



**HAL**  
open science

# Stress and toxicity of metal in photosynthetic bacteria : multi-scale study of the effects and the targets of metal ions and nanoparticles

Reem Tambosi

► **To cite this version:**

Reem Tambosi. Stress and toxicity of metal in photosynthetic bacteria : multi-scale study of the effects and the targets of metal ions and nanoparticles. Biotechnology. Université Paris-Saclay, 2020. English. NNT : 2020UPASL070 . tel-03169595

**HAL Id: tel-03169595**

**<https://theses.hal.science/tel-03169595>**

Submitted on 15 Mar 2021

**HAL** is a multi-disciplinary open access archive for the deposit and dissemination of scientific research documents, whether they are published or not. The documents may come from teaching and research institutions in France or abroad, or from public or private research centers.

L'archive ouverte pluridisciplinaire **HAL**, est destinée au dépôt et à la diffusion de documents scientifiques de niveau recherche, publiés ou non, émanant des établissements d'enseignement et de recherche français ou étrangers, des laboratoires publics ou privés.

# STRESS AND TOXICITY OF METAL IN PHOTOSYNTHETIC BACTERIA

Multi-scale study of the effects and  
the targets of metal ions and nanoparticles

## Thèse de doctorat de l'université Paris-Saclay

École doctorale n°577, structure et dynamique des systèmes vivants (SDSV)

Spécialité de doctorat : Sciences de la vie et de la santé

Unité de recherche : Université Paris-Saclay, CEA, CNRS, Institute for Integrative  
Biology of the Cell (I2BC), 91198, Gif-sur-Yvette, France.

Référent : Faculté des sciences d'Orsay

Thèse présentée et soutenue à Gif sur Yvette, le 15 Décembre 2020, par

**Reem TAMBOSI**

### Composition du Jury

**Nicolas BAYAN**

Professeur, Université Paris-Saclay

Président

**Francoise JACOB-DUBUISSON**

Directrice de recherche, CNRS, Institut Pasteur Lille

Rapportrice & examinatrice

**Francesca ZITO**

Directrice de recherche, CNRS, IBPC Paris

Rapportrice & examinatrice

**Alexandra FRAGOLA**

Maîtresse de conférences, LPEM, Sorbonne Université

Examinatrice

**Corinne CASSIER-CHAUVAT**

Directrice de recherche, CNRS, I2BC, Université Paris-Saclay

Examinatrice

**Soufian OUCHANE**

Directeur de recherche, CNRS, I2BC, Université Paris-Saclay

Directeur de thèse

**Nouari KEBAILI**

Maître de conférences CNRS, LAC, Université Paris-Saclay

Co-Encadrant de thèse

**Sylviane LIOTENBERG**

Maîtresse de conférences, CNRS, I2BC, Université Paris-Saclay

Co-Encadrante de thèse



# STRESS AND TOXICITY OF METAL IN PHOTOSYNTHETIC BACTERIA

Multi-scale study of the effects and  
the targets of metal ions and nanoparticles

**Thèse de doctorat de l'université Paris-Saclay**

École doctorale n°577, structure et dynamique des systèmes vivants (SDSV)

Spécialité de doctorat : Sciences de la vie et de la santé

Unité de recherche 1 : Université Paris-Saclay, CEA, CNRS, Institute for Integrative Biology of the Cell  
(I2BC), 91198, Gif-sur-Yvette, France.

Unité de recherche 2 : Université Paris-Saclay, CEA, CNRS, Laboratoire Aimé Cotton (LAC),  
91405, Orsay, France.

Référent : Faculté des sciences d'Orsay

**Thèse présentée et soutenue à Gif sur Yvette, le 15 Décembre 2020, par**

**Reem TAMBOSI**

## Composition du Jury

**Nicolas BAYAN**

Professeur, Université Paris-Saclay

**Francoise JACOB-DUBUISSON**

Directrice de recherche, CNRS, Institut Pasteur Lille

**Francesca ZITO**

Directrice de recherche, CNRS, IBPC Paris

**Alexandra FRAGOLA**

Maîtresse de conférences, LPEM, Sorbonne Université

**Corinne CASSIER-CHAUVAT**

Directrice de recherche, CNRS, I2BC, Université Paris-Saclay

**Soufian OUCHANE**

Directeur de recherche, CNRS, I2BC, Université Paris-Saclay

**Nouari KEBAILI**

Maître de conférences CNRS, LAC, Université Paris-Saclay

**Sylviane LIOTENBERG**

Maîtresse de conférences, CNRS, I2BC, Université Paris-Saclay

Président

Rapportrice & examinatrice

Rapportrice & examinatrice

Examinatrice

Examinatrice

Directeur de thèse

Co-Encadrant de thèse

Co-Encadrante de thèse



<b>Research Director</b>	<b>Soufian OUCHANE</b>	Directeur de Recherche CNRS Institute for Integrative Biology of the Cell Microbiology department Office : 33-1-69 82 31 37
<b>Co-Research Directors</b>	<b>Nouari KEBAILI</b>	Maître de conférence Université Paris-Saclay Laboratoire Aimé Cotton - Nanophysique Office : 01 69 35 20 61
	<b>Sylviane LIOTENBERG</b>	Maîtresse de conférence Université Paris-Saclay Institute for Integrative Biology of the Cell Office : 06 24 71 19 30
<b>Jury President</b>	<b>Nicolas Bayan</b>	Professeur Université Paris-Saclay Institute for Integrative Biology of the Cell Microbiology department.
<b>Reviewers</b>	<b>Françoise Jacob-DUBUISSON</b>	Directrice de Recherche CNRS Institut Pasteur, Lille
	<b>Francesca ZITO</b>	Directrice de Recherche CNRS Institute of Physico-Chemical Biology IBPC, Paris
<b>Examiners</b>	<b>Corinne CASSIER-CHAUVAT</b>	Directrice de Recherche CNRS Institute for Integrative Biology of the Cell Microbiology department
	<b>Alexandra FRAGOLA</b>	Maîtresse de conférence Sorbonne Université   UPMC Laboratoire de Physique et Etude des Matériaux (LPEM)



فوائد الأسفار

## The Benefits in Travelling

تغرب عن الأوطان في طلب العلى  
وسافر ففي الأسفار خمس فوائد

*Leave your country in search of loftiness  
And travel! For in travel there are 5 benefits,*

تفرج هم واكتساب معيشة  
وعلم وآداب وصحبة ماجد

*Relief of adversity and earning of livelihood  
And knowledge and etiquettes and noble companionship*

(*Al-Shafi'i (767-820)*)

---

*"Nothing in life is to be feared, it is only to be understood. Now is the time to understand more, so that we may fear less."*

(*Marie Curie (1867-1934)*)



*To my dear parents and my nieces,*



## Acknowledgment

This manuscript comes to embodiment almost four years of research carried out within the group of Microbiology, Bacterial Adaptation to Environmental Changes (I2BC Lab), and group of Physics, Nanoparticles, Nanostructures and Nanomaterials (LAC Lab). First and foremost, I would like to thank a number of people who have worked closely with this work and allowed it to exist.

Foremost, I would like to express my sincere gratitude to all my supervisors. Soufian OUCHANE, Sylviane LIOTENBERG and Nouari KEBAILI. For their effort and continuous support of my PhD study and research project. I am grateful for their patience, encouragement and non-stopped care. I have been extremely lucky to have these supervisors who cared so much about my work, and who responded to my questions and queries so promptly. I am grateful for helping me going through this path so I can achieve my dream and be who I am today. Also, you were there all the time asking and checking on me during the confinement time because of coronavirus. It was difficult time for all, yet my study was handled remarkably professionally. Thank you so much.

Special thanks for my thesis committee: Corinne CASSIER-CHAUVAT and Alexandra FRAGOLA for being there from year one. Making sure that I am making plans, following them, and I success. Special thanks for the rest of the jury Nicolas BAYAN, Françoise JACOB-DUBUISSON, and Francesca ZITO, for accepting to review my thesis and my research project.

My great sincere appreciation goes to the rest of the team members in the microbiology laboratory in I2BC. Marie-Line BOURBON, Anne-Soisig STENOUE, Marion BABOT, Anne DURAND, Chantal ASTIER, you were like my sisters here. I cannot thank you enough. You were there all the time for supporting, encouraging, teaching and directing me. Lots of things that we shared together, and I am blessed to have you all around me at this very important chapter in my life.

In Laboratory Aimé Cotton (LAC) my first thanks go to the directors that were always great support: Djamel BENREDJEM and Olivier DULIEU. My great sincere gratitude also to the other team members in the Nano<sup>3</sup> group (present and past) Thanks to Alain SARFATI, Vladimir AKOULINE, Frédéric CARLIER, Chloé GELLER, Gaylord TALLEC, Fano GONCALVEZ, Jamila DJAFARI... A special brotherhood and sisterhood mention to the other "doctorants" of the group and in the LAC, I had the pleasure to meet and share with, Luca, Julie, Abderaouf, Yassamine, Jack, Hiba, Aya, Clément, ... and to many othermaster's students and interns from all over the world (we were the nano (UNO) in LAC): Minji, Valeria, Fahim, Franck, Yassine...

I am grateful to my parents and my brothers and sisters, who have provided me through moral and emotional support in my life. For their patience being away for long time following my dreams. I am also grateful to my other family members and friends who have supported me along the way.

A very special gratitude goes to the Ministry of Education in Saudi Arabia, which is represented by the Embassy of the Kingdom of Saudi Arabia - Cultural Office in Paris, for the scholarship and funding my education during my Master in USA and my PhD study now, here, in France. Thanks to Dr. Abdullah AL-THONAIYAN, Dr. Bakheet AL-RESHEEDI and M. Jamal AL- ALSHEIBANI and all the employees in the Embassy of the Kingdom of Saudi Arabia - Cultural Office in Paris.

Special thanks to University Paris-Saclay, and the National Center of Scientific Research (Centre National de la Recherche Scientifique). It was a great opportunity to carry my project in such facilities.

Most to mention the effort of both Pierre CAPY and Jean-Luc PERNODET, the Director and Deputy Directors Doctoral School Structure and Dynamics of Living Systems (SDSV). Thank you so much for all the support and care you provide to all of us as PhD international students. With your instructions, it was always easy to understand the process of the ED SDSV during every year's registration. Thanks for your encouragement to participate at the (Journée de l'ED SDSV). A special thanks to Sandrine Le BIHAN (Assistante de l'ED SDSV) for her help and kindness.

Je suis également reconnaissant aux personnels de l'Université et du CNRS-I2BC, sans qui rien n'est possible aux chercheurs et étudiants, notamment Judith ELVER et tous les membres du Service Gestion des Personnels de l'I2BC.

À Marie-Line, j'ai la chance de ton amitié. Nous n'avons pas simplement partagé un bureau. Nous avons partagé des rires, des histoires, à la fois tristes et drôles. Nous avons partagé la route pour rentrer chez nous plusieurs fois. Me laisser avec un conseil, un commentaire et /ou un joli souhait comme dernière chose avant de me déposer au RER. J'ai toujours et constamment ressenti une énergie positive autour de toi. J'ai beaucoup appris de toi. Merci Marie-Line.

Last but by no means least, Thanks to all my friends here in France, the second family to me, who comforted and supported me to go through some tough times and issues I had with my health. Together, with you I were able to process and maintain the idea not to be able to see my family because borders were closed. I appreciated all the quality moments, and I cannot thank you enough.



# RÉSUMÉ

---

L'usage intensif des métaux et des ions métalliques dans l'industrie et l'agriculture représente une menace sérieuse pour l'environnement et pour tous les êtres vivants en raison de la toxicité aiguë de ces ions. Cependant, cette toxicité est aussi un outil prometteur dans le cadre de la résistance aux antibiotiques. En effet, les ions comme les nanoparticules ( $\text{Ag}^+$  ou  $\text{Cu}^+$ ) sont très utilisés dans diverses applications médicales, industrielles et sanitaires. L'effet antimicrobien de ces nanoparticules est en partie lié aux ions libérés et à leur capacité à interagir avec diverses protéines bactériennes. Le but de ce projet est d'étudier l'interaction entre un objet biologique (les bactéries) et des objets physiques (métaux), pour comprendre l'impact des métaux sous différentes formes (ions, nanoparticules et nanostructures) sur les cellules bactériennes en utilisant différentes approches : de physiologie, biochimie, génétique et de biologie cellulaire. Nous avons utilisé comme modèles biologiques, principalement la bactérie photosynthétique pourpre *Rubrivivax (R.) gelatinosus*, mais aussi *Escherichia coli*; et pour les objets physiques, nous avons utilisé l'argent comme métal principal mais aussi d'autres métaux (cuivre, cadmium et nickel) à titre de comparaison.

Les principaux objectifs de ce travail sont : **1-** d'étudier l'impact et les mécanismes de toxicité de ces ions métalliques / NPs sur les métabolismes bactériens respiratoire et photosynthétique. **2-** Identifier des gènes impliqués dans la réponse à un excès d'ions  $\text{Ag}^+$ . **3-** Etudier l'interaction des ions métalliques et des NP avec la membrane des bactéries. Ainsi, nous avons identifié, *in vitro* et *in vivo*, des cibles spécifiques d'ions  $\text{Ag}^+$  et  $\text{Cu}^+$  dans la membrane des bactéries. Cela inclut des complexes impliqués dans la photosynthèse et des complexes de la chaîne respiratoire. Il a été montré que les ions  $\text{Ag}^+$  et  $\text{Cu}^+$  ciblent spécifiquement une bactériochlorophylle exposée au solvant dans les antennes périphériques de collecte de lumière de *R. gelatinosus*. Nous avons aussi montré que ces ions cibles des complexes de la chaîne respiratoire chez *R. gelatinosus* et *E. coli*. Ceci présente à notre connaissance, la première preuve directe de dommages induits par des ions  $\text{Ag}^+$  sur les protéines membranaires impliquées dans ces métabolismes. Par ailleurs, nous avons également réalisé une étude comparative par microscopie (AFM/ SEM) de l'effet de l' $\text{Ag}^+$  en solution ou des Ag-NPs synthétisés dans notre laboratoire, sur la morphologie des cellules bactériennes.

**Mots-Clés** : argent / cuivre ; complexes membranaires ; homéostasie des métaux; photosynthèse ; respiration ; toxicité ; porphyrines ; AFM ; SEM

## I. Introduction

### Métaux essentiels et toxicité:

Certains métaux comme le  $\text{Fe}^{2+}$ , le  $\text{Mg}^{2+}$  ou le  $\text{Cu}^+$  etc, sont essentiels à la survie des organismes procaryotes et eucaryotes. Ils sont nécessaires à la croissance et à la survie des cellules en participant à de nombreux processus métaboliques vitaux. Par exemple, les métaux alcalins tels que le sodium, le potassium ou le calcium jouent un rôle crucial dans le métabolisme cellulaire et maintiennent le niveau ionique optimal.

D'autres métaux lourds tels que le  $\text{Fe}^{2+}$  ou le  $\text{Cu}^+$  sont des cofacteurs associés à plusieurs enzymes impliquées dans des processus cellulaires essentiels tels que la photosynthèse, la respiration aérobie et anaérobie, ou la détoxification d'espèces activées d'oxygène (Kim et al., 2008). Il est ainsi estimé que plus de 30% des protéines de la bactérie sont des métalloprotéines abritant des ions métalliques nécessaires à leurs structures ou leurs activités. Dans le cadre de cette étude, nous allons voir que des métalloprotéines comme les antennes collectrices de lumière, la succinate déshydrogénase ou la cytochrome *c* oxydase nécessaire à la croissance photosynthétique ou respiratoire sont des cibles d'ions métalliques.

La forte affinité des ions métalliques aux différents composants des cellules en particulier aux protéines et l'activité redox des ions sont à la base de la toxicité des ions. En effet un excès d'ions métalliques est souvent toxique pour les cellules. Cette toxicité est principalement médiée par une mauvaise métallation des protéines ou des cofacteurs, un mauvais repliement des protéines ou la génération d'un stress oxydatif.

Les protéines sont les principales cibles des ions métalliques. En effet, la plupart des ions métalliques peuvent interagir avec les polypeptides et peuvent ainsi inactiver les protéines. A titre d'exemple, le  $\text{Cu}^+$  va interagir avec le thiol des cystéines mais aussi avec le groupement imidazole de l'histidine et avec la méthionine. Il peut donc se substituer au véritable métal de transition lors de l'assemblage de la protéine ou au moins empêcher le métal de se lier à son site dans la protéine et conduire à son inactivation (**Fig. 1**).

L'impact le plus important et le plus étudié des métaux tels que le  $\text{Cu}^+$  ou l' $\text{Ag}^+$  est très probablement la dégradation des protéines à cluster [4Fe-4S] exposées. La dégradation des [4Fe-4S] a été décrite pour de nombreuses enzymes essentielles telles que la fumarase-A et la 6-phosphogluconate déshydratase dans *E. coli* (Macomber et Imlay, 2009; Xu et Imlay, 2012). L'enzyme HemN, contenant [4Fe-4S] est également une cible de l'excès de métal. La synthèse de l'hème et par conséquent de nombreuses

hémoprotéines sont impactées dans *Rubrivivax gelatinosus* et *Neisseria gonorrhoeae* (Azzouzi et al., 2013; Djoko & McEwan, 2013; Steunou et al., 2020a).

Les métaux à forte affinité peuvent également se substituer à d'autres ions lors de la synthèse de groupements prothétiques tels que les porphyrines (hème et chlorophylles). En effet, il a été montré *in vitro*, que la Ferro-chelatase qui catalyse l'insertion de  $Fe^{2+}$  dans la protoporphyrine IX, peut insérer du  $Zn^{2+}$  ou du  $Co^{2+}$  dans l'anneau porphyrine de la protoporphyrine IX (Hansson et al., 2011).

D'autre part, certains métaux comme  $Fe^{2+}$  et  $Cu^+$  sont capables de catalyser la réaction de Fenton et générer des radicaux hydroxyles ( $OH^{\cdot}$ ) extrêmement réactifs capables d'endommager les protéines, les lipides et l'ADN.

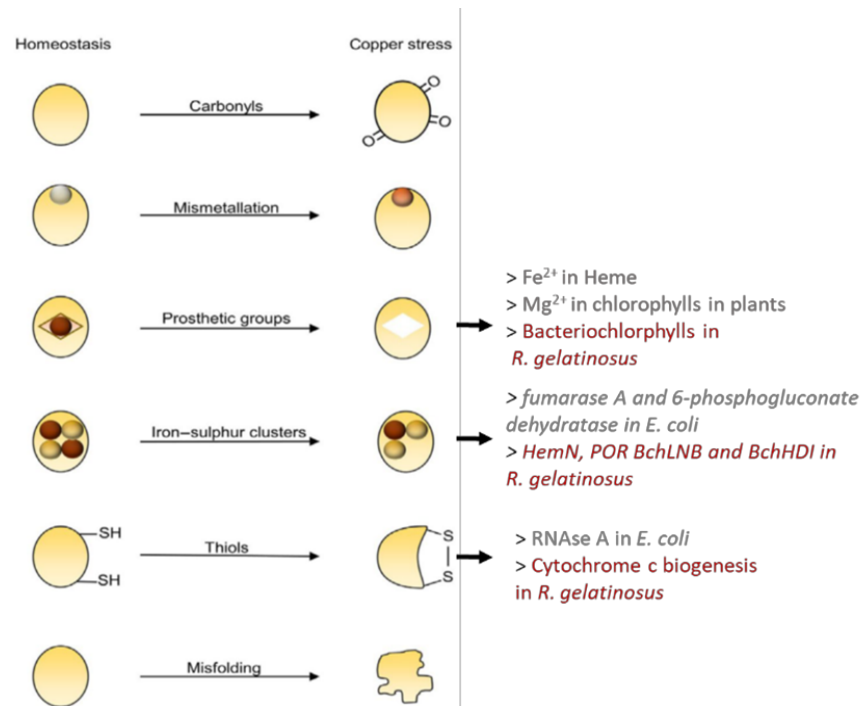


**Fig. 1** : Les métaux comme le cuivre peuvent induire la formation du carbonyle des protéines, provoquer une mauvaise métallation, interférer avec la biogenèse des groupes prothétiques, endommager les clusters [Fe-S], oxyder les thiols ou induire un mauvais repliement des protéines. Des exemples de ces effets ont été décrits dans *E. coli* et *R. gelatinosus* (en rouge). Modifié de (Dalecki et al., 2017).

L'accumulation de métaux dans l'environnement peut donc entraîner une toxicité et des défauts de métabolisme, conduisant à une croissance ralentie des micro-organismes, ainsi qu'à divers troubles métaboliques chez les organismes supérieurs. Heureusement, la présence de systèmes d'homéostasies efficaces des métaux permet d'échapper aux effets de l'excès des métaux, tant que les systèmes ne sont pas endommagés ou dépassés par l'excès métallique.

### **Homéostasie des métaux (stratégies de défense des bactéries) :**

Les cellules sont programmées pour maintenir un niveau optimal de métaux et résister ainsi à la toxicité de ces métaux. Ainsi, pour maintenir l'homéostasie des métaux, les cellules disposent de différents systèmes pour limiter l'import ou induire l'export en cas d'excès d'un métal. Ces mécanismes d'homéostasie impliquent des régulateurs capables de détecter les métaux et induire la réponse à l'excès, des moyens de séquestration extracellulaire ou intracellulaire des métaux, ou l'exclusion des métaux en limitant la perméabilité membranaire ou la détoxification par des systèmes d'efflux (P-type ATPase, protéines de la famille RND et protéines de la famille CDF).

Un dysfonctionnement du système d'homéostasie (import / efflux) de ces métaux peut provoquer d'importants troubles physiologiques aussi bien chez les procaryotes que chez les eucaryotes.

### **Contexte de santé public**

Depuis plus de vingt ans, les autorités de santé s'inquiètent d'une possible crise sanitaire liée surtout à la conjugaison de l'accroissement de bactéries multi-résistantes avec la pénurie dans le développement de nouveaux antibiotiques. En plus des efforts en pharmacie et médecine pour le soin et l'élaboration de médicaments, un effort important est apporté également dans la fabrication de matériaux, notamment de surface, avec une activité bactéricide ou permettant de réduire la prolifération bactérienne. Dans cette optique, l'utilisation de nanoparticules, notamment d'argent, et/ou de surfaces nano-structurées a connu un essor considérable ((Sánchez-López et al., 2020). C'est dans ce contexte et avec comme objectif à moyen terme l'élaboration de films anti-prolifération bactérienne, que se situe ce travail en nanobiotechnologie, fruit d'une collaboration multidisciplinaire, entre deux laboratoires. Toutefois, pour pouvoir utiliser ces matériaux métalliques, il est intéressant et important d'identifier les cibles moléculaires des métaux dans les bactéries pour comprendre les conséquences sur le métabolisme et décrire en détail les mécanismes de toxicité.

### **Interaction avec des nanoparticules et de nanostructures**

De nombreuses études ont été menées sur l'interaction des nanoparticules métalliques (essentiellement argent) avec les bactéries (essentiellement *E. coli*). Cependant les données restent limitées notamment car la complexité de cette étude nécessite une approche différente (multidisciplinaire) de celle des tests sur les antibiotiques ou de toxicité utilisés pour les composés classiques.

En effet les paramètres physicochimiques (stabilité, agrégation, dissolution et état de surface) des nanostructures dans le milieu de contact, influencent fortement la

toxicité observée sur les cellules. De plus, les interactions physicochimiques (floculation, adsorption, mécanismes redox) sont très souvent liées au modèle biologique. La plupart du temps les nanoparticules utilisées sont des nanoparticules commerciales pas toujours bien caractérisées et dont la stabilité en milieux biologiques induit une grande incertitude sur leurs tailles, leurs états de surface ou encore leur réactivité. La collaboration dans le cadre de cette thèse avec l'équipe Nano<sup>3</sup> (Nanoparticules, Nanostructures, Nanomatériaux) du laboratoire Aimé Cotton, nous a permis d'accéder à des nanoparticules synthétisées spécialement pour les manip, par voie chimique et/ou par voie physique avec un excellent contrôle de la taille, de la forme, et de la stabilité.

Les NPs sont fabriqués dans la plage (5-100 nm) pour des métaux, semi-métaux ou oxydes tels que : l'argent, l'antimoine ou l'oxyde de fer. Les techniques de synthèse sont de plus en plus nocif pour l'environnement (synthèse verte). Ces NP peuvent être préparées, en solution ou par dépôts sous ultra-vide sur des substrats différents tels que les matériaux carbonés (graphite, graphène, MWCNT) (Kébaïli et al., 2009). Le mica ou des substrats métalliques (cuivre, ...) ou d'oxydes (SiO<sub>2</sub>, TiO<sub>2</sub>, ...). L'enjeu est l'optimisation de cette production, l'adaptation à un milieu biologiquement compatible et leur transposition à un usage industriel.

### **Modèle d'étude :**

La majorité des études de la toxicité des métaux a porté sur des bactéries modèles et pathogènes (*E. coli*, *P. aeruginosa*, *S. typhimurium*, *B. subtilis*...). Peu d'études concernent des modèles environnementaux à l'exception de certaines bactéries pathogènes des plantes ou les cyanobactéries.

Comme les cyanobactéries, les bactéries pourpres offrent la possibilité d'étudier les effets des métaux aussi bien sur le métabolisme photosynthétique que respiratoire. Par ailleurs, 1- ces bactéries sont facilement cultivables et manipulables génétiquement en laboratoire sous différents modes trophiques, 2- Les outils génétiques nécessaires pour générer des mutants sont disponibles, et 3- le photosystème est relativement simple par rapport aux cyanobactéries et présente des homologies structurales et fonctionnelles avec le photosystème II des plantes supérieures (Donohue & Kaplan, 1991; Ouchane et al., 1996). La bactérie modèle de cette étude est *Rubrivivax gelatinosus*. C'est une bactérie environnementale, gram-négative introduite pour la première fois au laboratoire de photosynthèse de Gif-sur-Yvette en 1991 par F. Reiss et C. Astier pour développer les études génétiques (S. Ouchane) et structurelles du dispositif photosynthétique. Le nom *gelatinosus* provient de la capacité des cellules à dissoudre la gélatine. Cette bactérie a une forme en

bâtonnet et mobile grâce une paire de flagelles. La taille des cellules est comprise entre 0,4 et 0,5  $\mu\text{m}$  de largeur et entre 3 et 4  $\mu\text{m}$  de longueur. Les cellules poussent par photosynthèse en lumière et absence d'oxygène en utilisant un seul photosystème composé de deux antennes LH2 et LH1 et le centre réactionnel (RC) (**Fig. 2**).

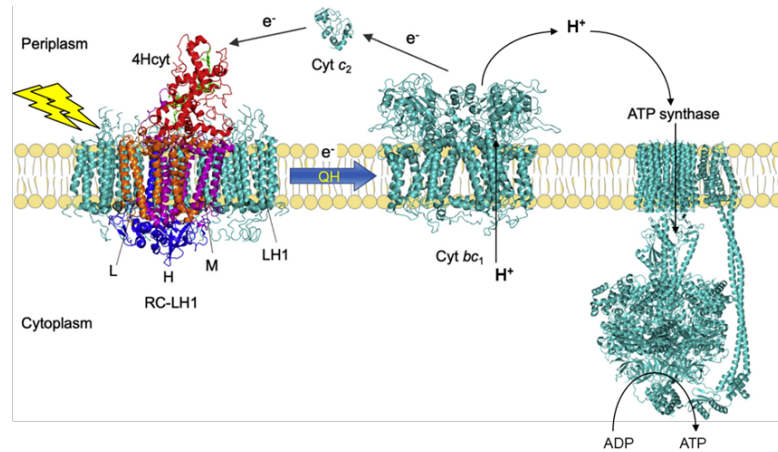


**Fig. 2** : Chaîne de transfert d'électrons dans les bactéries pourpres.

Les chlorophylles dans les complexes de collecte de lumière (LH) captent la lumière et la transfèrent au centre de réaction (RC). Le transfert entre le RC et le  $\text{cyt } bc_1$  génère un gradient de protons utilisé par l'ATPase pour produire de l'ATP.

A l'obscurité, la bactérie pousse par respiration aérobie grâce à une chaîne respiratoire composée des 4 complexes bactériens en plus de l'ATP synthase (**Fig. 3**).

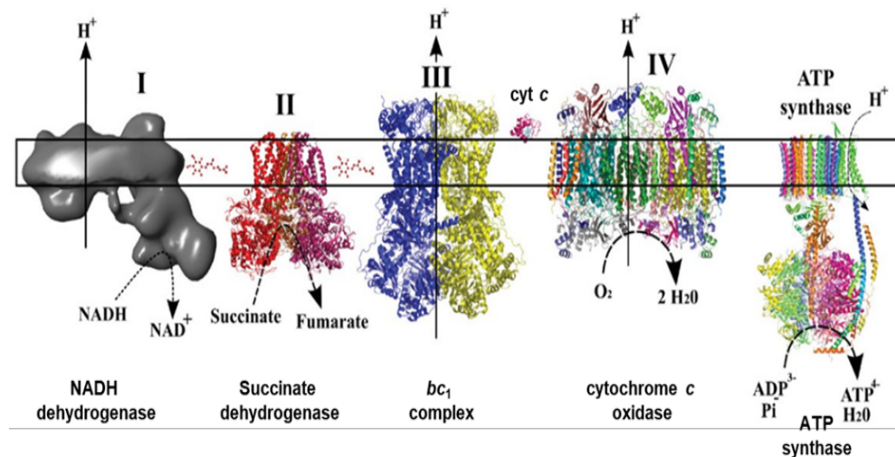


**Fig. 3** : Chaîne de transfert d'électrons dans les bactéries pourpres.

Le transport d'électrons entre ces complexes implique les quinones et le cytochrome  $c$  ( $\text{cyt } c$ ). Les protons transloqués par certains complexes sont utilisés pour la production d'énergie par l'ATPase.

## II. Résultats Majeurs

### 1. Cibles des ions argent et cuivre chez les bactéries :

Il a déjà été montré que l'exposition à un excès de métal altère le mécanisme photosynthétique des plantes et des algues. Nous avons montré, dans ce travail, que le complexe de collecte de lumière II (LH2) est la cible principale de l'exposition à l'Ag<sup>+</sup> et au Cu<sup>+</sup> chez la bactérie pourpre *Rubrivivax gelatinosus*. Nos recherches montrent en effet que *in vivo*, les ions Ag<sup>+</sup> ou Cu<sup>+</sup> inactivent spécifiquement la bactériochlorophylle *a* (B800) absorbant à 800 nm, alors que le même traitement avec Ni<sup>2+</sup> ou Cd<sup>2+</sup> des cellules n'a aucun effet. Les autres chlorophylles de l'antenne (B850) ne sont en revanche pas touchés par l'excès Ag<sup>+</sup> ou Cu<sup>+</sup>. Cela a été confirmé *in vitro* par l'analyse des protéines membranaires traitées aux ions Ag<sup>+</sup> ou Cu<sup>+</sup>. En effet, cela induit des modifications du spectre d'absorption de LH2 causées par perturbation de l'interaction des molécules B800 avec les protéines du complexe LH2. Cela a provoqué la libération de molécules B800 ce qui engendrera un impact sur les propriétés spectrales des caroténoïdes du complexe LH2 (**Fig. 4**).

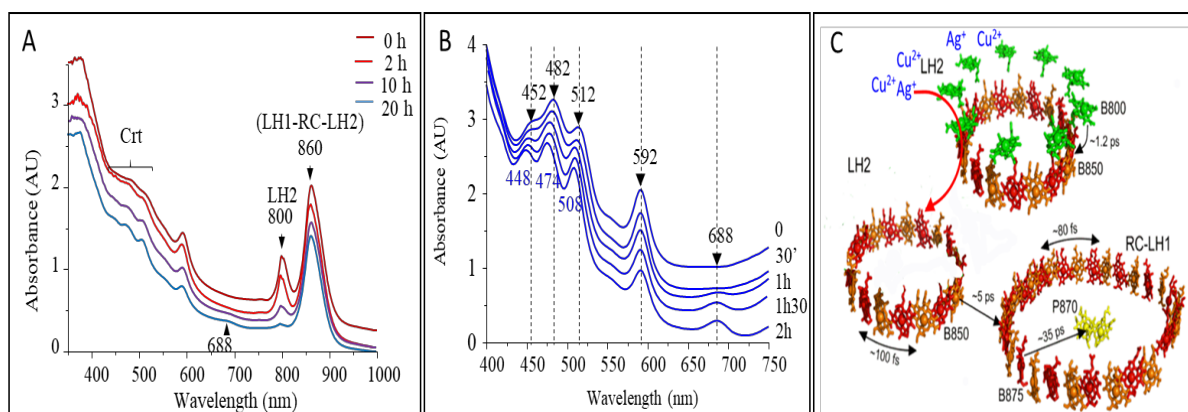


**Fig. 4 :** Effet d'AgNO<sub>3</sub> sur les complexes LH2 *in vivo* et *in vitro*.

**A-** Spectres d'absorption de cellules cultivées en photosynthèse puis exposées ou pas à 1 mM d'AgNO<sub>3</sub>. **B-** Spectres d'absorption montrant l'absorption des caroténoïdes dans des membranes exposées ou pas à 1 mM d'AgNO<sub>3</sub>. **C-** modèle montrant l'effet spécifique d'Ag<sup>+</sup> ou Cu<sup>+</sup> sur la chlorophylle B800 de LH2 dans le photosystème (LH2-LH1-RC).

D'autre part, des études antérieures ont suggéré que les ions Ag<sup>+</sup> peuvent affecter la chaîne respiratoire dans les mitochondries et dans les membranes des bactéries. Nous avons utilisé notre modèle bactérien *R. gelatinosus* pour essayer de révéler l'effet des ions Ag<sup>+</sup> sur la chaîne respiratoire bactérienne et identifier les

complexes impactés. Nos données ont démontré que l'exposition à  $\text{Ag}^+$ , à la fois *in vivo* et *in vitro*, provoquait une diminution des activités de la cytochrome *c* oxydase et du complexe I succinate déshydrogénase (**Fig. 5**). Une inhibition par les ions  $\text{Ag}^+$  de la succinate déshydrogénase a également été révélé lors de cette étude dans les cellules d'*E.coli*, mais pas chez *B. subtilis*.

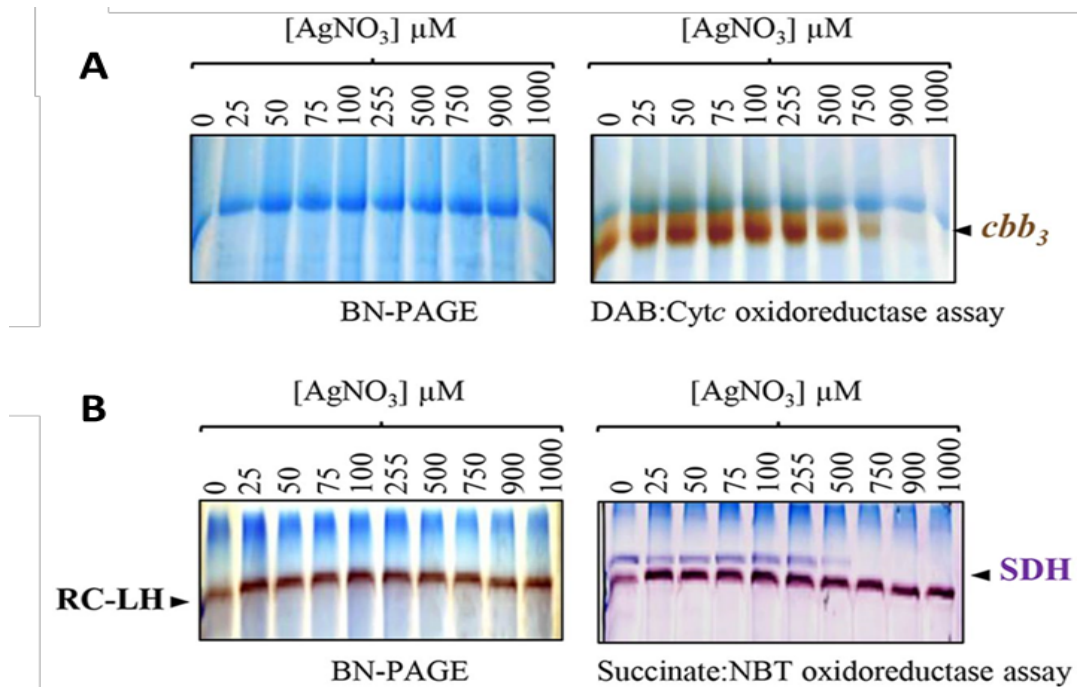


**Fig. 5.** Effet d' $\text{AgNO}_3$  sur les complexes respiratoires *in vitro*.

Les protéines membranaires exposées ou pas à des concentrations élevée d' $\text{Ag}^+$  ont été séparées sur une BN-PAGE de 5% à 12%. **A-** L'activité de la cytochrome *c* oxydase *cbb*<sub>3</sub> a été révélée DAB: test d'activité Cytc sur BN-PAGE. **B-** Test d'activité de la succinate déshydrogénase (SDH) sur BN-PAGE.

L'ensemble de ces résultats originaux ont fait l'objet d'une première publication dans MBio.

## **2. Recherche des gènes candidats impliqués dans la tolérance à l'argent**

Les cellules bactériennes induisent généralement les gènes codant les ATPases à efflux lors d'un stress métallique. La tolérance à l' $\text{Ag}^+$  chez *E. coli* implique par exemple l'ATPase CopA de type P1B, qui exporte le  $\text{Cu}^+$  et l' $\text{Ag}^+$  du cytoplasme vers le périplasma. Par conséquent, le mutant de délétion *copA* de *R. gelatinosus* a été utilisé pour vérifier l'implication de CopA dans l'efflux d' $\text{Ag}^+$ . Contrairement au  $\text{CuSO}_4$ , qui inhibe la croissance du mutant *copA*, aucune différence d'inhibition de la croissance n'a été observée entre les cellules mutantes *copA* et le type sauvage soumises à un

excès d'AgNO<sub>3</sub> (**Fig. 6**). Ces données suggèrent que contrairement à la tolérance Ag<sup>+</sup> chez *E. coli*, CopA n'est pas impliquée dans la tolérance Ag<sup>+</sup> chez *R. gelatinosus*. Des résultats similaires ont été obtenus avec le mutant *cadA* (*zntA*) déficient dans l'export du Zn<sup>2+</sup> ou Cd<sup>2+</sup>. Par ailleurs ces ATPases n'étaient pas induites par un excès de Ag<sup>+</sup>. Nous avons donc conclu que les ATPases CopA et CadA n'étaient pas impliquées dans la réponse à la présence d'AgNO<sub>3</sub>.

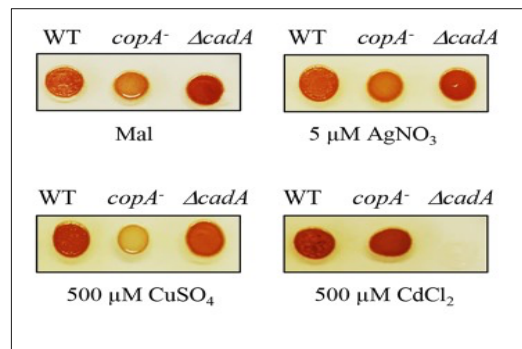


**Fig. 6** : Phénotype de croissance des mutants *copA* et  $\Delta$ *cadA*.

En présence des concentrations indiquées de AgNO<sub>3</sub>, CuSO<sub>4</sub> ou CdCl<sub>2</sub> sur milieu malate solide. Les cellules ont été cultivées en aérobic pendant 24 h à 30°C avant la photographie.

L'inactivation d'autres gènes codant des protéines de transport comme OmpA, Cus ou Cdf n'a donné aucun phénotype lorsque les mutants ont été poussés en présence d'Ag<sup>+</sup>. Ces résultats négatifs suggèrent que ces transporteurs ne sont pas nécessaires dans la toxicité à l'argent et que d'autres systèmes (à identifier) permettrait à la bactérie *R. gelatinosus* de tolérer la présence de ce métal dans son milieu.

### 3. Observations aux microscopes AFM/ SEM

Les résultats, présentés ici, complémentaires des mesures précédentes, montrent l'impact de l'effet toxique de l'argent sur la structure (morphologie et les propriétés mécaniques) de la membrane cellulaire. Nous avons utilisé les microscopes AFM et SEM pour observer les changements qui se produisent et visualiser l'effet des ions métalliques sur la surface de la membrane cellulaire.

Nous avons comparé différents modèles de bactéries, comme *Escherichia coli* et *Bacillus subtilis* comme contrôle, à l'observation sur *R. gelatinosus*. Les données collectées ont montré que les cellules bactériennes de *R. gelatinosus* étaient affectées par l'addition d'Ag<sup>+</sup>. La surface de la membrane cellulaire exhibe des modifications après 1 heure d'incubation et cela augmente avec un temps d'incubation prolongé (**Fig. 7**). Une observation similaire a été faite avec des cellules d'*E. coli* exposées à Ag<sup>+</sup>. Par contre, les cellules de *B. subtilis* n'ont montré aucun changement morphologique sur la structure cellulaire pendant la première heure d'incubation avec Ag<sup>+</sup>. Cependant,

les cellules ont été affectées et ont montré un changement de forme après 24 heures. Au-delà de 24 heures, les images de cellules incubées avec  $\text{Ag}^+$  montrent clairement la destruction de la membrane cellulaire menant à la mort des cellules.

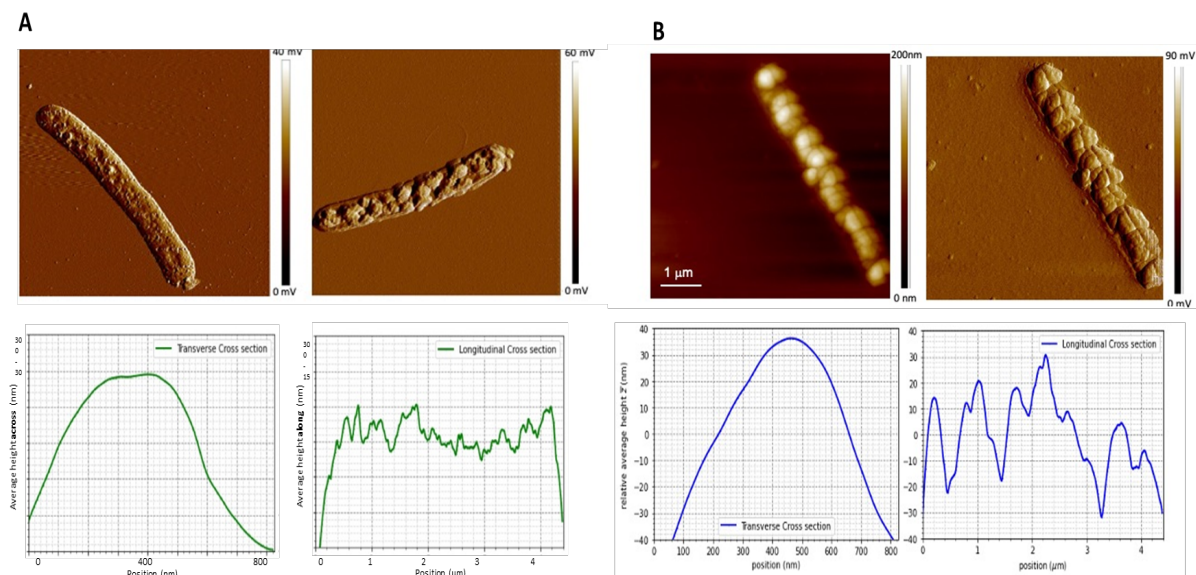


**Fig. 7:** Image AFM de cellules de *R. gelatinosus* exposées ou pas à  $\text{AgNO}_3$  pendant 1 h (A) ou après 24 h (B). Les courbes de profil correspondent à la hauteur moyenne relative le long de l'axe (longitudinal) et transversal des cellules bactériennes (transversales) pour les bactéries témoins prises comme références de profil.

De plus, l'analyse des données des images SEM a attiré notre attention sur la possibilité de modification de l'environnement cellulaire, par la formation de nouvelles particules. Ces particules adhèrent à la surface des cellules (Fig. 8) et pourraient augmenter la toxicité de l'argent si des ions sont libérés et pénètrent dans les bactéries ou au contraire réduire la toxicité si les particules sont insolubles.

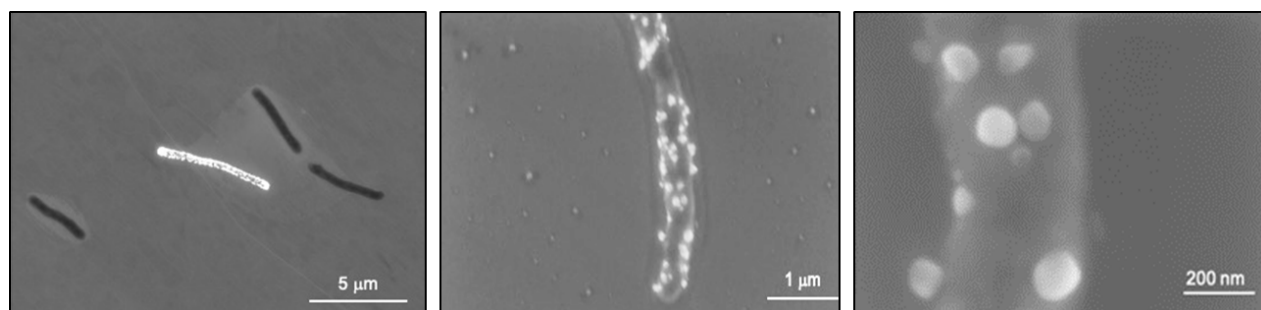


**Fig. 8 :** Formation des particules  $\text{Ag}^+$  et leur interaction avec les bactéries *R. gelatinosus*.

Ces particules sont formées vraisemblablement en raison de la réaction chimique entre les ions métalliques et les composants du milieu utilisé pour la culture des cellules bactériennes. Les résultats préalables montrent une précipitation de l'argent lié à la présence de phosphates dans certains milieux de culture. Ces données nous permettent également d'émettre l'hypothèse que les nouvelles particules formées peuvent avoir un impact en ce qui concerne la toxicité du métal utilisé sur les cellules et pourrait en outre expliquer en partie, les résultats très divergents dans la littérature.

#### 4. Nanoparticules : Synthèse et interactions avec les bactéries

La synthèse de NPs sphériques d'argent a été réalisée par un procédé de réduction chimique en utilisant du borohydrure de sodium comme agent réducteur et du citrate de sodium comme agent stabilisant (Ag-NPs1). Des NPs de plus grande taille ont été obtenues par une méthode de croissance par maturation à partir des germes de croissance précédent (Ag-NPs2) (**Fig. 9**). Pour la caractérisation des NPs, nous avons utilisé la spectroscopie UV-visible et la microscopie TEM. Les concentrations d'Ag-NPs ont été déterminées en utilisant le plasma à couplage inductif (ICP). Des solutions contenant des tailles différentes de nanoparticules d'argent ( $12 \pm 2$  nm à  $25 \pm 6$  nm) préparés à des concentrations élevées, ont été préparés pour évaluer leur impact sur la croissance des cellules de *R. gelatinosus*.

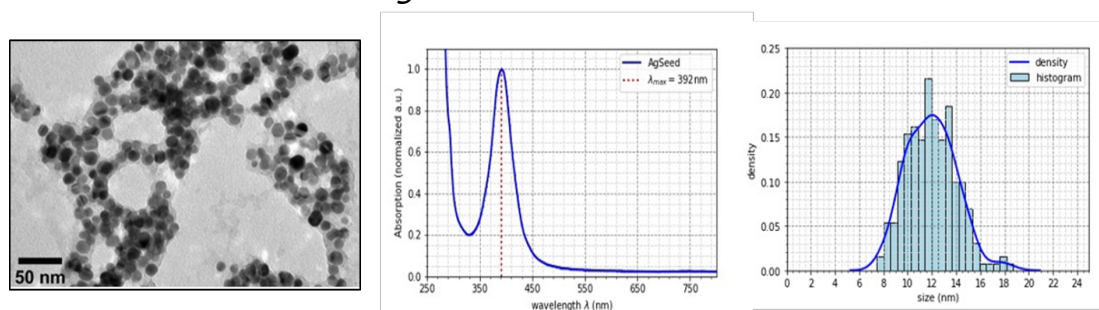


**Fig. 9.** Nanoparticules d'argents synthétisées au laboratoire

Images TEM, profil de spectroscopie d'absorption V-UV et distribution de taille de nanoparticules d'argent synthétisé par réduction chimique (Ag-NPs 1 (~12 nm)).

Nous avons testé lors d'expériences préliminaires (prometteuses) l'effet de ces NPs sur la croissance de *R. gelatinosus*. Nous avons ainsi comparé (des doses d'argent identiques de :  $\text{AgNO}_3$ , Ag-NPs 12 and 25 nm) l'effet des ions et des nanoparticules de 12 et 25 nm sur la croissance en milieu solide des cellules de *R. gelatinosus*. Les premiers résultats montrent que les ions  $\text{Ag}^+$  sont plus toxiques et que 1  $\mu\text{g} / \text{ml}$  d' $\text{AgNO}_3$  est suffisant pour inhiber la croissance des cellules. Pour les NPs, il faut 3  $\mu\text{g} / \text{ml}$  d'Ag-NPs (Ag-NPs 12 nm) pour avoir un impact sur la capacité des cellules à se

développer; et 5 µg/ ml pour l'inhiber complètement. L'effet des Ag-NPs 25 nm est significativement plus faible. Ceci montre clairement un effet de la taille des NPs sur la toxicité. Les NPs sont d'autant plus toxique qu'elles sont petites. Le mode probable d'interaction avec la surface bactérienne (contact de surface) augmente avec un rapport surface-volume plus élevé pour les NPs. De plus, les NP de plus petites ont une capacité de diffusion à travers la membrane cellulaire plus élevée (Acharya et al., 2018 ; Pal et al., 2007 ; Periasamy et al., 2012).

### **III. Conclusions et discussion**

L'argent, comme le cuivre, est utilisé depuis longtemps dans de nombreuses applications. Une faible concentration d'ions ou de nanoparticules d'argent peut être très toxique. Le but de ce travail est d'étudier l'impact des ions et NPs d'argent sur la bactérie photosynthétique pourpre *Rubrivivax gelatinosus*. Pour cela, un des premiers objectifs était d'identifier les cibles des ions Ag<sup>+</sup> pour pouvoir par la suite comprendre la toxicité des Ag-NPs, qui souvent agissent en laissant diffuser des ions de la nanoparticule.

Dans le cadre de ce travail de Thèse, nous avons montré que les deux métaux (Ag<sup>+</sup> et Cu<sup>+</sup>) ciblent l'antenne LH2 du photosystème et deux complexes respiratoires. Ces complexes sont des métalloprotéines contenant des cofacteurs porphyrines (chlorophylle (Mg<sup>2+</sup>) ou hème (Fe<sup>2+</sup>)) suggérant que les ions Ag<sup>+</sup> ou Cu<sup>+</sup> vont vraisemblablement interagir avec ces molécules et inhiber la fonction des complexes qui en dépendent.

En effet et en accord avec cette hypothèse, nous avons montré que les ions Ag<sup>+</sup> et Cu<sup>+</sup> affectent spécifiquement la chlorophylle B800 exposée de l'antenne LH2. Cette chlorophylle se détache du complexe ce qui modifie ces propriétés. En revanche les bactériochlorophylles B850 avec les molécules de caroténoïdes ne sont pas affectées, car non-exposées et enfouies dans la structure de la protéine. Le mécanisme par lequel Ag<sup>+</sup> ou Cu<sup>+</sup> libèrent le B800 du LH2 reste à étudier. Le Cu<sup>+</sup> ou l'Ag<sup>+</sup> pourrait rompre la liaison du Mg<sup>2+</sup> de la chlorophylle avec la protéine libérant ainsi la chlorophylle B800 (**Fig. 10**).

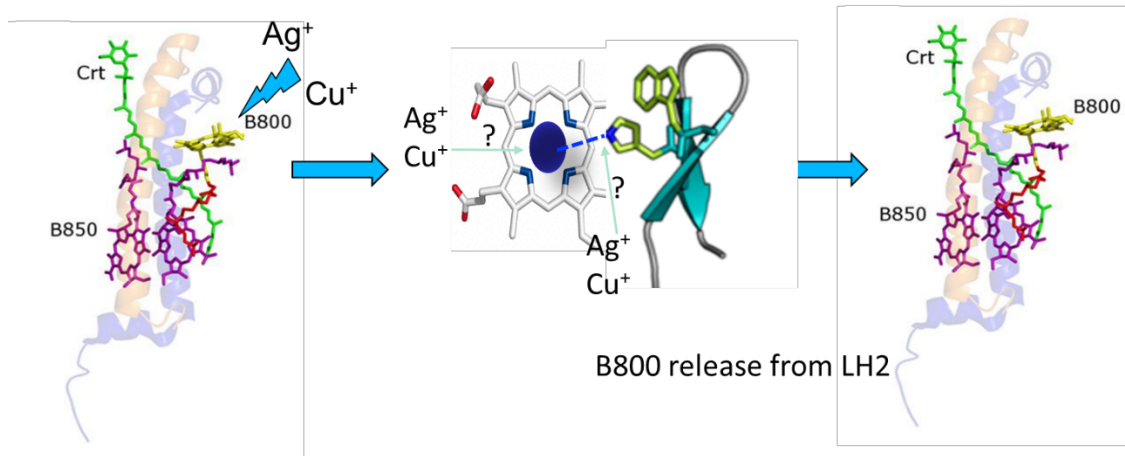


**Fig. 10.** Modèle proposé pour expliquer la perte de la chlorophylle B800.

Le  $\text{Cu}^+$  ou l' $\text{Ag}^+$  pourrait rompre la liaison du  $\text{Mg}^{2+}$  de la chlorophylle avec la protéine libérant ainsi la chlorophylle B800 de l'antenne LH2.

Les impacts de la présence d' $\text{AgNO}_3$  sur l'activité de la cytochrome *c* oxydase et de la succinate déshydrogénase chez *R. gelatinosus*, ainsi que sur la succinate déshydrogénase chez *E. coli*, ont été démontrés dans cette étude. Cela pourrait résulter de la perturbation par  $\text{Ag}^+$  de l'interaction entre les cofacteurs (hème ou [4Fe-4S]) et les protéines. Néanmoins, il faut noter que les effets de  $\text{Ag}^+$  sur les complexes rapportés dans cette étude ont été obtenus avec une concentration élevée d' $\text{AgNO}_3$ . Aucun effet n'a été montré chez la bactérie Gram-positif *B. subtilis*. Cela est sans doute lié à la différence de structure de la paroi cellulaire entre les bactéries Gram-positives et Gram-négatives. Les couches de peptidoglycane, beaucoup plus épaisses des bactéries Gram-positives, pourraient protéger la cellule du stress environnemental, y compris celui des ions métalliques externes. Les études menées jusqu'au aujourd'hui au laboratoire ont permis d'identifier diverses cibles des métaux dans la bactérie et proposer des mécanismes de toxicité. Mon travail permet de proposer un nouveau mécanisme, la libération des cofacteurs chlorophylles et hèmes exposés dans la membrane (**Fig. 11**).

-RÉSUMÉ-

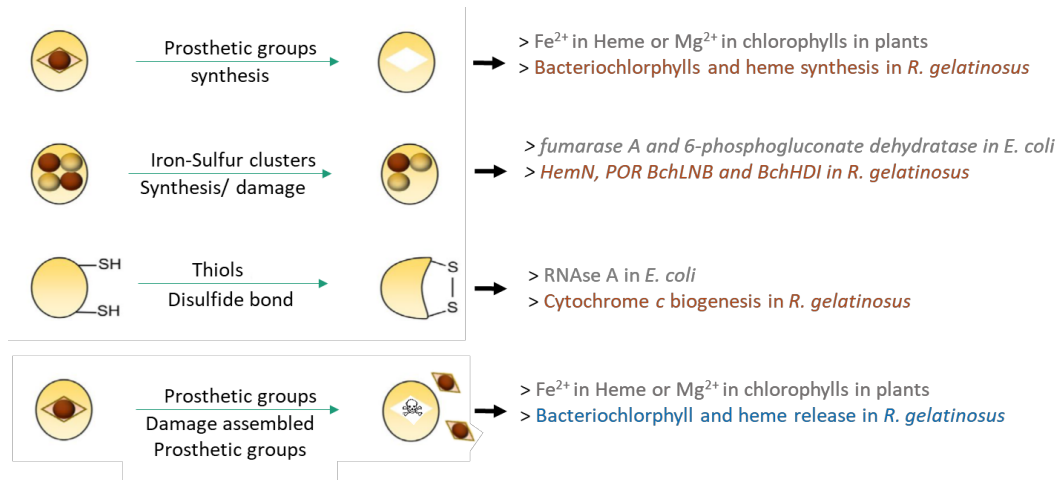


**Fig. 11.** Divers modèles proposés pour expliquer la toxicité des métaux dans les bactéries. Ce travail suggère que les porphyrines attachées mais exposées dans les protéines peuvent être des cibles directes des ions métalliques.

Les analyses par microscopie SEM ont révélé la formation de particules Ag<sup>+</sup>, dont la nature et composition reste à déterminer. Ces particules s'adsorbent à la surface des bactéries (**Fig. 12**). Par ailleurs, les analyses par microscopie AFM ont montré que le stress Ag<sup>+</sup> a augmenté la rugosité de la surface des bactéries exposées et provoqué des déformations et des cassures de la membrane cellulaire. Une différence totale moyenne de hauteur, de différentes vésicules, d'environ ± 30 nm se produit pendant la première heure d'exposition à Ag<sup>+</sup> chez *R. gelatinosus*. Alors que pour *E. coli*, Ag<sup>+</sup> fait apparaître des perturbations moins importantes, chez *B. subtilis*, l'impact Ag<sup>+</sup> est beaucoup plus lent. À notre connaissance, ces résultats sont les premières preuves directes et visuelles de dommages morphologiques causés par des ions Ag<sup>+</sup> sur la membrane des cellules de *R. gelatinosus*.

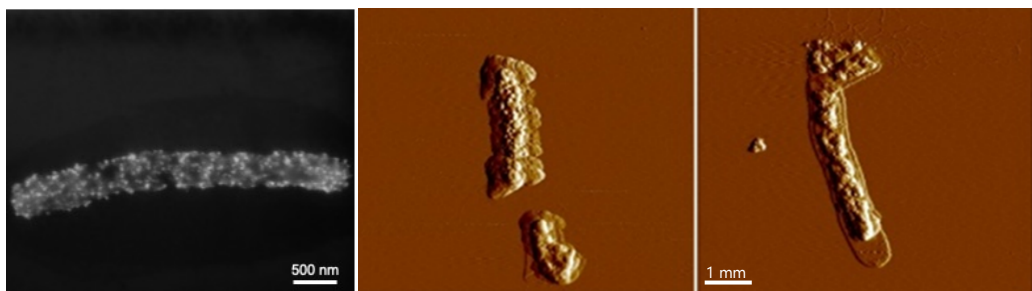


**Fig. 12 :** Formation des particules Ag<sup>+</sup> et leur interaction avec les bactéries *R. gelatinosus* SEM. Effet délétère des ions Ag<sup>+</sup> sur les cellules de *R. gelatinosus* après une exposition prolongée.

Dans cette étude, nous avons également synthétisé avec succès des nanoparticules d'argent en utilisant une méthode chimique. La forme sphérique des Ag-NP a des gammes de taille : de  $12 \pm 2$  nm à  $25 \pm 6$  nm. Outre la couleur invariable de la solution, les images TEM et les mesures spectrales ont démontré la stabilité des nanoparticules. Les Ag-NP ont été recouverts de citrate de sodium (agents de coating faiblement liés) pour éviter l'agrégation.

Des échantillons d'Ag-NP à différentes concentrations ont été préparés pour étudier leur effet sur la croissance des bactéries *R. gelatinosus*. Les résultats préliminaires ont montré que les plus petits Ag-NP sont les plus efficaces pour affecter la croissance des cellules à une concentration de  $3 \mu\text{g} / \text{ml}$ . Ces données ont été obtenues à partir de cultures cellulaires préparées sur milieu solide. En revanche, il n'y a pas eu de résultats probants concernant les cultures préparées en milieu liquide. Cela pourrait être dû à la facilité de diffusion à travers la membrane cellulaire et donc d'interaction avec les composants internes des cellules dans un milieu liquide plus que lorsqu'il s'agit d'un milieu solide, où le mouvement des NPs est restreint.

La plupart des études de toxicité des nanoparticules d'Ag<sup>+</sup> chez les bactéries et les eucaryotes mettent en lumière la réponse au stress oxydatif. Pour une caractérisation complète des mécanismes de toxicité des nanoparticules, les futures expériences devraient aborder la question de l'interaction entre les complexes membranaires impliqués dans la bioénergétique cellulaire et les nanoparticules d'Ag<sup>+</sup>.



# Table of Contents

---

INTRODUCTION	3
1. PHOTOSYNTHETIC PURPLE BACTERIA	1
1.1 Classification	1
1.2 Physiology and Habitat	2
1.3 Studied models	3
2. PHOTOSYNTHESIS IN BACTERIA	5
2.1 Photosynthetic membrane complexes	7
2.1.1 LH1 and LH2 Antennae	7
2.1.2 The Reaction Center	10
2.1.3 Photosynthetic pigments	12
2.1.3.1 Bacteriochlorophylls	12
2.1.3.2 Carotenoids	16
2.1.4 Organization of photosynthetic genes: the PS cluster	18
3. RESPIRATION IN PURPLE BACTERIA	19
3.1 Complex I: NADH	21
3.2 Complex II: succinate dehydrogenase (SDH)	22
3.3 Complex III: <i>bc<sub>1</sub></i>	23
3.4 Complex IV: Cytochrome <i>c</i> oxidase	24
4. REGULATION OF PHOTOSYNTHETIC GENES	26
4.1 The global anaerobic regulator FnrL	27
4.2. The transcriptional regulator PpsR	28
4.3 The RegB / RegA signal transduction system	29
5. GENERAL INTRODUCTION OF METALS IN BACTERIA	31
5.1 Metals and evolution	31
5.2 Selection of metal ions by proteins	32
5.3 Essential metallic ions and cofactors in bacteria	33
6. METALS IN THE ENVIRONMENT AND TOXICITY	35
6.1 Origin of metals in our environment	35
6.2 Toxicity caused by ion metals	35
7. METAL HOMEOSTASIS	39
7.1 Metal-sensing regulators	39
7.2 Extracellular sequestration of metals	42
7.3 Exclusion of metal by limiting membrane permeability	42
7.4 Intracellular sequestration of metals by chelating proteins	43

7.5 Enzymatic detoxification -----	44
7.6 Active efflux systems -----	44
7.6.1 P-type ATPases -----	44
7.6.2 Proteins of the RND family -----	47
7.6.3 The proteins of the cation diffusion facilitators (CDF family) -----	47
8. METALS NANOPARTICLES -----	49
8.1 Metal Nanoparticles -----	50
8.1.2 Optical properties -----	52
8.1.3 Physicochemical properties -----	54
8.1.4 Metal Nanoparticles synthesis -----	54
8.1.5 Metals nanoparticles as antimicrobial agent -----	57
8.2 Silver nanoparticles (Ag-NPs) -----	59
8.2.1 Silver nanoparticles as antimicrobial agent -----	60
8.2.3 Ag-NPs Synthesis methods -----	63
8.2.4 Ag-NPs characterization -----	65
8.3 Imaging and morphology analyzing tools -----	66
8.3.1 Electron Microscopy -----	67
8.3.2 Atomic Force Microscope -----	68
9. STATE OF THE ART -----	74
OBJECTIVE OF THE THESIS -----	83
RESULTS -----	87
1. IN VIVO TARGET OF SILVER AND COPPER -----	88
Introduction: -----	88
Summary and main findings: -----	89
Article I: Silver and Copper Acute Effects on Membrane Proteins. Impact on Photosynthetic and Respiratory Complexes in Bacteria -----	91
Supplemental results: -----	106
Additional results: -----	109
Discussion: -----	113
2. PUTATIVE TRANSPORT SYSTEMS INVOLVED IN METAL TOLERANCE IN <i>R. GELATINOSUS</i> -----	117
Introduction: -----	117
Results: -----	118
3. STRUCTURAL AND MORPHOLOGICAL ANALYSIS OF SILVER IONS IMPACT ON BACTERIA -----	130
Introduction: -----	130
Summary and main findings: -----	131
Additional result: -----	169
Discussion: -----	178

4. Silver Nanoparticle Synthesis and Their Effect on Photosynthetic Bacteria --	181
Introduction -----	181
Results -----	179
GENERAL DISCUSSION & PERSPECTIVES -----	190
APPENDIX -----	200
RELATED RESEARCH -----	200
ARTICLE IV: CROSS-TOLERANCE AND TARGETS OF METALS IN BACTERIA -----	201
Summary and main results in Article IV: -----	201
Article IV: Cadmium and Copper Cross-tolerance. Cu <sup>+</sup> alleviates Cd <sup>2+</sup> toxicity, and both cations target heme and chlorophyll biosynthesis pathway in <i>Rubrivivax gelatinosus</i> -----	203
ARTICLE V: INTERPLAY BETWEEN METALS EFFLUX AND ROS DETOXIFYING SYSTEMS -----	216
Summary and main results in Article V: -----	216
Article V: Additive effects of metal excess and superoxide, a highly toxic mixture in bacteria -----	218
MATERIALS & METHODS -----	231
REFERENCES -----	240

## Table of Figures

Figure 1. Photosynthetic prokaryotes habitat. ....	3
Figure 2. Photosynthetic purple bacteria. ....	5
Figure 3. Photosynthesis in bacteria. ....	6
Figure 4. Electron transfer chain in purple bacteria. ....	7
Figure 5. Photosystem arrangement and energy transfer.....	8
Figure 6. Cytoplasmic view of the LH2 antennae of <i>Rps. acidophila</i> .....	9
Figure 7. The LH2 pigment-protein from <i>Rps. acidophila</i> .....	10
Figure 8. Crystallographic structure of the reaction center of <i>Rhodospseudomonas (R.) viridis</i> . ....	11
Figure 9. Electron pathway between the cofactors in the reaction center. (Deisenhofer & Michel, 1989). ....	12
Figure 10. The tetrapyrrole biosynthesis pathway in purple bacteria.....	14
Figure 11. Structure of the 4Fe-4S cluster containing enzymes from the tetrapyrrole biosynthesis pathway in bacteria. ....	15
Figure 12. Regulatory pathways of photosynthesis in purple bacteria. ....	16
Figure 13. Carotenoid biosynthesis pathways in purple bacteria.....	18
Figure 14. Photosynthetic gene organization within the PS cluster in purple bacteria. ....	19
Figure 15. Complexes of the Respiratory chain of bacteria. ....	20
Figure 16. Crystal structure of the entire respiratory complex I (NADH dehydrogenase) from <i>Thermus thermophilus</i> bacterium.....	21
Figure 17. Crystal structure of Escherichia coli complex II (succinate dehydrogenase). ....	22
Figure 18. Structure of the <i>bc<sub>1</sub></i> complex.....	24
Figure 19. Structure of bacterial <i>aa<sub>3</sub></i> (left) and <i>cbb<sub>3</sub></i> oxidase (right).....	26
Figure 20. Schematic representation of gene regulation in purple bacteria.....	28
Figure 21. Evolution of oxygen, trace metal and metal ATPases on earth (A).....	32
Figure 22. Copper-induced damage. ....	37
Figure 23. Metalloregulatory and detoxification proteins involved in copper tolerance in <i>E. coli</i> (A). Structure of CueR from <i>E. coli</i> (B).....	41
Figure 24. Proteins involved in the tolerance of copper in <i>E. coli</i> .....	46
Figure 25. Structure of the CDF <i>YjiP</i> of <i>E. coli</i> involved in Zn <sup>2+</sup> efflux.....	48
Figure 26. Phase one of bacterial adhesion consists in the initial attraction of the cells to the surface through the effects of physical forces.....	49
Figure 27. The diversity of size and morphology of nanoparticles. ....	52
Figure 28. The different light-material interaction processes. ....	53
Figure 29. Localized Surface Plasmon Resonance of metallic nanoparticles under light illumination. ....	53
Figure 30. Different methods used for the synthesis of metal-based nanoparticles (MNPs). ....	55
Figure 31. NPs growth evolution involving different competitive mechanisms. ....	57
Figure 32. The appearance of antibiotics resistance versus antibiotics development. ....	58

Figure 33. Schematic representation of AgNPs mechanism of antimicrobial activity.	61
Figure 34. Process for the synthesis of AgNPs.	64
Figure 35. Silver nanoparticles by biosynthesis methods.	65
Figure 36. Optical extinction spectra and solution appearance of silver nanospheres.	66
Figure 37. EDX spectrum and electron images metal nanoparticle.	68
Figure 38. Schematic of the Atomic Force Microscope AFM.	70
Figure 39. Atomic force microscopy.	71
Figure 40. AFM cantilever and tip.	71
Figure 41. AFM images of bacteria and their aggregates with minerals in air.	72
Figure 42. Interplay between metal efflux, iron uptake and ROS detoxifying system.	77
Figure 43. Effect of Ag <sup>+</sup> and Cu <sup>2+</sup> on LH2 antennae.	90
Figure 44. Toxicity of CuSO <sub>4</sub> and AgNO <sub>3</sub> in cultures of high cells density.	106
Figure 45. Effect of CuSO <sub>4</sub> on LH2 complex.	107
Figure 46. LH2 monomer and its associated pigments.	108
Figure 47. Effect of AgNO <sub>3</sub> treatment on carotenoids in the LH2 complexes in membrane-enriched fractions.	109
Figure 48. Effect of Ag <sup>+</sup> on <i>cbb</i> <sub>3</sub> activity and amount in stressed cells.	110
Figure 49. Effect of Ag <sup>+</sup> on Complex I activity in stressed cells.	111
Figure 50. Effect of Ag <sup>+</sup> on Complex I activity in solubilized membranes.	112
Figure 51. Electronic absorption spectra of pheophytin (Pheo: chlorophyll without Mg <sup>2+</sup> ) and its complexes with Mg <sup>2+</sup> (Chla), Zn <sup>2+</sup> , Ni <sup>2+</sup> , and Pt <sup>2+</sup> .	114
Figure 52. Metal transporters identified in <i>R. gelatinosus</i> .	117
Figure 53. Gene inactivation by homologous recombination in <i>R. gelatinosus</i> .	118
Figure 54. Induction of CopI by metal ions.	119
Figure 55. <i>R. gelatinosus</i> proteins induction under silver stress.	120
Figure 56. <i>R. gelatinosus</i> CdfA sequence showing the His rich domain.	120
Figure 57. CdfA could be required for growth on silver but not on copper.	121
Figure 58. Role of CdfA in growth on cadmium or silver.	122
Figure 59. Growth curves of <i>R. gelatinosus</i> WT, <i>cdfA</i> <sup>-</sup> , <i>cadA</i> <sup>-</sup> and <i>cdfA-cadA</i> <sup>-</sup> in liquid medium under respiratory condition in the presence of CdCl <sub>2</sub> or AgNO <sub>3</sub> .	123
Figure 60. Gene organization of the putative <i>cusABC</i> operon in <i>R. gelatinosus</i> and <i>M. petroleiphilum</i> .	124
Figure 61. Role of <i>cusA</i> in growth on silver.	125
Figure 62. Role CusA in metal tolerance.	126
Figure 63. OmpW inhibition by CuSO <sub>4</sub> in <i>R. gelatinosus</i> .	127
Figure 64. Effect of <i>ompW</i> inactivation on Cu <sup>2+</sup> tolerance.	128
Figure 65. Substrates: mica and HOPG toxicity test comparing to other types of substrate.	169
Figure 66. Different form of droplets with water as solvent and drying time depending on substrate.	170
Figure 67. Ag-NPs on HOPG substrate.	172

Figure 68. AFM images of <i>R. gelatinosus</i> bacterial cells with Ag-NPs incorporated in the culture media. ....	173
Figure 69. AFM images of Ag-NPs after 7 days of deposition. ....	174
Figure 70. Mechanism of Ostwald Ripening. Size Distribution depending on the initial size distribution-7 days after. ....	174
Figure 71. SEM images of <i>B. subtilis</i> cells exposed or not to silver. ....	175
Figure 72. AgNO <sub>3</sub> effect on respiratory complexes in vivo. ....	177
Figure 73. TEM Images of seed silver nanoparticles AgSeed (left); and their characterization (right) using spectroscopy UV-Visble (up) and size distribution profiles and density given by images analysis (down). ....	183
Figure 74. TEM Images of grown silver nanoparticles AgSMG1 (left); and their characterisation (right) using spectroscopy UV-Visble (up) and size distribution profiles and density given by images analysis (down). ....	184
Figure 75. The <i>R. gelatinosus</i> growth under SC effect. ....	185
Figure 76. Growth phenotype of <i>R. gelatinosus</i> cells under silver stress. ....	186
Figure 77. <i>R. gelatinosus</i> growth under silver stress. ....	188
Figure 78. Ag <sup>+</sup> and Cu <sup>2+</sup> target B800 BCh and could decrease light capture by LH2. ....	193
Figure 79. Position of the Bch molecules and their ligands in the LH2 complex from <i>Rs. Molischanum</i> . ....	194
Figure 80. Different morphologies obtained through self-organization and driven organization of metal or semi-metal preformed nanoparticles deposited on substrate. ....	197

# INTRODUCTION

---

The objective of this thesis work is to study and try to understand the effect of metals on bacteria, in particular photosynthetic bacteria. The metabolism that interests us is photosynthesis, but the effect of metals is never very specific. Indeed, it is well established that metals can interact and affect the activity or integrity of various molecules in the cell. During my work I had to look at the effect of metals on photosynthesis, but also to assess the effect of metals on respiratory complexes. Therefore, in this introduction section, I have chosen to briefly describe the metabolisms and protein complexes involved in each metabolism in the model bacterium that I have studied. The objective is to have enough structural and functional elements to help us understanding the mechanisms of toxicity and the effects of metals on the bacterium.

## **1. Photosynthetic Purple Bacteria**

---

### **1.1 Classification**

---

Analyses of environmental metagenomes and proteomes from bacteria have revealed that photosynthesis is widely distributed among proteobacteria as demonstrated by the presence and phylogeny of the two subunits (PufL and PufM) of the Reaction center proteins (Imhoff et al., 2018). Among those bacteria, the purple photosynthetic bacteria is a major group of photosynthetic proteobacteria. They are Gram-negative bacteria able of autotrophic growth. They are around fifty genera, and some species are important models to study photosynthesis and related topics (Curtis, 2016; Guerrero, 2000). Purple photosynthetic bacteria are widely distributed in the nature due to their remarkable diverse metabolic pathways. In addition to their ability of photosynthetic growth, they can also grow by aerobic or anaerobic respiration. Based on their tolerance and use of sulfide compounds, the purple bacteria divided

into purple sulfur bacteria, and purple non-sulfur bacteria. They play very important roles in nature, for example: 1- consume toxic substances by their abilities of autotrophic process. 2- consume organic components by photoheterophy. 3- fix CO<sub>2</sub> and nitrogen. Thus, their use in different applications in industrial and agricultural fields are nowadays well developed (Guerrero, 2000; C. N. Hunter et al., 2009).

Based on 16S rRNA sequencing, purple non-sulfur bacteria, belongs to either  $\alpha$  or  $\beta$  proteobacteria (Imhoff, 2006). The  $\alpha$  sub-class species are the best studied up to date; and many strains of this subclass have their genome sequenced as *Rhodobacter (R.) capsulatus*, *Rhodobacter (R.) sphaeroides*, *Rhodopseudomonas (R.) palustris* and *Bradyrhizobium* ORS278 (Lang & Hunter, 1994). In the  $\beta$ -proteobacteria sub-group, *Rubrivivax (R.) gelatinosus* have been the model to focus on to study photosynthesis during the last twenty years. Four models of *R. gelatinosus* are studied, either to understand photosynthesis, hydrogen production or aromatic compounds and hydrocarbon-degradation: *Rubrivivax (R.) benzoatilyticus* JA2T, *Rubrivivax gelatinosus* IL144, *Rubrivivax gelatinosus* CBS and *Rubrivivax gelatinosus* S1 in our laboratory. Purple sulfur bacteria belong to the  $\gamma$ -proteobacteria sub-class, two species belonging to the family of *chromatiaceae* are the most studied, *Chromatium vinosum* and the marine bacterium *Congregibacter (C.) litoralis* strain KT71 (Fuchs et al., 2007).

## 1.2 Physiology and Habitat

---

Purple photosynthetic bacteria are widespread in nature, especially in aquatic environments. They are able to adapt to changing environmental conditions (light and oxygen) by using the required energy producing complexes and have the ability to use several sources of nutrients to feed a variety of metabolisms. Many of these bacteria can use different sources of carbon including CO and CO<sub>2</sub> and can fix nitrogen. For example, in the absence of oxygen and in the presence of light, they perform anoxygenic photosynthesis. In the opposite condition, in the dark, they generate their energy by aerobic respiration using oxygen, or by anaerobic respiration using other

acceptor of electrons such as nitrate, TMAO (trimethylamine N-oxide) or DMSO (dimethyl sulphoxide).

Some purple bacteria can adapt to high temperature, pH, or salinity environment (Lang & Hunter, 1994). Accordingly, these factors control the diversity of purple bacteria that can develop and grow in fresh water in lakes and estuaries, marine systems, and other aquatic environments (Fig. 1). In addition, some purple photosynthetic bacteria were isolated from plants (*Bradyrhizobium* ORS278), soil, or activated sludge (Curtis, 2016; Langridge et al., 2009).

Their growth and metabolic abilities make them a model of choice easy to grow and manipulate under laboratory conditions (Madigan & Jung, 2009).



**Figure 1. Photosynthetic prokaryotes habitat.**

On the left, green and purple bacteria grow in a hot spring run-off channel (Guerrero, 2000). On the right purple phototrophic bacteria growth in a water lake and in a domestic wastewater treatment using a continuous photo-anaerobic membrane bioreactor (Hülsen et al., 2016).

### 1.3 Studied models

---

Purple bacteria, in general, are suitable models to study not only photosynthesis, but also different metabolic and molecular mechanisms. Indeed, they were used to study cell division and chemotaxis (Porter et al., 2011), cytochrome *c* biogenesis (Verissimo & Daldal, 2014), heme synthesis, nitrogen and CO<sub>2</sub> fixation (Dangel & Tabita, 2015), gene regulation, biogenesis of respiratory complexes (Elsen et al., 2004), stress

response, etc. This was possible thanks to i) the ability to grow these bacteria in the laboratory easily under different trophic modes, and ii) the availability of genetic tools necessary to generate mutants with high efficiency of homologous recombination to perform site-specific mutagenesis (Donohue & Kaplan, 1991; Ouchane et al., 1996). Accordingly, many laboratories studied and reported the different aspects of photosynthesis in purple bacteria *R. capsulatus*, *R. sphaeroides*, *R. palustris*, *Bradyrhizobium* and *R. gelatinosus* (Allen et al., 1988; Bauer et al., 1993; Lang & Hunter, 1994).

Different biophysical technics, biochemical and structural studies (UV-Vis absorption, fluorescence, EPR, X-ray crystallography...) were used to study the photosynthetic complexes and mechanisms in these bacteria. In 1988, Deisenhofer, Huber and Michel who have described for first time the method of the membrane complex Reaction-center purification and crystallization using the purple bacterium *Rhodospseudomonas viridis*. They received the Nobel Prize in chemistry by solving the three-dimensional structure of the photosynthetic Reaction-center (RC) (Deisenhofer & Michel, 1989). Since then, most of the membrane photosynthetic complexes have been purified from other photosynthetic bacteria and their structures have been resolved.

Studies using these model purple bacteria, together with studies in green and cyanobacteria, have enabled significant advances in understanding the mechanisms of photosynthesis in eukaryotes including in algae and in plants. Furthermore, those bacterial models were also very useful in disentangling the pathways and steps of pigment (chlorophylls and carotenoids) biosynthesis in all phototrophs (Bryant et al., 2020; Liang et al., 2018).



**Figure 2. Photosynthetic purple bacteria.**

Growth and metabolic abilities make these microorganisms models of choice easy to grow and manipulate ("Phototropic Bacteria – Purple Non Sulfur Bacteria," 2012).

## **2. Photosynthesis in bacteria**

---

The photosynthetic process that requires light for growing, is a very important biological process where it converts solar/ light energy to chemical energy. In eucaryotes and cyanobacteria, it takes place in the thylakoid membranes and requires two photosystems, PSI and PSII (Fig. 3). In other bacteria, it takes place in the inner membrane and involves only one photosystem, PSI in the green bacteria and PSII in the purple bacteria. Cyanobacteria, the only prokaryote to perform the plant-like oxygenic photosynthesis are considered as the oldest phylum of bacteria that shaped the oxygenic atmosphere of our planet, and the progenitor of the plant-chloroplast. Like plants and algae, oxygen-producing cyanobacteria use PSII (Quinone-type RC), a *b<sub>6</sub>f* complex and PSI (4Fe-4S-type RC) in a linear electron flow to generate ATP and NADPH that drive carbon fixation (Azai et al., 2010).

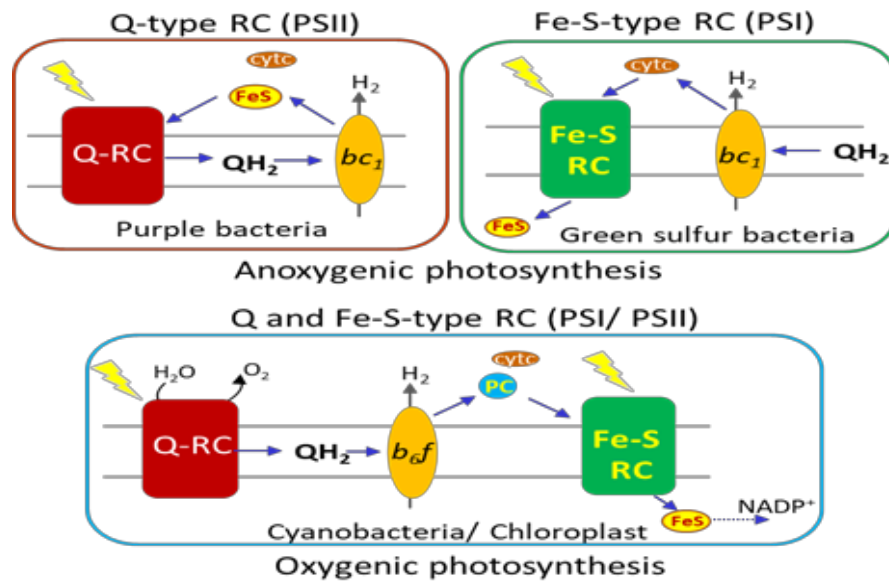


**Figure 3. Photosynthesis in bacteria.**

Photosynthetic electron transfer pathways in anoxygenic and oxygenic phototrophs. Purple bacteria use a Q-RC (PSII) type, while green sulfur bacteria use an Fe-S RC (PSI). Like plant and algae, cyanobacteria use both photosystems and produce oxygen.

In contrast, purple and green sulfur bacteria, perform anoxygenic photosynthesis. They respectively rely on a PSII or PSI photosystem and a *bc<sub>1</sub>* (*b<sub>6f</sub>*) complex for their growth under photosynthetic conditions (Fig. 3). In purple bacteria, the Q-type RC, the *bc<sub>1</sub>* complex and a soluble ferredoxin (HiPiP) or a cytochrome *c*, generate a cyclic electron transport flux and a membrane proton gradient for ATP synthesis. Green sulfur bacteria, use reduced sulfur compounds as electron source for their growth during photosynthesis to generate ATP and fix CO<sub>2</sub>. All these microorganisms use a light-harvesting antenna system, that transfer excitation to the RC. The structure and pigments (chlorophylls/phycobillins and carotenoids) in the antenna complexes vary between photosynthetic organisms. In the model cyanobacterium *Synechocystis*, light is collected by the phycobilisome; in green bacteria, a large chlorosome complex captures light; while purple bacteria contain an LH-type light harvesting system.

In purple bacteria, the LH1 complex is associated with the reaction center (RC) forming the core complex (Frank & Cogdell, 1996). A peripheral light-harvesting complex, LH2, induced under low-light conditions to increase light trapping efficiency is present in some species.

During photosynthesis, electron transfer takes place between these membrane components via liposoluble carriers (quinones) and water-soluble transporters (cytochromes *c* or HiPIP). Electron transfer is coupled to proton translocation from the cytoplasm to the periplasm, necessary for ATP production by the ATP synthase (Fig. 4).

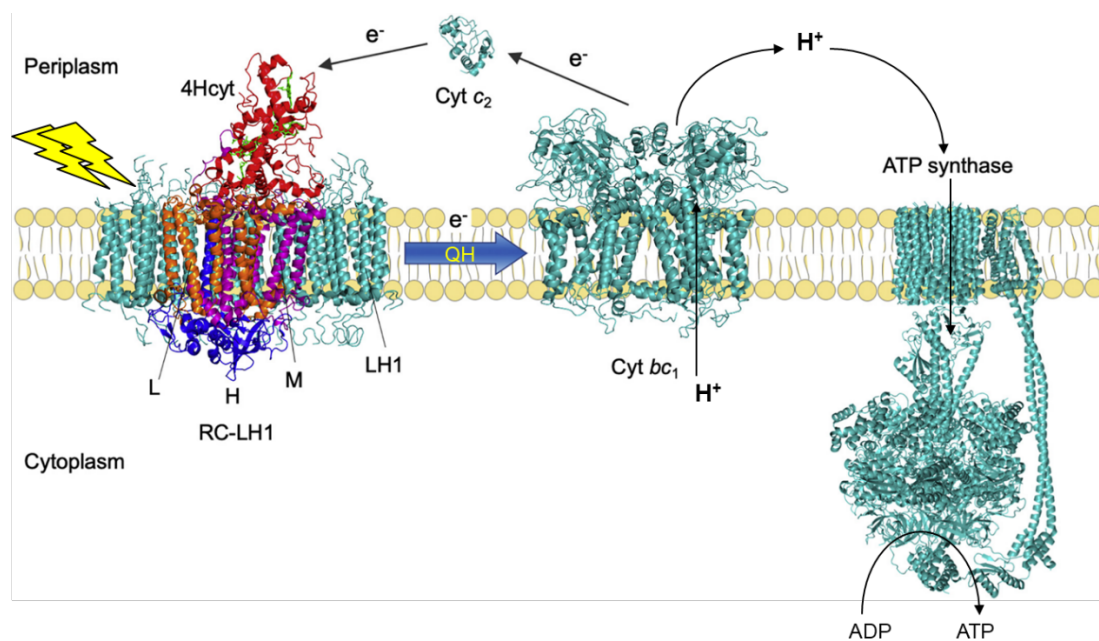


**Figure 4. Electron transfer chain in purple bacteria.**

The chlorophylls in the light harvesting complexes (LH) capture light and transfer it to the reaction center (RC). Cyclic electron transfer between the RC and *bc<sub>1</sub>* cytochrome generate a proton gradient used by the ATPase to produce ATP (Miller et al., 2020).

## 2.1 Photosynthetic membrane complexes

### 2.1.1 LH1 and LH2 Antennae

Light harvesting (LH) antennae are protein complexes that associated with pigments to absorb light energy. In general, in proteobacteria, there are two types of antennae, LH1 antennae and LH2 antenna. The LH1 associates with the reaction center, forming the core complex. Around them are organized the accessory antennae LH2 (Fig 5). The amount of LH2 is light-regulated, with increased LH2 under low light conditions (Saer & Blankenship, 2017; J. Zeilstra-Ryalls et al., 1998).

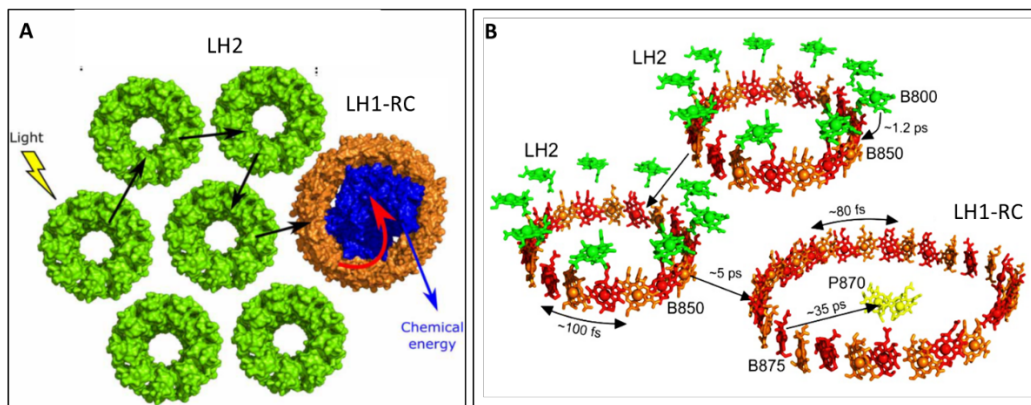


**Figure 5. Photosystem arrangement and energy transfer**

LH2 (green) absorb light energy and transfer the excitation to the core LH1 antenna (brownish orange). In the core antenna, energy is trapped by a final transfer step to the RC (blue), at which point the light energy is converted into chemical energy (QH<sub>2</sub>) (Saer & Blankenship, 2017). A- Protein complexes. B- Bacteriochlorophylls within the complexes. B800 BChls of LH2 are shown in green, B850 BChls of LH2 and B875 BChls of LH1 are shown in red and orange, and BChls P870 of the RC are shown in yellow (Sundström et al., 1999).

According to the crystal structure of LH2 from *Rhodospseudomonas (Rps). acidophila* and other species (Cogdell et al., 1999; McDermott et al., 1995), these antennae are heterodimers, and consist of two  $\alpha$  and  $\beta$  polypeptides associated with bacteriochlorophyll (BChls) and carotenoids pigments, non-covalently.  $\beta$  polypeptides are located on the outside of the cylindrical structure while the  $\alpha$  polypeptides buried inside. The heterodimers of the LH1 and LH2 antennae are associated with a different number of BChls and carotenoids molecules. The LH1 antennae binds two molecules of BChls and one or two molecules of carotenoids. On the other hand, the heterodimers of the LH2 antenna binds three molecules of BChls and one carotenoid molecule

(Cogdell et al., 1999; McDermott et al., 1995). These  $\alpha$  and  $\beta$  polypeptides form two concentric protein cylinders in the membrane, between which are sandwiched the light harvesting BChls and carotenoids (Fig. 6). The BChls of LH2 form two rings that are arranged approximately in the plane of the membrane. The first of these comprises 18 BChls, one for each  $\alpha$  and  $\beta$  polypeptide, oriented with the macrocycle of each BChls approximately perpendicular to the plane of the membrane (Fig 7). These "B850" BChls have a prominent UV-Vis absorbance band at 850 nm. The second ring comprises nine "B800" BChls, which are arranged with the macrocycle of each BChls parallel to the plane of the membrane and gives rise to a prominent absorbance band at 800 nm.

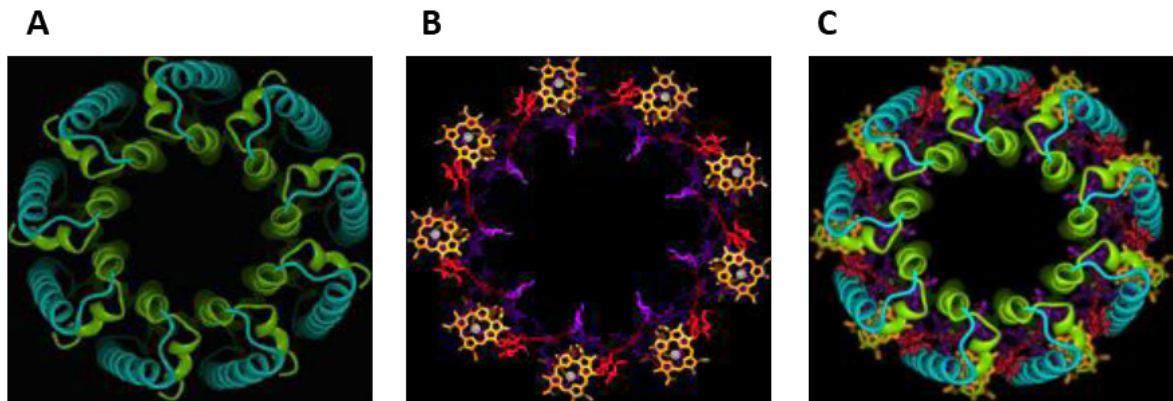


**Figure 6. Cytoplasmic view of the LH2 antennae of *Rps. acidophila*.**

A-Representation of  $\alpha$  and  $\beta$  polypeptides (Cytoplasmic view) B - Representation of the pigments (bacterio-chlorophylls carotenoids- (Cytoplasmic view)). C- Representation of the protein-pigment complex (periplasmic view). The  $\beta$ -polypeptides are represented in blue, the  $\alpha$ -apoproteins in green, the carotenoids in red, the 850-nm absorbing bacteriochlorophylls in violet and the bacteriochlorophylls absorbing at 800 nm in orange. Image from the photo gallery of Professor Richard Cogdell's laboratory.

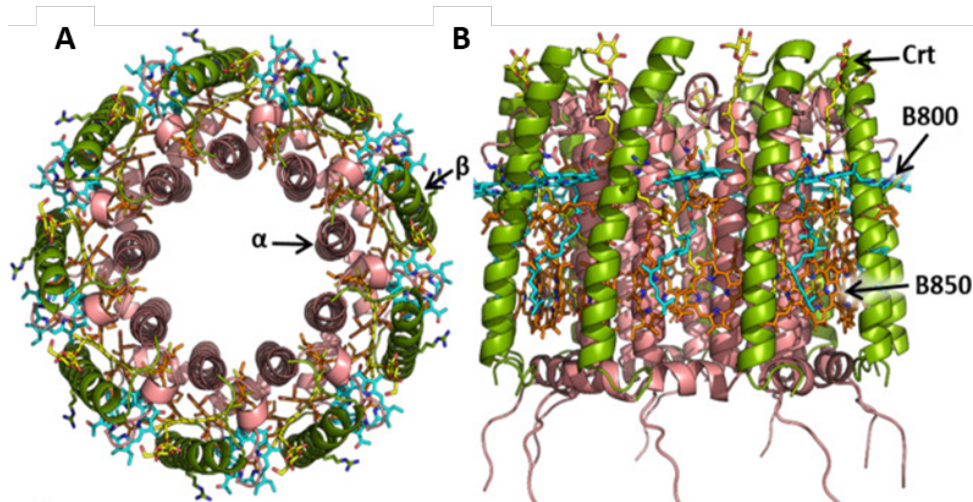


**Figure 7. The LH2 pigment-protein from *Rps. acidophila*.**

Views are parallel (A) and perpendicular (B) to the plane of the membrane. The protein scaffold comprises concentric cylinders of nine  $\alpha$  (inner), and nine  $\beta$  (outer) polypeptides (green and purple ribbons). The 18 B850 BChls (absorb at 850 nm) are shown in orange, and the 9 B800 BChls (absorb at 800 nm) are shown in cyan. The macrocycles of the B850 and B800 BChls are arranged perpendicular and parallel, respectively, to the plane of the membrane. Protein Data Bank (PDB) file 1NKZ (Papiz et al., 2003; Swainsbury et al., 2019).

### 2.1.2 The Reaction Center

The first three-dimensional structure of the Reaction Center complex was revealed in 1984. In general, the complex RC in the photosynthetic bacterium *Rhodospseudomonas viridis* is composed of multi-proteins PufL (light), PufM (medium) and PufH (heavy) polypeptides (Deisenhofer & Michel, 1989; S. Wang et al., 1994). PufL and PufM subunits have five transmembrane helices with associated four BChl $a$  cofactors. They are two Bchl $a$  called the special pair, two bacteriopheophytin, a carotenoid, a non-heme iron atom and two quinone electron acceptors ( $Q_A$  and  $Q_B$ ). The PufH subunit has a globular-shape, and it attached by a transmembrane helix from the cytoplasmic side. It plays an important role of the stability of the complex, and proton transfer to the quinone (Fig. 8).

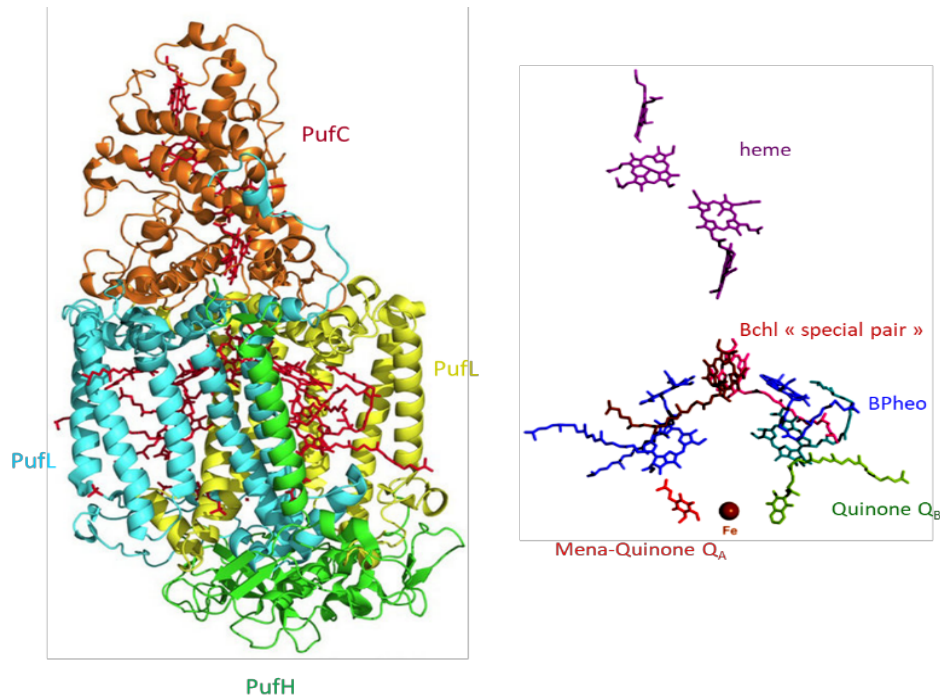


**Figure 8. Crystallographic structure of the reaction center of *Rhodospseudomonas (R.) viridis*.**

The blue is L subunit, yellow is the M subunit, the H subunit is in green and the cytochrome *c* subunit in orange. The cofactors are depicted on the right (Deisenhofer & Michel, 1989).

There is a fourth subunit of RC marked on the periplasmic side in *R. viridis* as well as in some species such as *R. gelatinosus* and *R. tenuis*. It is a tetra-heme cytochrome *c* (cyt<sub>c</sub>) involved in reducing the photooxidized special pair of BChl<sub>a</sub> (Agalidis et al., 1999).

During the electron transfer reactions, the primary electron transfer leads to charge separation on both sides of the membrane. The special pair of BChls carry a positive charge on one side of the membrane, and the Quinone carry a negative charge. Electron transfer leads to a fully reduced form of quinone Q<sub>B</sub>H<sub>2</sub>. The reduced Q<sub>B</sub> is released in the lipid phase of the membrane, which then reduces the *bc*<sub>7</sub> complex. The photo oxidized BChls dimer is then reduced by the cytochrome *c* through the *bc*<sub>7</sub> complex. This electron transfer leads to a proton gradient across the membrane that is used by the ATPase to produce ATP in the cytoplasm.

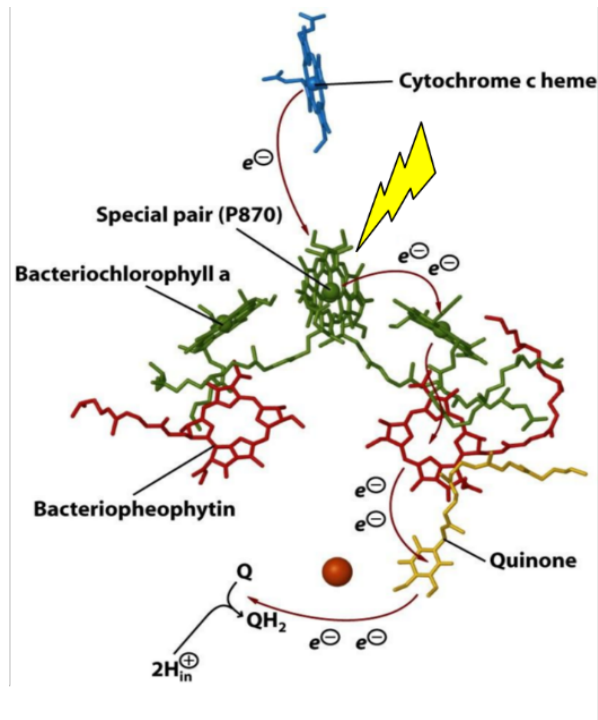


**Figure 9. Electron pathway between the cofactors in the reaction center.**  
(Deisenhofer & Michel, 1989).

### 2.1.3 Photosynthetic pigments

Plants, algae, cyanobacteria and photosynthetic bacteria, carry out a chlorophyll-based photosynthesis. All these phototrophs produce two pigments: 1- chlorophylls (bacteriochlorophylls for bacteria) required for both light harvesting and in photochemistry; and 2- carotenoids, which function primarily for the assembly of light harvesting antennae and photoprotection, but can also harvest light.

#### 2.1.3.1 Bacteriochlorophylls

The purple photosynthetic bacteria can generate the energy from light thanks to the Bchls presents in their photosynthetic complexes (Fig. 10). The purple bacteria contain bacteriochlorophylls that are essential for the assembly and the activity of the photosynthetic membrane. Bacteriochlorophylls are porphyrins (tetrapyrrolles) made from simple precursors (Glycine and Succinyl CoA) and the primary steps of

biosynthesis of these pigments are shared with heme and vitamin B<sub>12</sub> biosynthetic pathways.

In the pathway of biosynthesis of heme and bacteriochlorophylls, the consecutive action of the products of *the hemA, hemB, hemC* and *hemD* genes from L-Glutamate leads to the formation of the first tetrapyrrole, Uroporphyrinogen III (Dailey et al., 2017). Then, a reducing path follows this step which leads to the formation of vitamin B<sub>12</sub>, siroheme and heme *d*, or an oxidative path which catalyzed by the product of the *hemE* gene and leads to the formation of coproporphyrinogen III. The latter undergoes an oxidative decarboxylation step to protoporphyrinogen IX which can be catalyzed according to the oxygenation conditions by two structurally different enzymes. Under aerobiosis, this oxidation is catalyzed by the aerobic coproporphyrinogen III oxidase, HemF, which uses oxygen as an electron acceptor. Under microaerobic and anaerobic, the anaerobic coproporphyrinogen III oxidase enzyme HemN, containing a [4Fe-4S] cluster, provides oxidative decarboxylation of coproporphyrinogen III (Troup et al., 1995).

Protoporphyrinogen IX is oxidized by protoporphyrinogen IX oxidase (coded by *hemG, hemK* or *hemY*) to protoporphyrin IX, the precursor common to the biosynthesis of hemes and BChls.

From Protoporphyrin IX, an iron atom is introduced by the enzyme HemH (Ferrochelatase) at the center of the tetrapyrrole molecule, leading to the formation of protoheme IX (*heme b*) (Fig. 10) (Dailey et al., 2017). The latter is the precursor of heme *c*, heme *o* and heme *a*. The coordination of these different types of heme within apoproteins give rise to cytochromes, the main hemoproteins involved in the transport of electrons in the photosynthetic and respiratory chain.

Purple bacteria produce different types of BChls (*a, b, c, d*, and *e*). Nevertheless, most of them are BChls *a* type containing microorganisms. Protoporphyrin IX, is converted to Mg-Protoporphyrin IX (MgP) by the Mg-chelatase (BchHDI complex) that insert a magnesium atom in the tetrapyrrole ring (Fig 10) (Chew

& Bryant, 2007). A fifth cycle is then formed, and the reaction is catalyzed by an oxidative cyclase, BchE which is encoded by the *bchE* gene, to give Mg-divinyl-protochlorophyllide (PChlide *a*). However, a second enzyme, AcsF, has been identified in *R. gelatinosus* and catalyzes the same reaction as BchE although the two enzymes are structurally different. In fact, it has been shown that BchE catalyzes oxidative cyclization in the absence of oxygen, whereas AcsF catalyzes this reaction in the presence of O<sub>2</sub> (Ouchane et al., 2004; Pinta et al., 2002). PChlide *a* is the precursor compound of chlorophyllide *a*, itself precursor of BChl *a* and chlorophyll *a* in plants. The following steps of biosynthesis of the latter are shown schematically in (Fig. 10) with the different enzymes involved for each step.

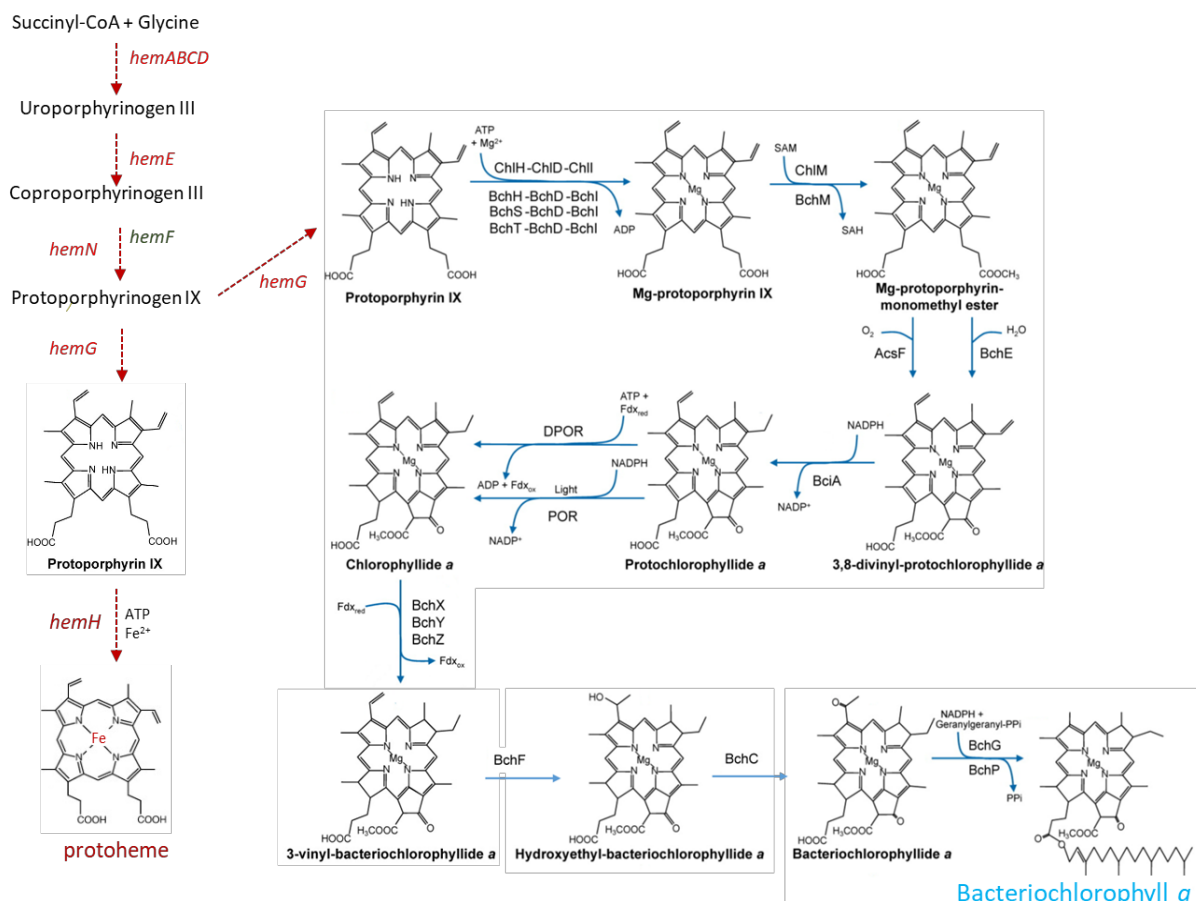


**Figure 10. The tetrapyrrole biosynthesis pathway in purple bacteria.**

This pathway is common to the biosynthetic pathway of vitamin B<sub>12</sub>, bacteriochlorophyll and heme. The genes coding for the enzymes that catalyze the different pathways are indicated. Modified from (Chew & Bryant, 2007).

The structure of some complexes involved in the tetrapyrroles, including heme and chlorophyll, biosynthesis pathways are available. It is the case of the bacterial anaerobic coproporphyrinogen III oxidase enzyme HemN from *E. coli* (Layer et al., 2003); the bacterial and eucaryotic protoporphyrinogen IX oxidase (HemG) (Koch et al., 2004) and ferrochelatase (HemH) from the common pathway (Hansson et al., 2011).

In the chlorophyll synthesis pathway the structure of the magnesium chelatase (BchHDI) (Chen et al., 2015), and the protochlorophyllide oxidoreductase (BchLNB) from photosynthetic bacteria and plants have been also solved (Muraki et al., 2010).

It should be noted, that both HemN and BchLNB structures showed the presence of 4Fe-4S clusters that are required for the activity of these enzymes. Exposed 4Fe-4S clusters have been described as targets of oxygen, reactive oxygen species and metal ions in many organisms and could be therefore targets in our model organism (Fig. 11).

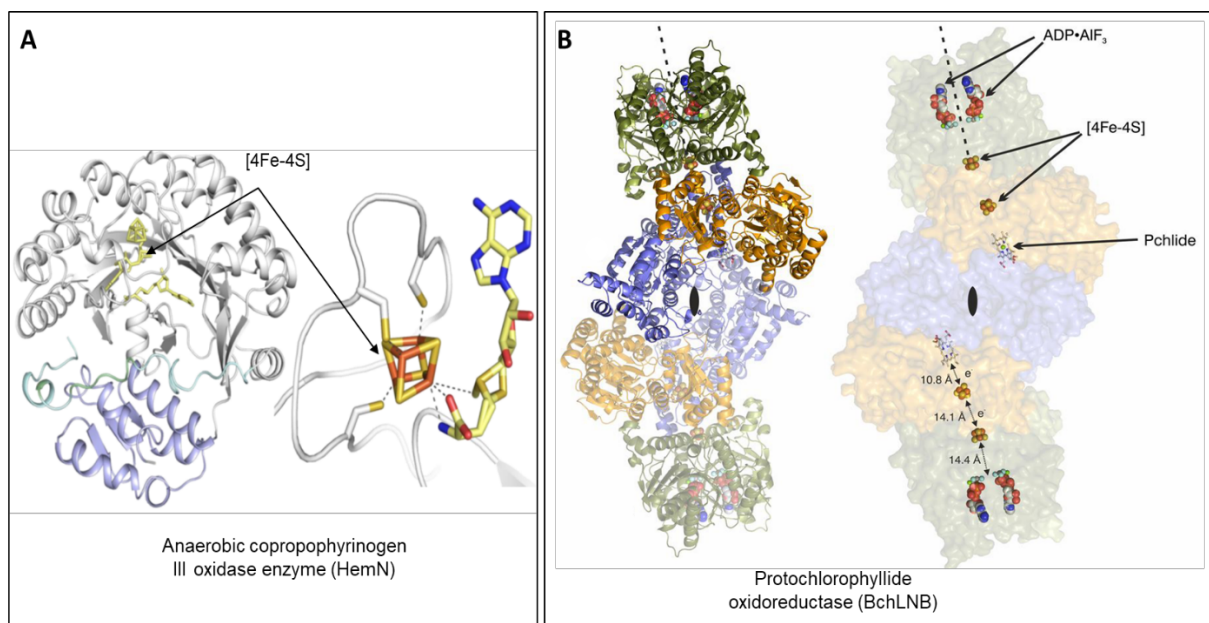


**Figure 11. Structure of the 4Fe-4S cluster containing enzymes from the tetrapyrrole biosynthesis pathway in bacteria.**

A- HemN (Layer et al., 2003). B- BchLNB (Moser et al., 2013).

The genes involved in the BChls biosynthesis pathway are very often organized into operons and grouped together in the photosynthetic gene cluster (40 to 50 kb) in purple bacteria (Fig. 12). Their expression is regulated by light and oxygen tension and involves two component systems (RegBA/PrrBA) and sensors of light or oxygen (AppA/PpsR/Aer/Fnr) (Pandey et al., 2011, 2017). Expression of photosynthetic genes is repressed under high oxygen tension; the bacterium will therefore favor aerobic respiration. Under micro-aerobic or anaerobic condition, the expression of photosynthetic genes is up regulated resulting in dark pigmented cells full of photopigments and photosynthetic complexes.

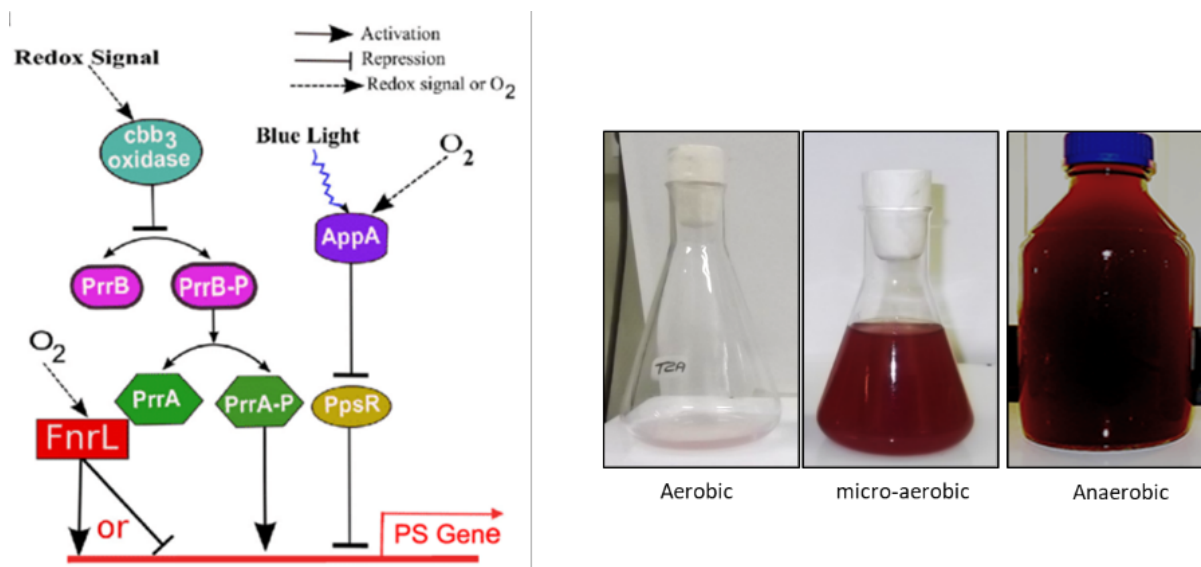


**Figure 12. Regulatory pathways of photosynthesis in purple bacteria.**

Proteins that govern photosynthetic gene expression in response to light and oxygen in photosynthetic bacteria (left) (Pandey et al., 2017). Growth of *R. gelatinosus* under different oxygen tension, showing the induction of photopigments with decreasing oxygen tension.

### 2.1.3.2 Carotenoids

Carotenoids are the second category of pigments present in the photosynthetic apparatus. They are synthesized by photosynthetic and non-photosynthetic organisms. These pigments have range of colors yellow, orange and

red. In phototrophs, carotenoids protect the reaction center from the damage caused by the photo oxidation resulting from the formation of oxygen singlets and the free radicals generated by the different cellular metabolisms in the presence of oxygen (Olson, 1993; Ouchane, 1997). They also play a structural role in the antennae assembly and stability (Cogdell & Gardiner, 1993; Gall et al., 2003). The carotenoids are also photo-collector pigments, they absorb light at wavelengths between 400 and 530 nm, and then they transfer the energy to the bacteriochlorophyll molecules.

Carotenoids are C<sub>40</sub>-compounds consisting of eight isopentenyl pyrophosphate units. Extensive studies in purple and cyanobacteria allowed the identification of all the genes involved in the biosynthesis pathways (Takaichi, 2013). Furthermore, analyses of carotenoid intermediates that accumulate in bacterial carotenoid mutants allowed the identification and the characterization of all the precursors and steps in the biosynthetic pathways. As for bacteriochlorophyll biosynthesis, most of the genes involved in carotenoid biosynthesis are in operons clustered within the photosynthetic gene cluster.

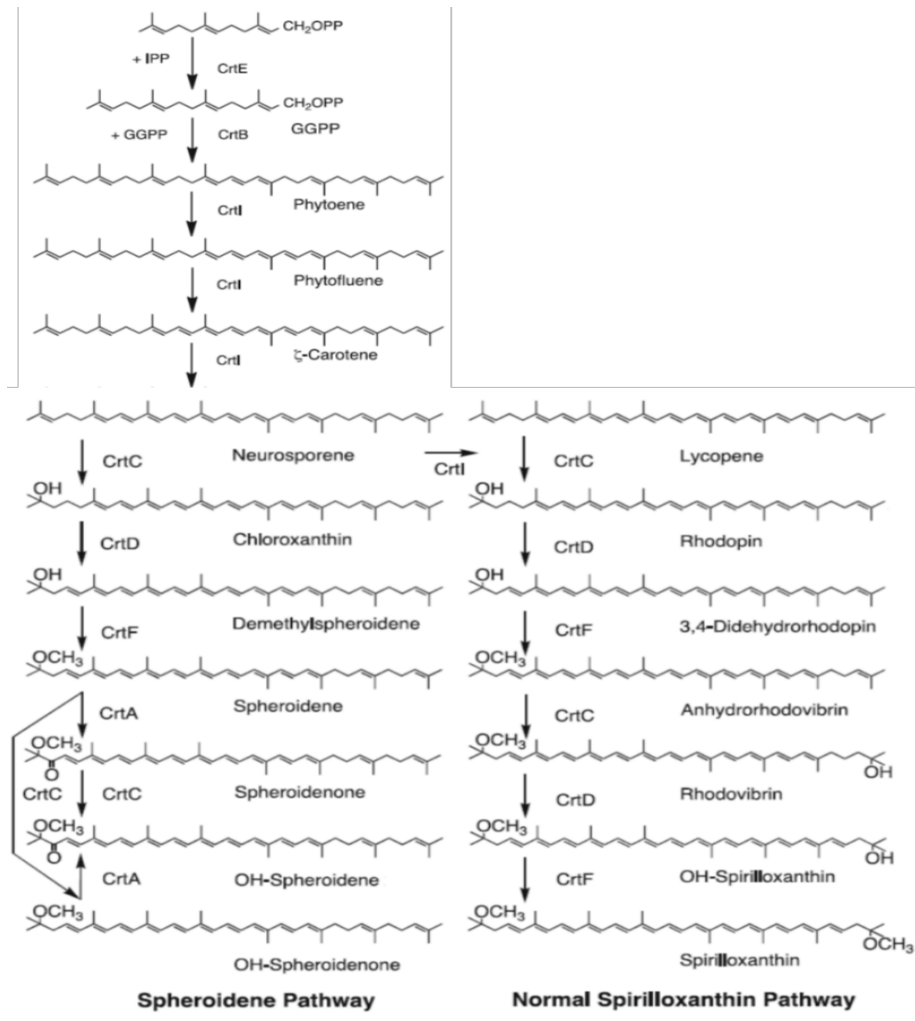


**Figure 13. Carotenoid biosynthesis pathways in purple bacteria.**

*Rhodobacter* produce only spheroidene. *R. gelatinosus* produces both spheroidene and spirilloxanthin (Takaichi, 2013).

#### 2.1.4 Organization of photosynthetic genes: the PS cluster

In purple bacteria, most genes involved in photosynthesis are very often found clustered and organized in operons in bacterial genomes (Choudhary & Kaplan, 2000; Igarashi et al., 2001). The photosynthetic gene cluster (about 40 kb) includes *puf* genes which encodes the L, M and C subunit of the reaction center, the *puhA* that encodes for the structural subunits of reaction center, the *pufB* and *pufA* genes encoding for LH1 antenna proteins. Also, most if not all the genes involved in the biosynthesis of

pigments (*bch* and *crt* genes) as well as genes required for the control of expression and synthesis of the different components of the photosystem, are localized in the same cluster.

It was shown in *R. capsulatus*, *R. sphaeroides* and *R. gelatinosus*, that operons are also grouped together with other operons to form super-operons (*crtEF-bchCXYZ-pufBALMC-crtADC*) (Choudhary & Kaplan, 2000; Elsen et al., 2005; Liotenberg et al., 2008; Youvan et al., 1984). This operon organization in operon and super-operons allow the coordination of gene expression and the rapid setup of the photosynthetic apparatus in response to light and drop in oxygen tension (Liotenberg et al., 2008).

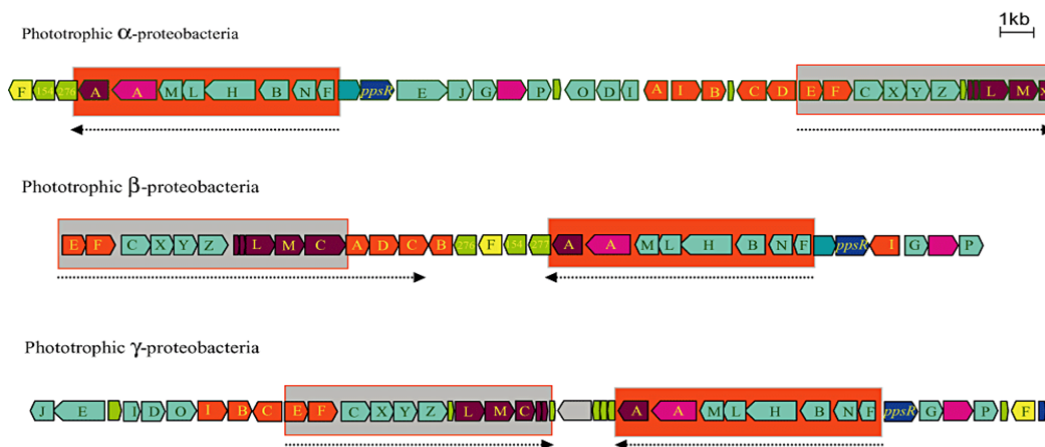


**Figure 14. Photosynthetic gene organization within the PS cluster in purple bacteria.**

*puf* genes are in dark red, *bch* genes in green and *crt* genes in orange. The superoperons are shown in the boxes and by the arrows (Liotenberg et al., 2008). The *crt-bch-puf* super-operon (gray frame) and *bch-puf* (orange frame).

### 3. Respiration in purple bacteria

In the absence of light, purple bacteria produce ATP through respiration. According to the final acceptor of electrons, there are two types of respiration: 1- Aerobic respiration, the final acceptor of the electrons of the respiratory chain is oxygen. 2- Anaerobic respiration, and the final electron acceptor is a compound

molecule such as nitrate, trimethylamine *N*-oxide (TMAO) and dimethyl sulfoxide (DMSO) (Richardson, 2000). I will focus only on aerobic respiration in this section.

As in mitochondria, the bacterial aerobic respiratory chain involves four to five membrane protein complexes where electrons transfer from a primary donor (NADH/ Succinate) to the terminal acceptor, oxygen. The electrons are transferred through the membrane complexes and pass from one complex to the other in the respiratory chain, via liposoluble or water-soluble carriers. In proteobacteria, there are two types of high potential electron carriers: membrane quinones that transfer electrons and protons from complex I (NADH dehydrogenase) and / or complex II (succinate dehydrogenase) to the cytochrome *bc*<sub>1</sub> complex (complex III) (R. K. Poole & Cook, 2000).

The periplasmic cytochrome *c* or the HiPIP (high potential ferredoxin) are involved in the transport of electrons to terminal oxidase (complex IV) to reduce oxygen into water molecules. (Fig. 15) (Rigoulet et al., 2007). Electron flow through the chain generates a proton gradient across the membrane that is used by the ATP synthase to generate ATP.

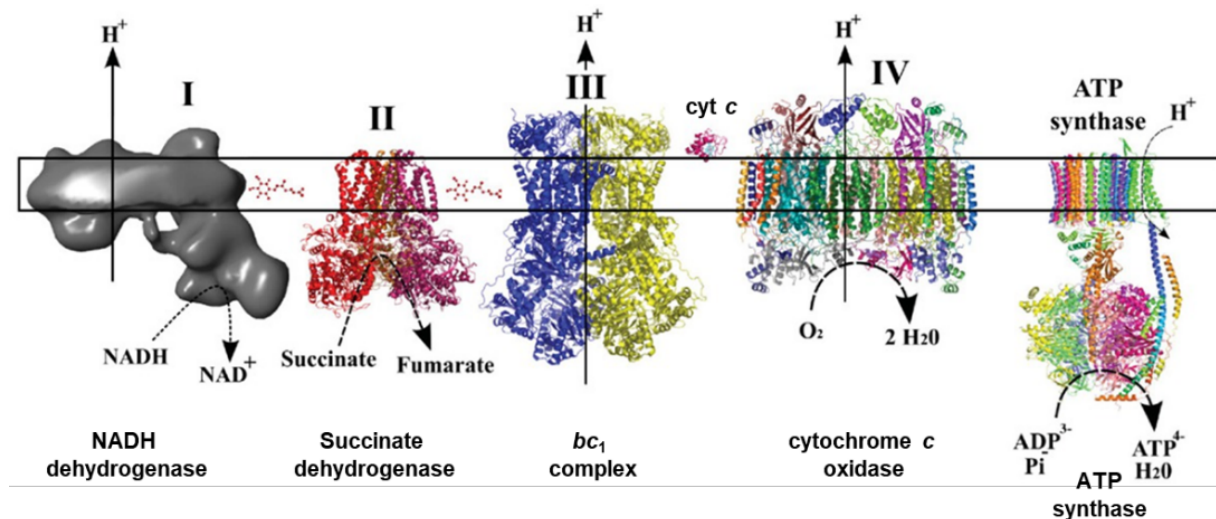


**Figure 15. Complexes of the Respiratory chain of bacteria.**

The transport of electrons between these complexes involves quinones (Q) and the cytochrome *c* (cyt<sub>c</sub>). The protons translocated by some complexes are used for the production of energy by the ATPase (Rigoulet et al., 2007).

### 3.1 Complex I: NADH

Complex I or NADH dehydrogenase is the first complex of the aerobic respiratory chain. It oxidizes NADH and reduces quinone pool in the membrane. It is the largest complex of the bacterial electron transfer chain and contains up to 16 (Nuo) different subunits. It contains a molecule of flavin mononucleotide (FMN) and a 9 iron-sulfur (Fe-S) clusters that participate in electron transfer. The NADH dehydrogenase complex (Fig. 16) catalyzes the transfer of two electrons from NADH to quinone coupled to the translocation of protons across the bacterial membrane participating therefore to generate the proton gradient for ATP synthesis (Baradaran et al., 2013).

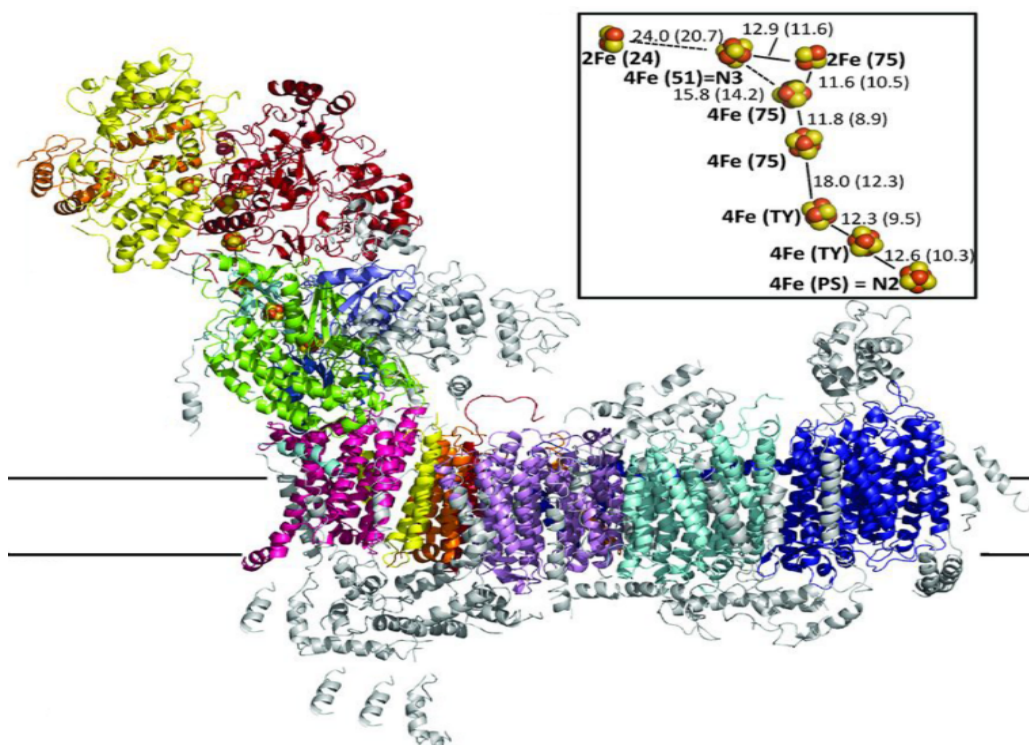


**Figure 16. Crystal structure of the entire respiratory complex I (NADH dehydrogenase) from *Thermus thermophilus* bacterium.**

(Zickermann et al., 2015).

### 3.2 Complex II: succinate dehydrogenase (SDH)

Succinate dehydrogenase (SDH or complex II) catalyzes the oxidation of succinate to fumarate. As for NADH dehydrogenase, the oxidation of succinate is coupled to the reduction of quinone pool in the respiratory chain. Nevertheless and unlike NADH dehydrogenase, this complex does not participate in translocation of protons; thus, its activity generates less ATP than NADH oxidation (Mills et al., 2016).

This complex has two domains. A membrane domain and soluble catalytic domain which is exposed to the cytoplasm in bacteria (Fig. 17). The (soluble) peripheral domain is composed of two subunits involved in the oxidation of succinate; SdhA, a flavoprotein, containing covalently attached flavin adenine dinucleotide (FAD) and SdhB containing three iron-sulfur clusters (Yankovskaya et al., 2003).

In *E. coli*, the membrane domain, where the reduction of the quinones takes place, contain two hydrophobic peptides (SdhC and / or SdhD) with heme *b* involved in the electron transfer.

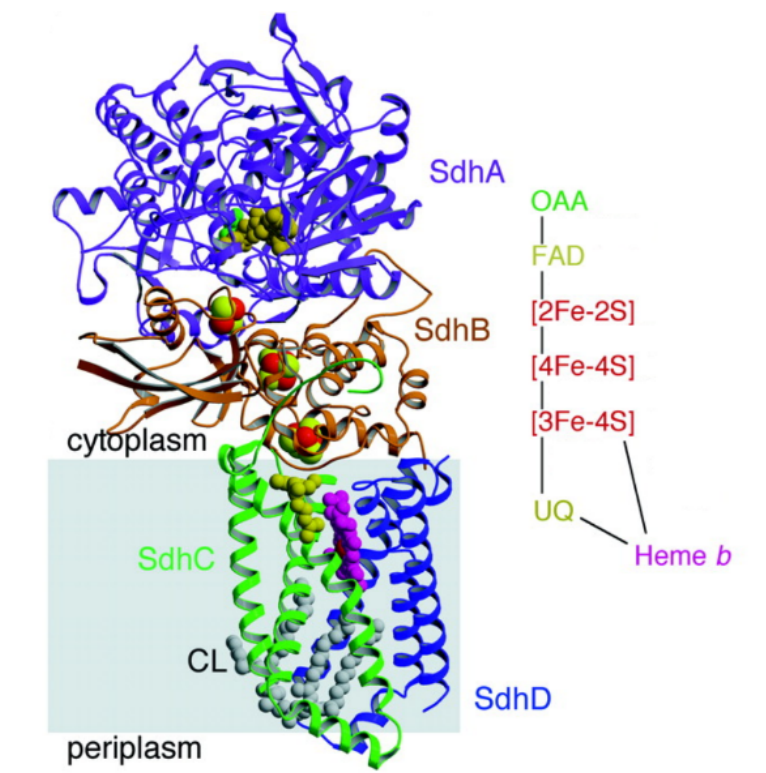


**Figure 17. Crystal structure of *Escherichia coli* complex II (succinate dehydrogenase).**

(Yankovskaya et al., 2003).

### 3.3 Complex III: *bc<sub>1</sub>*

---

The Ubihydroquinone cytochrome *c* oxidoreductase or cytochrome *bc<sub>1</sub>* (complex III) is a central complex involved in both respiration and photosynthesis in purple bacteria. It oxidizes quinols and reduces electron carriers, usually cytochromes *c* or ferredoxins. In parallel, it allows the translocation of protons across the membrane thus creating a gradient of proton and contributing to the ATP synthesis. The bacterial *bc<sub>1</sub>* complex consists of three major subunits (PetABC or QrcABC) with redox moieties (Fig. 18A): the Rieske protein, the cytochrome *b*, and the cytochrome *c<sub>1</sub>* (Gray & Daldal, 1995; Thöny-Meyer, 1997; Trumpower, 1990). Cytochrome *b* is a hydrophobic protein consisting of several transmembrane helices. It contains two type *b* heme, the high potential (*b<sub>H</sub>*) heme and the low potential (*b<sub>L</sub>*) heme. The Rieske protein contains a transmembrane domain attached to the membrane by its N-terminal extension. It contains a [2Fe-2S] cluster linked by two histidines and two cysteines. One of the interesting features of this protein is that its cluster is in a soluble and flexible periplasmic domain. Structural and spectroscopic data have made it possible to propose a model in which the passage of electrons in the *bc<sub>1</sub>* complex is controlled by the movement of the soluble domain (Darrouzet et al., 2000; Darrouzet & Daldal, 2003). The Cytochrome *c<sub>1</sub>* is inserted into the membrane by its hydrophobic C-terminal domain. It contains a *c*-type heme covalently attached by two cysteines, a histidine and a methionine as axial ligands. Structure of the *b<sub>6f</sub>* (*bc<sub>1</sub>*) complex from the alga *Chlamydomonas reinhardtii* was resolved and showed the presence of an additional heme (*c<sub>2</sub>*), a chlorophyll and carotenoid molecule within in the complex (Stroebel et al., 2003). More recently a structure of the *bc<sub>1</sub>* complex in super-complex with complex IV (cyt *c aa<sub>3</sub>*) from *Mycobacterium smegmatis* was reported (Fig. 18B) (Wiseman et al., 2018).



genome of this bacterium, *cbb<sub>3</sub>*, *bd*, *bo* and *caa<sub>3</sub>* type with a fused cytochrome *c*. The role of these terminal oxidases in respiration this bacterium has been studied. The results showed that only the *cbb<sub>3</sub>* and *bd* oxidases are functional in the wild strain (Hassani et al., 2010b). The activity of the *cbb<sub>3</sub>* and *bd* oxidases depends on the concentration of O<sub>2</sub>, the *cbb<sub>3</sub>* oxidase is involved in the micro-aerobic respiration (low oxygenation) whereas the quinol oxidase *bd* is important for the aerobic respiration (strong oxygenation).

The most common cytochrome *c* oxidase in bacteria is the *aa<sub>3</sub>* type very close to the mitochondrial cytochrome *c* oxidase. It is expressed under high oxygen tension and allow growth of most bacteria under aerobic condition. The enzyme contains four (Cox) subunits. It contains two copper centers and two heme *a* and *a<sub>3</sub>* molecules that participate in electron transfer and oxygen reduction (Fig. 19) (Nyquist et al., 2003). The second cytochrome *c* in bacteria correspond to the *cbb<sub>3</sub>* cytochrome *c* oxidase. This enzyme is specific to bacteria and in most species required for respiration under low oxygen tension. Indeed, except in few species, the enzyme is induced under micro-aerobiosis by the FNR regulator, and is required for growth when oxygen tension drops. The complex is composed of three to four subunits (Cco). The catalytic subunit CcoN contains two *b*-type heme, one of which forms with Cu the binuclear center where oxygen is reduced. The two other subunits are transmembrane proteins containing, in their soluble periplasmic domains, *c*-type hemes (Fig. 19) (Buschmann et al., 2010). These subunits allow the transfer of electrons from soluble cytochrome *c* to the catalytic site in CcoN subunit.

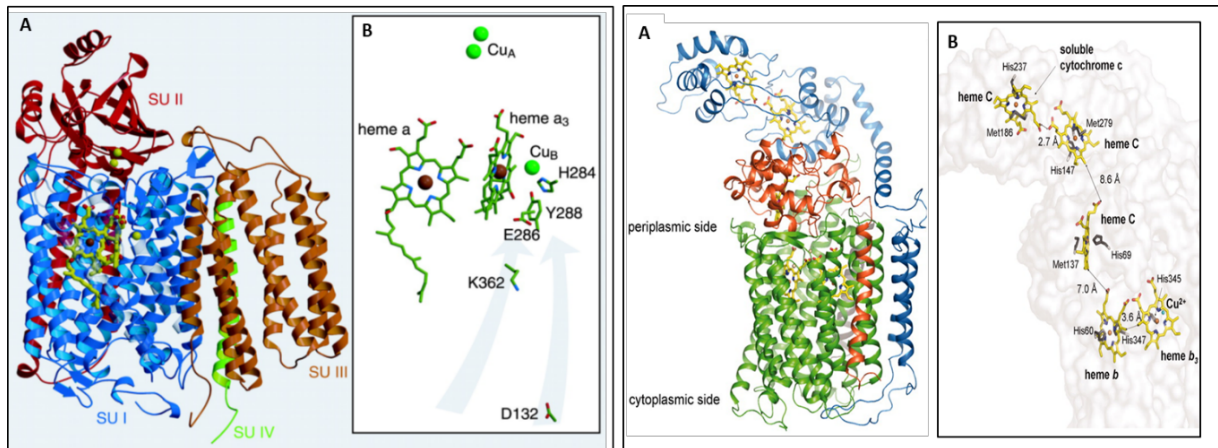


**Figure 19. Structure of bacterial *aa<sub>3</sub>* (left) and *cbb<sub>3</sub>* oxidase (right).**  
(Buschmann et al., 2010; Svensson-Ek et al., 2002).

## 4. Regulation of photosynthetic genes

Bacteria have the ability to adapt to different growth conditions. Thanks to their expansive metabolic versatility, they can adapt to different sources of nutrients and energy, optimize their growth, and thrive even under harsh and stress conditions. To this end, they need to control the gene expression to produce the required proteins in normal and/ or under stress conditions. Purple bacteria have the ability to detect variations in the light and oxygen conditions in their environment and optimize their energy production machinery. They sense the changes of oxygen availability and light intensity/quality, and assemble the complexes necessary for their growth either in photosynthesis or in respiration.

In the presence of light and anaerobiosis, these bacteria will synthesize the photosynthetic complexes that will ensure their growth *via* photosynthesis (Fig. 12). While in aerobic condition, the presence of oxygen promotes respiratory metabolism and the synthesis of the respiratory chain complexes. In anaerobic condition, dark and presence of nitrogen oxide (Nitrate / Nitrite) or DMSO, the cells produce the respiratory reductases of denitrification or DMSO reductase. To set up these metabolisms, bacteria

require specific regulation in order to ensure the synthesis of the complexes needed for each mode of growth.

The regulatory processes involve several sensors and transcriptional regulatory pathways that detect external inputs such as the change in O<sub>2</sub> or the intensity or quality of light. The regulatory pathways were mainly studied in *Rhodobacter sphaeroides* and *R. capsulatus*, nonetheless some of the regulatory proteins were identified in other purple bacteria including in *R. gelatinosus*. The three major oxygen regulatory systems that have been characterized in these bacteria are the FnrL, the PpsR / AppA and the two components system RegA/RegB systems. So far, the laboratory has identified in *R. gelatinosus* two factors sensitive to the concentration of O<sub>2</sub> in the medium: FnrL and PpsR (Ouchane et al., 2007; Steunou et al., 2004).

#### **4.1 The global anaerobic regulator FnrL**

---

FnrL (Fumarate and nitrate regulator), the global anaerobic transcription factor exists in the majority of proteobacteria. FnrL responds to oxygen concentration and controls the expression of hundred genes involved in the micro-aerobic or anaerobic growth in bacteria. The FnrL protein has four N-terminal cysteines that coordinate an oxygen-labile [4Fe-4S] center, a central dimerization domain and a helix-turn-helix domain for DNA-binding. This factor is able to detect the oxygen present in the medium thanks to its labile cluster (Mettert & Kiley, 2018). In absence of oxygen, FnrL forms a [4Fe-4S] cluster and binds to its target DNA (TTGA-N<sub>6</sub>-TCAA) sequence to induce the expression of the regulated genes. While in presence of oxygen, the [4Fe-4S] cluster will transform into [2Fe-2S], preventing the dimerization of the protein, thus rendering it inactive (Fig. 20). Through this reduction process of the cluster [4Fe-4S] and dimerization of the protein, FnrL indirectly detects the oxygen of the medium and trigger the required response (Moore & Kiley, 2001; J. H. Zeilstra-Ryalls & Kaplan, 2004).

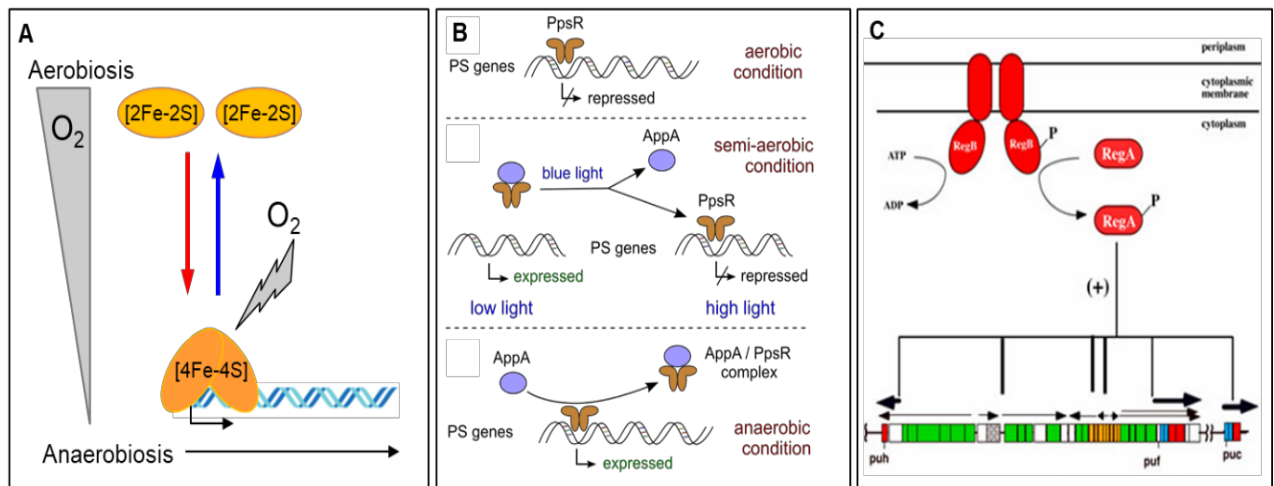


**Figure 20. Schematic representation of gene regulation in purple bacteria.**

A- In anaerobiosis, the formation of a cluster [4Fe-4S] allows the dimerization of FnrL which induces the expression of target genes. In aerobic, the [4Fe-4S] cluster is transformed into [2Fe-2S] preventing dimerization of the protein, making it inactive (Moore and Kiley 2001). B- Interaction of PpsR and AppA to modulate photosynthetic genes in response to oxygen and light. C- Regulation of PS genes by the two components system RegA/RegB.

In *R. sphaeroides*, *R. capsulatus* and *R. gelatinosus*, FnrL has an important role in the production of photosynthetic complexes. In fact, the FnrL factor is an activator of genes that are involved in porphyrin biosynthesis (Ouchane et al., 2007; J. Zeilstra-Ryalls et al., 1998; J. H. Zeilstra-Ryalls & Kaplan, 1995). It is required for the expression of several genes including *bchE* and *hemN*. FnrL is also involved in the expression of the *cbb<sub>3</sub>* cytochrome *c* oxidase required to reduce oxygen in the medium prior to start photosynthesis (Hassani et al., 2010b). By these means, FnrL is also important for photosynthesis in purple bacteria.

## 4.2. The transcriptional regulator PpsR

The PpsR factor regulates the photosynthetic genes in the presence of oxygen. It is mainly a repressor of gene expression, in the presence of  $O_2$ , that binds to a TGT-N<sub>12</sub>-ACA sequence in the promoter region. The PpsR protein has a C-terminal helix-turn-helix domain for DNA binding and contains two highly conserved cysteines, one located in the HTH domain and the other between two PAS domains. In *R. capsulatus*,

it has been shown that these cysteines play an important role in the activation of PpsR. In the presence of oxygen, they form a disulfide bond and increase thus the affinity of PpsR for its target promoters thus repressing the expression of carotenoids (*crt*) and bacteriochlorophyll (*bch*) synthesis genes (Fig. 20) (Masuda et al., 2002). In *R. gelatinosus*, it has been shown that PpsR represses the carotenoid gene *crtI* and activates the *pucBA* genes encoding the light-harvesting antennae LH2 (Steunou et al., 2004).

It was also shown in *Rhodobacter* that the activity of PpsR is controlled by a flavin containing antirepressor (AppA). AppA functions as a blue light-inhibited antirepressor. Under anaerobic condition, low light or in the dark, AppA interacts with PpsR, converting PpsR from an active into an inactive dimer, whereas under aerobic condition or blue light excited form, AppA is able to inhibit PpsR, resulting thus, in repression of photosynthetic genes by oxygen or blue-light (Gomelsky et al., 2008).

### **4.3 The RegB / RegA signal transduction system**

---

The two-component RegBA system (also annotated PrrBA) consists of the membrane-associated sensor kinase RegB and the cytoplasmic response regulator RegA. It was identified in *R. capsulatus* and *R. sphaeroides* (Sganga & Bauer, 1992), but not in *R. gelatinosus*. Although initially described as a regulator of photosynthesis, RegB/RegA system was found in other non-photosynthetic bacteria controlling a variety of metabolisms in response to oxygen (Elsen et al., 2004).

The redox signal that is detected by the membrane bound sensor kinase, RegB, would originate from the aerobic respiratory chain and the redox state of the quinol pool (Swem et al., 2006). RegB is inactive under aerobic condition, while under anaerobic condition, RegB autophosphorylates and subsequently phosphorelates RegA. Phosphorylated active RegA binds to promoter regions in the photosynthetic cluster inducing thus the expression of *puf* and *puc* genes encoding the reaction center

and the light harvesting complexes and genes involved in the synthesis of the photopigments (Schindel & Bauer, 2016).

## 5. General introduction of Metals in bacteria

---

### 5.1 Metals and evolution

---

Life on Earth appeared almost 4 billion years ago and since then it has been grown steadily to reach the biodiversity we know today. Throughout this process of evolution, living organisms have been able to draw from their environment all the elements derived from the, biosphere, hydrosphere, lithosphere and the atmosphere to ensure their survival, their development and their proliferation. The photosynthetic microorganisms appeared a little over 2 billion years ago and have modified the environmental conditions profoundly and in particularly the solubility of metal ions (Fig. 21).

In the anaerobic world,  $\text{Fe}^{2+}$  in the form of Fe-S clusters, mono or binuclear Fe-Fe centers or heme was required in many metabolisms and ensured the development of the living microorganisms. With the advent of oxygen, thanks to cyanobacterial photosynthesis, an important change occurred and led to the oxidation of reduced  $\text{Fe}^{2+}$  to insoluble  $\text{Fe}^{3+}$ , limiting thus the availability of iron. This posed both a challenge and an opportunity for the living organisms and many adaptations to the aerobic world have emerged.

Among these changes, the oxidation of other metals such as copper or zinc that became much more bioavailable. Since then for example, aerobic respiration has evolved thanks to the two  $\text{Cu}^{2+}$  centers within the oxygen reduction site of cytochrome oxidases. A second major change was the emergence of siderophores and  $\text{Fe}^{3+}$  uptake systems. In the meantime, these organisms have had to evolve systems to cope with the excess and toxicity of newly available and abundant metals (Dupont et al., 2011; Solioz, 2019) .

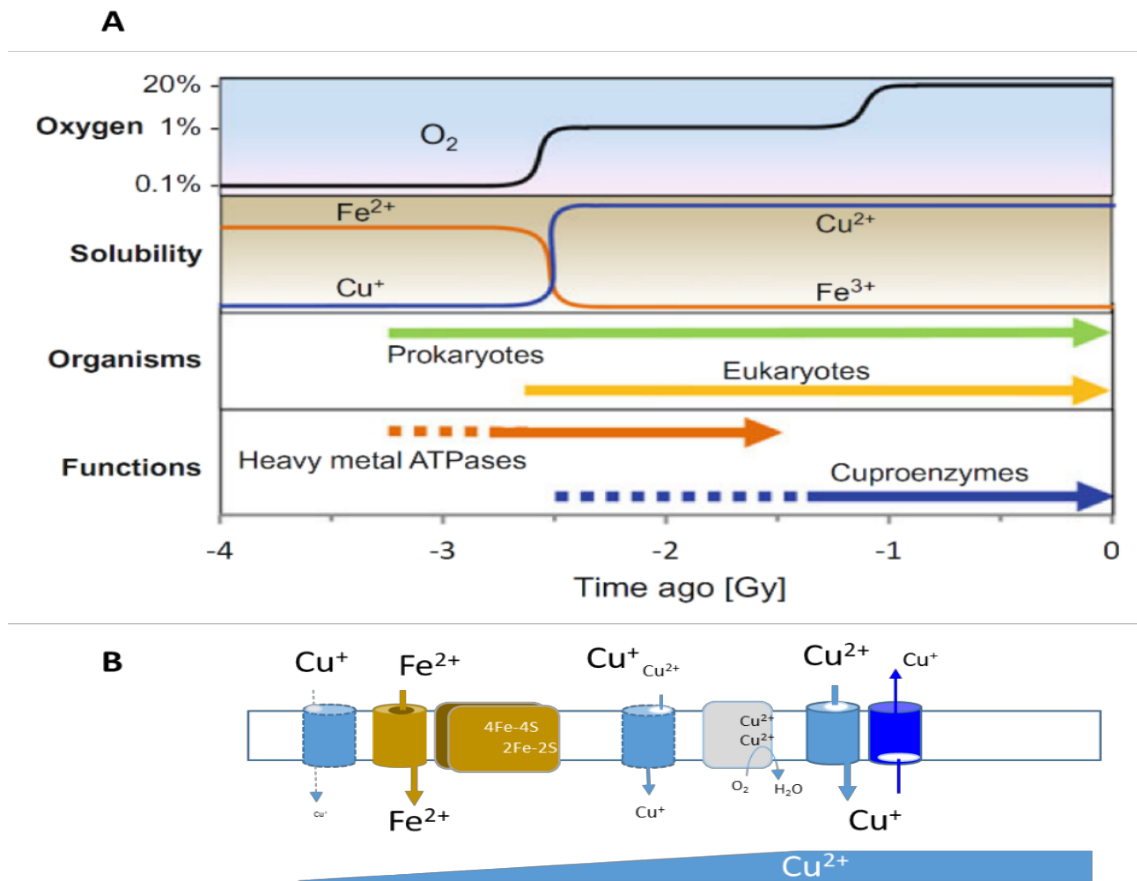


**Figure 21. Evolution of oxygen, trace metal and metal ATPases on earth (A).**

**B**-Iron was available in the anoxic world, but became insoluble under oxic conditions. On the contrary, copper became soluble with the advent of oxygen, but microorganisms had likely to deal its toxicity. Modified from (Dupont et al., 2011; Solioz, 2019).

## 5.2 Selection of metal ions by proteins

Ion metals are required for the activity of a variety of proteins involved in various processes such as respiration, photosynthesis, central metabolism, gene regulation, stress response *etc.* It is estimated that one-third to one-half of all enzymes in the cell requires a metal cofactor (Fe<sup>2+</sup>, Mg<sup>2+</sup>, Zn<sup>2+</sup>, Co<sup>2+</sup>, Cu<sup>+</sup> *etc.*) for their function (Osman et al., 2019). The majority of metallo-enzymes use a specific metal ion, and are inactive if de-metalated or mis-metalated and loaded with the wrong metal *in vivo* or *in vitro* (Barwinska-Sendra & Waldron, 2017). The selection of metals for biological

tasks is thus not arbitrary but extremely important. Specificity of metal binding is indeed important for the assembly, stability and the functioning of the metallo-proteins. Correct metalation is therefore an important step in the building and activity of these proteins. A way to ensure correct metalation is to maintain more competitive metals, ie: that can interact with many proteins in the cell, at very low concentrations and availabilities than the less competitive metals. In that sense, the metal homeostasis systems play a major role to keep the metals at the optimal and desired concentration for correct metalation of proteins (Osman et al., 2019). Another way to avoid mis-metalation, is to use specific metallo-chaperones to metalate proteins. Specific metallo-chaperones will assist the ion to reach its binding site without inflicting damage or becoming trapped in adventitious binding sites. This is the case of copper for example, that can form more tight complexes with many proteins than  $Mn^{2+}$  or  $Fe^{2+}$ . As a matter of fact, its insertion in the enzymes like the cytochrome oxidase requires many chaperones (Sco1, Cox11...) (Robinson & Winge, 2010).

Proteins are metal highly selective, and they can have multiple sites to bind metals. Nevertheless, the substitution of one metal by another can occur when the homeostasis system is deficient, and the mis-metalation can be the basis of metal toxicity in some cases.

### **5.3 Essential metallic ions and cofactors in bacteria**

---

Few metals are essential for the development and survival of living organisms. They are required for cells to grow and to live by participating in many essential metabolic processes and pathways. For example, alkali metals such as sodium, potassium or calcium play a crucial role in cellular metabolism and maintain the optimal ionic balance. Other metals such as  $Fe^{2+}$ ,  $Zn^{2+}$ ,  $Cu^+$ ,  $Ni^{2+}$ ,  $Mg^{2+}$  or  $Co^{2+}$  are associated with several enzymes or cofactors involved in essential cellular processes such as photosynthesis, aerobic and anaerobic respiration, or the detoxification of activated species of oxygen (Kim et al., 2008). Indeed, it is proposed that Metallo-enzymes

catalyze approximately half of the reactions of life (Osman et al., 2019). Some metals are directly inserted in the protein. For examples,  $\text{Cu}^{2+}$  in the cytochrome *c* oxidase, the carbon-monoxide dehydrogenase or the Cu-Zn superoxide dismutase (SodC).  $\text{Zn}^{2+}$  is found in the zinc-dependent phospholipase C;  $\text{Mn}^{2+}$  in the ribonucleotide reductase IV or the  $\text{Mn}^{2+}$  superoxide dismutase Mn-Sod (SodA);  $\text{Mg}^{2+}$  in the Adenylate cyclase.  $\text{Fe}^{2+}$  is found in many proteins as an iron mono-nuclear center like in the superoxide dismutase Fe-Sod (SodB), or as a binuclear center in the hydrogen:ferredoxin oxidoreductase (Foster et al., 2014).

Metals can also contribute to the activity of enzymes in which they are part of a complex inorganic or organic cofactor.  $\text{Fe}^{2+}$  can be part of the Fe-S clusters [2Fe-2S] or [4Fe-4S] for example, while  $\text{Cu}^{2+}$  can be active in interaction with the MoCo (molybdene cofactor) in the CO-dehydrogenase of some bacterial species (Gnida et al., 2003). Finally,  $\text{Fe}^{2+}$  is the main electron donor/acceptor in the heme moiety of hemoproteins and cytochromes, while  $\text{Mg}^{2+}$  is the metal required for the synthesis and activity of bacteriochlorophylls and chlorophylls in photosynthesis. An important cofactor of many enzymes is the cobalamin (vitamin B<sub>12</sub>) in which  $\text{Co}^{2+}$  is necessary for its activity.

As highlighted above, many metabolisms depend on essential metal ions, which enable enzymes to achieve vital chemical reactions. Yet, when present in excess, even at low concentration in the cells, the same life-enabling essential metals can be highly toxic. Toxicity is also a trait of some other metals that are not biologically active, but that can be toxic at almost any dose. Living organisms can also encounter these non-essential metals in their environment. This is the case of Silver, Gold, Arsenic, Lead or Cadmium. Nevertheless, some of these ions can have unexpected role in microorganisms. Indeed, it was shown in the marine diatom *Thalassiosira weissflogii*, and in several other diatom species, that cadmium ( $\text{Cd}^{2+}$ ) is required, instead of  $\text{Zn}^{2+}$ , for the activity of the Carbonic anhydrases that catalyze the inter-conversion of carbonic acid and carbon dioxide (Lane et al., 2005).

## **6. Metals in the environment and Toxicity**

---

### **6.1 Origin of metals in our environment**

---

Metals are naturally released in the environment after volcanic eruptions, forest fires, and wind-borne soil particles; but they are also released as a result of the anthropogenic activities related to agriculture and animal feeding (direct spreading or in fertilizers, pesticide insecticide and antimicrobial solutions), mining, or industrial and domestic sewages (He et al., 2005; Tchounwou et al., 2012). They are found in different forms such as hydroxides, oxides, sulphides, sulphates, phosphates, silicates and organic compounds. The most common heavy metals are lead, nickel, chromium, cadmium, arsenic, mercury, zinc, copper and silver (Masindi & Muedi, 2018). As they are not degradable, their accumulation will eventually have a detrimental effect due to their inability to undergo microbial or chemical degradation.

The overuse and the high doses of metals can have toxic effect. It influences the environment; thus, it loses its ability to foster life for human and all living organisms. Among different harmful sources to the environment, heavy metals pollution received a remarkable attention. They diffuse through environments in the soil, water, air, and their interfaces; and become toxic when they are not recovered or inactivated. They enter the human body through many ways: by eating and drinking contaminated food and water, breathing polluted air, and absorption through skin by the direct touch. For humans, serious body failures and diseases may attack the brain, immune system, kidney, liver, and lungs as consequences of the accumulation of toxic heavy metals in the tissues (Masindi & Muedi, 2018).

### **6.2 Toxicity caused by ion metals**

---

In general, the toxicity of a metal ion can be influenced by many abiotic factors, such as oxygen, temperature, pH, the ability to enter the cell, its interaction with organic

or inorganic molecules in the medium and its ability to interact with targets (proteins, lipid, DNA etc.) and interrupt metabolic pathways inside the cells. The intracellular concentration of each metal must be very well regulated to prevent cell overload, with unnecessary metal ions, that leads to toxic effect. This toxicity is mainly mediated by mis-metalation of protein or cofactors, mis-folding of proteins, or generation of oxidative stress.

The main targets of the deleterious effects of metal ions are the proteins. Indeed, most metal ions can interact with polypeptides, albeit with different affinities ( $Mn^{2+} < Fe^{2+} < Co^{2+} < Zn^{2+} < Cd^{2+} < Ni^{2+} < Cu^{2+}$ ) and can thus inactivate proteins.  $Cu^{2+}$  has the highest affinity for proteins and therefore, even at low concentration, can spontaneously bind to the proteins in a non-specific way. Thus, the concentration of  $Cu^{2+}$  in the cell is very low and tightly controlled (Robinson & Winge, 2010). In contrast,  $Mn^{2+}$ ,  $Mg^{2+}$  or  $Fe^{2+}$  display low affinity and their concentration in the cell is therefore higher.

The interaction with proteins can generate different damages. For example,  $Cu^{2+}$  will interact with different amino acids, in particular with thiol of cysteines but also with imidazole group of histidine and with methionine.  $Cu^{2+}$  can thus substitute to the genuine transition metal during the assembly of the protein or at least prevent the metal to bind to its site in the protein and lead to its inactivation (Fig. 22) (Dalecki et al., 2017; Solioz, 2018). Other amino acids like arginine, lysine or threonine, have side chains that are particularly sensitive to the  $Cu^{2+}$  generated hydroxyl radicals (Dalecki et al., 2017; Holm et al., 1996), leading to the formation of carbonyl groups.

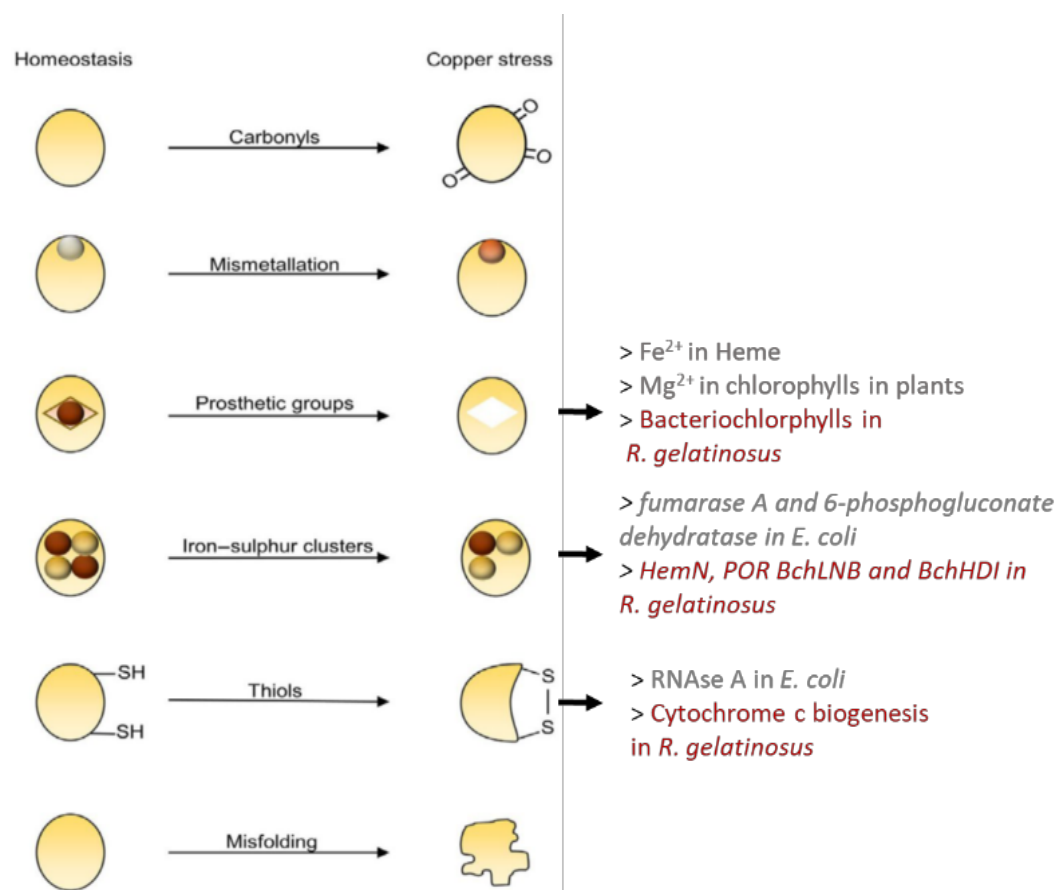


**Figure 22. Copper-induced damage.**

Copper mediates protein carbonyl formation, causes mis-metalation, interferes with the biogenesis of prosthetic groups, damages Fe-S clusters, oxidizes thiols, and induces protein mis-folding. Examples of these effects were described in *E. coli* and *R. gelatinosus* (in red). Modified from (Dalecki et al., 2017).

The most dramatic impact of metals such as  $\text{Cu}^{2+}$ ,  $\text{Co}^{2+}$ ,  $\text{Zn}^{2+}$ ,  $\text{Cd}^{2+}$  or  $\text{Ag}^+$  is very likely the disruption of exposed [4Fe-4S] clusters of proteins, within metal intoxicated cells (Macomber and Imlay, 2009). [4Fe-4S] was disrupted by these metals in many essential enzymes such as, the fumarase A and the 6-phosphogluconate dehydratase in *E. coli* (Macomber & Imlay, 2009; Xu & Imlay, 2012). The [4Fe-4S] HemN containing enzyme is also a target of metal excess. Heme synthesis and consequently many hemoproteins are impacted in *Rubrivivax gelatinosus* and *Neisseria gonorrhoeae* (Azzouzi et al., 2013; Djoko & McEwan, 2013; Steunou et al., 2020a). An additional stress imposed by metal excess was proposed to occur on the Fe-S cluster biogenesis machinery itself. Indeed,  $\text{Cu}^+$ ,  $\text{Co}^{2+}$  and  $\text{Cd}^{2+}$  appeared to directly bind and inhibit

components of the *E. coli* ISC machinery (Chillappagari et al., 2010; Montealegre et al., 2018; Tang et al., 2014).

Metals with strong affinity can also substitute others during the synthesis of prosthetic groups such as porphyrins (heme and chlorophylls). Indeed, it was shown *in vitro*, that Ferro-chelatase that catalyzes the insertion of Fe<sup>2+</sup> into protoporphyrin IX, can insert Zn<sup>2+</sup> or Co<sup>2+</sup> at a good rate in the porphyrin ring of protoporphyrin IX (Hansson et al., 2011). Similarly, but *in vivo*, substitution of Mg<sup>2+</sup> in chlorophyll molecules by Cu<sup>2+</sup>, Cd<sup>2+</sup>, Zn<sup>2+</sup> or Pb<sup>2+</sup> was reported in plants (Küpper et al., 1998a).

Damage may also occur through the disruption of the protein structure. Because redox active metals such as copper are potent oxidant, they can also catalyze the formation of nonnative disulfide bonds in proteins with nearby cysteines. Copper-mediated inactivation of the RNase A *via* formation of disulfide bonds within the protein was reported in *E. coli* (Hiniker et al., 2005), and our laboratory reported the inhibition of cytochrome *c* assembly by copper, very likely through formation of disulfide bonds (Durand et al., 2018).

On the other hand, some metal like Fe<sup>2+</sup> and Cu<sup>2+</sup> are able to catalyze the Fenton reaction:  $\text{Fe}^{2+} + \text{H}_2\text{O}_2 \rightarrow \text{Fe}^{3+} + \text{OH}^- + \text{OH}^\cdot$  or  $\text{Cu}^+ + \text{H}_2\text{O}_2 \rightarrow \text{Cu}^{2+} + \text{OH}^- + \text{OH}^\cdot$

Indeed, it was shown that the combination of Fe<sup>2+</sup> or Cu<sup>+</sup>, with hydrogen peroxide (H<sub>2</sub>O<sub>2</sub>) generates hydroxyl radicals (OH<sup>·</sup>) that is extremely reactive and will therefore react spontaneously and damage molecules (proteins, lipids, and DNA) present in its immediate surroundings. Other metals can indirectly induce such reaction. Fe<sup>2+</sup> release following the disruption of [4Fe-4S] clusters or the de-metalation of Ferro-proteins may generate hydroxy radicals, if its chelation or storage processes are deficient or slow.

## 7. Metal Homeostasis

---

Bacteria are programmed to deal with nutrient fluctuations (starvation or excess) in their environment, including for metal ions, to maintain essential metals at sufficient levels to meet cellular demands. In particular, to maintain metal homeostasis, they implement a variety of systems and strategies. To this end, they use metal ion sensors to induce or repress uptake transport or efflux systems, detoxification enzymes, storage proteins, and adapt their metabolism to cope with changes related to the metal imbalance (Mealman et al., 2012).

A dysfunction in the homeostasis system of these metals can cause physiological disorders both in prokaryotes and in eukaryotes. Given that, the topic of metal transport (uptake, efflux, storage...) and regulation is very large, with different systems described in the literature, I will only describe the response and the mechanisms to cope with excess metal with emphasis on copper.

### 7.1 Metal-sensing regulators

---

Metallo-regulatory proteins are the sentinels to ensure that metal needs are met, and to ensure a rapid response in case of depletion or excess metal. They operate by monitoring the pool of metal ions in the periplasm and cytoplasm of Gram-negative bacteria, and by modulating gene expression. Thus, metallo-regulatory proteins ensure that metal acquisition systems are expressed when metals are limiting for growth, and that storage and efflux systems are expressed under conditions of excess (Chandrangsu et al., 2017). For example, when the intracellular metal concentration is sufficient, a metal-bound repressor (case of Fur regulator that regulates iron uptake in bacteria) represses genes that involved in metal uptake. Whereas metalation of sensors that function under excess stress, will lead to increased expression of genes that are required for metal storage or efflux. Because in this work, I mainly focused on copper,

silver and cadmium, I will describe the copper efflux system and its regulation that is also active for silver and very similar to that of cadmium.

In proteobacteria, the most ubiquitous copper sensor system is a transcriptional regulator CueR (CopR in some bacteria) exhibiting both the role of a sensor and a regulator. This regulator is part of the MerR family, known to regulate metal homeostasis in bacteria. It has an N-terminal DNA binding domain, a dimerization domain in the middle of the protein and a C-terminal copper binding domain. In *E. coli* and other proteobacteria, the metal has been shown to be coordinated by a loop containing two conserved cysteines. Under non-stress conditions, the apo-CueR regulator bound to its operator DNA and represses expression. Cu<sup>+</sup> metal binding triggers conformational changes in CueR which in turn, activates the transcription of target genes (Fig. 23) (Philips et al., 2015; Rademacher & Masepohl, 2012). Indeed, CueR has an extremely high affinity for Cu<sup>+</sup>, in the order of zeptomolar range (Kd 10<sup>21</sup> M<sup>-1</sup>), indicating that, even extremely low changes in the copper concentration in the cell is monitored to avoid its accumulation. To this end, CueR induces, under copper (or silver in *E. coli*) excess, the expression of the copper efflux ATPase CopA and the periplasmic copper oxidase CueO to translocate excess copper out of the cell (Rensing & McDevitt, 2013).

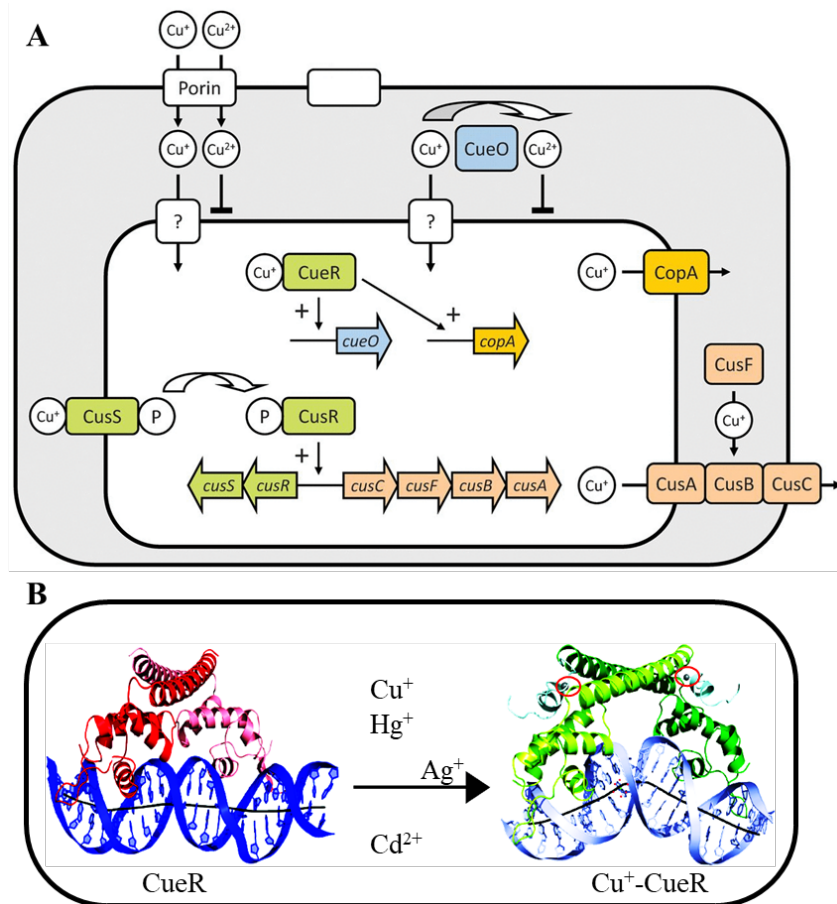


**Figure 23. Metalloregulatory and detoxification proteins involved in copper tolerance in *E. coli* (A). Structure of CueR from *E. coli* (B).**

The interaction with  $\text{Cu}^+$  induces conformation changes and promote expression. Other regulators (CadR or MerR) undergo the same changes to induce expression of the efflux systems (Philips et al., 2015; Rademacher & Masepohl, 2012).

The second sensor system, for regulating copper homeostasis in proteobacteria is the CusRS (or CopRS) system. It is a signal transduction two-component system that includes a transmembrane sensor kinase (CusS) and a cytoplasmic response regulator that binds DNA upon phosphorylation by CusS. In *E. coli*, this regulatory system modulates the expression of the RND CusCFBA transporter allowing copper extrusion from the periplasm outside the cell (Fig. 23) (Outten et al., 2001). This Cus efflux system and its regulatory signal transduction system is found only in few species. CusCFBA is induced in *E. coli* only under very high copper concentration and anaerobiosis (Outten et al., 2001). We should note that in *E. coli* these systems also respond to silver and are required for resistance to excess  $\text{Ag}^+$  (Chacón et al., 2014; Rensing et al., 2000).

Furthermore, similar Mer regulator system to CueR, required for the response to other metal ions including,  $Zn^{2+}$ ,  $Cd^{2+}$ ,  $Hg^{2+}$ , or  $As^{2+}$  were also identified in bacteria (Brown et al., 2003).

## 7.2 Extracellular sequestration of metals

---

Resistance to metal ions by extracellular sequestration is mostly found in yeasts and fungi, but some examples are also found in bacteria. Indeed, bacterial biofilm could be a barrier to different molecules. In particular, interaction of metal cations with the exopolysaccharides has been described and it can also limit the entrance of metals into the cells. In *Salmonella typhimurium* for example, it was reported that mucoid cells were more resistant to copper. In this bacterium  $Cu^{2+}$  excess induced the Rcs system that controls colanic acid, polysaccharides and capsule synthesis (Pontel et al., 2010). In *Acinetobacter baumannii*, the biofilm forming colonies were more resistant to copper than planktonic cells, very likely because components of the biofilm including polysaccharides may sequester copper (Williams et al., 2016). Similarly, cadmium was shown to induce secretion of exopolysaccharides in cyanobacteria and it was suggested that exopolysaccharides are efficient barrier that may allow to resist other heavy metal stresses in (Shen et al., 2018).

## 7.3 Exclusion of metal by limiting membrane permeability

---

Bacteria can sense the accumulation of excess metals and limit the entry of unnecessary metals into the cytoplasm. In *E-coli* for example, a study has shown that when stressing *E. coli* with  $Cd^{2+}$  ions, cells decrease the outer membrane porin *OmpF* protein synthesis (Faber et al., 1993). This protein is supposed to play a major role in the entry of metals into the periplasm. Similarly, in *P. aeruginosa*, the outer membrane porin *OprC* expression is down-regulated when copper is present in excess (Yoneyama & Nakae, 1996). Although these porins are not specific to copper, they contribute to

its entrance in these bacteria, and thus, reducing their expression would have an impact on the intracellular accumulation of metal ions (Faber et al., 1993). Limiting the uptake of metals is best documented for metals with specific uptake systems. This is the case for Zinc or iron (Pinochet-Barros & Helmann, 2018). Briefly, under  $\text{Fe}^{2+}$  starvation, Fur is demetalated and leads to derepression of the Fur regulon, including genes that are required for  $\text{Fe}^{2+}$  uptake (siderophore biosynthesis and import, and uptake of elemental iron import systems). On the contrary, under conditions of  $\text{Fe}^{2+}$  excess or intoxication, Fur directly binds  $\text{Fe}^{2+}$  and represses the uptake system, while inducing the expression of the  $\text{Fe}^{2+}$  efflux pump if present (Pi & Helmann, 2017). Similar regulation scheme occurs with  $\text{Zn}^{2+}$  via the Zur regulator (Pinochet-Barros & Helmann, 2018; Smith et al., 2009).

#### **7.4 Intracellular sequestration of metals by chelating proteins**

---

This defense mechanism is based on the production of metal-chelators that will interact with and sequester the excess of metal ions and thus protect the essential components of the cells. The best example is the production of metallothioneins by cyanobacteria (Cassier-Chauvat & Chauvat, 2014; Ziller & Fraissinet-Tachet, 2018). The metallothioneins are low-molecular weight and sulphhydryl rich proteins that have the capacity to bind ions through the thiol group of the cysteine residues. These unusual high cysteine content proteins can bind many metals including cadmium, mercury, silver, or copper and protect cells metal toxicity. Glutathione has a major in oxidative stress and redox balance in the cell, but is also able to interact with metal ions. Indeed, Glutathione synthesis is induced under copper or cadmium synthesis in *E. coli* and other bacteria and significantly contribute to the resistance to excess metal (Helbig et al., 2008).

More recently, copper storage protein (Csp), able to interact with and store  $\text{Cu}^+$  atoms were identified in many bacteria. These cysteine rich four-helix bundle proteins use thiolate to bind up to 80  $\text{Cu}^+$  ions and were found both in the cytoplasm and

periplasm of some bacteria. Their major role would be the delivery of  $\text{Cu}^+$  to cupro-proteins in the membrane, but their involvement in copper storage and tolerance was also reported (Dennison et al., 2018).

## 7.5 Enzymatic detoxification

---

Another way of resistance to certain metals is the chemical modification of a toxic metal ion to a less harmful component by modifying the oxidation-reduction state or by methylation. The best-known example is the mercury resistance in bacteria. The central enzyme in the microbial mercury detoxification system is the mercuric reductase MerA protein, whose expression is induced by MerR and catalyzes the reduction of  $\text{Hg}^{2+}$  to volatile  $\text{Hg}^0$ . In the case of copper,  $\text{Cu}^+$  is more reactive and more toxic than  $\text{Cu}^{2+}$ . Therefore,  $\text{Cu}^+$  oxidation in the periplasm of *E. coli* and other species by the multicopper oxidase CueO to  $\text{Cu}^{2+}$  is one of the main copper resistance mechanisms described in *E. coli* and CueO containing species.

Methylation of some ions is another bacterial detoxification pathway. Indeed, some bacteria are able to methylate toxic inorganic arsenite ( $\text{As}^{3+}$ ) via the  $\text{As}^{3+}$ -S-adenosylmethionine methyltransferase (encoded by the *arsM* gene) to form volatile mono or dimethyl-arsenite species (Huang et al., 2018).

## 7.6 Active efflux systems

---

### 7.6.1 P-type ATPases

---

P-type ATPases form a large superfamily of integral membrane proteins that pump ions and other molecules across cellular membranes. There are five subfamilies of P-type ATPases (P1-P5) and five subtypes, typically associated with different transport specificities. Our interest is P1B-ATPases which are pumping heavy-metal and transition-metal (Argüello et al., 2007; Palmgren & Nissen, 2011).

The Heavy-metal pumps (P1B-ATPases) are the most common P-type ATPases in bacteria and archaea. They are part of the large superfamily of ATP-driven pumps involved in metal transport across bacterial inner membrane (Argüello et al., 2007). These transporters extrude excess metal ions such as  $\text{Cu}^+$ ,  $\text{Zn}^{2+}$ ,  $\text{Cd}^{2+}$  or  $\text{Ag}^+$  from the cytoplasm to the periplasm. This P1B subfamily is divided into monovalent ( $\text{Cu}^+$ ,  $\text{Ag}^+$ ) and divalent ( $\text{Zn}^{2+}$ ,  $\text{Co}^{2+}$ ,  $\text{Pb}^{2+}$ ,  $\text{Cd}^{2+}$ ) metal pumps. In bacteria, the best-characterized heavy-metal pump is the  $\text{Cu}^+$ -efflux pump CopA that pumps  $\text{Cu}^+$  from the cytoplasm to the periplasm of Gram-negative bacteria. Homologues of CopA are present in most living organisms and can be involved in either  $\text{Cu}^+$  import or export. CopA is the homologue of the human  $\text{Cu}^+$ -ATPases ATP7A and ATP7B pumps (Yanfeng Wang et al., 2011) or the plant HMA6, located in the envelope and HMA8, localized in the thylakoid membranes of the chloroplast (Sautron et al., 2015).

In bacteria, the  $\text{Cu}^+$ -ATPase CopA is induced by copper and is required to tolerate excess  $\text{Cu}^{2+}$ . In some species like in *E. coli*, CopA is also involved in  $\text{Ag}^+$  tolerance (Rensing et al., 2000; Stoyanov et al., 2003).

-INTRODUCTION-

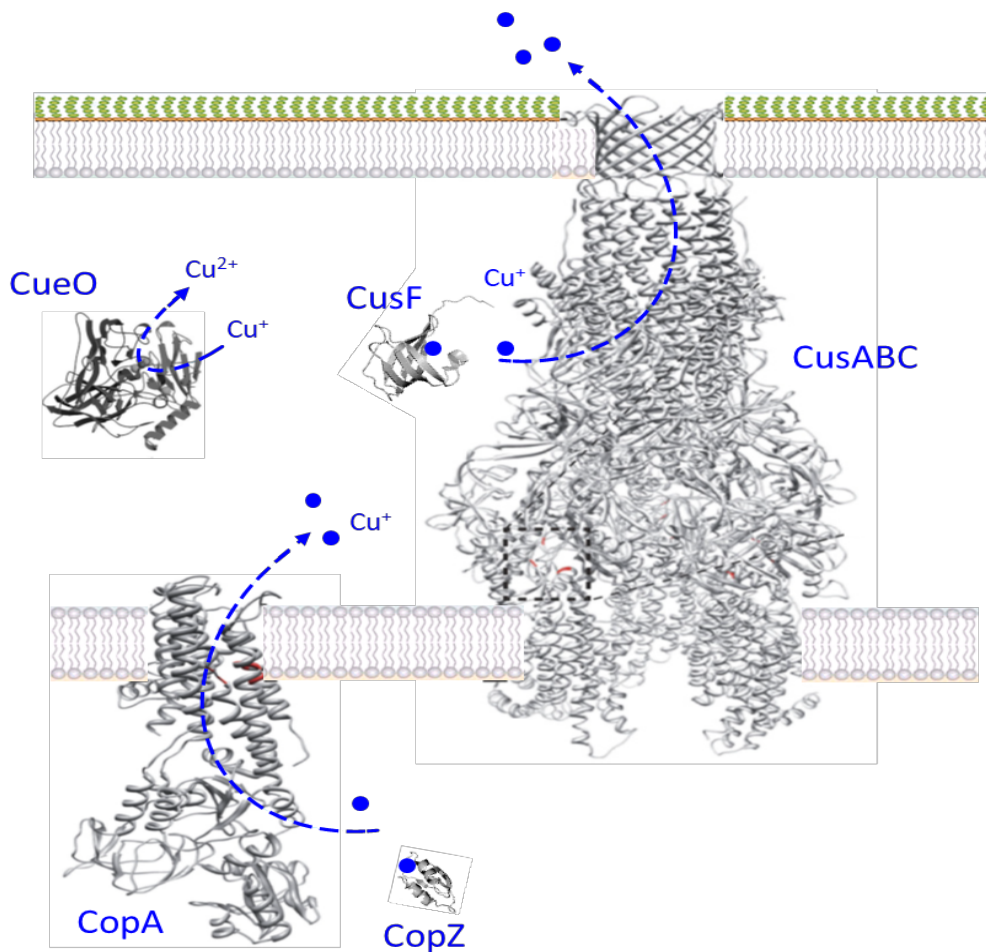


**Figure 24. Proteins involved in the tolerance of copper in *E. coli*.**

CopZ interact with  $\text{Cu}^+$  in the cytoplasm and deliver it to the CopA ATPase that translocate  $\text{Cu}^+$  to the periplasm. In the periplasm,  $\text{Cu}^+$  is oxidized by the  $\text{Cu}^+$ -oxidase CueO under aerobic condition, or extruded by the CusCFBA RND system (Rensing & Grass, 2003).

Similarly, to  $\text{Cu}^+$  efflux, ATPases specific to other cations are expressed when the metal exceeds the needs of the cell. It was shown that the ATPase ZntA (also called CadA) is induced by  $\text{Zn}^{2+}$  and extrude excess  $\text{Zn}^{2+}$ . Expression of this ATPase is also induced by  $\text{Cd}^{2+}$ , and is required in many species to tolerate cadmium in the medium (Sharma et al., 2000).

### 7.6.2 Proteins of the RND family

---

The members of the RND (Resistance-Nodulation-Cell-Division) superfamily are tripartite transporters widespread in Gram-negative bacteria. The RND systems are complex membrane proteins connecting the inner and outer-membrane (Delmar et al., 2015), allowing export of the substrate from the periplasm to the extracellular space using the motive proton force. These complexes consist of three proteins: an inner membrane protein, an outer membrane protein and a periplasmic adapter bridging the inner and outer membrane proteins. Two different types of RND systems were described (Delmar et al., 2015; Venter et al., 2015). 1- The HAE (Hydrophobic and Amphiphilic Efflux) system that extrude molecules such as antibiotics and 2- The HME (Heavy Metal Efflux) system such as the CusCBA or CzcCBA, that extrude  $\text{Cu}^+$  and  $\text{Ag}^+$  or  $\text{Zn}^{2+}$  and  $\text{Cd}^{2+}$  respectively. The best characterized RND heavy metal transporter is the *E. coli* CusCFBA system (Fig. 24) (Delmar et al., 2015). The CusCBA system interact with the periplasmic  $\text{Cu}^+$  chaperone CusF that deliver  $\text{Cu}^+$  to the metal-binding sites in the N-terminal domain of CusB, then  $\text{Cu}^+$  is exported to the outside trough the CusBC channel.

### 7.6.3 The proteins of the cation diffusion facilitators (CDF family)

---

CDF transporters are membrane proteins responsible for the cytosolic efflux of divalent cations coupled to the influx of  $\text{H}^+$  or  $\text{Na}^+$ . By this mean, they participate in metal detoxification or metal delivery for metalloprotein assembly in the membrane. These proteins belong to a family of metal transporters found in all three domains of life. They contain six transmembrane helices (TM) and a cytoplasmic hydrophilic C-terminal domain. In addition, all eukaryotic and some bacterial CDFs present a His-rich cytosolic region between TM4 and TM5. One of the best characterized CDF system in *E.coli* is the  $\text{Zn}^{2+}$  transporter YiiP (Fig 25). It presents a high-affinity to  $\text{Zn}^{2+}$  / $\text{Cd}^{2+}$ . It was shown that such transporter sense very low and subtle changes in the concentration of  $\text{Zn}^{2+}$  or  $\text{Cd}^{2+}$  and that YiiP is involved in the fine tuning of  $\text{Zn}^{2+}$  concentration in the

cell. In contrast to the ATPase ZntA, the deletion of the *yjiP* gene does not lead to an increase in zinc sensitivity (Nies, 2003).

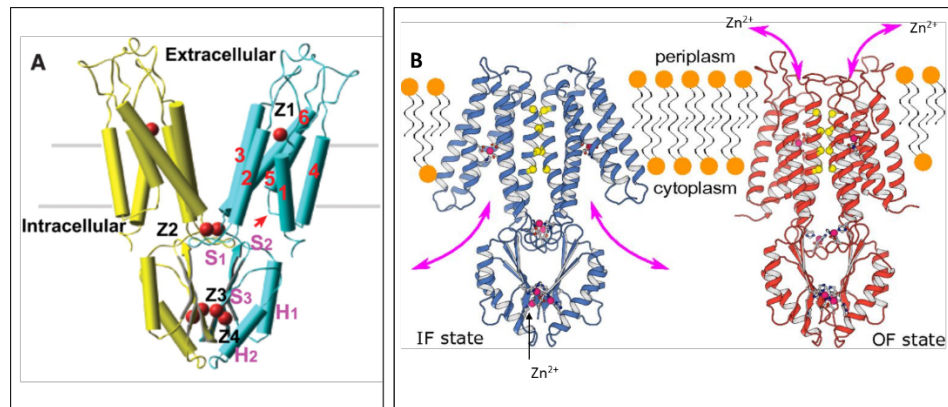


**Figure 25. Structure of the CDF *YjiP* of *E. coli* involved in Zn<sup>2+</sup> efflux.**  
(Lopez-Redondo et al., 2018; Lu & Fu, 2007).

In the last years, silver and silver-based nanoparticles (AgNPs) have been used for industrial and medical purposes and as antimicrobial agents (Sánchez-López et al., 2020). Nowadays, NPs are even increasingly used in various applications, as drug delivery, sensors, and painting, *etc.* Hence, we need to increase our understanding of toxicity mechanism of NPs. Metal toxicity can originate directly from ions but also from metal alloy and nanoparticles. In my project, I had also to analyze the effect of silver nanoparticles on *R. gelatinosus*. In the next section, I will introduce those particles and the approaches I used to analyses their interaction with bacteria.

## 8. Metals Nanoparticles

Bacteria have found their way to survive on earth for billion years. They are everywhere. They have the ability to colonize on most surfaces to communicate with the surrounded environment and/or to interact symbiotically with other organisms (Gallardo-Navarro & Santillán, 2019). The interaction between bacteria and physical materials involves the properties of these materials; which leads to different ranges of interactions. It is called long-range type when distance between the bacterial cell and the physical object is  $> 50$  nm. It is short-range interaction type when this distance is  $< 5$  nm distance. The hydrogen bonding and the ionic interactions are for examples of the latter type.

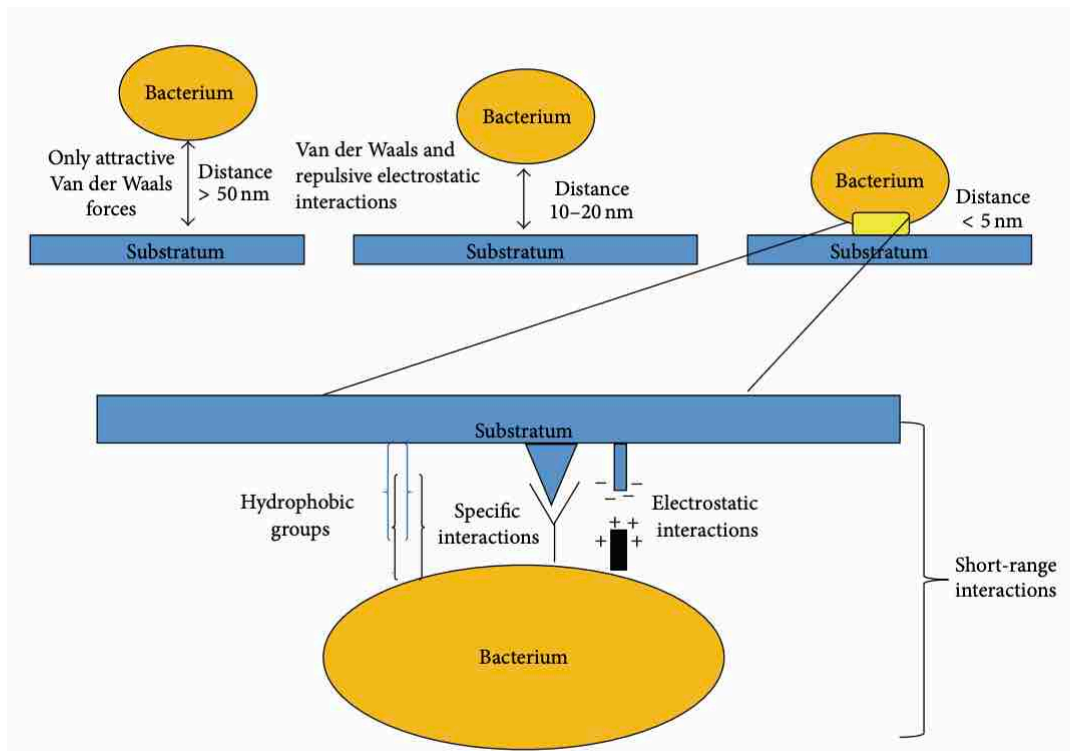


**Figure 26. Phase one of bacterial adhesion consists in the initial attraction of the cells to the surface through the effects of physical forces.**

(Gallardo-Navarro & Santillán, 2019).

Bacteria in their environments are exposed to various stress such as low/ high temperature, light and darkness and contact with metal pollution. Heavy metals

released in the environment are considered to be a serious threat to all type of living cells, not only to bacteria.

In the frame of this study, we focused on the effect of the interaction between physical objects (metals) and the biological subjects (bacteria). While bacteria use various strategies against excess of heavy metals; metals in different forms (ions/nanoparticles) have different impact.

Many studies are investigating, for instance, whether the toxicity of metal is caused by the nanoparticles themselves or by the ions that are released. We, also, have to consider that the impact of metals nanoparticles can be induced by their morphologies, their reduced size, their important effective surface or their selectivity for bacteria. In here, I am introducing the importance of metal nanoparticles as antimicrobial agent but pick out and emphasize the role of silver nanoparticles (Ag-NPs).

In this project, we had to synthesized Ag-NPs in the laboratory to ensure their properties (size, stability, composition, etc.) to control as much as possible the parameters of their interaction with bacteria. In this context, the collaboration with physicists and chemists demonstrated a very high added value. Their expertise was also very precious concerning imaging at the micro and nanoscale.

We used Scanning Electron Microscopy (SEM) and Atomic Force Microscopy (AFM) to monitor the activities at nanometer scale on the cell structure and to detect any morphological characterizations change.

## **8.1 Metal Nanoparticles**

---

It is not a very original idea to use metallic ions or nanoparticles as antimicrobial agent. For millennia, metals such as gold, silver or copper were used in different civilizations, like in Egypt and Mesopotamia for instance, for various purposes and among them for their observed or supposed properties against "evil". Over the time, improving techniques in smithy and mining such as heating, distillation, reflux, sublimation and metal technology (metallurgy) (Marambio-Jones & Hoek, 2010).

enable the design of more sophisticated metal tools and materials. In particular, and more recently, Nanotechnology, which can sometimes be defined as the engineering at nanoscale, permits huge progress in materials science, optics, electronics, ... and as far as we are concerned very promising solutions in medicine and in producing new pharmaceutical products made out of nanomaterials, nanoparticles and nanostructures (Zhang et al., 2016).

The word "Nano" derived from the Greek word "Nanos" that means "dwarf" or small. To be considered as nano, an object should have one or all of its dimensions in the range 1 to 100 nanometer (nm). A nanoparticle is also referred as a cluster usually when its size refers to the numbers of atoms contained. For example,  $\text{Ag}_{13}$  is a cluster containing 13 atoms of Ag. This particular clusters for example, possess 92 % of its atoms at its surface. This is very important because it means that when the size go down, the surface area/volume ratio increase (Yang et al., 2007). A large surface area/volume ratio means more amount of a substance comes in contact with the surrounding material, which leads for example to better catalysts due to maximum proportion exposed for potential reaction (Nel et al., 2006).

The conditions and parameters of nanoparticles synthesis affect strongly their characteristics that leads to a large variety of objects at all the dimensions, such as the 0D nanometer-size objects (e.g., nanodots), 1D nanometer-size objects (e.g., nanowires, nanorods and nanotubes), 2D nanometer-size objects (e.g. thin films) or the 3D nanometer-size objects (e.g., triangular prisms and cubes) (Fig. 27). The different nano morphologies create different surface chemistry, physical and optical properties that must be selected very carefully based on the desired function expected (Rai et al., 2012; Sondi & Salopek-Sondi, 2004).

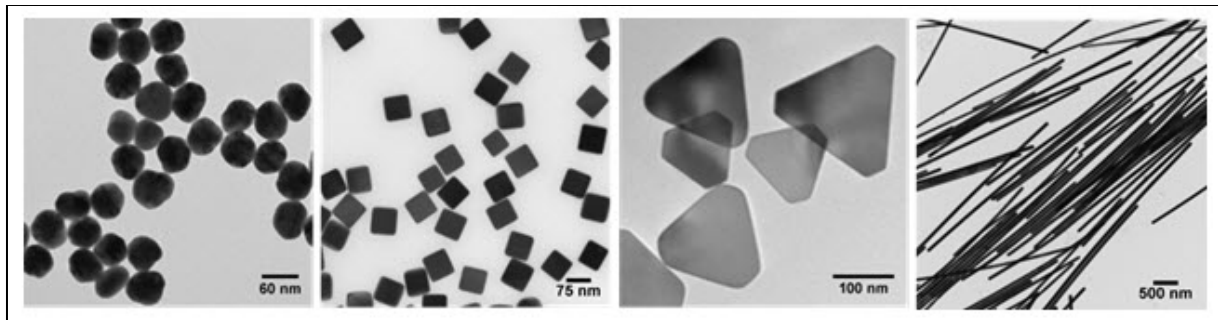


**Figure 27. The diversity of size and morphology of nanoparticles.**

Transmission electron micrographs demonstrating the possible sizes and morphologies that could be addressed by different chemical reaction and kinetics during the solution-phase synthesis of silver nanomaterials: (left to right) uniform 50 nm diameter spheres, 75 nm cubes, 120 nm triangular nanoplates, and silver nanowires (Oldenburg, Sigma.Aldrich).

The properties of the nanoparticles will be dependent of their characteristics (morphologies, composition, sizes, ...). These properties can be targeted for device design or used for their characterization.

### 8.1.2 Optical properties

One of the characteristics of the nanoparticles that can be used to distinguish and classified them is their colors. Indeed, different morphologies and/or sizes of nanoparticles of the same metal exhibits different colors. The optical properties can provide relevant dynamic and structural information. To understand this phenomenon, we must identify the processes involved in the interaction between light and an object at that scale. Light interacting with an object presents different pathways of behavior (Fig. 28). These pathways of interaction are reflection, when the light wave changes its direction after contact with the surface of an object. It is scattering when the light wave goes through all directions at different angles. It is absorption when it is absorbed by the object and transfer the light energy within the surface. It is a transmission when light pass through the object.

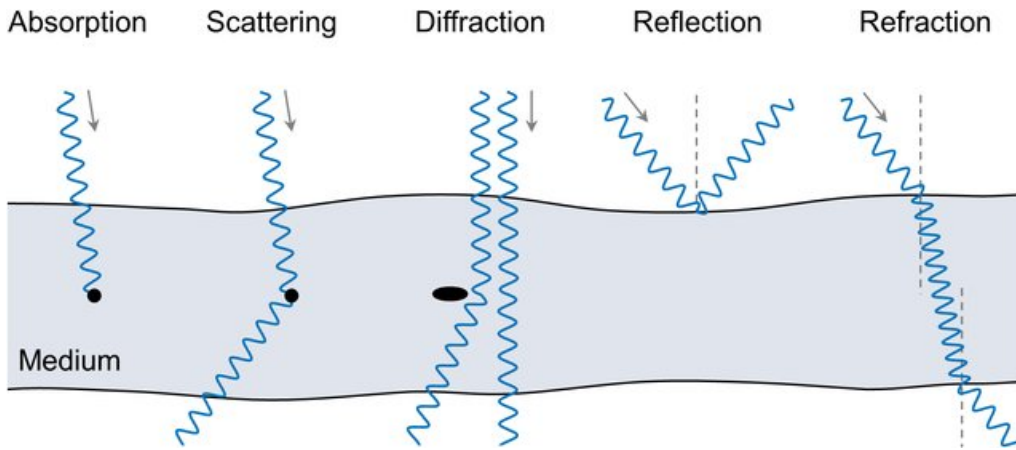


**Figure 28. The different light-material interaction processes.**

Absorption: transfer of light radiation to energy within a material. Scattering: change in light direction at different angles. Diffraction: light passes around the edge of an object. Reflection: change in light direction at a fixed angle. Refraction: light pass through one medium to another (Soliman, 2016).

Noble metal nanoparticles show strong interaction with light. This is because when they are excited by light at specific wavelengths, the conduction electrons on the metal surface undergo a collective oscillation. This oscillation is known as surface plasmon resonance (SPR). The absorption and scattering properties of metal nanoparticles can be tuned, for example, by controlling the particle size, shape, and the local refractive index near the particle surface (Fig. 29) (Moores & Goettmann, 2006). In the other hand plasmon profiles are unambiguous tools for nanoparticles characterization.

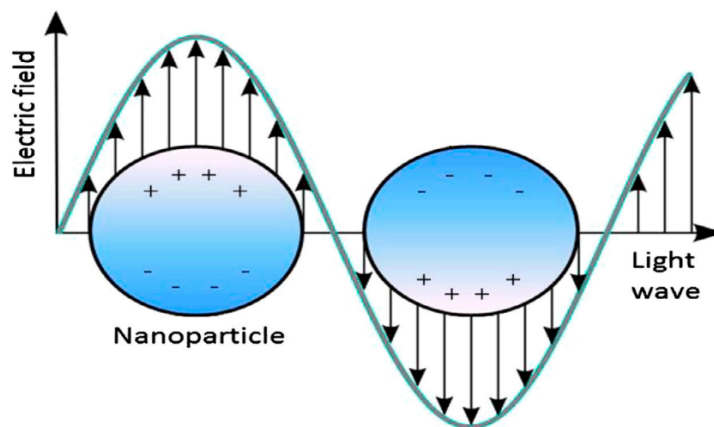


**Figure 29. Localized Surface Plasmon Resonance of metallic nanoparticles under light illumination.**

(Khlebtsov & Dykman, 2010).

### **8.1.3 Physicochemical properties**

---

At a nanoscale, the particle shows also specific physical and chemical properties comparing to the bulk. The physico-chemical properties of the surface of a particle such as the binding strength and size of the capping agents coating the particles, for example, can be very different. These properties provide an additional level of control over particle behavior. In aqueous media, many nanoparticles are electrostatically stabilized through the addition of charged agents at the particle surface. For example, the surface charge of silver nanoparticles can be controlled by coating the particles with citrate ions. This coating provides a strong negative charge. While using branched polyethylenimine (BPEI) would create an amine-dense surface with a highly positive charge. Other capping agents can provide additional functionality (Khan et al., 2019).

The physico-chemical properties including the surface charge, shape, size and agglomeration status are involved in the metal nanoparticles (MNP) effects and degree of toxicity; and their direct impact in biological interactions. Also, and from an application point of view, the MNP magnetic behavior is important as well (Alonso et al., 2018; K. Wu et al., 2019).

### **8.1.4 Metal Nanoparticles synthesis**

---

There are different methods for metal nanoparticles synthesis. The main methods to synthesize metal nanoparticles are classified as top-down and bottom-up techniques. Top-down strategy starts with making powder of raw material, then decreasing the size to nanoparticles. Bottom-up methods. start with the atoms of the element, as building block growing toward nanoparticles (Fig. 30) (Domenech et al., 2012; Yuliang Wang & Xia, 2004).

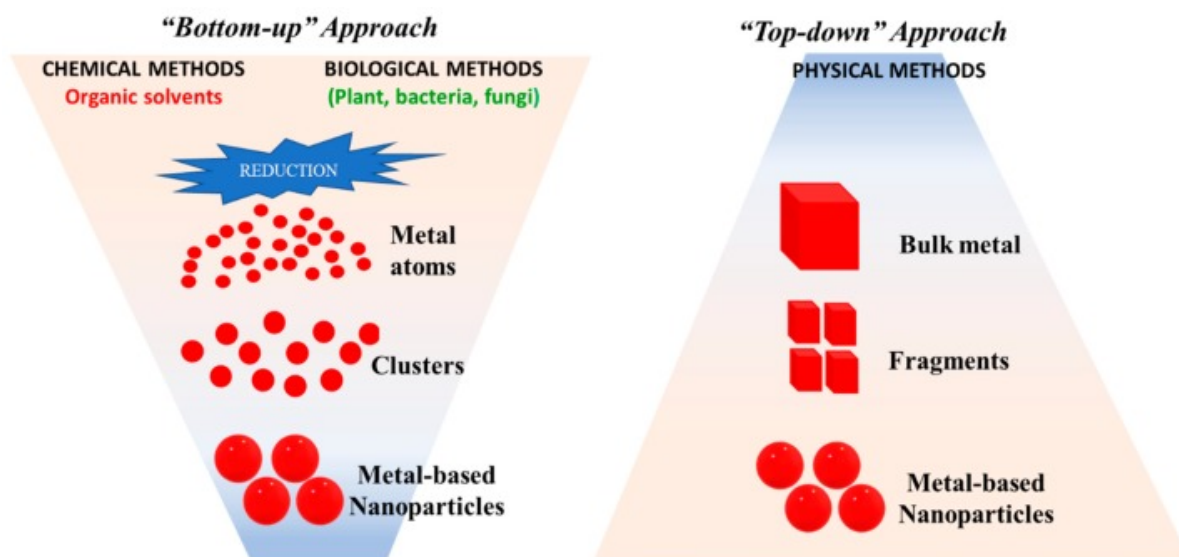


**Figure 30. Different methods used for the synthesis of metal-based nanoparticles (MNPs).**

(Sánchez-López et al., 2020).

The other methods to synthesize nanoparticles are for examples: thermolysis methods, photochemical methods, biological methods, chemical reduction methods, electrochemical methods and physical synthesis. Some methods as physical methods are considered as green synthesis because it causes less harm to the environment due to less chemical waste. Yet, it requires special and heavyweight equipment. Others, on the other hand, are faster, cheaper and do not require heavy and expensive instruments such some chemical methods. Overall, the MNPS synthesis method selection is mostly driven by the goal and the applications will be used for (Dias et al., 2015). The possibility to transpose the process industrially is also an interesting criterion to consider.

In chemical synthesis, NPs stabilization is one of the main challenges. Without stabilization, it is almost impossible to maintain initial size. Nanoparticles will undergo even under ambient conditions different process like evaporation and fragmentation. Thus, it needs the use of different additives to achieve stable NPs. Recently, the development of polymer-stabilized NPs, are considered to be the most promising solutions to stabilize the NPs (Pavičić et al., 2020).

Usually the commercial product of NPs contains sodium citrate as a coating agent. It is used to coat silver nanoparticles to stabilize them and prevent them from agglomerations. The sodium citrate is a small molecule with multiple carboxylic acid groups. There are many advantages of using sodium citrate such as negative charge, salt stability, and very low toxicity. It solves in water and/or weak buffers (Zhang et al., 2010).

The final products of chemical synthesis of NPs usually have a mesocrystalline or polycrystalline structure. In these non-classical nucleation and growth models, the nuclei reach a stable size which is used as a building block for the final nanomaterial structure. In general, the NPs addition forming meso or polycrystal structures can occur via an oriented attachment, coalescence or both mechanisms (Fig. 31) (José-Yacamán et al., 2005; Lee et al., 2005; Xia et al., 2017). The final formation of NPs and their attachment to each other have a great effect on their way to effect, to attach and to interact with material surfaces and biological microorganisms.

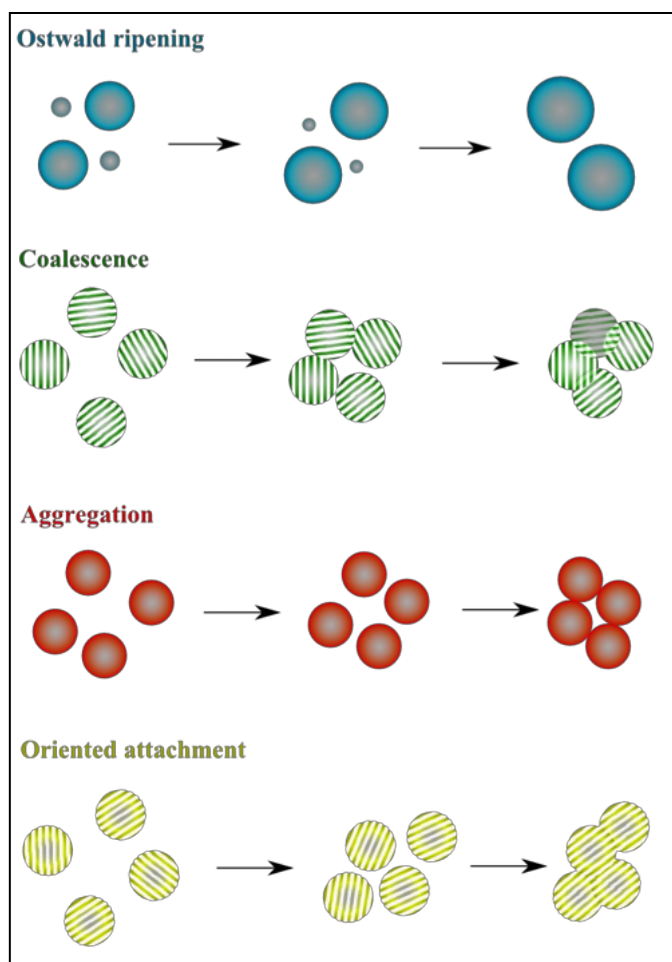


**Figure 31. NPs growth evolution involving different competitive mechanisms.** Representation of the different NPs growth evolution: Ostwald Ripening, Coalescence, Aggregation and Orientated Attachment (Djafari, 2019).

### 8.1.5 Metals nanoparticles as antimicrobial agent

One of the main and remarkable achievement of last century, was in medicine with the discovery of antibiotics, such as Salvarsan and Penicillin that were intensively used to cure patients who suffer of infection diseases (Khardori et al., 2020; Sánchez-López et al., 2020; Ventola, 2015). However, nowadays, the pharmaceutical industrial field has been facing a new challenge to evolve antimicrobial molecules because of the evolution of new antibiotics resistance bacteria (Aslam et al., 2018; Coates et al., 2011). This rapid emergence of resistant bacteria is occurring worldwide, endangering the efficiency of antibiotics, which have transformed medicine and saved millions of lives.

Many decades after the first patients were treated with antibiotics, bacterial infections have again become a threat. This type of bacteria is increasing in fast rate. Mainly through genetic modification, they exhibit new mechanisms against antibiotics by inactivating them or by effecting their therapeutic performance. Thus, and during the time, the world has been recording an increase of the mortality frequency due to infections disease issues; which consider in 2017 as global health crisis by the World Health Organization (Tacconelli & Magrini, 2017).

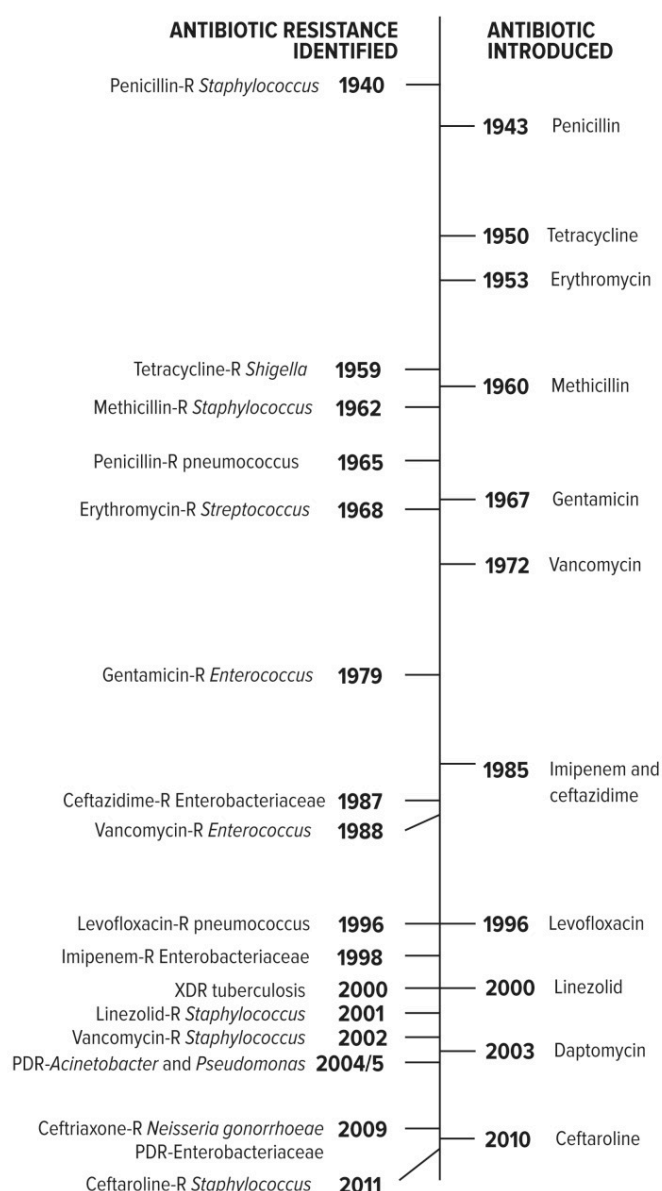


**Figure 32. The appearance of antibiotics resistance versus antibiotics development.**

PDR = pan-drug-resistant; R = resistant; XDR = extensively drug-resistant (Ventola, 2015).

The antibiotic resistance crisis could also be attributed to the overuse and misuse of these medications (transforming and weakening self-immunity), as well as a lack of new drug development by the pharmaceutical industry due among other things to reduced economic incentives and challenging regulatory requirements.

Therefore, there is an urgent call for new solutions with antibacterial properties (Tacconelli & Magrini, 2017). Coordinated efforts to implement new policies, renew research efforts, and pursue steps to manage the crisis are greatly needed. Among new research efforts, nanotechnology is playing an important role, to create non-traditional drugs and to develop and produce nanomaterials as promising agents against antibiotics resistance bacteria or bacteria proliferation.

Various heavy metals such as gold, copper and silver are known for their antimicrobial activities against both Gram-positive and Gram-negative bacteria. The activity comes from these metals in their nanoparticles form and/or through the released ions. The efficiency of their effect is attributed to the fact that there are no specific receptors on the surface of bacterial cell to bind with. However, the exact mechanism is not fully understood. Even if, some phenomena were identified, in the action of metals NPs or ions : specifically attracting to the surface of bacterial cell; attacking the cell membrane and cause changes in its permeability; inducing toxicity by generating the reactive oxygen species (ROS) and free radicals; and interrupt the cell's essential metabolism pathways (Dakal et al., 2016).

In here, we emphasize the role of silver ions and nanoparticles as antimicrobial agent and its toxicity toward bacteria. In addition, to the description of synthesis method and characterizations of silver nanoparticles.

## **8.2 Silver nanoparticles (Ag-NPs)**

---

Silver is not essential for cells to grow. The day-to-day contact with solid silver (bulk metal (Ag)) such as coins, spoons or jewelry showed, in the same time, no harmful effect on human health (Medici et al., 2019). Silver has been known since ancient times.

It has several properties: chemical, physical, and on atomic level, which made it a special element from many points of view. Its ability to be electrically conductive made it involved in many industrial uses like in high-end electronic devices. Its durability and appearance in addition to its antibacterial action (Medici et al., 2019), are advantages features to be used in everyday tools (musical instruments, dental filling, ...). The fields of nanoscience and nanoengineering are giving also a significant attention to Ag-NPs due to their uncommon physicochemical properties in producing new pharmaceutical products and new solutions in medicine (Lubick, 2008; Marambio-Jones & Hoek, 2010).

In the other hand, the overuse and overdoses released in the environment is a serious ecological issue. Sub micromolar concentrations of silver in the ionic state ( $\text{Ag}^+$ ), consider to be very toxic to human, plant and bacteria. Contaminated environments with silver enable metal accumulation inside bacterial cells and tissues of living organisms. These affected cells are reacting differently depending on several factors such as their immune systems, size and type of the living organism; dose, nature, size and shape of metals. Silver, in its both forms ions and/or NPs, impact cells of bacteria and plants by diffusing across the cell's membrane through unspecific pores. Human cells (skin and lung cells) can get exposed to silver nitrate or silver oxide by touching and breathing (Silver, 2003); which may lead to serious health issues, breathing problems, lung and throat irritation, stomach pain, and argyria (Butkus et al., 2003).

### **8.2.1 Silver nanoparticles as antimicrobial agent**

---

Antimicrobial properties of silver ions and nanoparticles make it the leading element to be used in cosmetics, food packaging, surgical coatings, medical implants, and water disinfection (Haider & Kang, 2015; Zhang et al., 2016). It has been used as antifungal, antiviral, antiamebial, anti-cancer and anti-inflammatory as well. However, the mechanism of its action is poorly understood.

Many studies have proposed scenarios about ways of damages caused by silver nanoparticles and/or ions. Mainly they attack living cells by interacting with cell membrane and change its permeability (Dakal et al., 2016). They are the cause of Reactive oxygen species (ROS) generation and free radicals. They can also inhibit bacterial growth via inactivating required proteins that important for cell metabolism. Silver atoms bind to thiol groups (-SH) in enzymes and inactivated them. It is also thought that silver can interrupt with ribosomes complexes and prevent protein translation process. The released silver ions, once they are inside in the cytoplasm, they have the ability to denature the DNA molecules (Fig. 33) (Klueh et al., 2000; Rai et al., 2012).

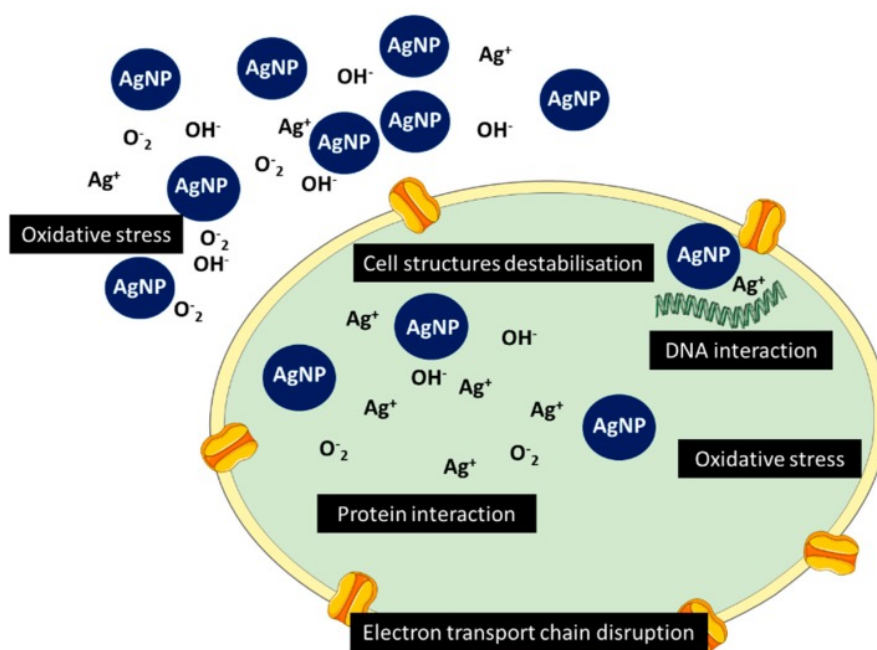


**Figure 33. Schematic representation of AgNPs mechanism of antimicrobial activity.**

(Sánchez-López et al., 2020).

The first interaction between Ag-NPs and bacterial cell membrane could be explained by the different electrical charges between them. While the surface of bacterial cell appears slightly negative in charge, positively charged Ag-NPs can

attached fast and strongly on the cell membrane. On the other hand, even neutral or negative charge of Ag-NPs can still increase their activity toward bacteria with an increased concentration; which result in attenuation of electrostatic repulsion by saturating the surface of a bacterial cell (Abbaszadegan et al., 2015).

Several studies have demonstrated that the bactericidal properties of the Ag-NPs are strongly influenced by their shape, size, and concentration (Bhattacharya & Mukherjee, 2008; Nateghi & Hajimirzababa, 2014; Pal et al., 2007; Rai et al., 2012; Raza et al., 2016). There is a shape-dependent manner for Ag-NPs to interact with bacteria, fungi and viruses (Galdiero et al., 2011; Panáček et al., 2009; Raza et al., 2016; Tamayo et al., 2014; J. Wu et al., 2014). It has been found that Ag-NPs size between 10 and 15 nm showed increased stability, biocompatibility and enhanced antimicrobial activity (Yacamán et al., 2001). Some other studies have revealed that smaller diameter (< 30 nm) of Ag-NPs are more effective against bacteria such as: *S. aureus* and *K. pneumoniae* (Dakal et al., 2016).

In addition to the importance of the size, the concentration (dose-dependent) of the NPs plays an important role as well. A study on both Gram-positive bacteria such as *S. aureus*, *P. aeruginosa*, and *V. cholera*, and Gram-negative bacteria such as *E. coli* and *S. typhi*, showed that the latter are more sensitive to lower concentrations. However, at higher concentrations (> 75 µg/mL) both type of bacteria exhibits complete growth inhibition (Kim et al., 2007).

Ag-NPs can be produced in different shapes like rod, triangle, round, cubes, wires, octahedral, polyhedral (Fig. 27) (Heiligtag & Niederberger, 2013). The shape of Ag-NPs plays also a specific role on their effect when interacting with bacteria. The triangle shape for example, can be more toxic than the spherical shape due to the high surface tension, and tip effects in efficient release of Ag ions. The presence of (111) atomic plans seems also to have more toxic impact against bacteria, probably because of the high atomic density (Djafari et al., 2019; Morones et al., 2005; Sadeghi et al., 2012).

In addition to the shape, size, and concentration of Ag-NPs, more investigations are necessary to assess the silver toxicity and its mechanism action. One important point is to understand whether its effect is because of the particles themselves or because of the silver ions released (Sánchez-López et al., 2020).

### 8.2.3 Ag-NPs synthesis methods

---

There are numerous methods to synthesize Ag-NPs as it was mentioned before. The chemical method is one of the most popular due to its fast process and being affordable comparing to other methods. A synthesis method is usually selected based on the purpose of uses. For example, in order to assess the Ag-NPs effect on biological application, it is ideal to have monodispersed small size (around 10 nm) NPs, in liquid solutions. Thus, to enhance their interaction with the cell surface and their transmission through nanometer size of canals in the cell membrane (Hamouda et al., 2019). Methods that produce deposited NPs on solid and dry substrates are less used since it difficult to assess the impact on living cell like bacteria due to the limitation of interactions.

The most common chemical method for Ag-NPs synthesis is based on the reduction of a metal precursor as ( $\text{AgNO}_3$ ) by a reducing agent as ( $\text{NaBH}_4$ ) (Mulfinger et al., 2007). The reduction reaction is given:



The reaction process undergoes two main stages: 1- the nucleation, and 2- the particles growth (Fig. 34). The particles produced needs to be stabilized, otherwise they aggregate and/or oxidize. Thus, the use of a stabilizing agent is very often required. There are many examples of common Ag-NPs stabilizers such as chitosan, gluconic acid, polyvinylpyrrolidone (PVP), polyvinyl alcohol (PVA), and sodium citrate (Dakal et al., 2016; Sánchez-López et al., 2020; Zhang et al., 2018).

The nucleation step of the process is an important issue, since it is the stage step where it is possible to control the size and shape of the nanoparticles. It requires to have the control on specific parameters during the reaction such as: the concentration of the agents used, the pH, temperature and the quality of the metal precursor and the reducing agent (Ho et al., 2012; Mulfingher et al., 2007).

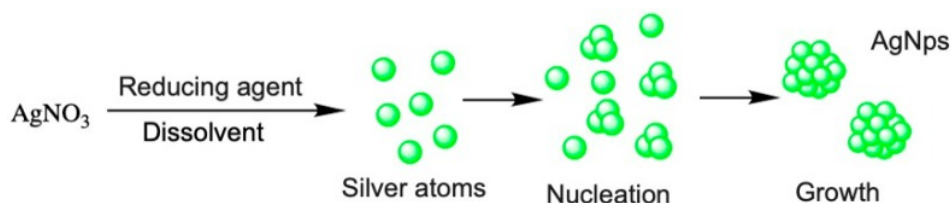


**Figure 34. Process for the synthesis of AgNPs.**

Schematic representations of synthesis of colloidal silver nanoparticles using chemical reduction process. Silver ions ( $\text{Ag}^+$ ) subjected to chemical reduction to form silver atoms ( $\text{Ag}^\circ$ ) (Sánchez-López et al., 2020).

Recently, biosynthesis method of NPs preparation has been under intense study. The interest toward NPs biosynthesis leads on using fewer chemical products and on involving biological entities: plants, fungi and bacteria. It is considered as an eco-friendly (green) method at also relatively low cost.

Interestingly it has been found that bacteria can use mainly, two ways to produce NPs. 1- It can use specific enzymes that are capable to react with addition of silver ions ( $\text{Ag}^+$ ) and transfer them to natural form of silver ( $\text{Ag}^\circ$ ). This process sort as intracellular biosynthesis method because of the use of enzymes formed by the bacterial cell. 2- The extracellular methods will refer to the use of, for example, the bacterial culture supernatant and the cell free extract.

Many studies have reported NPs biosynthesis using different models of bacterial cells (Gram-positive and Gram-negative) such as *E. coli*, *Pseudomonas stutzeri* AG29 and *Bacillus subtilis*. Depending on the method followed, NPs can be seen formed outside of the cells and/or accumulated inside the cells (Haefeli et al., 1984; Javaid et al., 2018; Mikhailov & Mikhailova, 2019).

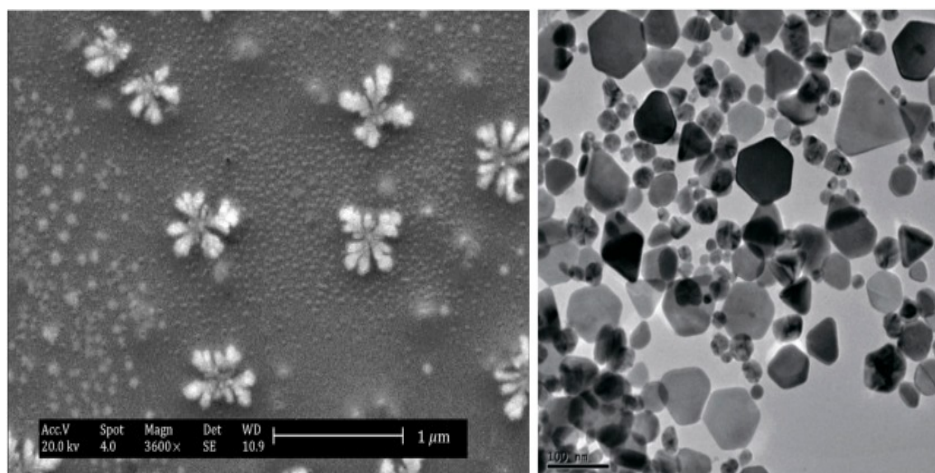


**Figure 35. Silver nanoparticles by biosynthesis methods.**

SEM image of Ag-NPs self-assembly by culture supernatant of *Streptomyces* sp. (left). TEM image of Ag-NPs by *Bhargavaea indica* DC1 (right) (Faghri Zonooz & Salouti, 2011; Singh et al., 2015).

#### **8.2.4 Ag-NPs characterization**

---

Among tools that are used to characterize the obtained Ag-NPs, UV–Vis spectrophotometry is the most common one, since it is possible to use the optical properties as spectral signature, giving likely direct access to size and shape for instance. The spectra of different sizes silver nanospheres and nanoplates and the appearance of dilute dispersions of the nanoparticles are shown in (Fig. 36). Smaller nanospheres absorb visible light and have plasmon resonance peaks near 400 nm (red). Larger spheres show increased scattering and have peaks near longer wavelengths (toward yellow). Silver nanoplates usually have large absorbing and scattering profile because of their anisotropic shape and then displays optical response at larger wavelength (toward the blue). The plasmon resonance can be tuned to peak at specific wavelengths by controlling the diameter, shape and thickness of the coating of the particle (Moores & Goettmann, 2006).

In addition, others technique and equipment are essential such as X-ray diffractometry (XRD), transmission electron microscopy (TEM), inductive coupled

plasma (ICP), and electrochemistry measurement (Zeta potential). The collective data given, can enable us to have fully Ag-NPs characterizations including shape, size, size distributions, particles stabilization and their concentration (Sánchez-López et al., 2020).

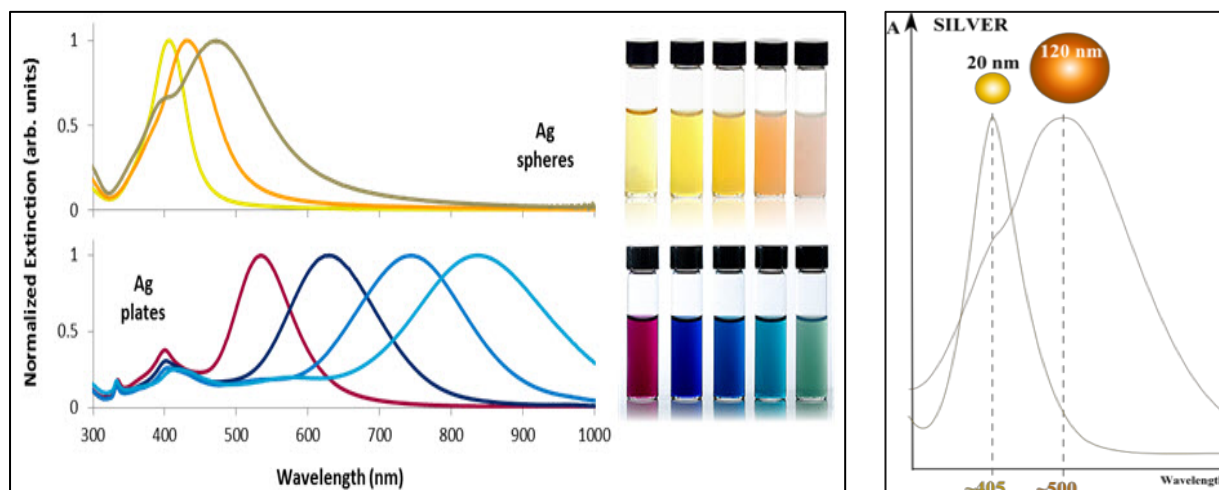


**Figure 36. Optical extinction spectra and solution appearance of silver nanospheres.**

On the right, selected optical extinction spectra and solution appearance of silver nanospheres between 10 and 100 nm in diameter (top) and silver nanoplates between 50 and 150 nm in diameter (bottom). Control over nanoparticle shape and size allows the plasmon resonance to be tuned across the visible and near-infrared portions of the spectrum (Djafari, 2019). On the left, UV-Vis spectra profile of metallic silver NPs in function of its size and composition (Oldenburg, Sigma.Aldrich).

### 8.3 Imaging and morphology analyzing tools

In the field of microbiology and nanotechnology, the microscope is a very important and essential apparatus for events characterizations and visualizing interaction that occur at nanometer average of size (Guerrero, 2000; Hamouda et al., 2019). In the frame of this study, it was used to try to visualize the mechanism of metal toxicity and describe the impact of the interaction between the biological subjects (the bacteria) and the physical objects (metal ions/NPs) on the surface of the cells. We have used the scanning electron microscope (SEM) and the atomic force microscope (AFM). Each microscope provides a significant analysis data from different perspectives that enables us to propose a novel mechanism of metal toxicity in bacteria.

Usually, these microscopes are associated with softwares and programs that are required to quantitatively analyze the obtained images. In this study, we have used for example ImageJ, Gwyddion or Nanoscope analysis.

### **8.3.1 Electron Microscopy**

---

The electron microscope is an important tool to image bacteria with great details. It enables us to access the morphology of bacterial cells and visualize their interaction with metals. There are two main types of it: the scanning electron microscope (SEM) and the transmission electron microscope (TEM).

In the SEM, electrons beams are used to generate a grayscale image of the sample at very high magnifications and resolution (Golding et al., 2016; Kaláb et al., 2008). The advantage of SEM is its ability to get a 3-dimension like images of bacteria and as closest to their natural appearance. It is also easy to manipulate for both sample introduction and progressive scales imaging.

In the case of TEM, the electrons beams pass through the sample exposed. It forms images as a shadow-like photographed on a fluorescent screen or CCD cameras (Kaláb et al., 2008).

The disadvantage of electron microscope, in general, is to take the bacterial samples through multiple steps of preparation such as: isolation, fixation, dehydration, and drying. There are other factors to have in consideration as well for after, when looking at the sample. Depends on the microscope used and the nature of the sample, the sample may be placed in a high vacuum chambre. For specimen sample such as bacteria, a special preparation is essential to protect the structure and the cell membrane that contain proteins, lipids, and high percentage of water. Thus, it this technique must be selected very carefully and have in consideration all the process of preparation that the sample will go through (Kaláb et al., 2008).

The Energy-Dispersive Spectrometer (EDS), is one among many associated tools for sample analysis. The (EDS) can get you an access to chemical analysis and mapping of

the sample; and the information can be acquired during imaging process. The generated data consists of spectra with peaks that corresponding to different elements signature, that are present in the sample. Every element has characteristic peaks of unique energy (Fig. 37) (Wang et al., 2016).

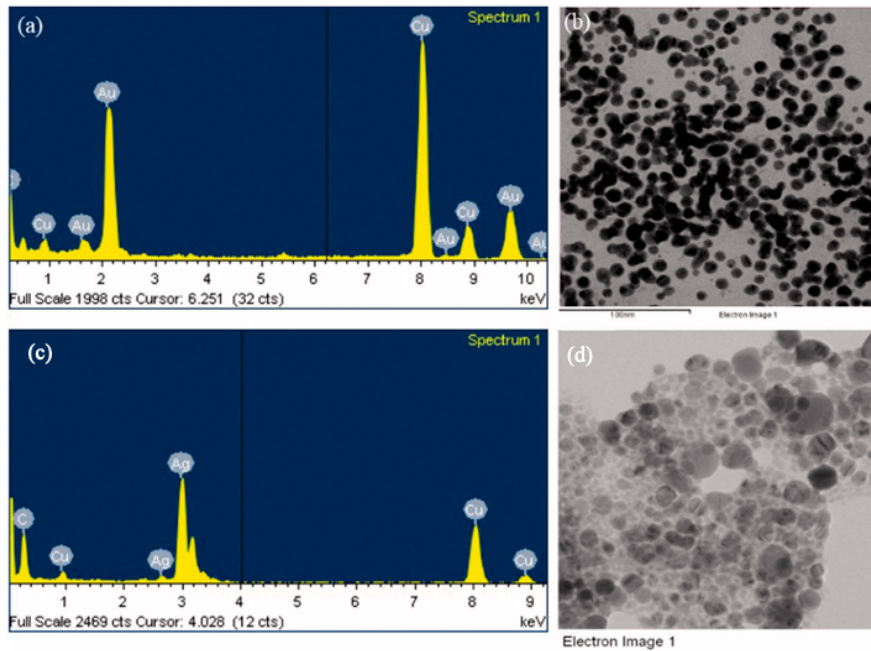


**Figure 37. EDX spectrum and electron images metal nanoparticle.**

EDX spectrum and electron micrograph region of gold nanoparticles (a) and (b). EDX spectrum and electron micrograph region of silver nanoparticles, (c) and (d) (Wang et al., 2016).

### 8.3.2 Atomic Force Microscope

Since it was invented in 1986 (Binnig et al., 1986), the atomic force microscope (AFM) has become an essential and common tool in microbiology and nanotechnology and it was our principal imaging device. Beside the ability to achieve nanoscale imaging and mechanical measurements, one can obtain images from dried microbial samples and/or live cells, since it can operate on soft and nonconductive materials. It can be combined with other analytical techniques for example with optical microscopy and spectroscopy, thus, providing great opportunities to collect more data of biological

samples in general and microbial samples (Flores & Toca-Herrera, 2009; Oreopoulos & Yip, 2008) in particular.

AFM enables high resolution images at nanoscale by scanning and sensing the small forces between the surface of a sample and sharp end tip (probe) (Dufrêne, 2014; Müller et al., 2009). The collected images are reproduced with the analysis of the position of reflected laser motion, on the tip at the end of a cantilever (Fig. 38). The image's resolution depends on the quality and nature of the tip; and can reach in some ideal conditions atomic scale resolution.

AFM operates in two main modes: contact mode and non-contact (tapping) mode. While contact mode detects the repulsion force, the non-contact mode detects the variation induced to tip oscillation by the Van der Waals force between the tip and atoms (samples scanned) (Fig. 39). The latter mode is most often used when contact mode can damage either the sample or the tip. This is almost always the most suitable mode for biological imaging (Dufrêne et al., 2017; Nguyen-Tri et al., 2020).

AFM is considered to be the best tool in the field of microbiology to observe morphological changes and to detect distortions that can occur on the surface of cell membrane and visualize it at a very high resolution (Liu & Wang, 2010). While SEM and TEM can also provide nanoscale images, yet, they require lots of sample preparation that include chemical metal coating, and/or ultrathin section. Such process for sample preparation leads to distort the microbial cells and the sample substantially (Liu & Wang, 2010).

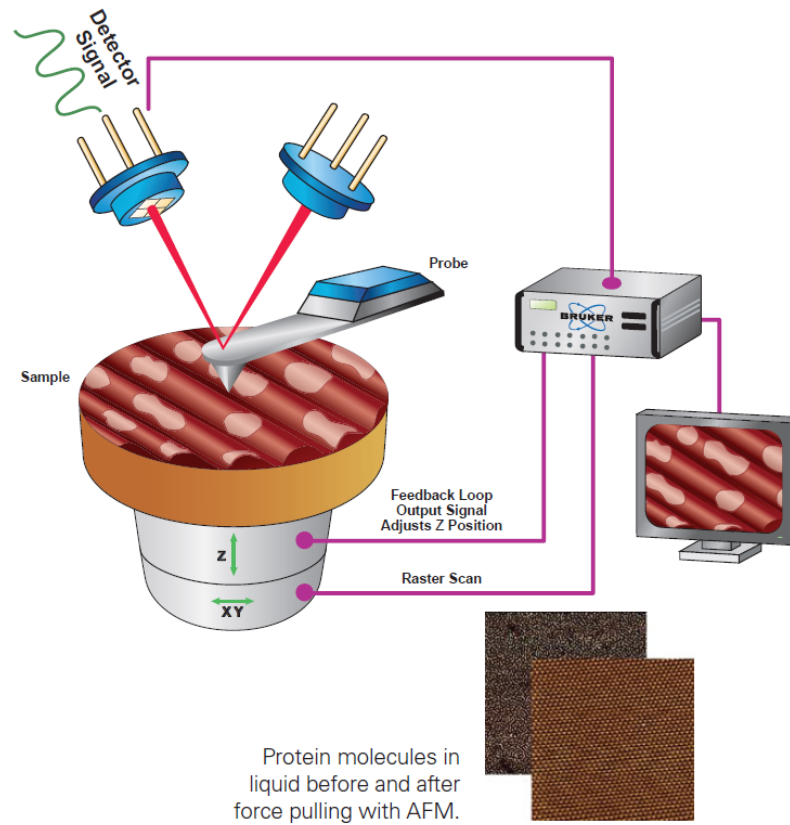


**Figure 38. Schematic of the Atomic Force Microscope AFM.**  
(*AFM Microscopes. Bruker, n.d.*)

The AFM images quality depends on many mechanical factors. The cantilever for example must be calibrated and installed well because the movement of the tip is depending on it. The tip must be selected carefully to be adapted to the nature of the examined sample. For correct images of a biological cell, it is necessary to avoid direct contact between the sharp tip and the surface of the cell membrane that may lead to damaging and changing the nature of cell's surface. The tip characteristics concerned tip geometry, its composition and mechanical properties. Tip and cantilever can undergo wide range of displacement, compression or distortion due the interaction forces between the tip and the surface at short ranges. We use cantilever with height about 10 – 15 mm and highly doped silicon to dissipate static charge (Fig. 40). It is also recommended to use a sharp tip and a soft cantilever for imaging biological sample,

so it adapts to surface roughness and surface fractal dimension. Another important point is to avoid having the tip contaminated (Raposo & Ferreira, 2007).

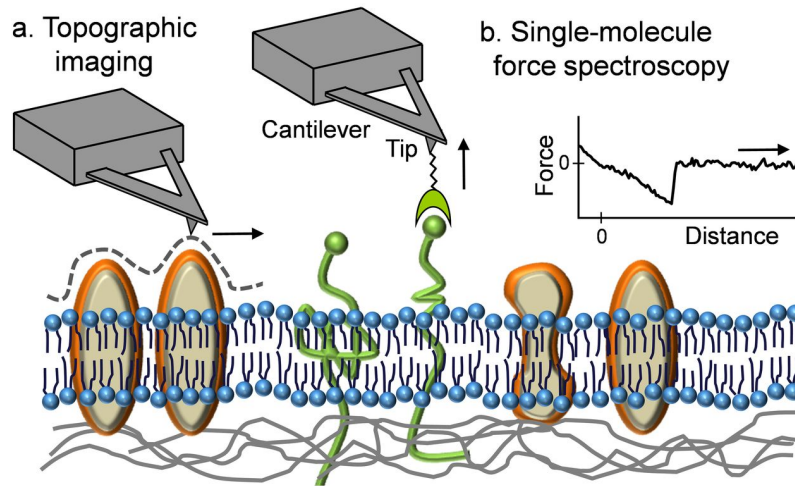


**Figure 39. Atomic force microscopy.**

AFM works by sensing the tiny forces between a sharp tip and the sample surface. (a) In topographic imaging, the tip scans the cell surface in buffer with nanometer-scale resolution. (b) In single-molecule force spectroscopy, the small interaction force between the tip and cell surface molecules is measured while the distance between the tip and cell is varied, thereby yielding a force-versus-distance curve; as shown in the cartoon, the tip is generally labeled with a ligand to detect, localize, and manipulate individual receptors (Dufrêne, 2014).

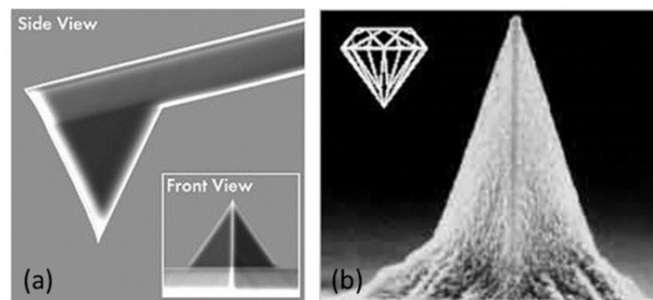


**Figure 40. AFM cantilever and tip.**

AFM Si<sub>3</sub>N<sub>4</sub> tip with Cantilever (a) and diamond coated AFM tip (b) (Nguyen-Tri et al., 2020).

The quantitative analysis of the surface profile is important to have in consideration even during imaging. There are several settings that are automatically saved while imaging but taking into account while imaging calibration, sampling,

elimination of offset, systematic slope correction, makes the post-imaging process easier and more relevant. The topological (height) and peak force error (mechanical) are the most analysed images. In (Fig. 41) we show an example of images regarding the interaction of bacterial cells with metals which appear in both phases height and peak force error (Huang et al., 2015).

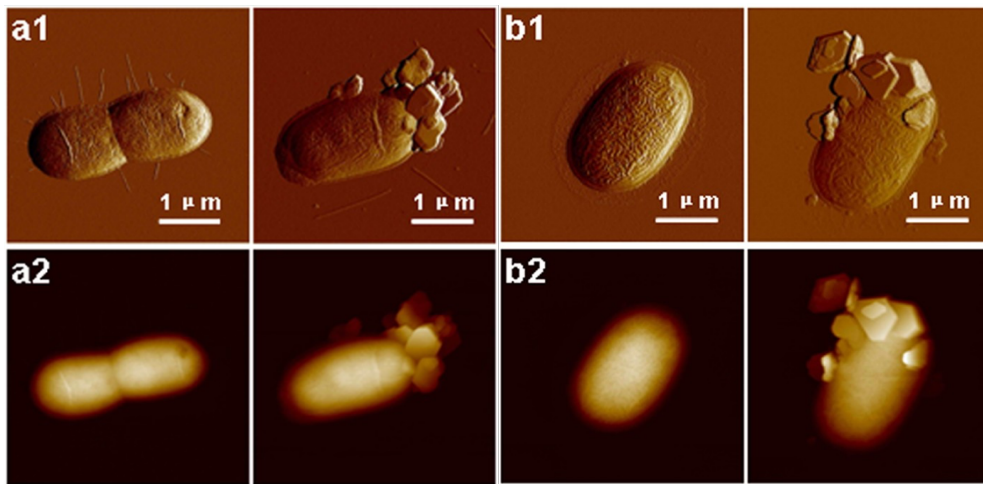


**Figure 41. AFM images of bacteria and their aggregates with minerals in air.**

Peak force error and height images of *E. coli* (a1,a2), *P. putida* (b1,b2) control and their aggregates with kaolinite (Huang et al., 2015).

The AFM overall data quality and accuracy of surface properties can be well accomplished through the control and adequation of tip and cantilever characteristics but also the scan feature (speed, resolution, sampling, ...). In addition, and for a complete morphology profile description of sample's surface, it is important to define and determine morphological reference parameters. A fully final morphology profile focusing on membrane cells change, for instance, will certainly include the distribution of heights, skewness and kurtosis moments as well (Raposo & Ferreira, 2007).



## 9. State of the Art

---

### i- Metal homeostasis in photosynthetic bacteria

The majority of studies regarding the characterization of metal homeostasis, including copper, zinc or iron, has been carried out in microorganisms such as *E. coli*, *Pseudomonas aeruginosa*, *Salmonella thyphimirium*, and *Bacillus subtilis* (Chandrangsu et al., 2017). In photosynthetic organisms, the homeostasis systems were also well studied in cyanobacteria (Cassier-Chauvat & Chauvat, 2014; Huertas et al., 2014; Shcolnick & Keren, 2006), algae (Blaby-Haas & Merchant, 2017), and plants (Pilon et al., 2009). In particular, it was shown that excess or limitation on copper in these photosynthetic organisms can affect photosynthesis and photopigments.

Very few studies refer to mechanisms of copper homeostasis and toxicity in photosynthetic bacteria.  $\text{Cu}^{2+}$  excess was mainly investigated in cyanobacteria; and it has received very little attention in purple bacteria. Studies of copper homeostasis was primarily investigated in the purple bacterium *Rhodobacter* species (Rademacher et al., 2012; Selamoglu et al., 2020). To overcome this lack of data, *R. gelatinosus* is also very good model to study and understand copper homeostasis and impact of copper excess on photosynthetic and respiratory complexes. In the last years, the group directed by S. Ouchane, started looking at the copper homeostasis system and its importance for respiration and photosynthesis in this bacterium. Bahia Hassani finished her PhD study with questioning the ability of *R. gelatinosus* to tolerate excess copper ions. Her thesis has highlighted the role of a  $\text{Cu}^+$ -ATPase CtpA, a homologue of CopA, in the biogenesis and activity of cuproenzymes (heme-copper  $\text{cbb}_3$  oxidase) in *R. gelatinosus*. However, it was found that CtpA is not necessary for the growth on a high copper concentration (Hassani et al., 2010a). Another PhD student, Asma Azzouzi, continued this study and identified the efflux system (CopA and CopI) in copper tolerance in *R. gelatinosus* (Azzouzi et al., 2013, Durand 2015). More importantly, she identified a direct target of copper (HemN) and her study allowed also the identification of targets within the chlorophyll biosynthesis pathway (Liotenberg et al 2015). Moreover, the group has also

started looking at the effect of non-redox active metal, cadmium, on photosynthetic and respiratory complexes. I arrived in 2016, with the interest to study silver and copper homeostasis and toxicity in *R. gelatinosus*. Because silver is one of the most used metal in the field of nanoparticle technologies and in healthcare facilities, we decided to study the effect of silver on *R. gelatinosus*.

Silver ions or silver alloy products are common in medical use and industrial applications as antimicrobial agents. Ag<sup>+</sup> resistant bacteria have been isolated (Asiani et al., 2016; Muller & Merrett, 2014; Sedlak et al., 2012), and despite the extensive use of this metal, the molecular basis for Ag<sup>+</sup> resistance and toxicity were studied in very few species like *E. coli* and *S. typhimurium* (Asiani et al., 2016; Rensing et al., 2000). In cyanobacteria (*Oscillatoria brevis*), Ag<sup>+</sup> induces metallothionein and an ATPase, but the effect on photosynthesis was not reported (Liu et al., 2004). There is no data on silver homeostasis and toxicity mechanisms in other photosynthetic bacteria.

### ***ii- Metal Homeostasis in the purple bacterium Rubrivivax gelatinosus***

The  $\beta$ -proteobacterium *Rubrivivax (R.) gelatinosus* has been introduced to the photosynthesis laboratory of Gif-sur-Yvette in 1991 by Françoise Reiss and Chantal Astier, to develop the genetic and structural studies of the photosynthetic apparatus in purple  $\beta$ -proteobacteria (Agalidis & Reiss-Husson, 1991). It is an environmental Gram-negative bacterium that thrive in soil and water biotopes (Uffen, 1976). The name *gelatinosus* is derived from its ability to dissolve gelatine. It has a rod shape and motile by single polar flagellum. The cell size in the range of 0.4 - 0.5  $\mu\text{m}$  width and  $\sim 4 \mu\text{m}$  length (Nagashima et al., 2012; Sheu et al., 2020; Willems et al., 1991). In the presence of light and anaerobically, the bacterium performs anoxygenic photosynthesis to produce ATP. In the presence of oxygen, *R. gelatinosus* uses a branched aerobic respiratory chain for ATP synthesis (Hassani et al., 2010b). The first studies carried out on this bacterium focused on the structural characterization of the photosynthetic complexes (Ranck et al., 2005; Scheuring et al., 2001), and the study of genes coding for the different components of the photosystem as well as the genes coding for the

enzymes of the photopigment synthesis pathway (Francki et al., 2000; Ouchane et al., 1995, 1997; Pinta et al., 2002). Then, studies were directed on regulation of bioenergetics pathways by light and oxygen (Liotenberg et al., 2008; Ouchane et al., 2007; Steunou et al., 2004).

These first studies have shown interesting characteristics of *R. gelatinosus* bacterium. These characteristics include: (i) the existence of a tetrameric cytochrome linked to the reaction center, (ii) the presence of a HiPIP (High Potential Iron Protein) and two light harvesting complex antennae, (iii) the existence of two carotenoid biosynthesis pathways; (iv) different organization of the genes involved in photosynthesis; and (v) different adaptation to oxygen. Also, Hassani and Steunou have demonstrated the role of terminal oxidases in the photosynthetic metabolism in *R. gelatinosus* (Hassani et al., 2010b). Studies on the biogenesis of the "heme-copper" *cbb<sub>3</sub>* oxidase have also been initiated with particular interest in the copper transport and insertion in the active site of the oxidase (Durand et al., 2018; Hassani et al., 2010a). These studies revealed also that *R. gelatinosus* has a relatively high tolerance to certain metals such as copper and cadmium (Hassani et al., 2010a).

Azzouzi's thesis work indicated that copper homeostasis involved the *cop* operon (*copARHLI*) that encode for the Cu<sup>+</sup>ATPase CopA, the Cu<sup>+</sup> sensor/regulator CopR (CueR) and three periplasmic proteins CopI, CopH and CopJ also required for copper tolerance. The operon is under the control of CopR. Asma also showed for the first time, that copper targeted many enzymes in the tetrapyrrole biosynthesis, namely, the coporphyrinogen III oxidase, the Mg-chelatase and the protochlorophyllide reductase, and thereby affects the cytochrome oxidase and the photosystem (Azzouzi et al., 2013; Liotenberg et al., 2015).

More recently, work conducted by Steunou revealed an interplay between the Cu<sup>+</sup> and Cd<sup>2+</sup> efflux ATPases. The efflux system required to tolerate Cd<sup>2+</sup> in *R. gelatinosus* correspond to the Zn<sup>2+</sup> and Cd<sup>2+</sup> ATPase CadA and its regulator CadR. Cadmium was also shown to induce copper tolerance system (CopA and CopI) in this

bacterium (Steunou et al., 2020a). Similarly, to copper, accumulation of cadmium in the bacterium also resulted in a porphyrin deficient phenotype. It was shown that  $Cd^{2+}$  target the coporphyrinogen III oxidase, HemN in the bacterium (Steunou et al., 2020a).

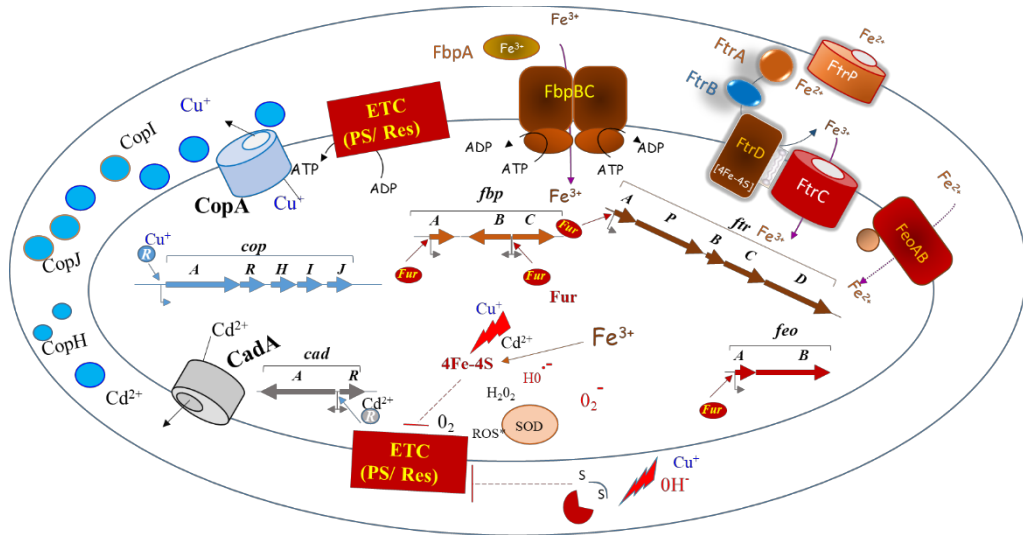


**Figure 42. Interplay between metal efflux, iron uptake and ROS detoxifying system.**

In the absence of the efflux ATPases CopA or CdaA accumulation of  $Cu^+$  or  $Cd^{2+}$  in the cytosol led to the degradation of [4Fe-4S] clusters. 'Released iron' originating from this degradation could rapidly be sequestered or exported out of the cells, thus generating an iron-depleted status in the poisoned cells. Consequently, iron uptake is induced to rebuild [4Fe-4S] clusters and the superoxide dismutases are induced. It was supposed that released iron could generate ROS, but oxidative stress may be further exacerbated by the induction of Fe-uptake in response to damaged Fe-S clusters. ETC: electron transfer chains (respiration or photosynthesis) are also poisoned by excess metal. ETC generate ATP for the ATPases but can also generate superoxide (Steunou et al., 2020c). Operons encoding efflux and import systems are shown.

Finally, to further characterize the mechanisms of response and toxicity of both metals, our group has highlighted the role of  $Fe^{2+}$  homeostasis and import in the response and resistance to  $Cu^+$  and  $Cd^+$  (Steunou et al., 2020c). At least three  $Fe^{2+}/Fe^{3+}$  uptake system were identified. Two of them (Fbp and Ftr) are involved in iron uptake in the bacterium and required in the response to excess metals. The overall findings of

all these previous studies depicted in (Fig. 42) rationalize metal excess toxicity in this bacterium and very likely in other organisms.

As reported above, consequences of  $\text{Cu}^{2+}$  or  $\text{Cd}^{2+}$  intoxication are direct damage to Fe-S proteins and ROS production. As cofactor, Fe-S clusters participate in many vital electron-transfer processes, especially in photosynthesis, respiration. Given their crucial role, intoxicated cells should repair or synthesize *de-novo* the Fe-S clusters, and for that purpose, they need to import iron. This work emphasized the importance of maintaining  $\text{Fe}^{2+}$  and Fe-S clusters homeostasis in response to metal intoxication by  $\text{Cu}^{2+}$  or  $\text{Cd}^{2+}$  in photosynthetic bacteria (Steunou et al., 2020c).

### ***iii- Specific actions of metal nanoparticles***

In the beginning of last century, the first observation and control of gold nanoparticles was achieved through the study of colloidal solution by Richard Adolf Zsigmondy who was awarded with Nobel prize for his extraordinary finds in 1925 (Zsigmondy, 1926). Since then, discovery of new techniques and strategies enable scientists to perform more efficient synthesis of NPs and get better control of their targeted properties. There are now a huge number of methods to synthesize metals nanoparticles (MNPs) in the laboratory. Methods for MNPs synthesis are even selected based on the goal and the application pursued (Brigger et al., 2002; Forestier et al., 1992; Merisko-Liversidge et al., 2003). Silver is one of the most used metal in the field of nanoparticles technologies and in healthcare facilities, but the actual mechanisms of its action as an antimicrobial agent and the specific impact of NPs due to their peculiar properties regards to silver ions actions is still not completely described (Möhler et al., 2018).

The complexity of this study requires a different (multidisciplinary) approach to that of antibiotic or toxicity tests used for conventional compounds. Indeed, the physicochemical parameters (stability, aggregation, dissolution and surface state) of nanostructures in the contact medium strongly influence the toxicity observed on cells (Ahmad et al., 2019; Nel et al., 2009). In addition, physicochemical interactions

(floculation, adsorption, redox mechanisms) are related to the biological model, in particular the presence of exopolysaccharides for some bacteria, as a natural barrier between the cell wall and nanoparticles (Ansari et al., 2018; Navarro Gallón et al., 2019). Culture media influence, since they contain chemical compounds that could precipitate or neutralized the metal ions, is too often ignored or underestimated (De Leersnyder et al., 2018; Johnston et al., 2018). Biosynthesis of nanoparticles is more and more reported and studied (Bao & Lan, 2019). Nanoparticles are biosynthesized when the microorganisms involved grab target ions from their environment and then transform the metal ions into metal nanoparticles or precipitates through enzymes generated by the cell activities for example. It can be classified into intracellular and extracellular synthesis according to the location where nanoparticles are formed (Mann, 2001; Simkiss & Wilbur, 2012). The intracellular method consists of transporting ions into the microbial cell to form nanoparticles in the presence of enzymes. The extracellular synthesis of nanoparticles involves trapping the metal ions on the surface of the cells and reducing ions in the presence of enzymes (Zhang et al., 2011). If we can consider naïvely, that the main purpose of fundamental cells as bacteria is to survive, it is understandable to link this ability in NPs synthesis to a protection mechanism toward survival (AbdelRahim et al., 2017).

It appears that the study of the compared effects of silver ions ( $\text{AgNO}_3$ ) and nanoparticles (AgNPs) on *R. gelatinosus* could be very interesting with a distinct goal of imaging the processes involved at submicron scale between the bacterial and the metal. The collaboration into a multidisciplinary team will have from this point of view, a special added value.

In the lab of NANO<sup>3</sup> (Nanoparticles, Nanostructures, Nanomaterials) – in LAC, research project concerns the synthesis and characterization of nanoparticles and nanostructures and their recovery in different applications: health, energy, or engineering. Nanoparticles and nanostructures are synthesized using physical process (gas aggregation source, UHV chamber deposition) or chemical synthesis (reduction of

precursors, electrospray deposition). These NPs can be prepared as dry samples which are deposited on different substrates such as: graphite, mica and metal or oxides substrates (Kébaïli et al., 2009) or in solution (Djafari et al., 2016, 2018, 2019). The main added value relies on the control of the size, shape, nature and stability of the obtained structures but also on the comprehension of the self-organisation mechanism on substrate, including the study of the effect of topology and surface curvature on the morphology of the nanostructures obtained (Kemper et al., 2009; Schmidt et al., 2008), the stability of fractal nanostructures and the mechanisms of their relaxation induced by chemical or thermal activation (Solov'yov et al., 2014; Wu et al., 2012), the possibility of using clusters through their interaction with the surface as a probe for fine characterization of these (Kébaïli et al., 2009) surfaces, the study of the aging of this structures (Lion, Sarfati, Kebaili., submitted 2020). This last study is essential for predicting the behavior and timekeeping of future applications. The team has also recognized skills in nanoscale characterization (SEM, STEM, AFM, STM microscopies, EDS, XPS, UV-V spectroscopies).

For my study, I focused on the synthesis of silver nanoparticles prepared in liquid solutions, thus, made it easier to manipulate experiments on bacterial cells culture; which usually prepared on liquid medium as well. I was able to synthesize silver NPs chemically in the lab. Successfully, we were able to obtain Ag-NPs in size rang (from  $12 \pm 2$  nm to  $25 \pm 5$  nm); in addition to the ability to control their size and have them stabilized. The aim is to study the Ag-NPs toxic effect on bacteria and compare the results to demonstrated data with Ag ions, in previous work of the same project (Tambosi et al., 2018), we have elucidated that silver is highly toxic and it inhibits the growth of bacteria even at a very low concentration. Also, that  $\text{Ag}^+$  have great impact on membrane proteins in both photosynthetic and respiration complexes.

Moreover, I have also built the skills to use microscopes as the atomic force microscope (AFM), the scanning electron microscope (SEM) and the transmission electron microscope (TEM). They are essentials tools in the field of nanoscience to

characterize the NPs prepared. Also, in the field of microbiology to study the interactions between the physical objects (metal) and biological subject (bacteria) at the relevant scale. This was one of the main goals of this study which basically aim to understand the interaction, the localization and the morphological structure change occur on the cell's membrane under metal stress.



# OBJECTIVE OF THE THESIS

---

Given their importance in sustaining life, and/or their acute toxicity, many studies have investigated the homeostasis and impact of metals in both prokaryotes and eukaryotes. Yet, there are still important gaps regarding our comprehension of metal homeostasis and toxicity mechanisms. Several reasons for this, among which: i- some metals have attracted more attention than others, ii- most studies of metal toxicity focus on one type of metal, although organisms face mixture of metals in their environment and iii- in many cases, bacteria whose metal homeostasis have been studied are primarily pathogenic bacteria, although biodiversity can be an inexhaustible source of new discoveries...

For photosynthetic bacteria, most studies focus on cyanobacteria, which is very understandable given their role in biomass production, their contribution to shaping our atmosphere and their functional and structural homologies with the photosystems from algae and plants. Nevertheless, photosynthetic proteobacteria are also environmental bacteria that have other advantages such as the simplicity of their photosystem and photo-pigments (while showing similarities with algae and plants), their growth and adaptive abilities and the availability of many molecular and genetic tools. In this context, I was interested in investigating the impact of silver and copper excess on the purple photosynthetic bacterium *R. gelatinosus*. The goal of this project is to study the interaction between biological subject (bacterial cell) and physical objects (metals), and to understand the impact of these metals in different forms (ions and nanoparticles) on photosynthetic and respiration growth of the bacterium.

In order to gain mechanistic insights into the adaptive responses of *R. gelatinosus* to metal stress, the essential objectives are i) to study the impact and the

mechanisms of toxicity of these metallic ions/NPs on the bacterial respiratory/photosynthesis metabolisms. ii) to identify the bacterial genes involved in response to excess  $\text{Ag}^+$  ions, and iii) to study the interaction of metal ions and NPs with cell surface.

The data obtained during my PhD thesis term are presented in four parts in the results section:

**Part I:** In this study, we were interested in silver and copper targets and their effect on photosynthetic and respiration membranes and complexes. Data was published (Tambosi et al., 2018).

**Part II:** This part presents our tentative approach to identify genes that may play role in silver tolerance in *R. gelatinosus*.

**Part III:** This part focus on the effect of silver on bacterial cell structure and morphology using microscopy (SEM and AFM). The aim is to give a second perspective (morphological characterization) to the first part regarding the interaction between silver ions and the bacterial membrane (Tambosi et al., submitted 2020).

**Part IV:** This part shows results regarding metal nanoparticles synthesis, characterization, and preliminary results on biological applications using these NPs.

Finally, some of my contributions to ongoing projects in the laboratory with other members of the team, are presented as additional research. One study highlighted the cross-tolerance between cadmium and copper efflux systems (Steunou et al., 2020a). The second paper reports the importance of superoxide dismutase (SodB) and its requirement to protect exposed cells to heavy metals (Steunou et al., 2020b).

-

More recently, we got preliminary results on the effect of silver in the culture mediums, regarding silver ions precipitations and NPs synthesis (Djafari et al., submitted 2020).



# RESULTS

---

Metals such as  $\text{Cu}^{2+}$ ,  $\text{Zn}^{2+}$  or  $\text{Ag}^+$  compounds are widely used in many fields for their antimicrobial properties. Nevertheless, the extensive use and spread of metal ions or nanoparticles represent a serious threat to the environment and to all living organisms because of the acute toxicity of most metal ions. Nowadays,  $\text{Ag}^+$  nanoparticles are one of the most widely used nanoparticles in many industrial and healthcare applications. The antimicrobial effect of  $\text{Ag}^+$  nanoparticles is in part, related to the released  $\text{Ag}^+$  ions. It is therefore important to characterize the toxicity of  $\text{Ag}^+$  ions and to identify cellular targets of this metal to foresee the toxicity of nanoparticles.

My work focused thus, on understanding the impact of silver and other metals on purple photosynthetic bacteria. I used silver in forms of ions ( $\text{AgNO}_3$ ) and nanoparticles (Ag-NPs). For the biological model, I used the photosynthetic bacterium *R. gelatinosus* and other non-photosynthetic bacteria as a control. This project included also other metals, as control, such as copper and cadmium. The main reasons are that  $\text{Cu}^+$  and  $\text{Ag}^+$  follow the same efflux and detoxification routes in *E. coli* and other species, while cadmium has its own efflux system. In addition,  $\text{Ag}^+$  is not redox active as  $\text{Cd}^{2+}$ , in contrast to  $\text{Cu}^{2+}$ .

# 1. In Vivo Target of Silver and Copper

---

## Introduction:

---

The homeostasis and toxicity of biological active metals ( $\text{Fe}^{2+}$ ,  $\text{Cu}^{2+}$ ,  $\text{Zn}^{2+}$ ,  $\text{Co}^{2+}$ ,  $\text{Mg}^{2+}$ , etc) have been widely studied because of the importance of these metals in various metabolisms within the cell. Non-essential metals, however, were less attractive, but due to their toxicity and industrial or medical interest, many studies were conducted in the last years to have a better understanding of their toxicity mechanisms in both prokaryotes and eukaryotes. Furthermore, the fast rate of the development in the nanotechnology field using metals have raised awareness and prompted to study their impact on the environment and organisms.

Silver is a non-essential, but a potent toxic metal including in bacteria. In *E. coli*,  $\text{Ag}^+$  ions damage the [4Fe-4S] exposed clusters in dehydratases (Xu & Imlay, 2012). *E. coli* uses the  $\text{Cu}^+$  efflux systems (CopA and CusCFBA) to extrude  $\text{Ag}^+$  from the cell (Bondarczuk & Piotrowska-Seget, 2013). Very few studies refer to mechanisms of  $\text{Ag}^+$  homeostasis and toxicity in cyanobacteria, while no study was reported to date on photosynthetic proteobacteria.

*R. gelatinous* is a good model to assess the effect of metal on the photosynthetic and respiratory complexes. Indeed, previous studies in the laboratory had identified targets of copper and cadmium, in particular in the biosynthesis pathway of heme and bacteriochlorophylls (Azzouzi et al., 2013; Steunou et al., 2020a).

In this first study, we investigated the *R. gelatinosus* behavior under  $\text{Ag}^+$  stress under different growth conditions. The aim is to assess the effect of  $\text{Ag}^+$  on growth and to identify the proteins that can be damaged by this metal. As a control for the specific effects of  $\text{Ag}^+$ , we used  $\text{Cd}^{2+}$  and  $\text{Cu}^{2+}$ , and to confirm our results, we assess the effect of  $\text{Ag}^+$  on *E. coli* and *B. subtilis*. Our results showed that silver and copper affect the activity of membrane complexes involved both in photosynthesis and in respiration and suggested that  $\text{Ag}^+$  and  $\text{Cu}^+$  could damage exposed prosthetic groups such as

chlorophylls and heme in proteins as explained in the introduction section of this manuscript (Fig. 22) (Dalecki et al., 2017).

### **Summary and main findings:**

---

In this work, we started looking at the effect of silver on the growth of wild type (WT) *R. gelatinosus* in comparison with  $\text{Cu}^{2+}$  and  $\text{Cd}^{2+}$ . Interestingly, the analyses showed that  $\text{Ag}^+$  was very toxic even at very low concentration compared to  $\text{Cu}^{2+}$  and  $\text{Cd}^{2+}$ . It is established that, thanks to the ATPases CopA and CadA, *R. gelatinosus* tolerates high concentration of  $\text{Cu}^{2+}$  and  $\text{Cd}^{2+}$  respectively (Azzouzi et al., 2013; Steunou et al., 2020a). This was the first indication that  $\text{Ag}^+$  does not induce or use Cop or Cad efflux systems in this bacterium, in contrast to other species. This was confirmed by western blot and analyses of the growth of the *copA*<sup>-</sup> deficient mutant.

The presence of photopigments in the bacterium allows a rapid investigation of the effect of metals on photosynthesis. Indeed, UV-Vis spectra can provide qualitative and quantitative data regarding the photosynthetic complexes within the membrane of the bacterium. In this respect, analyses of WT cells grown photosynthetically and exposed to  $\text{Ag}^+$  ions, revealed a significant decrease in the amount of the light harvesting LH2 (B800-850). More specifically, the decrease affects only the 800 nm bacteriochlorophyll of the LH2 complex. This 800 nm specific decrease was also observed when cells were exposed to  $\text{Cu}^{2+}$ , but not to  $\text{Cd}^{2+}$  or  $\text{Ni}^{2+}$ .

Moreover, analyses of these spectra and the position of the Bch 800 and 850 in the crystal structure of the LH2 allowed us to conclude that  $\text{Ag}^+$  and  $\text{Cu}^{2+}$  damage the light harvesting LH2 by targeting the exposed Bch 800 (Fig. 43). The bacteriochlorophylls within the LH1 or RC or the Bch 850 of LH2 should be protected by the protein structure against metal damages.

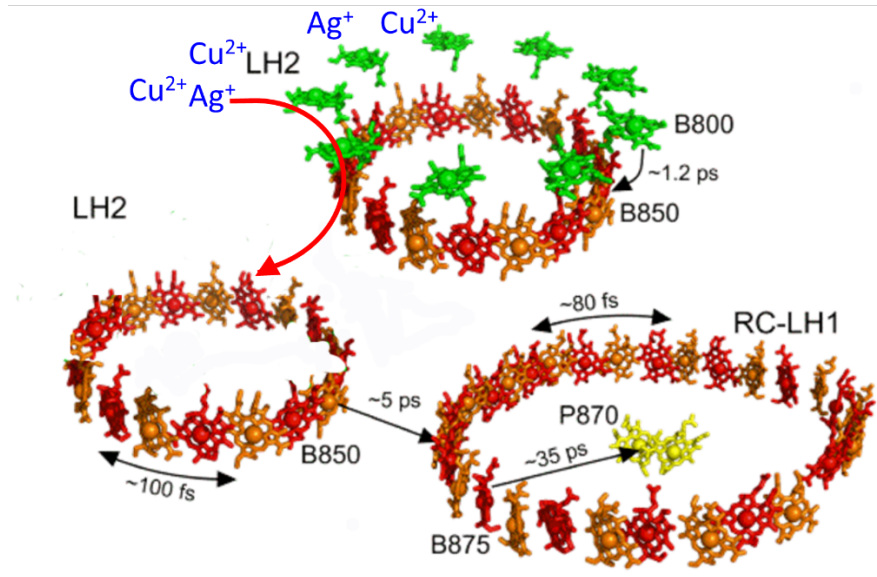


**Figure 43. Effect of Ag<sup>+</sup> and Cu<sup>2+</sup> on LH2 antennae.**  
Only the Bch 800 is damaged upon Ag<sup>+</sup> and Cu<sup>2+</sup> exposure.  
Modified from (Jones, n.d.) lab Bristol.

We also took advantage of the ability of the bacterium to grow also by respiration to check the effect of Ag<sup>+</sup> on complexes required for respiration. In fact, many previous studies have suggested that Ag<sup>+</sup> can affect the respiratory chain in mitochondria and bacteria, nevertheless a direct evidence showing the activity inhibition of respiratory complexes were missing. In the laboratory, we can reveal the activity of most complexes in native membranes. I therefore assessed the effect of Ag<sup>+</sup> on respiratory complexes from cells grown with Ag<sup>+</sup> or in purified membranes exposed *in vitro* to excess Ag<sup>+</sup>. Our data demonstrated that exposure to Ag<sup>+</sup>, resulted in a decrease of the cytochrome *c* oxidase (complex IV) and the succinate dehydrogenase (complex II) activities. To verify our data in other bacteria, I also checked the effect of Ag<sup>+</sup> on respiratory complexes from *E. coli* and *B. subtilis*. The effect of Ag<sup>+</sup> was also found on complex II in *E. coli* but not in *B. subtilis*. To explain this effect on complex IV and II, we suggested that Ag<sup>+</sup> might affect heme moieties in both complexes.

**Article I: Silver and Copper Acute Effects on Membrane Proteins. Impact on Photosynthetic and Respiratory Complexes in Bacteria**

---

**\*Published. MBio 2018**

-RESULTS-



# Silver and Copper Acute Effects on Membrane Proteins and Impact on Photosynthetic and Respiratory Complexes in Bacteria

Reem Tambosj,<sup>a</sup> Sylviane Liotenberg,<sup>a</sup> Marie-Line Bourbon,<sup>a</sup> Anne-Soisig Steunou,<sup>a</sup> Marion Babot,<sup>a</sup> Anne Durand,<sup>a</sup> Nouari Kebaili,<sup>b</sup> Soufian Ouchane<sup>a</sup>

<sup>a</sup>Institute for Integrative Biology of the Cell (I2BC), Université Paris Saclay, CEA, CNRS, Université Paris Sud, Gif-sur-Yvette, France

<sup>b</sup>Laboratoire Aimé Cotton (LAC), CNRS, Université Paris Sud, ENS Paris Saclay, Campus d'Orsay, Université Paris Sud, Orsay, France

**ABSTRACT** Silver (Ag<sup>+</sup>) and copper (Cu<sup>+</sup>) ions have been used for centuries in industry, as well as antimicrobial agents in agriculture and health care. Nowadays, Ag<sup>+</sup> is also widely used in the field of nanotechnology. Yet, the underlying mechanisms driving toxicity of Ag<sup>+</sup> ions *in vivo* are poorly characterized. It is well known that exposure to excess metal impairs the photosynthetic apparatus of plants and algae. Here, we show that the light-harvesting complex II (LH2) is the primary target of Ag<sup>+</sup> and Cu<sup>+</sup> exposure in the purple bacterium *Rubrivivax gelatinosus*. Ag<sup>+</sup> and Cu<sup>+</sup> specifically inactivate the 800-nm absorbing bacteriochlorophyll *a* (B800), while Ni<sup>2+</sup> or Cd<sup>2+</sup> treatment had no effect. This was further supported by analyses of CuSO<sub>4</sub>- or AgNO<sub>3</sub>-treated membrane proteins. Indeed, this treatment induced changes in the LH2 absorption spectrum related to the disruption of the interaction of B800 molecules with the LH2 protein. This caused the release of B800 molecules and subsequently impacted the spectral properties of the carotenoids within the 850-nm absorbing LH2. Moreover, previous studies have suggested that Ag<sup>+</sup> can affect the respiratory chain in mitochondria and bacteria. Our data demonstrated that exposure to Ag<sup>+</sup>, both *in vivo* and *in vitro*, caused a decrease of cytochrome *c* oxidase and succinate dehydrogenase activities. Ag<sup>+</sup> inhibition of these respiratory complexes was also observed in *Escherichia coli*, but not in *Bacillus subtilis*.

**IMPORTANCE** The use of metal ions represents a serious threat to the environment and to all living organisms because of the acute toxicity of these ions. Nowadays, silver nanoparticles are one of the most widely used nanoparticles in various industrial and health applications. The antimicrobial effect of nanoparticles is in part related to the released Ag<sup>+</sup> ions and their ability to interact with bacterial membranes. Here, we identify, both *in vitro* and *in vivo*, specific targets of Ag<sup>+</sup> ions within the membrane of bacteria. This include complexes involved in photosynthesis, but also complexes involved in respiration.

**KEYWORDS** chlorophyll, copper, membrane complexes, metal homeostasis, photosynthesis, respiration, silver, toxicity

**M**etal accumulation in the environment results in toxicity and defects in metabolism, leading to impaired growth of microorganisms, as well as to a variety of metabolic disorders in higher organisms. In most bacteria, metals such as Cu<sup>+</sup>, Cd<sup>2+</sup>, or Ag<sup>+</sup> would diffuse through nonspecific importers within the membrane. This induces the expression of the detoxification systems that allow the cell to tolerate the presence of metals in its environment (1–6). Among these systems, metal efflux systems are very efficient to detoxify excess metal. The P<sub>1</sub>B-type ATPases are the most fre-

**Received** 13 July 2018 **Accepted** 3 October 2018 **Published** 20 November 2018

**Citation** Tambosj R, Liotenberg S, Bourbon M-L, Steunou A-S, Babot M, Durand A, Kebaili N, Ouchane S. 2018. Silver and copper acute effects on membrane proteins and impact on photosynthetic and respiratory complexes in bacteria. *mBio* 9:e01535-18. <https://doi.org/10.1128/mBio.01535-18>.

**Invited Editor** Fevzi Daldal, University of Pennsylvania

**Editor** Howard A. Shuman, University of Chicago

**Copyright** © 2018 Tambosj et al. This is an open-access article distributed under the terms of the [Creative Commons Attribution 4.0 International license](https://creativecommons.org/licenses/by/4.0/).

Address correspondence to Soufian Ouchane, [soufian.ouchane@i2bc.paris-saclay.fr](mailto:soufian.ouchane@i2bc.paris-saclay.fr).

quently present heavy metal transporters in bacteria (7). They extrude excess or toxic metal ions such as  $\text{Cu}^+$ ,  $\text{Zn}^{2+}$ ,  $\text{Cd}^{2+}$ ,  $\text{Co}^{2+}$ ,  $\text{Pb}^{2+}$ , or  $\text{Ag}^+$  from the cytoplasm to the periplasm, where metal is handled by other detoxifying proteins. In *Escherichia coli*, the  $\text{Cu}^+$  detoxifying system includes the  $\text{Cu}^+$  efflux ATPase CopA, the CusFCBA efflux system, and the CueO oxidase (8, 9). These systems are also involved in  $\text{Ag}^+$  detoxification in *E. coli* and other species (9–11). In mutants defective in the efflux system, metal accumulation in the cytoplasm can disrupt different metabolic pathways. Indeed,  $\text{Cu}^+$ ,  $\text{Ag}^+$ , or  $\text{Cd}^{2+}$  can disrupt the solvent-exposed 4Fe-4S clusters of dehydratases (12, 13). In the purple photosynthetic bacterium *Rubrivivax gelatinosus*,  $\text{Cu}^+$  induces the expression of the CopA-ATPase and the periplasmic blue copper protein CopI (14, 15). Recent *in vivo* studies showed that  $\text{Cu}^+$  accumulation in *R. gelatinosus* and the human pathogen *Neisseria gonorrhoeae*  $\Delta\text{copA}$  mutants affects cell growth by altering heme biosynthesis in the cytoplasm (14, 16) or cytochrome *c* assembly in the periplasm for the  $\Delta\text{copI}$  mutant in *R. gelatinosus* (15). Interestingly, similar effect of tellurite on cytochrome *c*-type assembly was recently reported in *Rhodobacter capsulatus* (17).  $\text{Cu}^+$  can also compete with iron for the metal binding site of IscA and inhibit the 4Fe-4S cluster assembly pathway in *E. coli* (18). In plants and algae, metals exert their toxic action mostly by damaging chloroplasts, which leads to decreased efficiency of photosynthesis. Plants subject to excess metals usually exhibit a decrease in the photosystem amount and chlorophyll content (19–22). However, the toxicity mechanisms are not well known. Assessing the effect of metals on the growth of photosynthetic bacteria can provide new insights into the toxicity mechanisms and identify metal targets in phototrophs. Purple photosynthetic nonsulfur bacteria can grow by aerobic and anaerobic respiration or photosynthetically in the light under anaerobic or microaerobic conditions, using a cyclic electron transport chain. Aerobic respiration usually involves a branched energy-transducing electron transfer chain (23). The cytochrome *c*-dependent branch usually involves the NADH dehydrogenase, succinate dehydrogenase, the *bc<sub>1</sub>* complex, and the terminal cytochrome *c* oxidase (*aa<sub>3</sub>* or *cbb<sub>3</sub>*). Under light-exposed condition, photosynthesis takes place within the membranous photosynthetic apparatus. The photosystem is usually composed of three pigment-protein complexes, namely, the two light-harvesting antennae (light-harvesting complex I [LH1] and light-harvesting complex II [LH2]) and the reaction center (RC), associated with carotenoids and bacteriochlorophylls (24). During the process, the light-harvesting complexes (LH) capture light energy and direct it to the RC, where conversion of the excitation energy/charge separation takes place. The LH antenna system consists of two large pigment-protein complexes, the core light-harvesting complex, LH1, that surrounds the RC, and the peripheral light-harvesting complex, LH2, induced under low-light conditions to increase light trapping efficiency in some species. Both LH antennae are composed of two integral membrane polypeptides ( $\alpha$  and  $\beta$ ) that associate with bacteriochlorophyll (BChl) and carotenoid molecules (25–27). The LH2 antennae contain two spectrally distinct bacteriochlorophylls, *a* (B800) and B850, which absorb in the near-infrared range, at 800 and 850 nm, respectively. The crystal structure of the LH2 from *Rhodospseudomonas acidophila* was previously resolved (25). The B850 molecules are sandwiched between the  $\alpha$  and  $\beta$  subunits and are perpendicular to the membrane surface. In contrast, the B800 molecules are localized between the  $\beta$  subunits and aligned parallel to the membrane surface. The structures of the RC-LH1 core complexes of *Rhodospseudomonas palustris* and *Thermochromatium tepidum* are available (26, 27). In this study, we analyzed the effect of extended exposure to metals on photosynthesis and respiration in the photosynthetic purple bacterium *R. gelatinosus*. The data indicated that the B800 of LH2 was specifically removed upon exposure to  $\text{AgNO}_3$  and  $\text{CuSO}_4$ . We then assessed the impact on the respiratory chain and showed that metal ions also damaged the succinate dehydrogenase and the terminal cytochrome *c* oxidase, thereby affecting respiration.

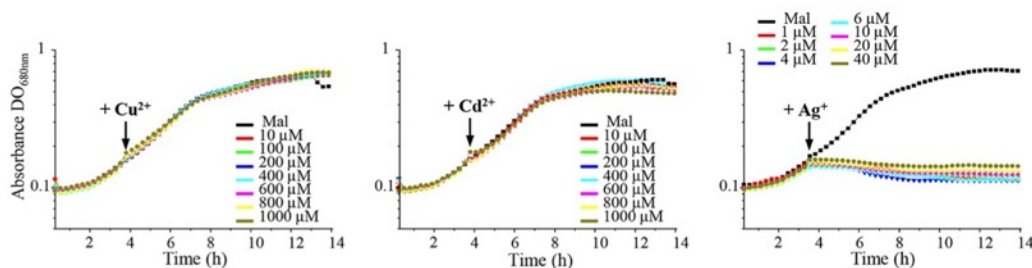


**FIG 1**  $\text{AgNO}_3$  growth inhibition of *R. gelatinosus*. Wild-type cells were grown in 96-well microplates in the Tecan Infinite M200 luminometer. Indicated concentrations of  $\text{CuSO}_4$ ,  $\text{CdCl}_2$ , or  $\text{AgNO}_3$  were added to the growth medium after 3.5 h, when cells reached an  $\text{OD}_{680}$  of 0.16 (arrow). Black line represents growth curves of untreated cells (malate) and red, green, blue, cyan, magenta, yellow, and brown lines represent growth curves of cells treated with increasing concentrations of  $\text{Cu}^{2+}$ ,  $\text{Cd}^{2+}$ , or  $\text{Ag}^+$ , as indicated.

## RESULTS

### Silver is highly toxic for *R. gelatinosus*, and the $\text{Cu}^+$ -ATPase CopA is not involved in $\text{Ag}^+$ response.

To assess the toxicity of  $\text{Ag}^+$  in comparison with those of other toxic metals, wild-type cells were treated with increasing concentration of  $\text{AgNO}_3$ ,  $\text{CuSO}_4$ , or  $\text{CdCl}_2$  during the exponential growth phase, and overnight growth was monitored. Growth was not affected by the addition of  $\text{CuSO}_4$  or  $\text{CdCl}_2$ , even at 1 mM. In contrast, addition of 1  $\mu\text{M}$   $\text{AgNO}_3$  was enough to fully inhibit growth (Fig. 1). Similar results were reported in *E. coli* cells, highlighting the acute toxicity of  $\text{Ag}^+$  compared to that of other metal cations (13). We should note that toxicity was reduced when  $\text{AgNO}_3$  was added to a higher density of cells (Fig. S1), as previously reported for *E. coli*. It was suggested that metal ions could interact and be sequestered on the cell surface; the high cell density will therefore affect the dose response (13). To cope with excess toxic metal, bacteria usually induce the genes encoding the metal-efflux ATPases.  $\text{Ag}^+$  tolerance in *E. coli* involves the metal efflux  $\text{P}_1\text{B}$ -type ATPase CopA, which translocates  $\text{Cu}^+$  and  $\text{Ag}^+$  from the cytoplasm to the periplasm (4, 9). Therefore, the *R. gelatinosus* efflux-defective *copA* mutant was used to check the involvement of CopA in  $\text{Ag}^+$  efflux. Unlike  $\text{CuSO}_4$ , which inhibits *copA* mutant growth (Fig. 2A), no difference in growth inhibition was observed between *copA* mutant and wild-type cells subjected to excess  $\text{AgNO}_3$ . These data suggested that in contrast to  $\text{Ag}^+$  tolerance in *E. coli*, CopA is not involved in  $\text{Ag}^+$  tolerance in *R. gelatinosus*. Although the ZntA/CadA ATPase is known to translocate divalent cations, we also checked whether the  $\Delta\text{cadA}$  mutant was sensitive to  $\text{Ag}^+$  (A. S. Steunou, A. Durand, M.L. Bourbon, M. Babot, S. Liotenberg, and S. Ouchane, submitted for publication). As for the *copA* mutant strain, no difference in growth was observed between wild-type and  $\Delta\text{cadA}$  strains in the presence of  $\text{AgNO}_3$  (not shown). Cells were also spotted on solid medium supplemented with the same metals. Both *copA* and  $\Delta\text{cadA}$  mutants showed growth inhibition on 500  $\mu\text{M}$   $\text{CuSO}_4$  and 500  $\mu\text{M}$   $\text{CdCl}_2$ , respectively. However, none of the mutants exhibited an altered growth phenotype on 5  $\mu\text{M}$   $\text{AgNO}_3$  (Fig. 2B). We therefore concluded that the CopA and CadA ATPases were not involved in the  $\text{AgNO}_3$  response. To further support this conclusion, we analyzed by Western blot the expression of CopA and CopI in response to metal shock in a strain expressing a His-tagged version of CopA (CopA-H<sub>6</sub>) (Fig. 2C). Cells were grown under photosynthetic condition and shocked with  $\text{CuSO}_4$  and  $\text{CdCl}_2$ , known to induce the expression of the  $\text{Cu}^+$  efflux system (Steunou et al., submitted for publication), or with  $\text{AgNO}_3$ . Untreated cells showed a basal level of CopA and CopI expression because of the presence of 1.6  $\mu\text{M}$   $\text{CuSO}_4$  in the growth medium. As expected, addition of  $\text{CuSO}_4$  or  $\text{CdCl}_2$  to the growing cells led to significant increases in the amounts of CopA and CopI (Fig. 2C). In contrast,  $\text{AgNO}_3$  did not induce the expression of both proteins. Collectively, these results showed that the *R. gelatinosus* CopA efflux ATPase is not involved in  $\text{AgNO}_3$  stress response and detoxification, in contrast to that in *E. coli*.

### Silver and copper excess specifically affected the LH2 complexes in the membrane.

To assess the effects of  $\text{Ag}^+$  ions on photosynthesis, cells (optical density at

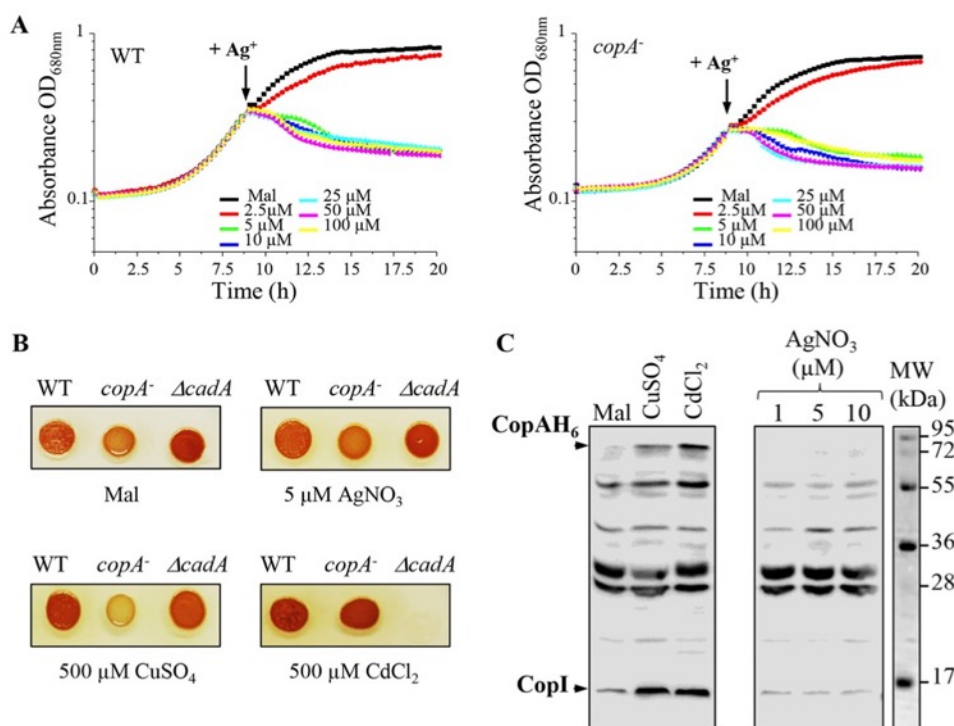


**FIG 2** CopA and CadA are not involved in  $AgNO_3$  response. (A) Wild-type (WT) and *copA* mutant (*copA*<sup>-</sup>) cells were grown in microplates under microaerobic conditions. Indicated concentrations of  $AgNO_3$  were added to the growth medium after 8.5 h, when cells reached an  $OD_{680}$  of 0.3 (arrow). (B) Growth phenotype of the WT, *copA* and  $\Delta cadA$  mutants in the presence of indicated concentrations of  $AgNO_3$ ,  $CuSO_4$ , or  $CdCl_2$  on solid malate media. Cells were grown aerobically for 24 h at 30°C prior to photography. (C) Induction of CopA-H<sub>6</sub> and CopI expression in cells shocked for 1 h with 0.5 mM  $CuSO_4$ , 0.5 mM  $CdCl_2$ , or 1 to 10  $\mu M$   $AgNO_3$ . Cells were grown in photosynthetic condition and metals were added to the growth medium when cells reached an  $OD_{680}$  of 0.8. Total protein extracts from the same amount of cells ( $OD_{680}$  of 0.1) were separated on 14% SDS-PAGE. The proteins were revealed on a Western blot using an HisProbe-HRP.

680 nm [ $OD_{680}$ ] = 2) grown overnight under photosynthetic condition were treated with 1 mM  $AgNO_3$  and grown further for 2, 10, or 20 h. The bacteriochlorophyll *a* absorbance in the photosynthetic complexes was measured to monitor changes in response to excess  $AgNO_3$  in the cell in the reaction center and in light-harvesting antenna LH1 complexes and LH2 complexes. The effect of  $Ag^+$  on the photosynthetic (PS) complex spectra are presented in Fig. 3A. The B860 (RC-LH1-LH2) and B800 (LH2) wavelength band intensity variations, depending on the length of  $AgNO_3$  exposure, are represented.  $Ag^+$  induced no apparent effect on the 860-nm band. However, a time exposure-dependent decrease of the B800 band intensity was observed (Fig. 3A). This suggested that the LH2 antennae were affected by  $AgNO_3$  exposure. We also question whether this effect was specific to  $AgNO_3$ . For that purpose, cells were also subjected to metal excess stress as described above, but with different metal cations (Fig. 3B). Interestingly, only  $CuSO_4$  caused the same effect as  $AgNO_3$  on the LH2 complexes. Exposure to  $CdCl_2$  or  $NiSO_4$  did not affect the photosynthetic complexes. These data demonstrated that  $AgNO_3$  and  $CuSO_4$  extended exposure affected the LH2 in the photosynthetic membranes.

**Silver and copper specifically induced the loss of the 800-nm absorbing bacteriochlorophyll *a* in LH2.** The LH2 antenna (B800 and B850) complexes are spectrally characterized by the 800- and 850-nm absorption bands that arise from the near-infrared (Qy) transitions of the bacteriochlorophyll *a*. The loss of the B800 band suggested the loss of the LH2 in the membrane. However, the spectra presented in Fig. 3 also suggested that the LH2 B850 bacteriochlorophyll was not affected, since no shift was observed in the 860-nm band that encompasses the RC (870-nm), the LH1

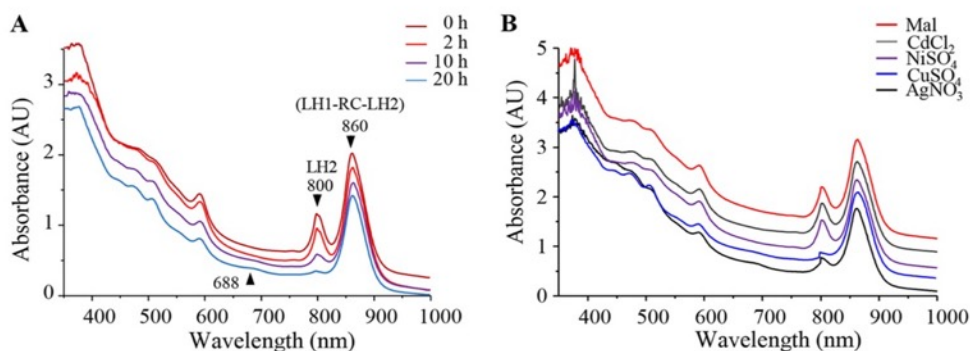


**FIG 3** AgNO<sub>3</sub> exposure impact on photosystem *in vivo*. (A) Spectral analyses of wild type (WT) cells grown overnight by photosynthesis and exposed or not to 1 mM AgNO<sub>3</sub> after they reach an OD<sub>680</sub> of 2. Spectra (350 to 1,000 nm) were recorded after 2- (light red line), 10- (purple line), or 20-h (blue line) exposure on a double-beam Cary 500 spectrophotometer. (B) Spectral analyses of the WT cells exposed or not to 1 mM CdCl<sub>2</sub> (gray line), NiSO<sub>4</sub> (purple line), CuSO<sub>4</sub> (blue line), or AgNO<sub>3</sub> (black line) after they reached an OD<sub>680</sub> of 2. Spectra were recorded after 20 h of exposure. Mal (dark red line), untreated cells grown in malate medium.

(875-nm), and the LH2 (850-nm) bands. To confirm this assumption, we compared the spectra of the untreated or AgNO<sub>3</sub>-shocked wild-type cells to the spectrum of the *pucBA* LH2-deficient mutant (28) that only assembles the RC-LH1 core (Fig. 4A). Deletion of the LH2 genes resulted in a significant decrease of the 800-nm band and a substantial red shift of 15 nm (from 860 to 875 nm) of the 860-nm band (28). The resulting peak at 875 nm corresponds to the RC-LH1 core absorption bands. In sharp contrast with the LH2-deficient mutant, the AgNO<sub>3</sub>-shocked wild-type cell spectrum showed the decrease of the 800-nm band and no changes in the 860-nm-absorbing bacteriochlorophyll molecules arising from the RC-LH1 core and a modified (B800-free) LH2 (Fig. 4A). Similar impact on LH2 complexes was observed when cells were subjected to CuSO<sub>4</sub> treatment (Fig. S2). These spectra showed that the B800 molecules can selectively be extracted or released from the LH2 complexes in the presence of metals without disrupting the interaction of the LH2 polypeptides with the B850 molecules.

The effect of metals on the RC-LH1 core was also assessed using the *pucBA* LH2-deficient mutant. Spectra of the exposed cells showed that AgNO<sub>3</sub> and CuSO<sub>4</sub> slightly affected the amount of the RC-LH1 (Fig. 4B). Moreover, total protein lysates from all untreated or treated samples were also loaded onto SDS-PAGE. The Coomassie blue staining showed that all wild-type samples have comparable amounts of LH2 subunits, indicating that the release of B800 molecules did not affect the LH2 protein

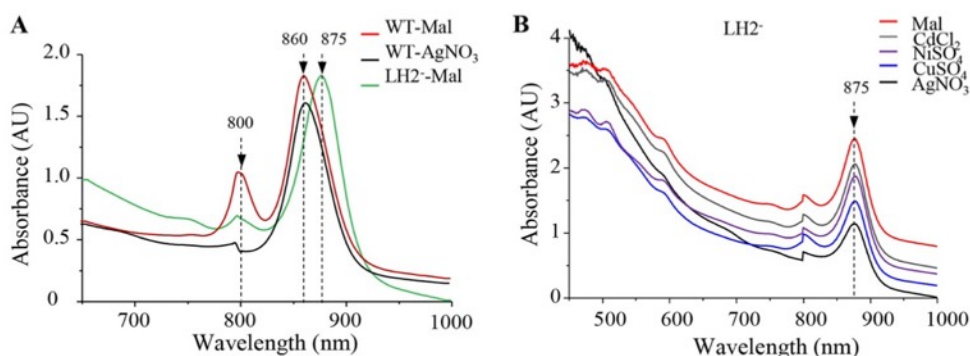


**FIG 4** Effect of AgNO<sub>3</sub> on LH2 complexes *in vivo*. (A) Absorption spectra of wild-type (WT) cells grown overnight by photosynthesis untreated (Mal, red line) or exposed to 1 mM AgNO<sub>3</sub> (black line) in comparison with LH2-deficient mutant (LH2<sup>-</sup>) cells grown overnight by photosynthesis in malate medium (green line). (B) Spectral analyses of the LH2-deficient mutant cells untreated (Mal, red line) or exposed to 1 mM CdCl<sub>2</sub> (gray line), NiSO<sub>3</sub> (purple line), CuSO<sub>4</sub> (blue line), or AgNO<sub>3</sub> (black line) after they reach an OD<sub>680</sub> of 2. Spectra were recorded after 20 h of exposure.

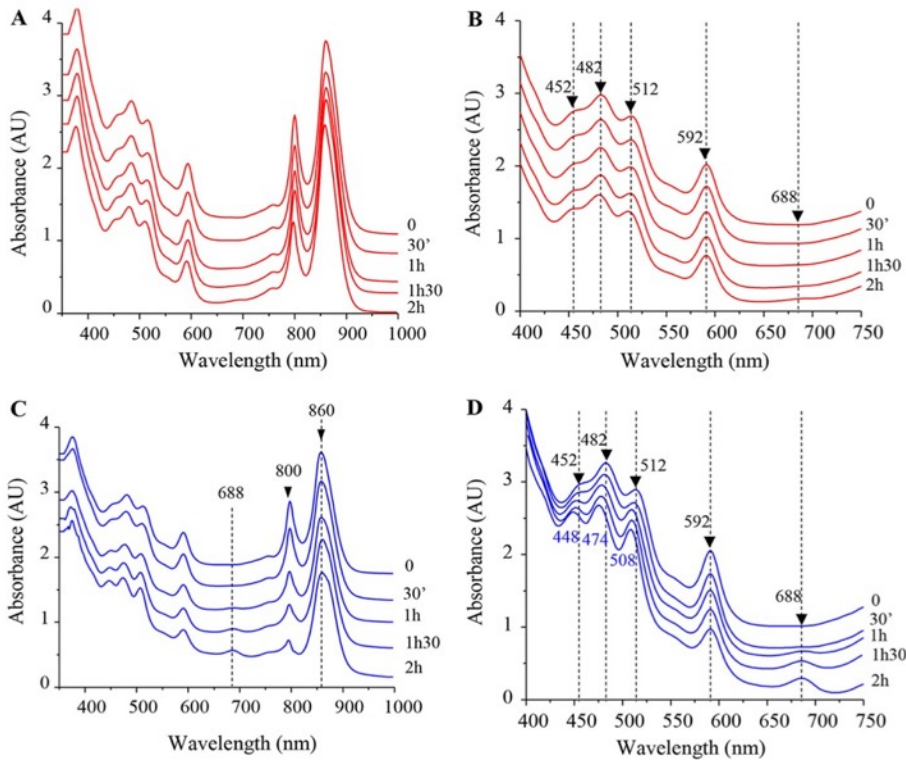


**FIG 5** Effect of  $\text{CuSO}_4$  on LH2 complexes of isolated membranes. (A) Spectra (350 to 1,000 nm) of untreated membranes were recorded every 30 min. (B) Enlargement of the 400- to 750-nm spectrum absorbance region of untreated membranes. (C) Enriched membrane fractions were mixed with  $\text{CuSO}_4$  at 2 mM final concentration; 350- to 1,000-nm spectra were then recorded every 30 min. (D) Enlargement of the 400- to 750-nm spectrum absorbance region, highlighting the shift in the carotenoids bands and the increase in the 688-nm band in the  $\text{CuSO}_4$ -treated membranes.

stability (Fig. S2). Altogether, these data indicated that  $\text{AgNO}_3$ - and  $\text{CuSO}_4$ -induced alterations in the structure of the LH2 complexes, targeting the B800 molecules of the complex. However, this specific and rather limited effect on B800 and the LH2 could not explain the drastic growth inhibition by  $\text{Ag}^+$ , suggesting that  $\text{Ag}^+$  affects other crucial components or complexes of the cell.

**Metal-specific impact on the 800-nm band attested by the release of bacteriochlorophyll and shift in carotenoid absorbance.** In the LH2 structure of *Rhodospirillum rubrum*, the 800-nm absorbing bacteriochlorophyll *a* molecules lie between the  $\beta$ -apoprotein helices, where phytol moieties interact with the carotenoids. The structural data showed that at least one of the carotenoid molecules makes close Van der Waals contacts with the B800 pigment (25, 29). We therefore assumed that the release of B800 molecules following metal stress should also impact the B800-carotenoid interaction. To verify this assumption, enriched membranes from wild-type cells were incubated in phosphate buffer supplemented or not with 2 mM  $\text{CuSO}_4$  or  $\text{AgNO}_3$ . Spectra were then recorded every 30 min to monitor the effect of metals on photosynthetic complexes on isolated membranes (Fig. 5). For untreated membranes, no changes in the amount or in the spectral properties of the RC, LH1, and LH2 were observed (Fig. 5A and B). However, in the membranes subjected to  $\text{CuSO}_4$  treatment, a significant decrease in the intensity of the 800-nm band was observed in association with an absorption increase at 688 nm (Fig. 5C and D). This later absorption peak very likely arose from oxidized Bchl in solution, as previously reported (30). Furthermore, with extended exposure to  $\text{CuSO}_4$ , a shift was also observed in the carotenoid absorption region. Indeed, untreated proteins exhibited three peaks at 452, 482, and 512 nm (Fig. 5B), while  $\text{CuSO}_4$  treatment resulted in a shift of the carotenoid absorbance to 448,

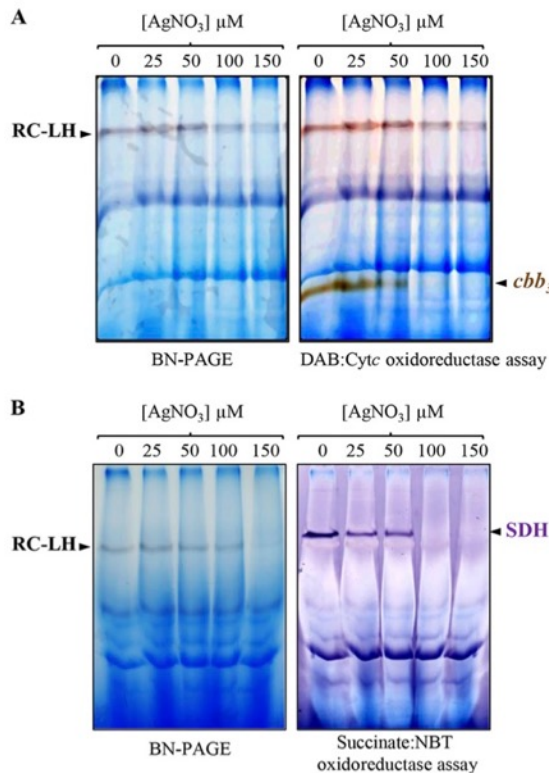


**FIG 6** AgNO<sub>3</sub> effect on respiratory complexes *in vivo*. The wild-type (WT) cells were grown under microaerobic respiratory condition and shocked for 1 h with increasing concentration of AgNO<sub>3</sub>. DDM-solubilized membrane proteins were separated on a 5% to 12% BN-PAGE. (A) *cbb*<sub>3</sub> cytochrome c oxidase DAB:Cyt c in-gel activity assay. (B) Succinate dehydrogenase (SDH) in-gel activity assay.

474, and 508 nm (Fig. 5D). Similar effects were obtained in the presence of AgNO<sub>3</sub> treatment (Fig. S3). Thus, we concluded that in the presence of CuSO<sub>4</sub> or AgNO<sub>3</sub>, changes in the LH2 absorption spectrum are related to the disruption of the interaction of B800 molecules with LH2, which causes the release of the B800 molecules and subsequently impacts the spectral properties of the carotenoids within the B850 LH2.

**Silver damages the cytochrome c oxidase and the succinate dehydrogenase in the respiratory chain.** Previous studies in 1974 and 2005 established that Ag<sup>+</sup> ions inhibit the respiratory chain of *E. coli* (31, 32). In eukaryotes, Ag<sup>+</sup> ions can induce mitochondrial dysfunction, partly by inhibiting respiration (33, 34). However, the complexes targeted by Ag<sup>+</sup> ions were not yet identified. To check the effect of AgNO<sub>3</sub> on two respiratory complexes (succinate dehydrogenase and *cbb*<sub>3</sub> cytochrome c oxidase) from *R. gelatinosus*, exponentially growing wild-type cells under respiratory conditions were subjected to increasing concentration of AgNO<sub>3</sub> (25 to 150 μM) and grown for another hour. To examine the effect of AgNO<sub>3</sub> on the *cbb*<sub>3</sub> oxidase, membrane proteins were solubilized and cytochrome c oxidase activity was assayed on blue native PAGE (BN-PAGE) (35). As shown in Fig. 6A, comparable diaminobenzidine (DAB)-positive bands corresponding to the *cbb*<sub>3</sub> oxidase were revealed in the solubilized membrane proteins from untreated and 25 μM AgNO<sub>3</sub>-stressed cells. Decreased activity was detected in the 50 μM AgNO<sub>3</sub>-stressed cells. However, no active *cbb*<sub>3</sub> oxidase was detected on membrane fractions isolated from 100 and 150 μM AgNO<sub>3</sub>-stressed cells (Fig. 6A). We should note that there was a slight effect on the amount of RC-LH with 100 and 150 μM AgNO<sub>3</sub>. This could be the consequence of membrane protein solubilization; indeed, the loss of B800 may destabilize LH2 in the presence of detergent. Nonetheless, the other blue-stained complexes on BN-PAGE did not seem to be affected (Fig. 6A and B), suggesting that AgNO<sub>3</sub> targets only some complexes, including

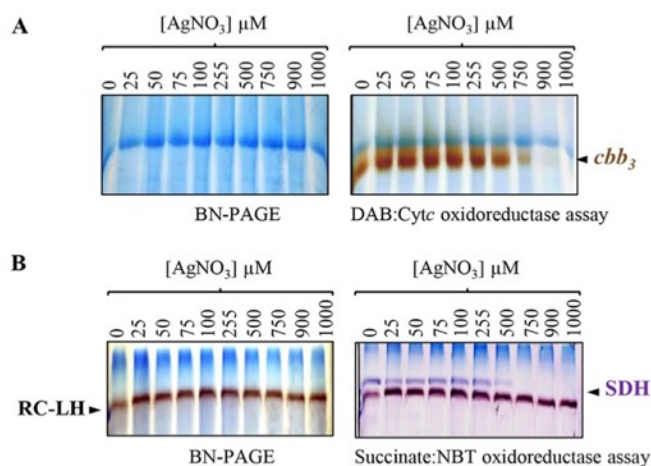


**FIG 7** Effect of AgNO<sub>3</sub> treatment on respiratory complexes in membrane-enriched fractions. These fractions were mixed with increasing concentration of AgNO<sub>3</sub> for 1 h. DDM-solubilized membrane proteins were then separated on a 5% to 12% gradient BN-PAGE. (A) *cbb*<sub>3</sub> cytochrome *c* oxidase in-gel activity assay. (B) Succinate dehydrogenase (SDH) in-gel activity assay.

the *cbb*<sub>3</sub> cytochrome *c* oxidase and the RC-LH. Similarly, succinate:nitroblue tetrazolium (NBT) *in gel* assay revealed an active band, likely corresponding to succinate dehydrogenase (SDH). Treatment with increasing concentration of AgNO<sub>3</sub> resulted in a partial or full inhibition of this activity (Fig. 6B) suggesting that AgNO<sub>3</sub> also affected succinate dehydrogenase in exposed cells.

As for photosynthetic complexes, we analyzed the *in vitro* effect of AgNO<sub>3</sub> on respiratory complexes in isolated membrane protein fractions (Fig. 7). For that purpose, membranes from wild-type cells were incubated in buffer supplemented or not with increasing concentration of AgNO<sub>3</sub> (from 25 to 1,000 μM). Similarly to the *in vivo* data, incubation of membrane proteins with increasing concentration of AgNO<sub>3</sub> led to a decrease in cytochrome *c* oxidase *cbb*<sub>3</sub> (Fig. 7A) and succinate dehydrogenase activities (Fig. 7B). Altogether, these data suggested that AgNO<sub>3</sub> could inhibit respiration by directly damaging the respiratory complexes, including cytochrome *c* oxidase and succinate dehydrogenase.

**Silver damages respiratory complexes in *Escherichia coli* but not in *Bacillus subtilis*.** The findings above prompted us to test the activity of respiratory complexes in other bacterial species after AgNO<sub>3</sub> treatment. To this aim, *E. coli* and *Bacillus subtilis* cells grown to exponential phase were subjected to increasing concentration of AgNO<sub>3</sub> (25 to 150 μM) and grown for another hour. Membranes proteins were isolated, and activity assays for respiratory complexes were performed by BN-PAGE. As *E. coli* cells do not express any cytochrome *c* oxidase, we only assayed the activity of succinate dehydrogenase. We detected changes in the activity of this complex when cells were subjected to AgNO<sub>3</sub> stress, as the SDH activity decreased with increasing concentration of AgNO<sub>3</sub> (Fig. 8A). To ascertain that the detected band corresponds to the SDH, the succinate-NBT in-gel assay was also performed with membrane proteins isolated from the *sdhA* deletion mutant (36) (Fig. 8A). These results confirmed that AgNO<sub>3</sub> can affect respiration in *E. coli* and provide evidences that the SDH complex is a target of AgNO<sub>3</sub>. In *B. subtilis*, however, AgNO<sub>3</sub> treatment did not affect the activity of the cytochrome *c* oxidase *caa*<sub>3</sub>, nor the activity of the SDH (Fig. 8B).

## DISCUSSION

The use and spread of metal ions or nanoparticles represent a serious threat to the environment and to all living organisms because of the acute toxicity of these ions. Silver and copper ions have been used for their antimicrobial activities for several years. Nowadays, Ag<sup>+</sup> nanoparticles are one of the most widely used nanoparticles in many industrial and health applications (37). The antimicrobial effect of Ag<sup>+</sup> nanoparticles is

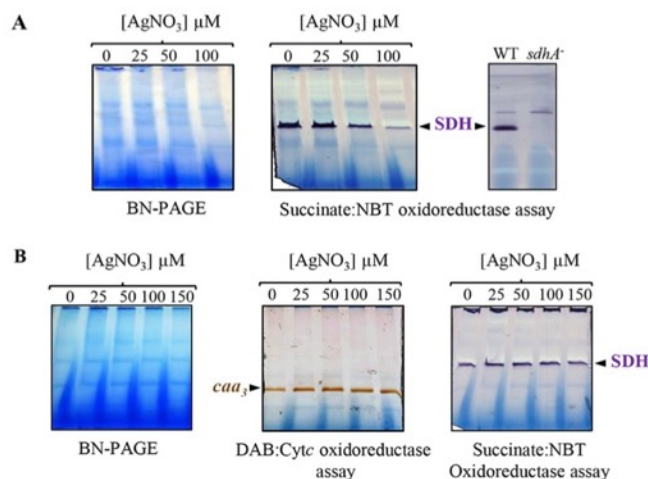


**FIG 8** AgNO<sub>3</sub> effect on respiratory complexes in *E. coli* and *B. subtilis* cells. Strains were grown under aerobic respiratory condition and shocked for 1h with increasing concentration of AgNO<sub>3</sub>. DDM-solubilized membrane proteins were separated on a 5% to 12% gradient BN-PAGE. (A) Succinate dehydrogenase (SDH) in-gel activity assay of *E. coli* membrane fractions. Membrane fraction from the SDH-deficient mutant (*sdhA*<sup>-</sup>) was used as a control. (B) *caa*<sub>3</sub> cytochrome *c* oxidase and succinate dehydrogenase (SDH) in-gel activity assays of *B. subtilis* membranes.

in part related to the released Ag<sup>+</sup> ions and their ability to interact with bacterial membranes (37–39). It is therefore important to characterize the toxicity of Ag<sup>+</sup> ions and to identify cellular targets of this metal. Previous studies reported that the acute toxicity of Ag<sup>+</sup> lies in its ability to interact with membranes but also in its ability to affect iron sulfur proteins (13). To identify targets of Ag<sup>+</sup>, we compared the impact of different metal ions on the stability and activity of membrane complexes in the purple photosynthetic bacterium *R. gelatinosus*. AgNO<sub>3</sub> was found to be more toxic than the other ions used, including CuSO<sub>4</sub> and CdCl<sub>2</sub>. This may be related to the absence of an efficient efflux system to detoxify Ag<sup>+</sup> and/or to its bioactivity and ability to damage molecules. Indeed, the Cop system involved in detoxification of Ag<sup>+</sup> in other bacteria (9–11) is not induced by AgNO<sub>3</sub> in *R. gelatinosus*, which may increase the susceptibility of the bacterium to AgNO<sub>3</sub>. In *E. coli*, although the Cop efflux is effective in expelling Ag<sup>+</sup> ions outside the cells, AgNO<sub>3</sub> remains very toxic and targets different cellular components. In *Chlamydomonas reinhardtii* (39, 40) and *Arabidopsis thaliana* (41), Ag<sup>+</sup> and Cu<sup>+</sup> exposures were both found to significantly inhibit growth and to induce decreases in photosynthesis and chlorophyll content. Here, we found that both metals target the bacterial LH2. Both Ag<sup>+</sup> and Cu<sup>2+</sup> specifically target the B800 molecules but not the B850 ones (Fig. 9). Similar results were reported when LH2 complexes from *R. sphaeroides* and *R. acidophila* were subjected to high atmospheric pressure (30). This could be related to the structure of this complex and the position of the chlorophyll molecules in the complex. In fact, the B850 bacteriochlorophylls with the carotenoid molecules are buried between the concentric rings formed by the α and β subunit outer rings (25) and are therefore well shielded from the external buffer. In contrast, the B800 molecules are located between the outer rings formed by helices of the β subunits and are parallel to the lipid surface near the cytosolic side (Fig. 9). This positions the B800 molecules in contact with the solvent, where they would be more exposed than the B850 molecules, in agreement with water molecules being found close to the B800 molecules in the *R. acidophila* LH2 crystal structure (25, 29). The effect on B800 did not modify the complex stability, since the B850 molecules were not affected. Nevertheless, the resulting complex would be inefficient for light energy capture and photon transfer to the photochemical reaction center. Indeed, the LH2 light energy is transferred from B800 to B850. Energy transfer then occurs between B850 and B875 molecules in the light-harvesting complex LH1 to the RC (42). Thus, we

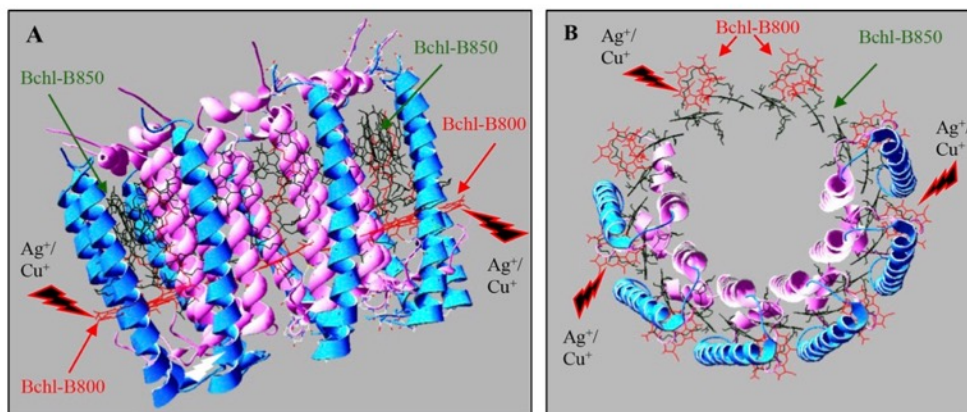


**FIG 9**  $\text{Ag}^+$  and  $\text{Cu}^+$  specifically target the B800 within the LH2. Structure of the LH2 and arrangement of pigments within the complex from *Rhodospseudomonas acidophila* (1KZU.pdb) (25). The figure was generated using the Protein Data Bank (Swiss-PdbViewer). View parallel to the plane of the membrane (A) and from the top of the complex (B) showing the exposed B800 molecules (in red) located between the  $\beta$  subunit helices, which form the outer ring (cyan). The B850 molecules (green) are buried between the concentric rings formed by the helices of the  $\alpha$  subunits (pink) and the outer  $\beta$  subunit helix ring. For better viewing, carotenoids and helices of  $\alpha$  and  $\beta$  subunits were hidden.

assume that  $\text{Ag}^+$  or  $\text{Cu}^+$  exposure will result in reduced excitation transfer to the B870 in the RC and decreased photosynthesis yield. Only a slight effect of  $\text{Ag}^+$  and  $\text{Cu}^+$  was observed on the LH1-RC in the LH2-deficient strain. In the LH1-RC structures from *R. palustris* and *T. tepidum* (26, 27), the bacteriochlorophyll molecules in LH1 complexes are found sandwiched between the concentric ring formed by the  $\alpha$  subunits and the external ring formed by the  $\beta$  helices, like the B850 molecules in the LH2 structure. These Bchl molecules and the RC-Bchls could therefore be shielded from the external buffer and therefore from damages that may be caused by the presence of metal ions. The mechanism by which  $\text{Ag}^+$  or  $\text{Cu}^+$  release B800 from the LH2 remains to be studied. Nonetheless, previous studies have shown that  $\text{Mg}^{2+}$  in chlorophylls could be substituted, both *in vitro* and *in vivo*, by heavy metal ions (20, 43, 44). It was shown that *in vivo* substitution of the  $\text{Mg}^{2+}$  atom of chlorophyll by heavy metals, including  $\text{Cu}^+$ ,  $\text{Cd}^{2+}$ , or  $\text{Pb}^{2+}$ , is a major damage mechanism in stressed plants. Indeed, substitution of  $\text{Mg}^{2+}$  affects the LHCII and the photosystem PSII, thereby causing a decrease in photosynthesis (20). Likewise, it was shown that  $\text{Ni}^{2+}$ ,  $\text{Cu}^{2+}$ , and  $\text{Zn}^{2+}$  induced a destabilization of heme binding to *b*-type hemoproteins and led to the release of heme from myoglobin, ferricytochrome *b<sub>s</sub>*, indoleamine-dioxygenase, hemopexin, and cytochrome P450 (45, 46). Formation of a bioconjugate of human hemoglobin with  $\text{Ag}^+$  ions was also reported (47, 48). Finally, both  $\text{Ag}^+$  and  $\text{Cu}^+$  can displace metal- or damage-exposed 4Fe-4S clusters in proteins (13). By these means, such metal ions can inhibit the activity of hemoproteins and metalloproteins in the membrane and the cytosol.  $\text{AgNO}_3$  impacts on the activity of cytochrome *c* oxidase and succinate dehydrogenase in *R. gelatinosus*, as well as on the succinate dehydrogenase in *E. coli*, were demonstrated in this study. This could arise from the disruption of the interaction between the cofactors (heme or 4Fe-4S) and the proteins. Nevertheless, we should note that the effects of  $\text{Ag}^+$  on complexes reported in this study were obtained with high concentration of  $\text{AgNO}_3$ . No effect was shown in the Gram-positive bacterium *B. subtilis*. This may be related to the difference in the cell wall structure between Gram-positive and Gram-negative bacteria. The much thicker peptidoglycan layers in Gram-positive bacteria are crucial in protecting the cell from environmental stress, including that of external metal ions (49). In agreement with this, *Staphylococcus aureus* is less sensitive to  $\text{AgNO}_3$  than *E. coli*, as  $\text{AgNO}_3$  treatment was shown to strongly affect the membrane integrity of *E. coli* but not that of *S. aureus* (50–52). In a recent study,  $\text{AgNO}_3$  was shown to affect the activity of the cytochrome *c* oxidase in *B. subtilis* (53). However,  $\text{AgNO}_3$  interfered with the biogenesis process of the oxidase by displacing  $\text{Cu}^{2+}$  from the Sco

assembly protein (53). In our study, we checked the impact of  $\text{AgNO}_3$  on already-assembled complexes. Nevertheless, prolonged exposure to metal should be further studied to better characterize the response to  $\text{Ag}^+$  stress in *B. subtilis*. Beside the direct effect of  $\text{Cu}^{2+}$  and  $\text{Ag}^+$  on these membrane complexes, heme or 4Fe-4S cluster degradation is expected to release iron, which may magnify the toxicity of metals, as excess free iron gives rise to hydroxyl radicals and induces oxidative stress. Most toxicity studies of Ag nanoparticles in bacteria and eukaryotes shed light on oxidative stress response. For a full characterization of nanoparticle toxicity mechanisms, future experiments should address the issue of interaction between membrane complexes involved in cellular bioenergetics and Ag nanoparticles.

## MATERIALS AND METHODS

**Bacterial strains and growth.** *E. coli* and *B. subtilis* cells were grown aerobically (500-ml flasks containing 50 ml medium) at 37°C in LB medium. *R. gelatinosus* cells were grown at 30°C, in the dark microaerobically (low oxygenation in 50-ml flasks containing 50 ml medium) or in light by photosynthesis (filled tubes with residual oxygen in the medium) in malate growth medium (54). The antibiotics kanamycin (Kan) and trimethoprim (Tpm) were used at a final concentration of 50  $\mu\text{g}/\text{ml}$ .

Growth inhibition curves were monitored at  $\text{OD}_{680}$  with measurements taken every 15 min for 24 h, using an Infinite M200 luminometer (Tecan, Mannerdorf, Switzerland) for aerobic condition. For photosynthesis conditions, strains were grown as described above, and OD was measured after 24 h using the Tecan luminometer.

**Membrane protein preparation.** Cells were disrupted by sonication in 0.1 M sodium phosphate buffer (pH 7.4) containing 1 mM phenylmethylsulfonyl fluoride. Unbroken cells were removed by a low-speed centrifugation step (25,000  $\times g$ , 30 min, 4°C), and supernatants were subjected to ultracentrifugation (200,000  $\times g$ , 90 min, 4°C) to collect the membrane fraction. Membrane fractions were then resuspended in the same buffer. Membrane protein concentration was estimated using the bicinchoninic acid assay (Sigma), with bovine serum albumin as the standard. For membrane protein metal treatment, required concentrations of metal solution were mixed with 50 mg/ml membrane proteins at room temperature. Spectra were recorded every 30 min.

**Spectrophotometric measurements.** Absorption spectroscopy was performed with a Cary 500 spectrophotometer. For spectra on whole cells, cells were resuspended in a 60% (wt/vol) sucrose solution. Membrane fractions were in 0.1 M sodium phosphate buffer (pH 7.4).

**Blue native gel electrophoresis and in-gel assays.** To assay *cbb*<sub>3</sub> and succinate dehydrogenase activities, *R. gelatinosus* wild-type cells were grown microaerobically. For *E. coli* and *B. subtilis*, cells were grown aerobically. Membranes were prepared as previously described. Blue native polyacrylamide gel electrophoresis (BN-PAGE) and in-gel Cox activity assays (DAB:Cytc staining) were performed as described in (35), and succinate dehydrogenase activity was assayed using succinate and NBT (nitroblue tetrazolium), as described in reference (55).

**Western blot analysis and HisProbe-HRP detection.** Equal amounts of cells ( $\text{OD}_{680} = 1$ ) were disrupted in SDS loading buffer, and proteins were then separated on a 15% SDS-PAGE and further transferred to a Hybond ECL polyvinylidene difluoride (PVDF) membrane (GE Healthcare). Membranes were then probed with the HisProbe-horseradish peroxidase (HRP) (Pierce), according to the manufacturer's instructions, and positive bands were detected using a chemiluminescent HRP substrate, according to the method of Haan and Behrmann (56). Image capture was performed with a ChemiDoc camera system (Bio-Rad).

## SUPPLEMENTAL MATERIAL

Supplemental material for this article may be found at <https://doi.org/10.1128/mBio.01535-18>.

**FIG S1**, PDF file, 0.1 MB.

**FIG S2**, PDF file, 0.1 MB.

**FIG S3**, PDF file, 0.1 MB.

## ACKNOWLEDGMENTS

We gratefully acknowledge the support of the CNRS and the Microbiology Department of I2BC. We are grateful to Yoshiharu Yamaichi from I2BC and to The National Bioresource Project, National Institute of Genetics, Japan, for providing *E. coli* strains.

We declare that we have no conflicts of interest with the contents of this article.

## REFERENCES

1. Barwinska-Sendra A, Waldron KJ. 2017. The Role of intermetal competition and mis-metalation in metal toxicity. *Adv Microb Physiol* 70: 315–379. <https://doi.org/10.1016/bs.ampbs.2017.01.003>.
2. Capdevila DA, Edmonds KA, Giedroc DP. 2017. Metallochaperones and metalloregulation in bacteria. *Essays Biochem* 61:177–200. <https://doi.org/10.1042/EBC20160076>.

3. Chandrangu P, Rensing C, Helmann JD. 2017. Metal homeostasis and resistance in bacteria. *Nat Rev Microbiol* 15:338–350. <https://doi.org/10.1038/nrmicro.2017.15>.
4. Rensing C, Grass G. 2003. *Escherichia coli* mechanisms of copper homeostasis in a changing environment. *FEMS Microbiol Rev* 27:197–213. [https://doi.org/10.1016/S0168-6445\(03\)00049-4](https://doi.org/10.1016/S0168-6445(03)00049-4).
5. Solioz M. 2018. Copper and bacteria: evolution, homeostasis, and toxicity. Springer International Publishing, Cham, Switzerland.
6. von Rozycki T, Nies DH. 2009. *Cupriavidus metallidurans*: evolution of a metal-resistant bacterium. *Antonie Van Leeuwenhoek* 96:115–139. <https://doi.org/10.1007/s10482-008-9284-5>.
7. Arguello JM, Eren E, Gonzalez-Guerrero M. 2007. The structure and function of heavy metal transport P1B-ATPases. *Biomaterials* 20:233–248. <https://doi.org/10.1007/s10534-006-9055-6>.
8. Outten FW, Huffman DL, Hale JA, O'Halloran TV. 2001. The independent *cue* and *cus* systems confer copper tolerance during aerobic and anaerobic growth in *Escherichia coli*. *J Biol Chem* 276:30670–30677. <https://doi.org/10.1074/jbc.M104122200>.
9. Rensing C, Fan B, Sharma R, Mitra B, Rosen BP. 2000. CopA: an *Escherichia coli* Cu(II)-translocating P-type ATPase. *Proc Natl Acad Sci U S A* 97:652–656. <https://doi.org/10.1073/pnas.97.2.652>.
10. Mandal AK, Cheung WD, Arguello JM. 2002. Characterization of a thermophilic P-type Ag<sup>+</sup>/Cu<sup>+</sup>-ATPase from the extremophile *Archaeoglobus fulgidus*. *J Biol Chem* 277:7201–7208. <https://doi.org/10.1074/jbc.M109964200>.
11. Stoyanov JV, Magnani D, Solioz M. 2003. Measurement of cytoplasmic copper, silver, and gold with a *lux* biosensor shows copper and silver, but not gold, efflux by the CopA ATPase of *Escherichia coli*. *FEBS Lett* 546:391–394. [https://doi.org/10.1016/S0014-5793\(03\)00640-9](https://doi.org/10.1016/S0014-5793(03)00640-9).
12. Macomber L, Imlay JA. 2009. The iron-sulfur clusters of dehydratases are primary intracellular targets of copper toxicity. *Proc Natl Acad Sci U S A* 106:8344–8349. <https://doi.org/10.1073/pnas.0812808106>.
13. Xu FF, Imlay JA. 2012. Silver(I), mercury(II), cadmium(II), and zinc(II) target exposed enzymic iron-sulfur clusters when they toxify *Escherichia coli*. *Appl Environ Microbiol* 78:3614–3621. <https://doi.org/10.1128/AEM.07368-11>.
14. Azzouzi A, Steunou AS, Durand A, Khalfaoui-Hassani B, Bourbon ML, Astier C, Bollivar DW, Ouchane S. 2013. Coproporphyrin III excretion identifies the anaerobic coproporphyrinogen III oxidase HemN as a copper target in the Cu<sup>+</sup>-ATPase mutant *copA*<sup>−</sup> of *Rubrivivax gelatinosus*. *Mol Microbiol* 88:339–351. <https://doi.org/10.1111/mmi.12188>.
15. Durand A, Azzouzi A, Bourbon ML, Steunou AS, Liotenberg S, Maeshima A, Astier C, Argentini M, Saito S, Ouchane S. 2015. c-type cytochrome assembly is a key target of copper toxicity within the bacterial periplasm. *mBio* 6:e01007-15.
16. Djoko KY, McEwan AG. 2013. Antimicrobial action of copper is amplified via inhibition of heme biosynthesis. *ACS Chem Biol* 8:2217–2223. <https://doi.org/10.1021/cb4002443>.
17. Borsetti F, Borghese R, Cappelletti M, Zannoni D. 2018. Tellurite processing by cells of *Rhodobacter capsulatus* involves a periplasmic step where the oxyanion causes a malfunction of the cytochrome c maturation system. *International Biodeterioration & Biodegradation* 130:84–90. <https://doi.org/10.1016/j.ibiod.2018.04.002>.
18. Barillo DJ, Marx DE. 2014. Silver in medicine: a brief history BC 335 to present. *Burns* 40:53–58. <https://doi.org/10.1016/j.burns.2014.09.009>.
19. Chandra R, Kang H. 2016. Mixed heavy metal stress on photosynthesis, transpiration rate, and chlorophyll content in poplar hybrids. *Forest Science and Technology* 12:55–61. <https://doi.org/10.1080/21580103.2015.1044024>.
20. Kupper H, Kupper F, Spiller M. 1996. Environmental relevance of heavy metal-substituted chlorophylls using the example of water plants. *J Exp Bot* 47:259–266. <https://doi.org/10.1093/jxb/47.2.259>.
21. Lee S, Kim YY, Lee Y, An G. 2007. Rice P1B-type heavy-metal ATPase, OsHMA9, is a metal efflux protein. *Plant Physiol* 145:831–842. <https://doi.org/10.1104/pp.107.102236>.
22. Sabatini SE, Juarez AB, Eppis MR, Bianchi L, Luquet CM, Rios de Molina MC. 2009. Oxidative stress and antioxidant defenses in two green microalgae exposed to copper. *Ecotoxicol Environ Saf* 72:1200–1206. <https://doi.org/10.1016/j.ecoenv.2009.01.003>.
23. Borisov VB, Verkhovsky MI. 2015. Oxygen as acceptor. *EcoSal Plus* 6. <https://doi.org/10.1128/ecosalplus.ESP-0012-2015>.
24. Saer RG, Blankenship RE. 2017. Light harvesting in phototrophic bacteria: structure and function. *Biochem J* 474:2107–2131. <https://doi.org/10.1042/BCJ20160753>.
25. McDermott G, Prince SM, Freer AA, Hawthornthwaite-Lawless AM, Papiz MZ, Cogdell RJ, Isaacs NW. 1995. Crystal structure of an integral membrane light-harvesting complex from photosynthetic bacteria. *Nature* 374:517–521. <https://doi.org/10.1038/374517a0>.
26. Roszak AW, Howard TD, Southall J, Gardiner AT, Law CJ, Isaacs NW, Cogdell RJ. 2003. Crystal structure of the RC-LH1 core complex from *Rhodospseudomonas palustris*. *Science* 302:1969–1972. <https://doi.org/10.1126/science.1088892>.
27. Yu LJ, Suga M, Wang-Otomo ZY, Shen JR. 2018. Structure of photosynthetic LH1-RC supercomplex at 1.9 Å resolution. *Nature* 556:209–213. <https://doi.org/10.1038/s41586-018-0002-9>.
28. Steunou AS, Ouchane S, Reiss-Husson F, Astier C. 2004. Involvement of the C-terminal extension of the alpha polypeptide and of the PucC protein in LH2 complex biosynthesis in *Rubrivivax gelatinosus*. *J Bacteriol* 186:3143–3152. <https://doi.org/10.1128/JB.186.10.3143-3152.2004>.
29. Freer A, Prince S, Sauer K, Papiz M, Hawthornthwaite-Lawless A, McDermott G, Cogdell R, Isaacs NW. 1996. Pigment-pigment interactions and energy transfer in the antenna complex of the photosynthetic bacterium *Rhodospseudomonas acidophila*. *Structure* 4:449–462. [https://doi.org/10.1016/S0969-2126\(96\)00050-0](https://doi.org/10.1016/S0969-2126(96)00050-0).
30. Gall A, Ellervee A, Sturgis JN, Fraser NJ, Cogdell RJ, Freiberg A, Robert B. 2003. Membrane protein stability: high pressure effects on the structure and chromophore-binding properties of the light-harvesting complex LH2. *Biochemistry* 42:13019–13026. <https://doi.org/10.1021/bi0530351>.
31. Bragg PD, Rainnie DJ. 1974. The effect of silver ions on the respiratory chain of *Escherichia coli*. *Can J Microbiol* 20:883–889. <https://doi.org/10.1139/m74-135>.
32. Holt KB, Bard AJ. 2005. Interaction of silver(I) ions with the respiratory chain of *Escherichia coli*: an electrochemical and scanning electrochemical microscopy study of the antimicrobial mechanism of micromolar Ag<sup>+</sup>. *Biochemistry* 44:13214–13223. <https://doi.org/10.1021/bi0508542>.
33. Miyayama T, Arai Y, Suzuki N, Hirano S. 2013. Mitochondrial electron transport is inhibited by disappearance of metallothionein in human bronchial epithelial cells following exposure to silver nitrate. *Toxicology* 305:20–29. <https://doi.org/10.1016/j.tox.2013.01.004>.
34. Yuan L, Gao T, He H, Jiang FL, Liu Y. 2017. Silver ion-induced mitochondrial dysfunction via a nonspecific pathway. *Toxicology Res (Camb)* 6:621–630. <https://doi.org/10.1039/c7tx00079k>.
35. Khalfaoui Hassani B, Steunou AS, Liotenberg S, Reiss-Husson F, Astier C, Ouchane S. 2010. Adaptation to oxygen: role of terminal oxidases in photosynthesis initiation in the purple photosynthetic bacterium, *Rubrivivax gelatinosus*. *J Biol Chem* 285:19891–19899. <https://doi.org/10.1074/jbc.M109.086066>.
36. Baba T, Ara T, Hasegawa M, Takai Y, Okumura Y, Baba M, Datsenko KA, Tomita M, Wanner BL, Mori H. 2006. Construction of *Escherichia coli* K-12 in-frame, single-gene knockout mutants: the Keio collection. *Mol Syst Biol* 2:2006–0008.
37. De Matteis V, Cascione M, Toma CC, Leporatti S. 2018. Silver nanoparticles: synthetic routes, *in vitro* toxicity and therapeutic applications for cancer disease. *Nanomaterials (Basel)* 8:319. <https://doi.org/10.3390/nano8050319>.
38. Ivask A, Elbadawy A, Kaweeteeraw C, Boren D, Fischer H, Ji Z, Chang CH, Liu R, Tolaymat T, Telesca D, Zink JL, Cohen Y, Holden PA, Godwin HA. 2014. Toxicity mechanisms in *Escherichia coli* vary for silver nanoparticles and differ from ionic silver. *ACS Nano* 8:374–386. <https://doi.org/10.1021/nn4044047>.
39. Navarro E, Piccapietra F, Wagner B, Marconi F, Kaegi R, Odzak N, Sigg L, Behra R. 2008. Toxicity of silver nanoparticles to *Chlamydomonas reinhardtii*. *Environ Sci Technol* 42:8959–8964. <https://doi.org/10.1021/es801785m>.
40. Navarro E, Wagner B, Odzak N, Sigg L, Behra R. 2015. Effects of differently coated silver nanoparticles on the photosynthesis of *Chlamydomonas reinhardtii*. *Environ Sci Technol* 49:8041–8047. <https://doi.org/10.1021/acs.est.5b01089>.
41. Li X, Ke M, Zhang M, Peijnenburg W, Fan X, Xu J, Zhang Z, Lu T, Fu Z, Qian H. 2018. The interactive effects of diclofop-methyl and silver nanoparticles on *Arabidopsis thaliana*: growth, photosynthesis and antioxidant system. *Environ Pollut* 232:212–219. <https://doi.org/10.1016/j.envpol.2017.09.034>.
42. Luer L, Moulisova V, Henry S, Polli D, Brotsudarmo TH, Hoseinkhani S, Brida D, Lanzani G, Cerullo G, Cogdell RJ. 2012. Tracking energy transfer between light harvesting complex 2 and 1 in photosynthetic membranes grown under high and low illumination. *Proc Natl Acad Sci U S A* 109:1473–1478. <https://doi.org/10.1073/pnas.1113080109>.
43. Baumann HA, Morrison L, Stengel DB. 2009. Metal accumulation and

- toxicity measured by PAM-chlorophyll fluorescence in seven species of marine macroalgae. *Ecotoxicol Environ Saf* 72:1063–1075. <https://doi.org/10.1016/j.ecoenv.2008.10.010>.
44. Kupper H, Kupper F, Spiller M. 1998. *In situ* detection of heavy metal substituted chlorophylls in water plants. *Photosynthesis Res* 58:123–133. <https://doi.org/10.1023/A:1006132608181>.
  45. Mauk MR, Mauk AG. 2010. Metal ions and electrolytes regulate the dissociation of heme from human hemopexin at physiological pH. *J Biol Chem* 285:20499–20506. <https://doi.org/10.1074/jbc.M110.123406>.
  46. Mauk MR, Rosell FI, Mauk AG. 2009. Metal ion facilitated dissociation of heme from b-type heme proteins. *J Am Chem Soc* 131:16976–16983. <https://doi.org/10.1021/ja907484j>.
  47. Mahato M, Pal P, Kamilya T, Sarkar R, Chaudhuri A, Talapatra GB. 2010. Hemoglobin-silver interaction and bioconjugate formation: a spectroscopic study. *J Phys Chem B* 114:7062–7070. <https://doi.org/10.1021/jp100188s>.
  48. Mahato M, Pal P, Tah B, Ghosh M, Talapatra GB. 2011. Study of silver nanoparticle-hemoglobin interaction and composite formation. *Colloids Surf B Biointerfaces* 88:141–149. <https://doi.org/10.1016/j.colsurfb.2011.06.024>.
  49. Silhavy TJ, Kahne D, Walker S. 2010. The bacterial cell envelope. *Cold Spring Harb Perspect Biol* 2:a000414. <https://doi.org/10.1101/cshperspect.a000414>.
  50. Feng QL, Wu J, Chen GQ, Cui FZ, Kim TN, Kim JO. 2000. A mechanistic study of the antibacterial effect of silver ions on *Escherichia coli* and *Staphylococcus aureus*. *J Biomed Mater Res* 52:662–668. [https://doi.org/10.1002/1097-4636\(20001215\)52:4<662::AID-JBM10>3.0.CO;2-3](https://doi.org/10.1002/1097-4636(20001215)52:4<662::AID-JBM10>3.0.CO;2-3).
  51. Jung WK, Koo HC, Kim KW, Shin S, Kim SH, Park YH. 2008. Antibacterial activity and mechanism of action of the silver ion in *Staphylococcus aureus* and *Escherichia coli*. *Appl Environ Microbiol* 74:2171–2178. <https://doi.org/10.1128/AEM.02001-07>.
  52. Sutterlin S, Tano E, Bergsten A, Tallberg AB, Melhus A. 2012. Effects of silver-based wound dressings on the bacterial flora in chronic leg ulcers and its susceptibility *in vitro* to silver. *Acta Derm Venereol* 92:34–39. <https://doi.org/10.2340/00015555-1170>.
  53. Hussain S, Andrews D, Hill BC. 2018. Exposure of *Bacillus subtilis* to silver inhibits activity of cytochrome c oxidase *in vivo* via interaction with SCO, the CuA assembly protein. *Metallomics* 10:735–744. <https://doi.org/10.1039/C7MT00343A>.
  54. Agalidis I, Rivas E, Reiss-Husson F. 1990. Reaction center light harvesting B875 complexes from *Rhodocyclus gelatinosus*: characterization and identification of quinones. *Photosynth Res* 23:249–255. <https://doi.org/10.1007/BF00034855>.
  55. Wittig I, Karas M, Schagger H. 2007. High resolution clear native electrophoresis for in-gel functional assays and fluorescence studies of membrane protein complexes. *Mol Cell Proteomics* 6:1215–1225. <https://doi.org/10.1074/mcp.M700076-MCP200>.
  56. Haan C, Behrmann I. 2007. A cost effective non-commercial ECL-solution for Western blot detections yielding strong signals and low background. *J Immunol Methods* 318:11–19. <https://doi.org/10.1016/j.jim.2006.07.027>.



## Supplemental results:

### S1- Toxicity of CuSO<sub>4</sub> and AgNO<sub>3</sub> in high-density culture.

In the article (Fig. 1), it was shown that cells growth was not affected by the addition of CuSO<sub>4</sub> or CdCl<sub>2</sub>, even at 1 mM. In contrast, addition of 1 μM AgNO<sub>3</sub> was enough to fully inhibit cells growth. These data were obtained when adding metal ions during early stage of the exponential growth phase. However, the effect of these metals is different when adding them during the late exponential growth phase or stationary phase, where cultures have high-density of cells. While the effect of CuSO<sub>4</sub> remains the same, Ag<sup>+</sup> toxicity was reduced (Fig. 44). Cells were able to resist up to 6 μM of AgNO<sub>3</sub>. Similar results were reported for *E. coli* (Xu & Imlay, 2012). The ability of cations to interact with polysaccharides and cell surface could explain this difference. It was indeed suggested, that metal ions could interact and be sequestered on the cell surface; therefore, the high cell density will affect the metals dose response (Xu & Imlay, 2012).

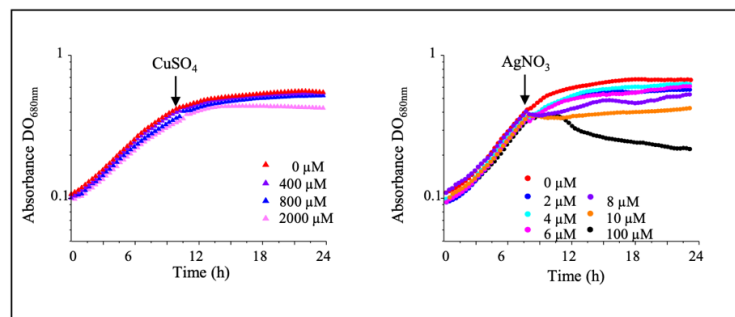


**Figure 44. Toxicity of CuSO<sub>4</sub> and AgNO<sub>3</sub> in cultures of high cells density.**

Toxicity of CuSO<sub>4</sub> and AgNO<sub>3</sub> in high cell density culture. Cells were grown in micro-aerobiosis on microplates in the Tecan Infinite M200 luminometer. Indicated concentrations of CuSO<sub>4</sub> or AgNO<sub>3</sub> were added to the growth medium after cells reached OD<sub>680nm</sub>=0.4 (arrow).

### S2- Effect of CuSO<sub>4</sub> on LH2 and LH1-RC complexes.

In the course of this work, it was shown that both Ag<sup>+</sup> and Cu<sup>2+</sup> are specifically stimulating the loss of the 800 nm bacteriochlorophyll, but not the 850 nm in the LH2 antennae. The impact of CuSO<sub>4</sub> on the RC-LH1 core was also assessed using the *pucBA*

LH2<sup>-</sup> deficient mutant. Spectra of the exposed cells showed that CuSO<sub>4</sub> only very slightly affected the amount of the RC-LH1 (Fig. 45).

Moreover, total protein lysates from all untreated or treated samples were loaded onto SDS-PAGE. The Coomassie blue staining showed that all wild-type samples have comparable amounts of LH2 subunits, indicating that the release of B800 molecules did not affect the LH2 protein stability (Fig. 45D) in agreement with the UV-Vis spectra.

Altogether, these data indicated that Ag<sup>+</sup> and Cu<sup>2+</sup> induced alterations in the structure of the LH2 complexes, targeting the B800 molecules of the complex, while the RC-LH complex is rather well protected.

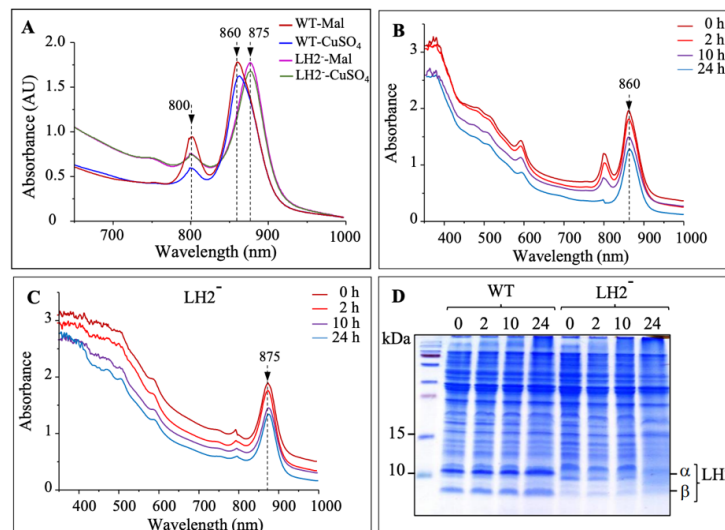


**Figure 45. Effect of CuSO<sub>4</sub> on LH2 complex.**

**A-** Absorption spectra of WT and LH2 deficient mutant cells grown overnight under photosynthetic condition exposed or not to 1 mM CuSO<sub>4</sub>. **B-** Absorption spectra of WT cells grown overnight under photosynthetic condition and exposed to 1 mM CuSO<sub>4</sub>. The 350-1000 nm spectra were recorded after 2, 10 and 24 h. **C-** Spectral analyses of the LH2 deficient mutant cells exposed to 1 mM CuSO<sub>4</sub>. Spectra were recorded after 2, 10 and 24 h. **D-** Coomassie blue staining of total protein lysate from untreated or CuSO<sub>4</sub> treated cells.

### S3- Effect of AgNO<sub>3</sub> treatment on carotenoids in the LH2 complexes

In the LH2 antennae structure of *Rhodospseudomonas acidophila*, the 800-nm absorbing bacteriochlorophyll *a* molecules lie between the α-apoprotein helices, where the phytyl moieties of B800 interact with the carotenoids (Fig. 46). Since Ag<sup>+</sup> or Cu<sup>2+</sup>

affected the B800 BCh, it was expected that loss of this bacteriochlorophyll might affect carotenoids within the LH2 complex exposed to metals.

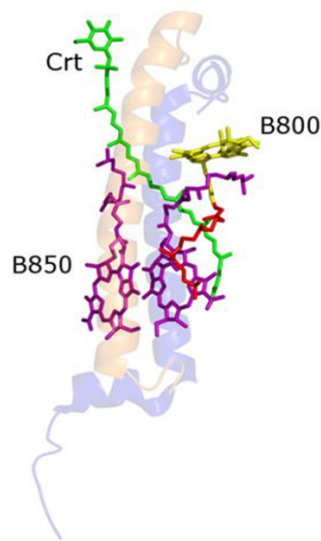


**Figure 46. LH2 monomer and its associated pigments.**

(view parallel to the plane of the membrane).  $\alpha$  and  $\beta$  subunits are in blue and orange, the B800 BCh are in yellow, the B850 are colored purple, and the carotenoids are in green (Saer & Blankenship, 2017).

Purified membranes subjected to  $\text{Ag}^+$  or  $\text{Cu}^{2+}$  treatment, showed a significant decrease in the intensity of the 800 nm band with an absorption of increase at 688 nm. While the spectra of untreated membranes showed no changes in the amount of the RC, LH1, and LH2 were observed.

A close analyses of the spectra showed that indeed, carotenoids were also affected by  $\text{Cu}^{2+}$  (Fig. 5 in the paper) and by  $\text{Ag}^+$  as evidenced by the shift in their absorbance spectra (Fig. 47). The spectra of untreated proteins exhibited three peaks at 452, 482, and 512 nm. On the other hand, the spectra showed that with extended exposure to  $\text{AgNO}_3$ , a shift was observed in the carotenoid absorption region.  $\text{AgNO}_3$  treatment resulted in a shift of the carotenoid absorbance to 448, 474, and 508 nm.

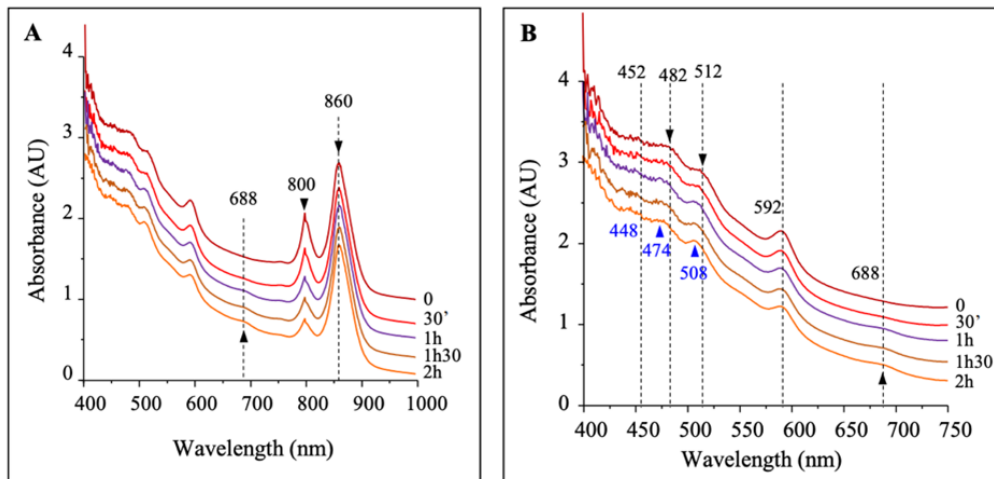


**Figure 47. Effect of  $\text{AgNO}_3$  treatment on carotenoids in the LH2 complexes in membrane-enriched fractions.**

**A-** Cells membrane fractions were mixed with  $\text{AgNO}_3$  at a final concentration of 2 mM and 350-1000 nm spectra were recorded every 30 min. **B-** Zoom in the 400-750 nm spectrum absorbance highlighting the shift in the carotenoid bands and the increase in the 688 nm band.

Thus, we concluded that in the presence of  $\text{CuSO}_4$  or  $\text{AgNO}_3$ , changes in the LH2 absorption spectrum are related to the disruption of the interaction of B800 molecules, which causes the release of the B800 bacteriochlorophylls and subsequently impacts the spectral properties of the carotenoids within the B850 LH2 complex.

### **Additional results:**

I will present some data that were collected during my study. They are also important to complete our understanding regarding silver and copper effect on membrane proteins, and their impact on photosynthetic and respiratory complexes in *R. gelatinosus*.

#### **1- Effect of $\text{AgNO}_3$ treatment on *cbb*<sub>3</sub> oxidase.**

In this work, it was shown that  $\text{AgNO}_3$  damage the B800 of LH2 complex and inhibits the activity of respiratory complexes in the purified membrane including *cbb*<sub>3</sub> cytochrome *c* oxidase. This indicated that the  $\text{Ag}^+$  ions can damage assembled complexes within the membrane. We have shown that the loss of B800 did not affected

-RESULTS-

or degraded the LH2 complex (Fig. 45), very likely because the remaining B850 chlorophylls and the carotenoids are sufficient to stabilize and maintain the LH2 complex. We question whether inhibition of the *cbb<sub>3</sub>* oxidase is related only to the putative loss of heme, or whether Ag<sup>+</sup> damage, leads to degradation and loss of the complex?

To test this different hypothesis, we have specific antibodies raised against *cbb<sub>3</sub>* of *R. gelatinosus*. I therefore, checked the activity (DAB cyt c oxidase activity assay) and amount of *cbb<sub>3</sub>* (Western blot using CcoP antibodies) in solubilized membranes from grown cells exposed to AgNO<sub>3</sub>.

The results are presented in (Fig. 48) and clearly showed that both *cbb<sub>3</sub>* activity and amount are decreased in Ag<sup>+</sup> exposed cells. It is known that absence or loss of heme from cytochromes leads to rapid degradation of the apoprotein, we therefore propose that if Ag<sup>+</sup> damage heme in respiratory complexes, this will ultimately lead to the degradation of these complexes.

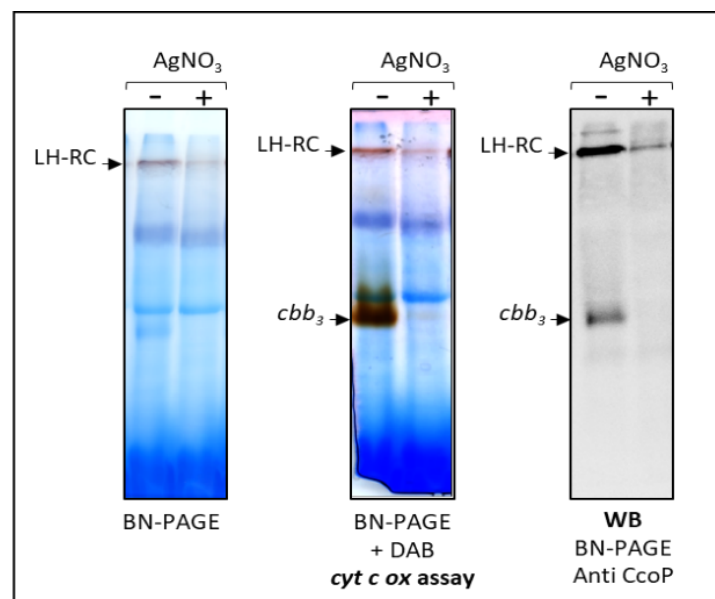


**Figure 48. Effect of Ag<sup>+</sup> on *cbb<sub>3</sub>* activity and amount in stressed cells.**

The wild-type cells were grown over night under micro-aerobic condition and shocked for 1 h with AgNO<sub>3</sub>. Equal amount of membranes were solubilized and subjected to BN electrophoresis. The gel was cut in three parts and the activity of *cbb<sub>3</sub>* was revealed using DAB assay, while the amount of the complex was revealed on Western blot using CcoP subunit antibodies.

## 2- Effect of AgNO<sub>3</sub> treatment on the NADH dehydrogenase, in *vivo* and *vitro*.

In the published work we have presented data regarding the effect of AgNO<sub>3</sub> on two complexes among the five complexes of the the respiratory chain. I also wanted to study the effect of AgNO<sub>3</sub> on the NADH dehydrogenase complex I *in vivo* and *in vitro* as well. For that purpose, grown cells of *R. gelatinosus* were exposed to increased concentrations of AgNO<sub>3</sub> (25, 50, 100 and 150 μM) for 1 hour, and the activity of complex I was detected in purified membranes on BN-PAGE using the NADH/NBT oxidoreductase assay.

As shown in (Fig. 49) bands corresponding to the putative complex I were revealed in the solubilized membrane proteins from untreated and 25 μM AgNO<sub>3</sub> stressed cells. Decreased activity was detected in the 50 μM AgNO<sub>3</sub> stressed cells. However, no active band could be detected in the membrane fractions isolated from 100 and 150 μM AgNO<sub>3</sub> stressed cells.

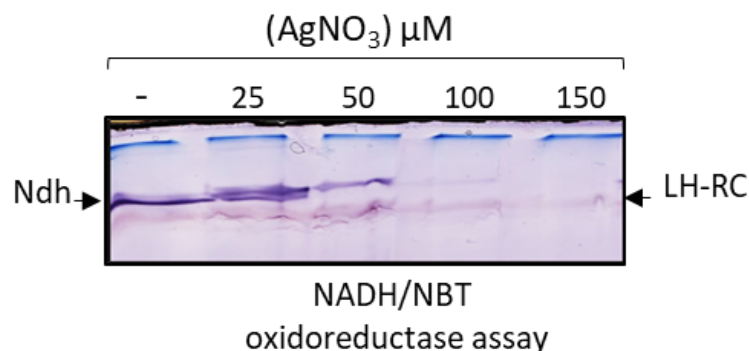


**Figure 49. Effect of Ag<sup>+</sup> on Complex I activity in stressed cells.**

The wild-type cells were grown under micro-aerobic condition and shocked for 1 h, with increasing concentration of AgNO<sub>3</sub>. Equal amount of membranes were solubilized and subjected to BN electrophoresis. The activity of complex I was revealed using NADH/NBT oxidoreductase assay.

Similarly, to the *in vivo* data, incubated membrane proteins with increasing concentration of AgNO<sub>3</sub> led to a decrease in NADH activity; and completely inhibited at 750, 900 and 1000 μM (Fig. 50).

-RESULTS-

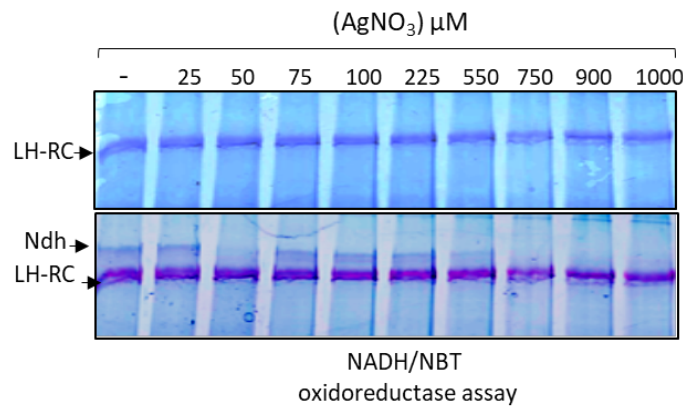


**Figure 50. Effect of Ag<sup>+</sup> on Complex I activity in solubilized membranes.**

Equal amount of membranes from WT were mixed with increasing concentration of AgNO<sub>3</sub> for 1 h. DDM solubilized membrane proteins were then separated on a 5% to 12% gradient BN-PAGE. The activity of complex I was revealed using NADH/NBT oxidoreductase assay.

Altogether, these data suggested that AgNO<sub>3</sub> could inhibit respiration by damaging the respiratory complexes, including cytochrome *c* oxidase, succinate and NADH dehydrogenases. These results on complex I were not shown in the published paper because we were missing the NADH mutant strain to be used as control. In fact, other complexes that exhibit NADH dehydrogenase activity may be present in the membrane fraction. Nevertheless, our data strongly support that AgNO<sub>3</sub> could inhibit respiration by directly damaging the respiratory complexes, including cytochrome *c* oxidase, succinate and NADH dehydrogenases.

## Discussion:

---

Metals such as silver and copper are known for their use as antimicrobial agents. However, the overuse of such metals is a serious threat to the environment and to all living organisms. Furthermore, the toxic effect of metal nanoparticles is very often related to the released metal ions and their ability to interact with bacterial membranes and proteins. Thus, this study aims to characterize the toxicity of silver and copper ions and to identify some of their cellular targets. We should note that metal ions, targets a variety of molecules and proteins in the cells, and thus the identified targets in my work are related to the growth conditions and the phenotype we observe. We should keep in mind that there are many potential metal targets in the cell, as explained in the introduction section.

Our results indicated that silver in its ionic form is very toxic even at very low concentration in *R. gelatinosus*. This is may be related to the absence of an efficient efflux system to detoxify  $\text{Ag}^+$  and/or to its bioactivity and ability to damage specific molecules. Through this study, it was found that silver completely inhibits the growth of *R. gelatinosus* if coinoculated with diluted cells. Thus, to assess the effect of  $\text{Ag}^+$ , we first grow cells and then shock them with  $\text{Ag}^+$  to study its impact. Another fact is that while the CopA efflux is effective in expelling  $\text{Ag}^+$  ions outside the cells in *E. coli*, it was not involved in *R. gelatinosus*.  $\text{Ag}^+$  does not induce *cop* operon, and the mutant *copA* behave as the wild type when exposed to  $\text{Ag}^+$ . More studies are required to characterize the gene response to silver stress in *R. gelatinosus*. For example, a transcriptomic or proteomic study could reveal the genes or proteins that are up-regulated or down-regulated after  $\text{Ag}^+$  shock. Genetic analyses of these genes can confirm the role of the candidate genes. Otherwise, the use of a transposon library mutant could also be an effective approach to identify genes involved in  $\text{Ag}^+$  response. Indeed, mutants that do not tolerate  $\text{Ag}^+$  would be affected in the efflux or detoxification systems, while mutants that tolerate  $\text{Ag}^+$  shock will be affected in the import system or regulatory pathways for examples.

In our model *R. gelatinosus*, we found that both metals  $\text{Ag}^+$  and  $\text{Cu}^{2+}$  target the LH2 complex in the PS apparatus; specifically targeting the B800 molecules but not the B850 Bch. We have proposed that this could be related to the structure of the LH2 complex. On one hand, the B850 bacteriochlorophylls with the carotenoid molecules are buried between the  $\alpha$  and  $\beta$  subunit outer rings and are therefore well shielded from the external buffer (Fig. 9 in the paper). On the other hand, the B800 molecules are located within the outer rings formed by helices of the  $\beta$  subunits and are parallel to the lipid surface near the cytosolic side. This makes them in contact with the solvent, thus, become more exposed than the B850 molecules. The mechanism by which  $\text{Ag}^+$  or  $\text{Cu}^{2+}$  release B800 from the LH2 remains to be studied. However, it is tempting to speculate that  $\text{Ag}^+$  or  $\text{Cu}^{2+}$  may damage or de-metalate the exposed B800 bacteriochlorophylls. This could be tested *in vitro*. In fact, we can expose purified or commercial chlorophyll to metal ions and check the presence of  $\text{Mg}^{2+}$  or other metals in the porphyrin by UV-Vis absorbance as shown in (Fig. 51) (Karcz et al., 2014).

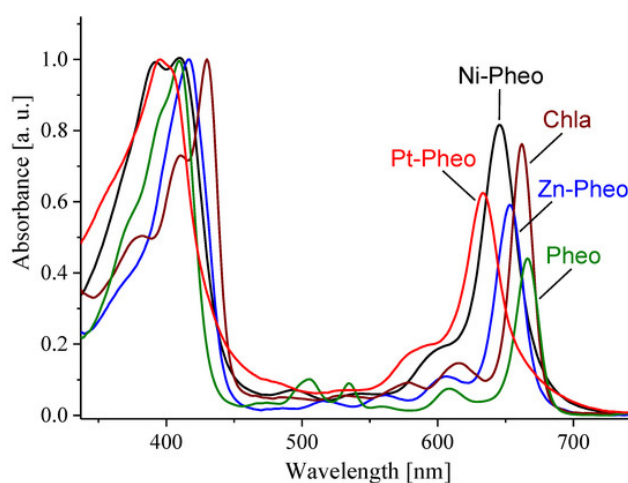


**Figure 51. Electronic absorption spectra of pheophytin (Pheo: chlorophyll without  $\text{Mg}^{2+}$ ) and its complexes with  $\text{Mg}^{2+}$  (Chla),  $\text{Zn}^{2+}$ ,  $\text{Ni}^{2+}$ , and  $\text{Pt}^{2+}$ .**

The spectra were recorded at ambient temperature in acetone, normalized to the Soret bands' maxima (Karcz et al., 2014) .

## -RESULTS-

Provided that the LH2 structure is conserved in purple bacteria, we would expect and suggest that similar effects of  $\text{Ag}^+$  or  $\text{Cu}^{2+}$  would occur in other LH2 containing bacteria. It is also tempting to suggest that exposed chlorophyll molecules, in any photosynthetic complex, might be damaged by metals. It is known that metal ions affect photosynthesis and the amount of chlorophylls in plants (DalCorso et al., 2013). Inhibition of chlorophyll synthesis or degradation of photosystem can explain the decrease of chlorophyll. A direct damage of plant chlorophylls by metals as previously shown (Küpper et al., 1998b) and shown in our study can also explain chlorophyll decrease in metal stressed plants.

Also, we have found that  $\text{Ag}^+$  or  $\text{Cu}^{2+}$  have an impact on the activity of cytochrome *c* oxidase and succinate dehydrogenase (SDH) in *R. gelatinosus*, as well as SDH in *E. coli*. The effect of metals on these complexes was first observed *in vivo* and could thus be related to inhibition of the assembly of the complexes or to a direct damage. Nevertheless, the *in vitro* data showed that even assembled complexes can be damaged by excess metal.

Based on our finding that  $\text{Ag}^+$  or  $\text{Cu}^{2+}$  directly dissociate exposed chlorophyll from LH2, we suggest that inhibition of cytochrome *c* oxidase and succinate dehydrogenase might be also the consequence of porphyrin (heme) dissociation from these complexes both *in vivo* and *in vitro* under metal excess. Yet, we cannot exclude an effect of  $\text{Ag}^+$  or  $\text{Cu}^{2+}$  on the 4Fe-4S clusters in the SDH (complex II). In this regard, damage of 4Fe-4S clusters in complex I by  $\text{Ag}^+$  or  $\text{Cu}^{2+}$  would also explain the inhibitory effect observed when we assayed for the NADH dehydrogenase activity of the complex.

-RESULTS-

## 2. Putative transport systems involved in metal tolerance in *R. gelatinosus*

### Introduction:

To resist metal toxicity, cells use various strategies to survive. Limiting the uptake or inducing the required detoxification enzymes and activating the efflux pumps are examples of cell defence against metal toxicity. Silver tolerance in bacteria rely on the induction of the efflux ATPase and RND systems to expel the ions. In *E. coli* and other species, the copper efflux system is induced by  $\text{AgNO}_3$  and both CopA and CusCFBA are involved in  $\text{Ag}^+$  efflux and tolerance (Gudipaty et al., 2012; Rensing et al., 2000).

In the frame of my research study, I was interested in identifying the genes that might be involved in silver tolerance in *R. gelatinosus*. We decided to test known candidate genes encoding ion transporters in *R. gelatinosus*. These include *copA*, *cadA* but also genes encoding putative proteins displaying homologies with the RND Cus system or the cation diffusion facilitator CdfA. In addition, an outer membrane OmpW was identified in the laboratory as a putative copper importer, *ompW* was also selected to check whether it is involved in  $\text{Ag}^+$  import.

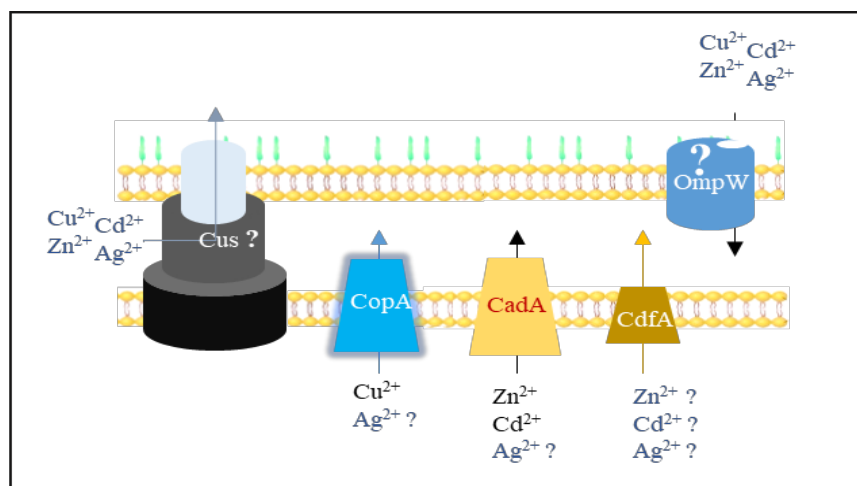


**Figure 52. Metal transporters identified in *R. gelatinosus*.**

Scheme showing the known (CopA/ CadA) and the putative metal transporters in *R. gelatinosus*.

The approach was to use available *copA* and *cadA* deficient mutants and generate deletion mutation in the three other genes, and then assay for the Ag<sup>+</sup> and other metals tolerance/ sensitivity in these mutants in comparison with the wild type strain.

*R. gelatinosus* can be transformed by electroporation and selection of double cross-over event (inactivated gene) can be achieved on selective media (kan<sup>R</sup>, Amp<sup>S</sup>) as depicted in (Fig. 53). Then gene inactivation is tested by PCR to ensure that the gene is inactivated and that the wild type gene is absent in the strain.

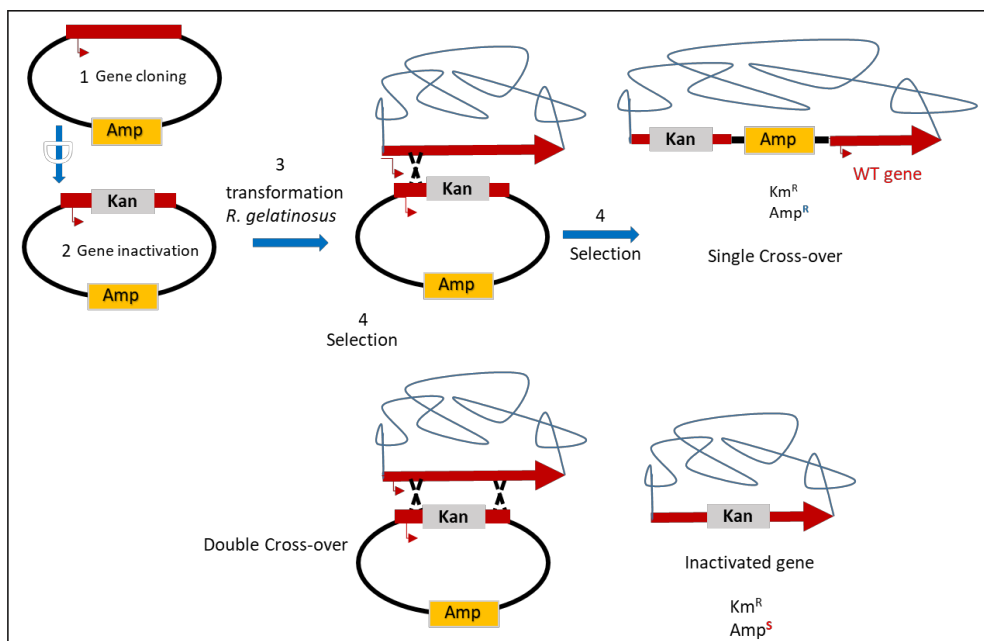


**Figure 53. Gene inactivation by homologous recombination in *R. gelatinosus***

## Results:

### 1- The *copA*, *copI* and *cadA* proteins are not involved in silver tolerance.

*copA* was identified as coding for the Cu<sup>+</sup> efflux ATPase in *R. gelatinosus* (Azzouzi et al., 2013). As mentioned above and in the published data, CopA was not involved in Ag<sup>+</sup> response as shown by growth of the *copA*<sup>-</sup> mutant in the presence of indicated concentration of AgNO<sub>3</sub> on solid and liquid malate medium (Tambosi et al.,

2018). Furthermore, the CopI protein, also involved in copper tolerance, was found to be induced by cadmium and other metals ( $\text{Ni}^{2+}$  and  $\text{Zn}^{2+}$ ) but not by  $\text{Co}^{2+}$  (unpublished by the laboratory). CopI is also involved in  $\text{Cd}^{2+}$  tolerance (Steunou et al., 2020a). Thanks to the presence of 5 histidine residues in the N-ter of CopI protein, it can be detected on Western blot using a His-probe that recognize and interact with the His stretch in the protein. I have tried to detect CopI when cells were exposed to increasing concentration of  $\text{AgNO}_3$ . The western blot showed no induction of CopI by  $\text{AgNO}_3$ , in contrast to  $\text{Cu}^{2+}$  or  $\text{Cd}^{2+}$ .

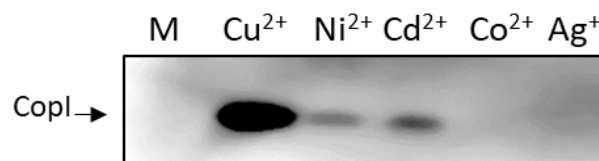


**Figure 54. Induction of CopI by metal ions.**

Cells were grown under photosynthesis and exposed overnight to 1 mM  $\text{Cu}^{2+}$ ,  $\text{Ni}^{2+}$ ,  $\text{Cd}^{2+}$ ,  $\text{Co}^{2+}$  or 2  $\mu\text{M}$   $\text{Ag}^+$ . Western blot on total extract was revealed using the His probe.

These data showed that in contrast to *E. coli*, *S. typhimurium* and other bacteria (Gudipaty et al., 2012; Rensing et al., 2000), the copper efflux system is not involved in  $\text{Ag}^+$  response in *R. gelatinosus*. Similarly, based on the growth phenotype of *cadA* mutant on  $\text{AgNO}_3$  it was concluded that the  $\text{Zn}^{2+}/\text{Cd}^{2+}$ -ATPase CadA is not involved in  $\text{Ag}^+$  tolerance (Tambosi et al., 2018).

## 2- The Cation diffusion facilitator CdfA

The cation diffusion facilitator CDF family are transporters involved in metal import into the cytoplasm, but some are also involved in the efflux of metals such as  $\text{Zn}^{2+}$  or  $\text{Cd}^{2+}$  (Nies 2003). While analyzing the soluble and membrane fractions of *R. gelatinosus* cells exposed to increasing  $\text{AgNO}_3$  using the His probe to detect CopI, we observed a slight increase in a membrane protein around 37 kDa in response to  $\text{AgNO}_3$ . We thought that  $\text{Ag}^+$  might therefore regulate this protein.

## -RESULTS-

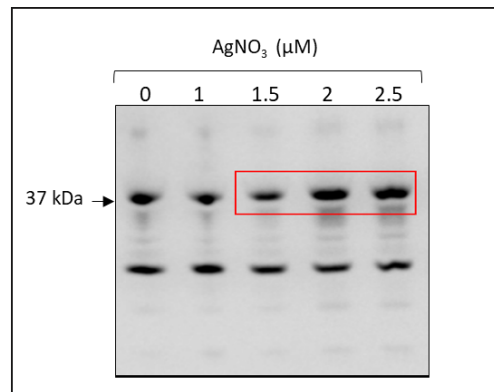


**Figure 55. *R. gelatinosus* proteins induction undress silver stress.**

Five cultures of *R. gelatinosus* were grown under photosynthetic condition; four of them were exposed to (1, 1.5, 2, and 2.5  $\mu\text{M}$ ) of  $\text{AgNO}_3$ . After overnight growth, membrane fractions were used for WB to detect induced proteins under silver stress by using His-probe.

The fact that we revealed this protein with the His probe, indicated that it should be a histine rich protein, with domain of at least 5 histidines. Search of proteins with histidine clusters in the genome of *R. gelatinosus*, pointed out to a His rich 35 kDa protein annotated as "putative cation transmembrane transporter". Analyses of the sequence showed indeed a His rich sequence (Fig. 56), and blast analyses showed that it has similarities with the CDF proteins YiiP or ZitB from *E. coli* and other bacteria. YiiP or ZitB are involved in the efflux of  $\text{Zn}^{2+}$  in *E. coli* and other organisms (Lu & Fu, 2007).

```
MSSHHQDLSPLPHPAFADEGVARREKALLQVTLTLVTMAVEVGAGWWTGSLALLADGWWMGTHALALGGAVLAYRLARR  
ASAHGGYAFGGWKIEVLAAYTSGLLLLAAAAGIAWDAIATLREPRPIAFGEAMGVAVLGLVNLASAWLLSRGGHDHHHHHHHD  
HHHGHADDHNDHDDHDPHGHHHHDANFGAAYLHVLADLMTSVLAI AALAGGLWAGWRWLDPAVALLGALVVGQWALG  
VLRQSSRALVDATADPEISGRIRTLIEADGDARLSDLHVWQVGAQAWSAAIAIVADRPLPAAVYRARLAEIVPLRHVTVEVHRCE  
GCGEACPRG
```

**Figure 56. *R. gelatinosus* CdfA sequence showing the His rich domain.**

To check if CdfA is involved in  $\text{Ag}^+$  tolerance, I have cloned and inactivated the *cdfA* gene in *R. gelatinosus* and tested the resistance of the mutant in comparison with the wild type when exposed to excess  $\text{Cu}^{2+}$ ,  $\text{Ag}^+$  and  $\text{Cd}^{2+}$ .

As shown in figure (Fig. 57), WT and *cdfA*<sup>-</sup> strains were grown overnight on malate plates containing  $\text{CuSO}_4$  and  $\text{AgNO}_3$ . Under  $\text{Cu}^{2+}$  stress, CdfA is not required since the mutant growth was not affected. However, on  $\text{Ag}^+$  containing plates, the

-RESULTS-

growth of *cdfA*<sup>-</sup> mutant was affected in contrast with the wild type. These data suggested that CdfA might be involved in Ag<sup>+</sup> tolerance.

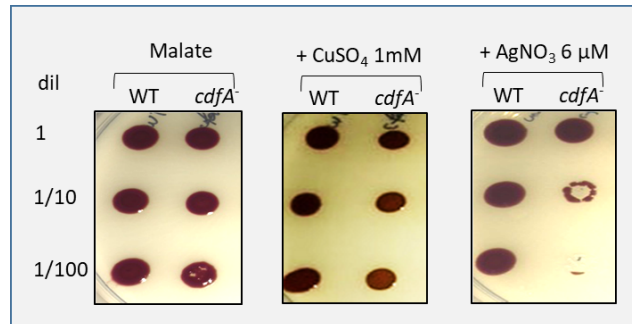


**Figure 57. CdfA could be required for growth on silver but not on copper.**

8 μl drop of undiluted, 10- and 100-times dilution of WT and *cdfA*<sup>-</sup> mutant cultures were spotted on plates and incubated for growth overnight by photosynthesis (30°C).

Given that homologues of CdfA (YiiP/ ZitB) were identified as Zn<sup>2+</sup> or Cd<sup>2+</sup> transporters, we also checked the importance of CdfA in Cd<sup>2+</sup> tolerance. To this aim we also generated a double mutant in which both CdfA and the Cd<sup>2+</sup>-ATPase CadA were inactivated. The ability of these strains to tolerate cadmium or Ag<sup>+</sup> was tested as above on plates containing CdCl<sub>2</sub> or AgNO<sub>3</sub> under photosynthetic and respiratory conditions. As shown in (Fig. 58), on CdCl<sub>2</sub>, *cdfA*<sup>-</sup> growth was not affected by Cd<sup>2+</sup>, while CadA growth was limited. Inactivation of *cdfA*<sup>-</sup> in *cadA*<sup>-</sup> background did not increase the sensitivity of *cadA*<sup>-</sup> mutant to Cd<sup>2+</sup>. These results showed that CdfA did not contribute to cadmium tolerance in *R. gelatinosus*. On AgNO<sub>3</sub> containing plates, no difference was

-RESULTS-

observed between all the strains in contrast to the previous experiment showing sensitivity of the *cdfA*<sup>-</sup> mutant to silver.

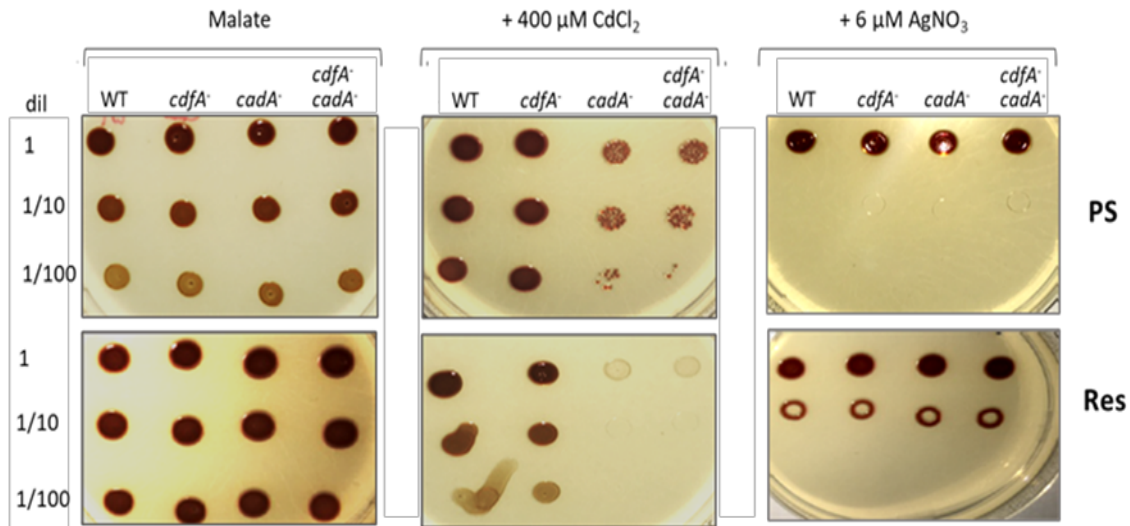


**Figure 58. Role of CdfA in growth on cadmium or silver.**

8 μl drop of undiluted, 10- and 100-times dilution of WT, *cdfA*<sup>-</sup>, *cadA*<sup>-</sup> and *cdfA*<sup>-</sup>*cadA*<sup>-</sup> mutant cultures were spotted on plates and incubated for growth overnight by photosynthesis (PS) or respiration (Res) at 30°C.

Unfortunately, for unknown reason, the phenotype of *cdfA*<sup>-</sup> strain on Ag<sup>+</sup> plates was not very stable. We also checked the phenotype in liquid growth conditions (Fig. 59). Under cadmium stress condition, *cdfA*<sup>-</sup> strain did not exhibit any phenotype, while when *cdfA* gene was inactivated in *cadA*<sup>-</sup> strain, the double mutant exhibited a stronger phenotype than the single mutant *cadA*<sup>-</sup>. These data in liquid, in contrast to the solid medium, suggested a role of CdfA in cadmium tolerance only when the efflux ATPase CadA is missing. In contrast, under silver stress condition, *cdfA*<sup>-</sup> mutant exhibited a very strong phenotype while the double mutant *cdfA*<sup>-</sup>*cadA*<sup>-</sup> strain exhibited only a slight phenotype.

We should note the lag time in growth in liquid medium for all strains in presence of AgNO<sub>3</sub>. This lag is more important for the mutants than the wild type. Many hypotheses can be put forward to explain this phenotype, among these, growth started after cells have expressed detoxification or buffering systems, or after the silver

-RESULTS-

precipitate in the medium decreasing thus the concentration of the metal in the medium.

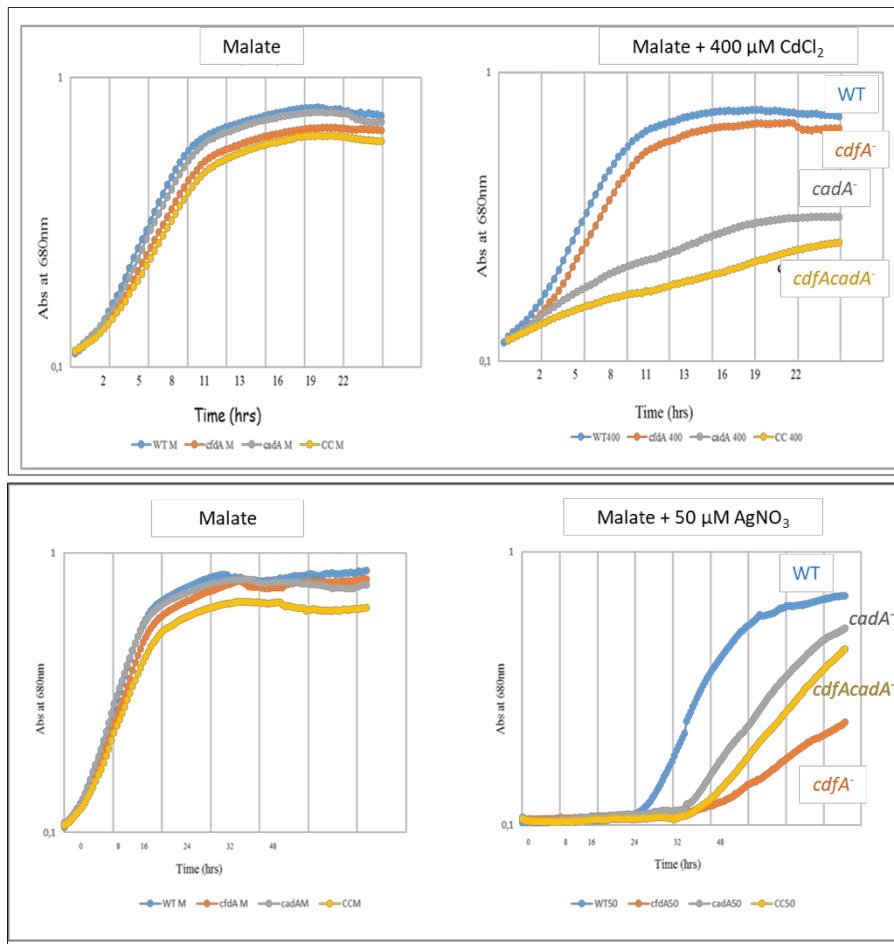


**Figure 59. Growth curves of *R. gelatinosus* WT, *cdfA*<sup>-</sup>, *cadA*<sup>-</sup> and *cdfA-cadA*<sup>-</sup> in liquid medium under respiratory condition in the presence of  $\text{CdCl}_2$  or  $\text{AgNO}_3$ .**

Cells were grown in 96-well microplates in the Tecan Infinite M200 luminometer (30°C). 400  $\mu\text{M}$   $\text{CdCl}_2$  or 50  $\mu\text{M}$   $\text{AgNO}_3$  were added in the beginning of the culture preparation. Growth with  $\text{CdCl}_2$  was stopped after 24 h, while with  $\text{AgNO}_3$  it was stopped after 48 hrs.

These experiments on plates or in liquid have been repeated several times, and unfortunately, we were not able to conclude on the putative involvement of CdfA in silver or even in cadmium tolerance.

### 3- The putative *Cus* system

A gene annotated *czcA* or *cusA* "potentially involved in copper tolerance", was found in the genome sequence of *R. gelatinosus*. This gene encodes a protein that shared only 29% homology with the CusA from *E. coli*. The two genes *czcB* and *czcC* that encode the two other subunit of the RND system are found downstream *cusA*, but encode proteins that share homology with other RND of *E. coli* and but not CusBC. Nevertheless, in *Methylibium petroleiphylum*, a close bacterium to *R. gelatinosus*, the *cusABC* operon is found in a cluster that encode for proteins involved in copper tolerance, suggesting that this RND system may encode a second Cu<sup>+</sup> efflux system in *R. gelatinosus*.

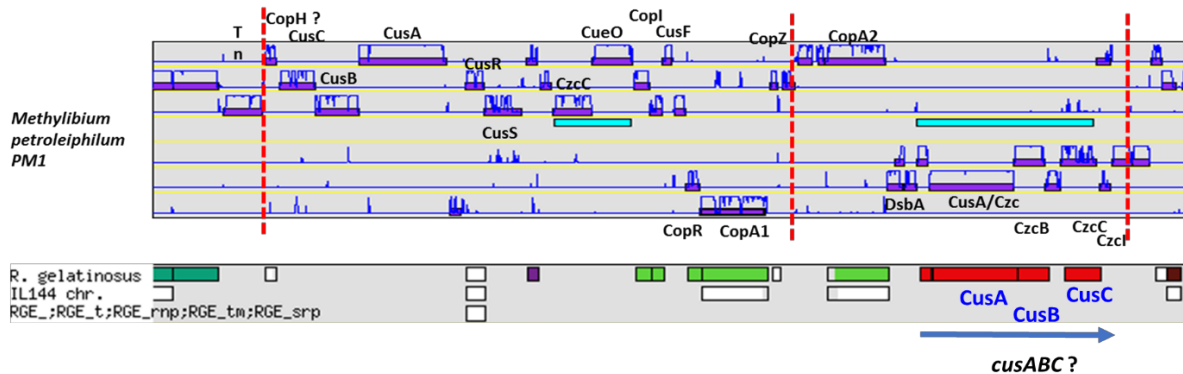


**Figure 60. Gene organization of the putative *cusABC* operon in *R. gelatinosus* and *M. petroleiphylum*.**

The *cus* operon is found in a large cluster probably involved in Cu<sup>+</sup> tolerance.

Despite the low homology with *E. coli* Cus, we decided to consider these genes as candidate genes and check if *cus* is involved in copper or silver tolerance in *R. gelatinosus*. For that purpose, I cloned *cusA* and generated a single mutant *cusA*<sup>-</sup>. The mutant strain *cusA*<sup>-</sup> was exposed to increased concentration of AgNO<sub>3</sub> and compared to this of the wild type (Fig. 61).

-RESULTS-

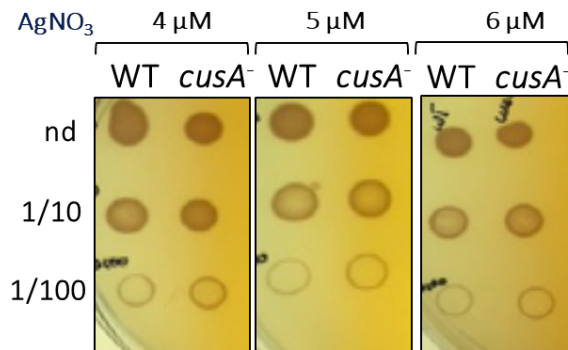


**Figure 61. Role of *cusA* in growth on silver.**

8 μl drop of undiluted, 10- and 100-times dilution of WT and *cusA*<sup>-</sup> mutant cultures were spotted on plates and incubated for growth overnight by photosynthesis (30°C). No difference was observed between the mutant and the wild type.

Because CopA and CopI play a major role in Cu<sup>+</sup> efflux and are still effective in *cusA*<sup>-</sup> strain, I also made the double mutants *cusAcopA*<sup>-</sup> and *cusAcopI*<sup>-</sup> strain and compared their tolerance to AgNO<sub>3</sub> and CuSO<sub>4</sub> and other ions, in comparison with the single mutants *cusA*<sup>-</sup>, *copA*<sup>-</sup>, *copI*<sup>-</sup>, and the wild type. The growth is presented in (Fig. 62). Under Zn<sup>2+</sup>, Cd<sup>2+</sup> or Ni<sup>2+</sup> stress, no effect on the growth of all strains was observed as expected. In contrast, under Cu<sup>2+</sup> stress, the growth of both *copA*<sup>-</sup> and *copI*<sup>-</sup> was affected as previously showed (Azzouzi et al., 2013; Durand et al., 2015). Inactivation of *cusA* did not increased the growth defect in any mutant, suggesting that the inactivated Cus is not involved in copper tolerance. Surprisingly, when exposed to silver, the double mutant *cusAcopA*<sup>-</sup> but not *cusAcopI*<sup>-</sup> was more sensitive to AgNO<sub>3</sub> than the single mutant *copA*<sup>-</sup> or *cusA*<sup>-</sup>. More studies are required in order to reveal the role of this *cus* homologue in efflux/ transport of ions in *R. gelatinosus*. In fact, a recent proteomic study showed that Cus is induced in *R. gelatinosus* under CuSO<sub>4</sub> excess stress (Unpublished).

## -RESULTS-

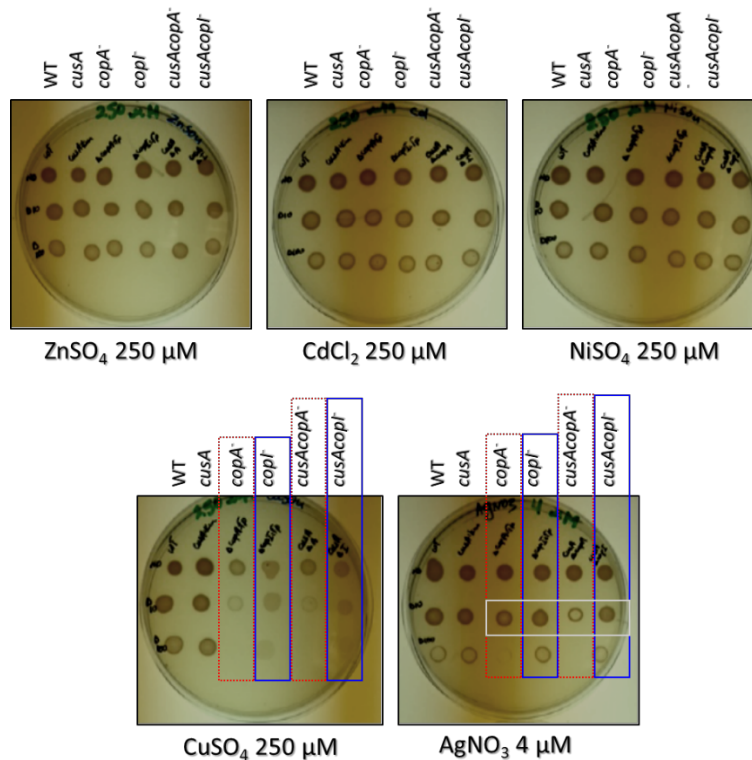


**Figure 62. Role CusA in metal tolerance.**

8 μl drop of undiluted, 10- and 100-times dilution of WT, *cusA*<sup>-</sup>, *copA*<sup>-</sup>, *copI*<sup>-</sup>, *cusAcopA*<sup>-</sup> and *cusAcopI*<sup>-</sup> cultures were spotted on plates supplemented with 250 μM of ZnSO<sub>4</sub>, CdCl<sub>2</sub>, NiSO<sub>4</sub>, CuSO<sub>4</sub> or 4 μM AgNO<sub>3</sub> and incubated for growth overnight by photosynthesis (30°C).

#### 4- The outer membrane protein (*ompW*)

The outer membrane proteins (OMP) family are widespread proteins in Gram-negative bacteria. Among their roles is the passive diffusion of nutrients from the medium into the periplasm. In *R. gelatinosus*, Anne Durand using Mass spectrometry analyses had found a relation between increasing copper concentration and decrease of OmpW, suggesting that OmpW might play a role in copper toxicity. To explain this observation, it was suggested that cells under excess copper may inhibit the expression of OmpW to limit the entrance of copper.

-RESULTS-

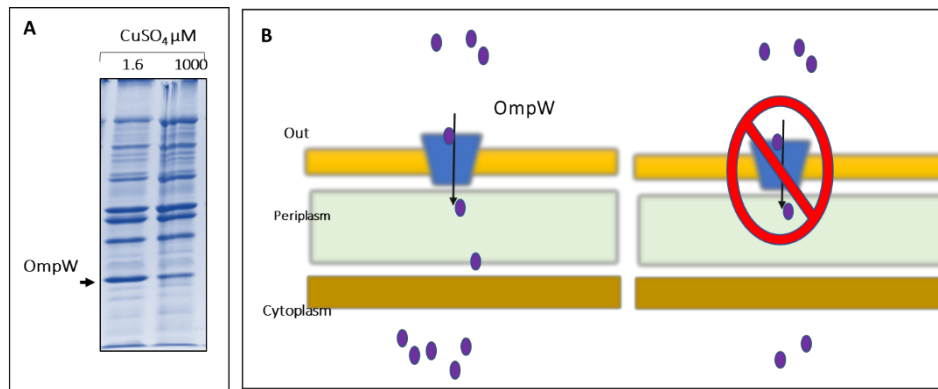


**Figure 63. OmpW inhibition by CuSO<sub>4</sub> in *R. gelatinosus*.**

**A-** SDS PAGE showing the decreased amount of OmpW in the membrane fraction due to increased copper concentration. **B-** Inactivation of *ompW* would limit the entrance of metal into the cells through the outer membrane, thus, protecting the cells from metals excess (From A. Durand).

As for the other candidate genes, I cloned *ompW* gene and generated a single and double mutant in which the *ompW* or the *ompW* and *copA* were inactivated. Growth of the mutants in the presence of CuSO<sub>4</sub> was compared to that of the WT and the single mutants (Fig. 64). The data showed that inactivation of *ompW* did not improve the growth of CopA. Similar results were obtained with Cd<sup>2+</sup> and Ag<sup>+</sup>. No phenotype was observed with *ompW* mutation, very likely because metal ions can enter through other porins in the outer membrane.

-RESULTS-

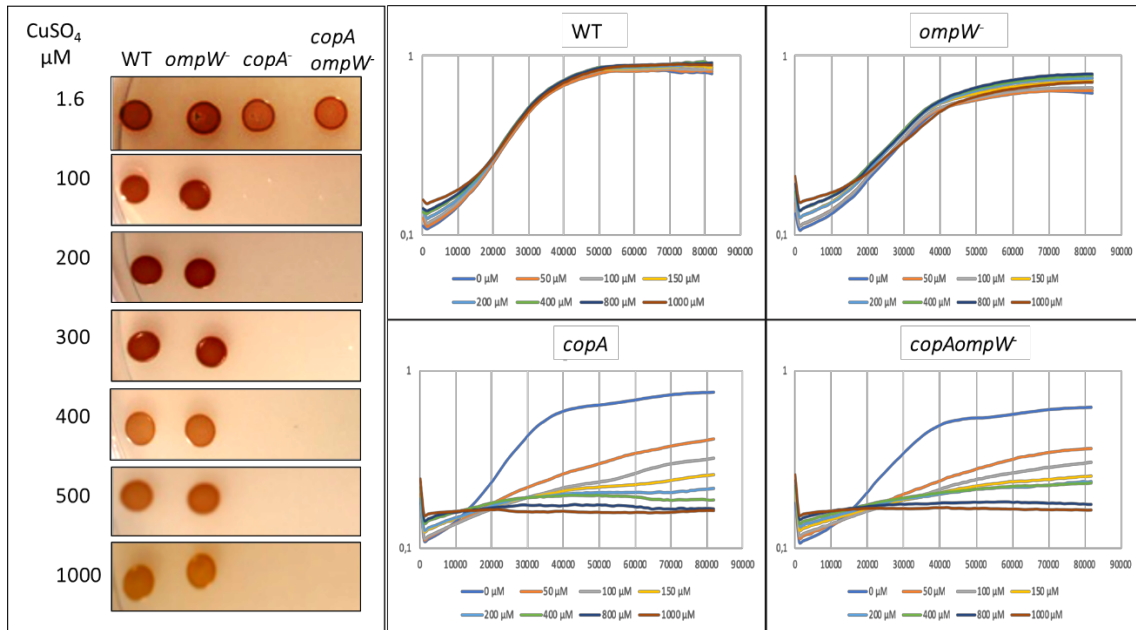


**Figure 64. Effect of *ompW* inactivation on Cu<sup>2+</sup> tolerance.**

A- Growth of WT and the mutants on plates containing increasing concentration of CuSO<sub>4</sub> under PS condition. Growth curves of WT and the mutants in liquid under aerobic condition with increasing concentration of CuSO<sub>4</sub>.

-RESULTS-

### 3. Structural and morphological analysis of silver ions impact on bacteria

---

#### Introduction:

---

The metal homeostasis and metals toxicity are crucial field to study because of the omnipresence of metals in our daily life (Barwinska-Sendra & Waldron, 2017; Lubick, 2008). Furthermore, heavy metals like copper, gold and silver are playing an increasing role as antimicrobial agents (Sánchez-López et al., 2020; Zhang et al., 2016). There is still a clear deficiency on the understanding of exact toxic mechanism that occur inside the cells; in both prokaryotes and eukaryotes in general, and in the photosynthetic proteobacteria in particular.

This study deals with the effect of silver ions on the photosynthetic bacterium *Rubrivivax (R.) gelatinosus*. The main goal was to be able to propose a mechanism that explains silver toxicity from the characterization of the structural and morphological modification induced on the bacteria cell. It aims to give a second perspective to the first paper (Tambosi et al., 2018), which demonstrated the impact of silver and copper on membrane proteins within the photosynthetic and respiratory complexes in bacteria.

The *Rurivivax (R.) gelatinous* is a gram-negative and environmental bacterium. It was selected as a main model for this study to overcome the lack of data regarding the effect of heavy metals on the morphological changes in photosynthetic proteobacteria. In addition, we used other models of bacteria such as *Escherichia coli* and *Bacillus subtilis* as a comparison, since they were both widely considered in previous studies (Chandrangsu et al., 2017; Liu & Wang, 2010; Sondi & Salopek-Sondi, 2004; Xu & Imlay, 2012; Zhou et al., 2012).

The results obtained lean on SEM (Scanning Electron Microscopy) and AFM (Atomic and Molecular) imaging. The high-resolution images and their analysis had enabled us to picture the silver interaction with the bacteria and its impact on the

membrane structure. In addition, the images had also revealed the dependencies of the growth culture medium on the metal toxicity and a possible scenario for a defense mechanism against it.

### **Summary and main findings:**

---

Our investigation started by observing the behavior of *R. gelatinosus* cells under the stress of silver ions (silver nitrate) under different conditions of growth. Bacterial cultures were prepared in both solid and liquid media. It was observed that silver seems to be more toxic in liquid environment than in solid one. This is clearly due to the limitation of  $\text{Ag}^+$  ions mobility and consequently its interaction with cell's membrane in the solid medium; while in liquid higher mobility enhanced the interaction between both. Also, it was found that it is difficult to detect the growth of cells under silver stress which was added from the beginning using the adaptation method of growth. Cells challenge the stress for almost 24 hours till the  $\text{Ag}^+$  precipitate then they start to regrow in the case of those that were exposed to a maximum of 50 mM. For more concentration, cells could not recover. Accordingly, we followed the so-called shocking method to pursue our study. We added silver at different stage of cells growth. It was found that the higher density of cells is the most resistant. This could be due to segregation and sequestering of  $\text{Ag}^+$  ions on the surface of the cell membrane of some bacteria.

We carried on our investigation to visualize the cells behavior under silver pressure using microscopes: SEM and AFM. They were adequate tools to observe the  $\text{Ag}^+$  interaction with bacterial cells metals. Cells of *R. gelatinosus* already grown were exposed to  $\text{AgNO}_3$ , and images were taken during different incubation times. *E. coli* and *B. subtilis* bacteria were also used in this study, as control and comparison. Both microscopes used have provided valuable and complementary data from this point of view.

## -RESULTS-

The images have shown a two stages scenario for the description of the interaction between silver ions and bacteria cells: a first stage (occurring into the first hour of exposure) where silver ions precipitate, around and on the bacteria membranes, following apparently different stochastic nucleation and growth mechanism. And a second stage (around 24 hrs.) where silver ions and/or small particles impact and penetrate cell's membrane inducing huge transformation of bacteria membranes morphology and mechanical properties leading to breaking and apoptosis.

The surface of the cell membrane undergoes larger damage with increasing time of incubation and exposition. While untreated cell remains unaffected. Similar observation was done with exposed *E. coli* cells. On the other hand, *B. subtilis* cells showed no similarities on the cells structure modification during the first hour of the incubation. However, cells had been affected and showed drastic morphological change after 24 hrs. After more than 24 hrs., they all showed weak, fallen apart cell membrane and broken cells. We were able to give more quantitative analysis through rugosity change analysis for instance.

Our results show also clearly, the effect of culture media on those processes. There are crucial differences on the possibility of forming new particles due to the chemical reaction between  $\text{Ag}^+$  ions and the components of the medium used for bacterial cells culture. Thus, we started to look to the impact of different media on silver and their overall effect on bacteria. Interestingly, the new formed particles have been detected in malate medium but not in LB; and more interestingly, this could be a reason on increasing or decreasing the toxicity of metal used. We should also consider the effect of the bacteria in this precipitation process as a possible defence mechanism. This should address the issue of interaction between membrane complexes involved in cellular bioenergetics and silver in its ions and NPs forms.

**Article II: Silver Effect on Bacterial Cell Membrane Structure Investigated by Atomic Force and Scanning Electron Microscopes**

---

\*Submission process 2021

## Revealing Silver Effects on Bacterial Cell Structure by Atomic Force and Scanning Electron Microscopies

Reem Tambosi<sup>a,b</sup>, Jamila Djafari<sup>a</sup>, Sylviane Liotenberg<sup>b</sup>, Soufian Ouchane<sup>b</sup> and Nouari Kebaili<sup>a</sup>

<sup>a</sup> Université Paris-Saclay, CNRS, Laboratoire Aimé Cotton, 91405, Orsay, France.

<sup>b</sup> Université Paris-Saclay, CEA, CNRS, Institute for Integrative Biology of the Cell (I2BC),  
91198, Gif-sur-Yvette, France.

# Correspondence should be addressed to: [nouari.kebaili@universite-paris-saclay.fr](mailto:nouari.kebaili@universite-paris-saclay.fr) and  
[soufian.ouchane@i2bc.paris-saclay.fr](mailto:soufian.ouchane@i2bc.paris-saclay.fr)

**Keywords:** Silver, Toxicity, Bacteria, Atomic Force Microscopy (AFM), Scanning Electron Microscopy (SEM).

**Running Title:** Silver effect on cell structure by AFM-SEM microscopies

## **Abstract**

The use of silver ( $\text{Ag}^+$ ) as an antimicrobial under different forms and at different scales, appears in numerous applications such as in health care, food industry, clothing, fabrics and disinfectants. Yet, there is still important gaps regarding the complete comprehension of the mechanisms of its actions on bacteria. In a previous work (Tambosi et al., *mbio*, 2018)<sup>1</sup>, we demonstrated that, silver and copper severely damage membrane proteins involved in photosynthesis and respiration in bacteria exposed to metal excess. Here, we are presenting complementary data using AFM and SEM microscopies, that reveals (i) the drastic effects of  $\text{Ag}^+$  ions on the morphology and structure of cell membrane and (ii) the formation of  $\text{Ag}^+$  aggregates that adhere to the bacterial cell surface in *R. gelatinosus*. Impacts of  $\text{Ag}^+$  ions on *R. gelatinosus* are compared to those on the most commonly studied bacteria (*E. coli* and *B. subtilis*), while considering the effect of culture grown media on the modification of silver ions. Altogether, these results reveal other levels and subtle aspects of  $\text{Ag}^+$  toxicity to be taken into account in understanding the general mechanisms of metal toxicity in bacteria.

## Introduction

In the context of antibiotic crisis, where lack of efficiency is linked to both multi-resistance bacteria and increasingly reduced offer of antibiotic solutions<sup>2-5</sup>, silver has been considered as a very promising alternative proposal<sup>4,6</sup>. It is therefore, widely used in industry, agriculture and health care as an antimicrobial agent<sup>5,7,8</sup>. It can be found as pure and/or alloy with other metals, at different scale and forms. It inhibits, causes or enhances mechanisms of bacterial death, disrupts growth or reduces bacterial biofilm proliferation<sup>9,10</sup>. However, its use is not without danger, since excess of silver in both ions ( $\text{Ag}^+$ ) and nanoparticles ( $\text{Ag-NPs}$ ) forms shows toxic impact toward all types of living cells. Yet, the underlying mechanisms driving its toxicity and its impact on bacteria, are still under intense investigations<sup>11-13</sup>.

Unlike copper, iron or zinc for example<sup>14</sup>, silver is not an essential metal for cell growth. In bacteria, iron or zinc enter the cell through specific import systems. Silver ions could diffuse and enter the cells through the outer membrane via nonspecific importers and poison the membrane or the cytoplasm of the bacterium<sup>15</sup>.  $\text{Ag}^+$  could also affect the membrane integrity and damage the cell structure if it accumulates outside the cell, although direct evidences are still missing. In general, bacterial cells are programmed to maintain and to resist metal effects and toxicity. They have the ability to reach metal homeostasis by using different defense systems. They can, for example, repress the import system, induce the required detoxification enzymes including metal sequestration and/or active efflux systems<sup>16,17</sup>. A dysfunction in the homeostasis system (import/efflux) of these metals can cause physiological disorders in both prokaryotes and eukaryotes cells<sup>18</sup>. Many studies have reported these damages<sup>1,4,12,19</sup>. For example, human cells (skin and lung cells) are easily exposed to silver nitrate or silver oxide by touching and breathing<sup>20</sup>; this exposure can cause breathing problems, lung and throat irritation, stomach pain, and argyria<sup>21,22</sup>. In the green algae *Chlamydomonas reinhardtii*, silver ions disrupt cellular metabolism and inhibit important functions such as photosynthesis<sup>23,24</sup>. In

## -RESULTS-

*Escherichia (E.) coli*, *Bacillus (B.) subtilis* or *Salmonella (S.) typhimurium* model bacteria,  $\text{Ag}^+$  inhibits the growth by targeting various metabolisms<sup>25-28</sup>. In photosynthetic bacterium only few studies have addressed metal toxicity mechanisms and homeostasis of silver. Therefore, we used to tackle the effect of  $\text{Ag}^+$  on photosynthesis and respiration.

In a previous study<sup>1</sup>, we have reported results on a molecular level regarding the metals ( $\text{Cu}^+$  and  $\text{Ag}^+$ ) toxicity in *Rubrivivax (R.) gelatinosus* an environmental and gram-negative photosynthetic purple bacterium. The results revealed new findings on the targets of both  $\text{Cu}^+$  and  $\text{Ag}^+$  ions in the inner membrane<sup>1</sup>. The membrane complexes affected are specifically the peripheral light harvesting complex LH2 and the cytochrome *c* oxidase; required for photosynthesis and respiration respectively. Moreover, our data showed that  $\text{Ag}^+$  has effects on the succinate dehydrogenase (SDH) complex in *E. coli*, but not in *B. subtilis*<sup>1</sup>. In this study, we carried out an investigation, using Scanning Electron Microscope (SEM) and Atomic Force Microscope (AFM), to provide data on the morphological and structural changes that occur upon exposure of bacteria to silver ions due to metals influence. The aim of these investigations, in this context, was to elucidate the influence of silver  $\text{Ag}^+$  ions outside the bacterial cells and essentially to reveal  $\text{Ag}^+$  interaction with the cell membrane surface. The results showed that high resolution images could discern and characterize the detailed changes that occurred on the bacterial cell membrane after treatment with  $\text{AgNO}_3$ . To our knowledge, this presents the first direct evidence of  $\text{Ag}^+$  silver ions morphological damages to *R. gelatinosus* cell membrane. Our data analyses showed drastic changes that increased with the increasing of incubation time, while untreated samples remain unaffected.  $\text{Ag}^+$  exposure leads to i- the formation of irregular deep grooves vesicles on the cell surface, ii- to cell membrane shrinking and iii- to structure breaking in the extreme case of extended exposure. A phenomena of silver particles accumulation on the membrane surface has also been observed using SEM, raising the questions

-RESULTS-

of the media effect on silver precipitation, the influence of cell membrane surface and eventually suggest a hypothetical scenario of cell defense.

## Results and discussion

### *Consequences of Ag<sup>+</sup> exposure on cell surface and morphology revealed by SEM and AFM microscopy*

To assess the toxicity effect of Ag<sup>+</sup> on cell's morphology and structure, we imaged *R. gelatinosus* cells that were exposed to 1 mM of AgNO<sub>3</sub> and deposited using dip coating on substrate for both SEM (on freshly cleaved graphite HOPG) and AFM (on freshly cleaved Mica). We have prepared same samples, under same conditions, for both untreated and treated cultures after 1 and 24 hours (h) incubation with AgNO<sub>3</sub>. Results showed that untreated cells of *R. gelatinosus* have rod-shape and a relatively smooth surface with no ruptures or swellings (**Fig. S1**). The images, at the same scales, showed also that the morphology and physical appearance of the untreated bacteria were not dependant on the imaging tool (AFM vs SEM) or the nature of the substrate (HOPG vs Mica). Bacteria were sometimes grouped in clusters, but most often isolated cells were easily detected, enabling individual and non-perturbed study of their morphology. No modification due to the deposition on the substrate and no physical stress or surface deformation were observed. No ageing effect or alteration during the observation time window was observed. Furthermore, there was no effect of different deposition procedure, nor drying technics, nor ambient air or high vacuum. Membranes cells were continuous, and homogeneous. We did not observe any charge effect on the bacteria in SEM images and there was no observable effect of electron beam tension. For the AFM imaging in non-contact mode, we did not saw displacement of cells, and the tip interaction with the membrane caused no damage. Thus, bacteria were completely stable (shape and position) during the observation time window.

Interestingly, in the samples that were exposed to 1 mM of AgNO<sub>3</sub> for one hour, SEM images showed accumulation of metals around some bacteria (**Fig. 1**). With a bigger scale we observed bacteria that appeared very bright (statistically one fourth, at that concentration of

cells and ions) (**Fig. 1A**). Higher magnification showed an impressive accumulation of metallic aggregates on the cell surface (**Fig. 1B and Fig. S2**). The size distribution of these aggregates on the membrane was compared with the distribution size of the ones that can be observed also around the cells (**Fig. 1C**). It seems, that during the first hour, the first stage was silver precipitation to form these aggregates. The superposition of several normal distributions of the aggregates size distribution suggested several, may be competitive, stochastic nucleation processes<sup>29,30</sup>. However, we observed a difference between distribution on and around the cell's membrane. Some of the aggregates around the cells (2<sup>nd</sup> and 3<sup>rd</sup> pics of density profile) can be attributed directly to detached particles from the membranes. These data raised questions related to the interaction of bacteria with silver ions in the medium. First, since not all bacteria displayed these particles on their surface, this may suggest a difference in the surface component (exopolysaccharides/ capsule) of our cells, and/or a difference in the growth stage (dividing *versus* static or dying cells). Second, we might consider that these particles arose from interaction of silver with components in the growth media. Nevertheless, we can also speculate at that point, that precipitation of silver ions was mediated by cells eventually as a first stage of a defence mechanism, since insoluble particles could be more difficult to penetrate into the cell with increasing size of the particles. This was suggested in *Pseudomonas aeruginosa* in which extracellular synthesis of nanoparticles was also observed after exposure to cadmium or selenium<sup>31-33</sup>. This mechanism was suggested to contribute to metal resistance in *Pseudomonas*.

Furthermore, the AFM images of untreated or exposed bacteria to AgNO<sub>3</sub> for one hour, confirmed the presence of silver aggregates on the cell's membrane (**Fig. 2**). The size distribution corresponds to the one observed with the SEM. Aggregates on the cells were not displaced by the scanning and showed important adhesion to the cell surface. Yet, we cannot exclude that some aggregates grown on cell surface can be detached during washing and deposition on substrate processes. No membrane deformation, breaking or change in hardness-

softness were observed at that point. We imaged also, using AFM, bacteria cells after extended incubation time (24 h) to AgNO<sub>3</sub>. **Figure 3** shows the comparison between untreated cells, and AgNO<sub>3</sub> exposed bacteria after 24 h incubation. The figure shows, again topography and peak force error images, but also longitudinal and transverse cross section profiles. These images indicated that silver stress caused the cell surface to become rough in *R. gelatinosus*. Cells start to lose their clear-cut rod-shaped morphologies with the increasing of incubation time. We could not observe metallic aggregates on the membranes. The edges of the cells seem to be petrified as shown on the peak and Force Error and we can see numerous large patches.

Cross section curves showed clearly an increase of the rugosity, leading to cell's membrane breaks transversally to the bacteria length axis. However, to establish a better quantitative analysis of the morphology, we focused our study on the distribution of heights, skewness and kurtosis moment who are known to be fundamental for describing surface asymmetry and flatness features<sup>34</sup>. We measured for that the following parameters, along (longitudinal) and across (transverse) bacteria length axis, taking into account only the cell, without substrate variation possible modification:

- Arithmetic average height ( $\bar{z}$ ) gives general description of height variation:

$$\bar{z}(N) = \frac{1}{N} \sum_{i=1}^N z(x, y)$$

- RMS roughness ( $R_q$ ) represents the standard deviation of surface heights:

$$R_q(N) = \sqrt{\frac{1}{N} \sum_{i=1}^N [z(x, y) - \bar{z}(N)]^2}$$

- Average total roughness ( $R_{tm}$ ), the sum of mean of maxima profile for peak height ( $R_{pm}$ ) and for valleys depths ( $R_{vm}$ ), calculated over the surface  $R_{tm} = R_{pm} + R_{vm}$  with

$$\mathbf{R}_{\text{pm}} = \frac{1}{N} \sum_{i=1}^N \max(z_j - \bar{z}) ; 1 < j < M \text{ and } \mathbf{R}_{\text{vm}} = \frac{1}{N} \sum_{i=1}^N |\min(z_j - \bar{z})| ; 1 < j < M$$

- Skewness (**Sk**), the 3<sup>rd</sup> moment of profile amplitude probability density function, measures the profile symmetry about mean line.

$$\mathbf{Sk} = \frac{1}{NR^3} \sum_{i=1}^N [z_i - \bar{z}]^3.$$

If the height distribution is symmetrical **Sk** is zero. It is positive if the surface has more peaks than valleys and negative if the valleys are predominant.

- Kurtosis (**Ku**), the 4<sup>th</sup> moment of profile amplitude probability function, measure surface sharpness

$$\mathbf{Ku} = \frac{1}{NR^4} \sum_{i=1}^N [z_i - \bar{z}]^4.$$

When **Ku**, is equal to 3, this indicates a gaussian amplitude distribution, smaller than 3 means that the surface is flattening and higher than 3, that the surface has a lot of peaks.

**Table 1**, summarize these morphological parameters for the control and the exposed bacteria to silver ions. Errors on the values are estimated around 10% for average height and rugosities, and around 20% for 3<sup>rd</sup> and 4<sup>th</sup> moments.

The most important change was an important increasing of surface roughness, along bacteria length axis, till the integrity of cell's membranes was not ensured anymore. It was difficult to localise silver aggregates under these extended exposure condition. Cells with longer incubation time (> 24 h) showed greater damages (**Fig. 4**) and the broken cells were difficult to locate by the microscope. Interestingly, for those we were able to locate, they were so fragile that they were broken in parts after being deposited (during drying process) on the surface of the substrate or during the tip scanning.

***Morphological alterations caused by silver ions, comparison with other bacteria***

There are various studies which have reported the effect of silver on other bacteria such as *E. coli* and *B. subtilis*<sup>35,36</sup>. It was then important to extend our study to these two species as controls and comparison to our results on the photosynthetic model bacterium *R. gelatinosus*. In these experiments, Ag<sup>+</sup> stress was applied to *E. coli* and *B. subtilis* cells grown in LB medium since it was difficult to grow them in Malate. Experiments were achieved with the same concentration of Ag<sup>+</sup> ions (1 mM), and on cultures with same optical density. Samples were collected after incubation time and they were prepared to be imaged by SEM and AFM, using same protocol for deposition and same substrate as above for *R. gelatinosus*. For *E. coli*, the results showed that cells in the control sample had smooth and soft surface, with intact rod-shaped cells (**Fig. S3**). The AFM images (**Fig. 5**) confirmed the SEM results on untreated *E. coli* as cells appeared regular and smooth. In contrast, exposure to silver ions, affected the surface topology. Indeed, cells exhibited more irregular membrane surface and some grooves appeared on the top even after just one hour of exposure (**Fig. 5**). The grooves increased with increasing incubation time up to 24 h and very likely Ag<sup>+</sup> stress could promote cell wall breakdown and cytoplasm release after extended exposure (24 h in **Fig. 5**). Similar AFM experiments on *E. coli* exposed to Ag<sup>+</sup> ions were previously reported<sup>37</sup> and showed that vesicles appeared on the bacterium surface and became larger with the increase of the incubation time. Nevertheless, contrary to *R. gelatinosus* samples, no accumulation of metallic aggregates on *E. coli* cells was observed. In the case of *B. subtilis*, we observed electron beam charge effect, and brighter aspect in the case of SEM imaging. In addition, silver exposed *B. subtilis* cells were most often aggregating in clusters, while the control sample cells were evenly individually distributed on the surface of the substrate (**Fig. S4**). For AFM imaging, we could observe a slight displacement of the cells under tip scanning, suggesting a weaker adhesion to the Mica substrate than previous cases. The cells aggregation effect on the other hand, might relate to the

interactions between cells and  $\text{Ag}^+$  that accumulate on the surface of the cells; in addition to the interaction with the substrate used. This phenomenon was reported with *E. coli* cells exposed to carbon dots stress for instance<sup>38</sup>. The imaging of *B. subtilis* exposed to silver ions showed that  $\text{Ag}^+$  had less effect comparing to *R. gelatinosus* and *E. coli* during the first hour of incubation (**Fig. 6**). Cell morphology differs slightly from control one. However, we could observe a drastic effect after 24 h exposition to silver. Apparent smaller size and irregular shape were the main morphological transformations, as reported for *E. coli* cells exposed to silica nanoparticles<sup>39</sup>.

Collectively, these results showed that silver has a strong impact on bacteria. It changes the structure of the cell surface which could be due to the accumulation of ions on the surface or/and deterioration of specific components of the cell wall. The impact of silver on bacteria differed from one type to another. The most drastic effect was observed with *R. gelatinosus*. This could originate from various factors. The thickness and structure of the cell wall for instance, is considered to be an important factor of metal stress resistance<sup>40</sup>. Another difference could arise from culture media composition: the speciation and bioavailability of metals in malate vs LB medium.

#### ***Effect of culture media (malate medium versus LB medium) on $\text{Ag}^+$ toxicity in *R. gelatinosus****

Studies have reported that bacterial growth media could impact on ions bioavailability and therefore on cell's response and shape under stress condition<sup>41-43</sup>. We can suspect that, since culture media contains different chemical compounds as phosphates and chlorates, silver precipitation may occur distinctly depending on the medium composition. Growth of *E. coli* and *B. subtilis* in malate medium is very limited and did not allowed analyses of cells in this culture medium. In contrast, *R. gelatinosus* has the ability to grow on both malate and LB, although growth is slower in LB medium. To assess the effects of culture medium content on

## -RESULTS-

Ag<sup>+</sup> toxicity, we first monitor the effect of Ag<sup>+</sup> in LB, in comparison with malate medium, on the photosynthetic complexes of *R. gelatinosus*. In this experiment, *R. gelatinosus* cells were grown in malate or in LB medium. AgNO<sub>3</sub> was then added, and spectra were recorded after different incubation times. In agreement with our previous data<sup>1</sup>, the results showed that for cells grown in malate medium, the light harvesting LH2 bacteriochlorophyll Bch800 decreased with the increasing incubation time. After 10 h of incubation, the Bch800 bacteriochlorophyll was completely lost (**Fig. 7A**). On the other hand, and in contrast to malate, for cells grown in LB, Ag<sup>+</sup> took longer time to show the same impact on LH2. After 10 h of incubation, Bch800 decreased only slightly and was lost only after 24 h post incubation (**Fig. 7B**). These results indicate that silver in LB medium still affect LH2 but its impact and interaction with the membrane complexes, could be slowed down by Ag<sup>+</sup> ligands in the LB medium.

### ***Effect of culture media (malate medium versus LB medium) on the interaction of R. gelatinosus with silver ions.***

Given that accumulation of silver aggregates was observed for *R. gelatinosus* in Malate medium, but not in *E. coli* or *B. subtilis* in LB, we asked whether these aggregates could also form when *R. gelatinosus* was grown in LB medium. To answer this question, bacteria were grown as previously in Malate or LB medium. SEM imaging was used to discriminate any effects between untreated or AgNO<sub>3</sub> exposed cells in LB or Malate medium. The images revealed several differences. First for unknown reason, *R. gelatinosus* cells grown in LB were longer than those grown in Malate medium (**Fig. S5**). Second, the comparison between exposed bacteria to silver showed that unlike malate case, bacteria grown in LB did not exhibit any silver accumulation on their surface. Bright halos were observed around the cells; likely, due to trace of the medium, but we did not observe any metallic aggregates on the bacterial surface (**Fig. 8**) in the LB medium. Together with the effects of Ag<sup>+</sup> in LB medium on the photosynthetic LH2

complexes, the SEM results showed and confirmed that the susceptibility of bacterial cells to silver ions and very likely to AgNPs is dependent on the culture medium content. This is in agreement with previous studies showing that the thiol-containing compounds and some amino acids of LB medium could sequester  $\text{Ag}^+$  and other cations, protecting thus bacteria from  $\text{Ag}^+$  toxicity<sup>44,45</sup>. Indeed, while Malate medium includes high concentration of phosphate ( $\text{K}_2\text{HPO}_4$ ), LB on the other hand contains NaCl and reduced amount of phosphate. Both react with  $\text{AgNO}_3$  and can lead to precipitate  $\text{Ag}^+$  as  $\text{Ag}_3\text{PO}_4$  and  $\text{AgCl}_3$ <sup>46</sup>, respectively. Accordingly, we suggest that in Malate medium,  $\text{Ag}_3\text{PO}_4$  precipitate forms aggregates in the medium and adhere to some cells, while in LB most  $\text{Ag}^+$  could be sequestered by ligands such as thiols preventing thus formation of  $\text{AgCl}_3$  aggregates.

#### **Formation of $\text{Ag}^+$ aggregates in Malate/LB or citrate.**

It was difficult, at that point to identify precisely the composition of these aggregates, the focusing of the electron beam for EDX analysis for instance, induced contamination and charge effect on the sample and the signal even accumulated was difficult to separate from the carbon (HOPG) main signal. Furthermore, we suggest that these dots/aggregates may correspond to the forming of  $\text{Ag}_3\text{PO}_4$  particles due to the reaction between  $\text{AgNO}_3$  and  $\text{K}_2\text{HPO}_4$ <sup>47,48</sup>. The latter is considered to be a necessary component for Malate medium formulation, beside other chemical elements, at the reactant's concentration range of phosphate derivatives and malate molecule in malate medium. Indeed, these components are the more concentrated in the malate medium, and their reaction with  $\text{AgNO}_3$  is thus more probable. The reaction between silver nitrate and phosphate is:  $2\text{K}_2\text{HPO}_4 + 3\text{AgNO}_3 \rightarrow \text{Ag}_3\text{PO}_4 + 3\text{KNO}_3 + \text{KH}_2\text{PO}_4$ . The chlorate can also lead to  $\text{AgCl}$  precipitates<sup>49</sup>, but since there are present in both media, and before further and more detailed study, we decided to drive them away at that point. Phosphates as far as they are concerned are at very low concentration in LB formulation. As shown in figure 1, the size

## -RESULTS-

distribution density profiles show different superposed size distribution, suggesting that the nucleation stochastic process leading to the first distribution (red line) around the cells is different from the double centred distribution (blue line) on the membranes. We hypothetically attributed the first process, to silver precipitation due to chemical compounds present into malate medium, distinguished from other process involving bacteria response to the metallic stress concerning as showed in previous work<sup>1</sup> membranes proteins.

To demonstrate rapidly this assumption, we carried the following experiment. 6 mM of AgNO<sub>3</sub> was directly added to the media, malate and LB, under same conditions. The concentration was increased to enhance the suspected effects. We analysed then the optical properties, using spectrophotometry, of the compounds to detect possible formation of silver nanoparticles through their well-known plasmonic response<sup>50-52</sup>. (**Fig. 9**) shows the optical absorption for AgNO<sub>3</sub> added to culture media (Malate vs LB) and for comparison with citrate that is commonly used to reduce AgNO<sub>3</sub> to produce Ag nanoparticles. Usually in citrate assisted production of silver nanoparticles, borates are used instead of phosphates<sup>53</sup>. The spectrophotometric curve showed clearly in all cases the formation of silver nanoparticles with a higher efficiency in the case of Malate compare to LB. The nanoparticles were not very stable and underwent probably fragmentation process and dilution into the solution. We can see that in case of Malate and LB, nanoparticles underwent fragmentation and/or dilution, while for citrate they underwent also growing mechanisms.

More details analysis, trying to distinguish between several chemical compounds (phosphates, malic acid, carboxylates, chlorates, ...) in broth composition<sup>42,43,53,54</sup> and also light effect, is actually carried in our group. Furthermore, these preliminary results are sufficient to establish a link between observed aggregates and silver precipitation process due to medium solution. Considering Mie theory for the plasmonic response of silver nanoparticles, we can establish that the response around 440 nm corresponds to an average size distribution around

20 nm, in agreement with the distribution size observed around the cells but not the one on the membranes. The second distribution seems induced by species on the membranes, and hypothetically considered as a part of a defense mechanism.

### **Conclusions and perspectives**

Metals antimicrobial activity has been investigated in different model bacteria. Metals exert their antimicrobial activity by affecting various components of the cell, including very likely, the cell envelope integrity. In this context, we present here, the morphological changes triggered by  $\text{Ag}^+$  ions on the structure of *R. gelatinosus*, *E. coli* and *B. subtilis* cells, using AFM and SEM microscopies. It is obvious from this study and others, that AFM and SEM can provide a useful information regarding the antimicrobial mechanisms of metal ions. The results helped us to build a 2 steps scenario: a first step (occurring in the 1st hour of exposure) where silver ions precipitate around and on the bacterial membrane following apparently different stochastic nucleation and growth mechanism. A second step (extended exposure) where silver ions and/or small particles impact and penetrate cell's membrane inducing huge transformation of bacterial membranes morphology and mechanical properties leading to cell wall breaking. However, several open questions remain concerning the localisation of silver fixation points, defense mechanism implying diffusion and nucleation of silver ions on the membranes and optimal particles size for membranes penetration. Interaction with synthesized nanoparticles with controlled size and shapes is under investigation to clarify that point.

Comparison between bacteria and media enable to clarify specific behaviour of some species. While *R. gelatinosus* cells showed high susceptibility to  $\text{Ag}^+$  after short exposure, in *B. subtilis*, the impact of  $\text{Ag}^+$  took longer. Only cells incubated for 24 h with  $\text{AgNO}_3$  appeared in smaller size and irregular shape. This might be explained by the cell wall structure of *B. subtilis* and very likely of other gram-positive bacteria. The thicker membrane built of layers

## -RESULTS-

of peptidoglycan in gram-positive species, could improve the cell ability to resist external environmental stress including metals stress<sup>40</sup>. On the other hand, our results showed also clearly the effect of culture media on those processes. A better understanding of the specific role of the different chemical components present in the media should help addressing this issue. It was found that silver reacts differently in different media used for cells growth. It has more toxic impact on cells in Malate than in LB medium, at least for *R. gelatiosus*, due, as we suggest, to the presence of phosphate in Malate medium. The reaction between  $\text{AgNO}_3$  and  $\text{K}_2\text{HPO}_4$  lead to the precipitation of  $\text{Ag}_3\text{PO}_4$  that appeared as whitish particles adhering to the cells surface. These dots were detected by the SEM due to the backscattered light of identified Ag atoms on the sample surface. It is tempting to suggest that the accumulation of  $\text{Ag}_3\text{PO}_4$  particles on cell surface could enhance or accelerate the toxic effect of silver. Indeed, because of their direct attachment to the membrane they could potentially release  $\text{Ag}^+$  ions inside the cells. Nevertheless, we should also consider the opposite hypothesis. Indeed, reduction of soluble  $\text{Ag}^+$  to colloidal or nanoparticles in Malate medium could protect cells if insoluble particles are too large to enter into the cells as reported in *Pseudomonas aeruginosa*<sup>55,56</sup>. The composition of the Ag precipitates is not yet known. It could correspond to  $\text{Ag}_3\text{PO}_4$ , nevertheless, there is also a strong reaction between  $\text{AgNO}_3$  and Malic acid (main ingredient for Malate medium formula). More investigations are required to determine the nature of these precipitates in Malate medium.

Figures

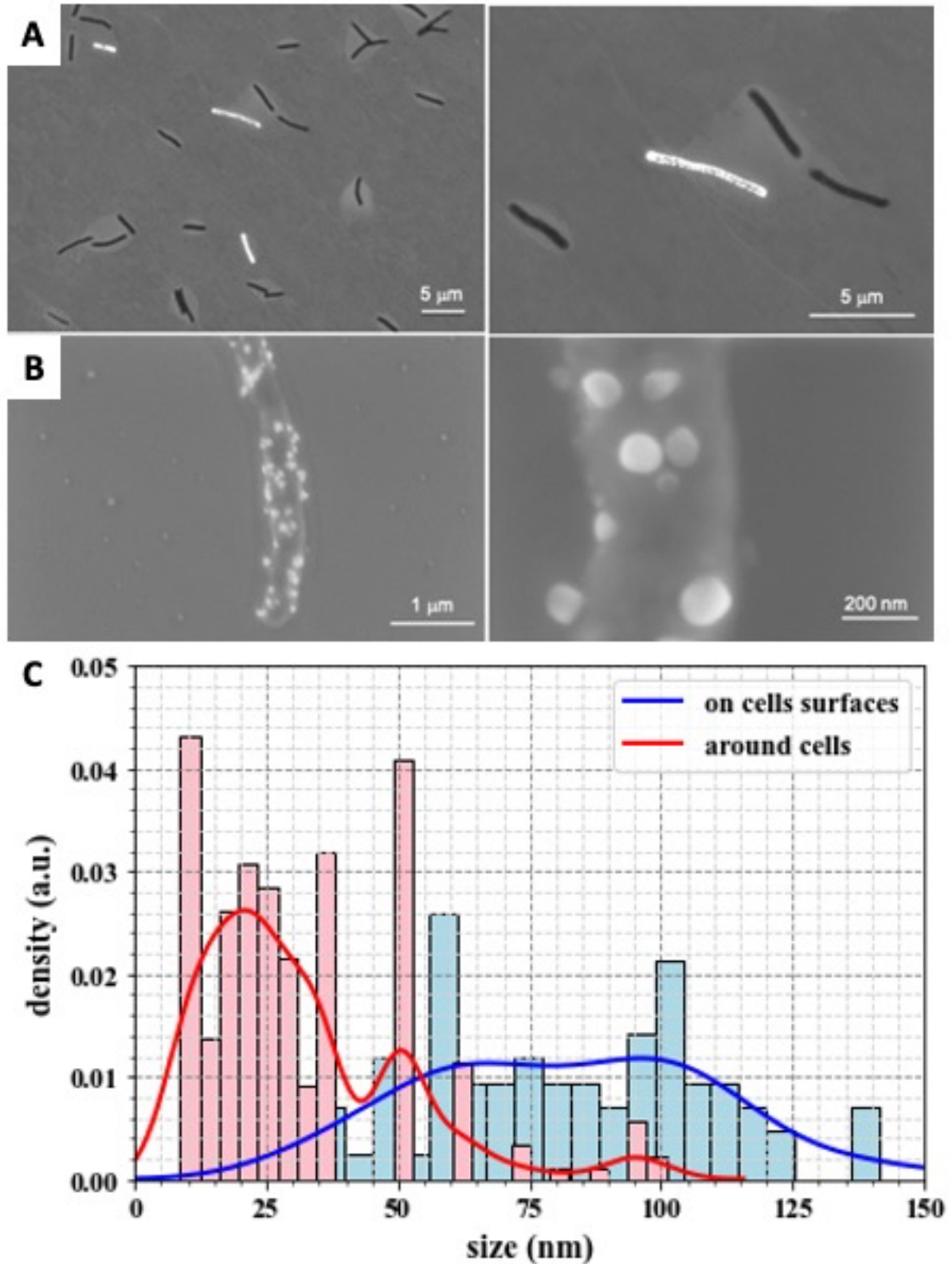


**Fig. 1** - SEM image at different scale (A) and their zoom (B) of *R. gelatinosus* bacteria, exposed to  $\text{AgNO}_3$  for 1 h, deposited on HOPG graphite as described previously. One can observe silver (bright dots) concentration on the outer membrane. In (C) the graph shows the size distribution (histogram and density) of metallic aggregates on cells surface and around the cells.

-RESULTS-

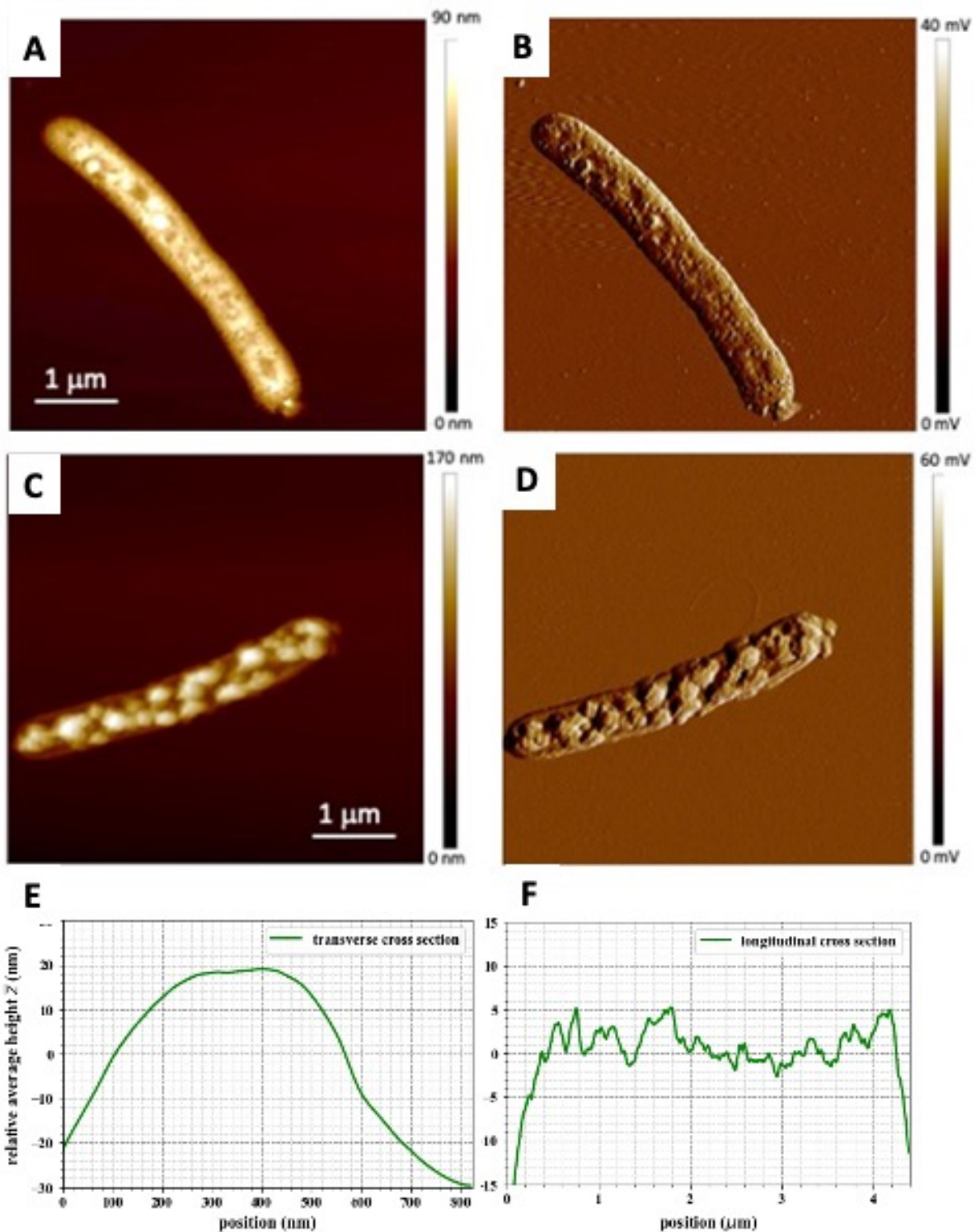


**Fig. 2** - AFM image of *R. gelatinosus* deposited as described previously. Images shows topological i.e. height (A and C) and peak force error (B and D) of untreated bacteria (1<sup>st</sup> line) and bacteria exposed to  $\text{AgNO}_3$  for 1 h (2<sup>nd</sup> line). The profile curves correspond to relative (difference with mean height) average height across (transversal (E)) and along (longitudinal (F)) bacteria cell axis for control bacteria as profile references.

-RESULTS-

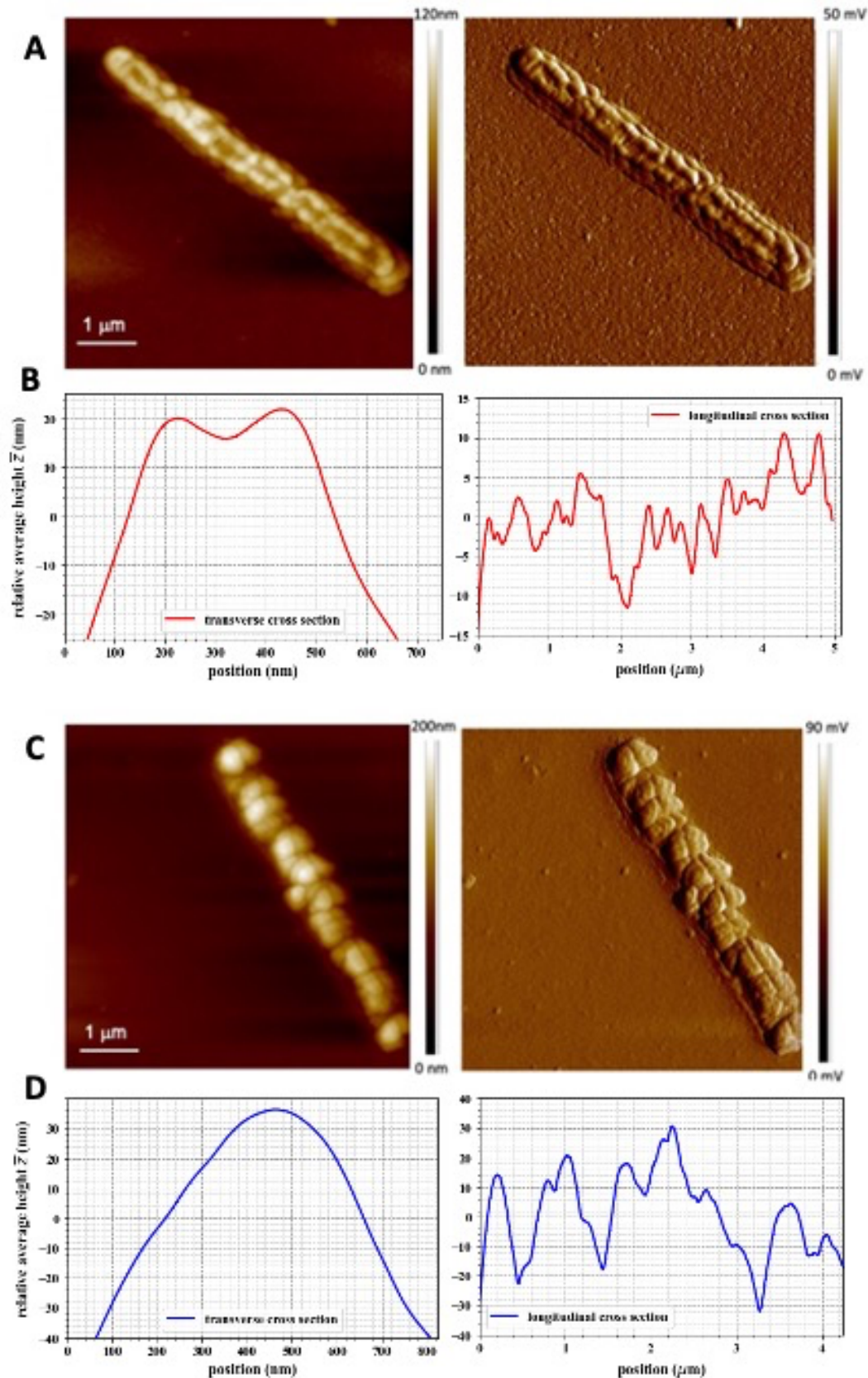


**Fig. 3** – Images show topological, peak force error and profile cross section analysis. AFM image of *R. gelatinosus* bacteria untreated (A) and exposed (C) to AgNO<sub>3</sub> for 24 h. Relative average heights are, calculated compared to height mean value, along and across the bacteria cell's length axis (B and D).



**Fig. 4** - AFM image topology (upper group) and peak force error (lower group) of several *R. gelatinosus* bacteria exposed to  $\text{AgNO}_3$  for 24 h or more, showing as examples the important damages caused to membranes and cells.

-RESULTS-

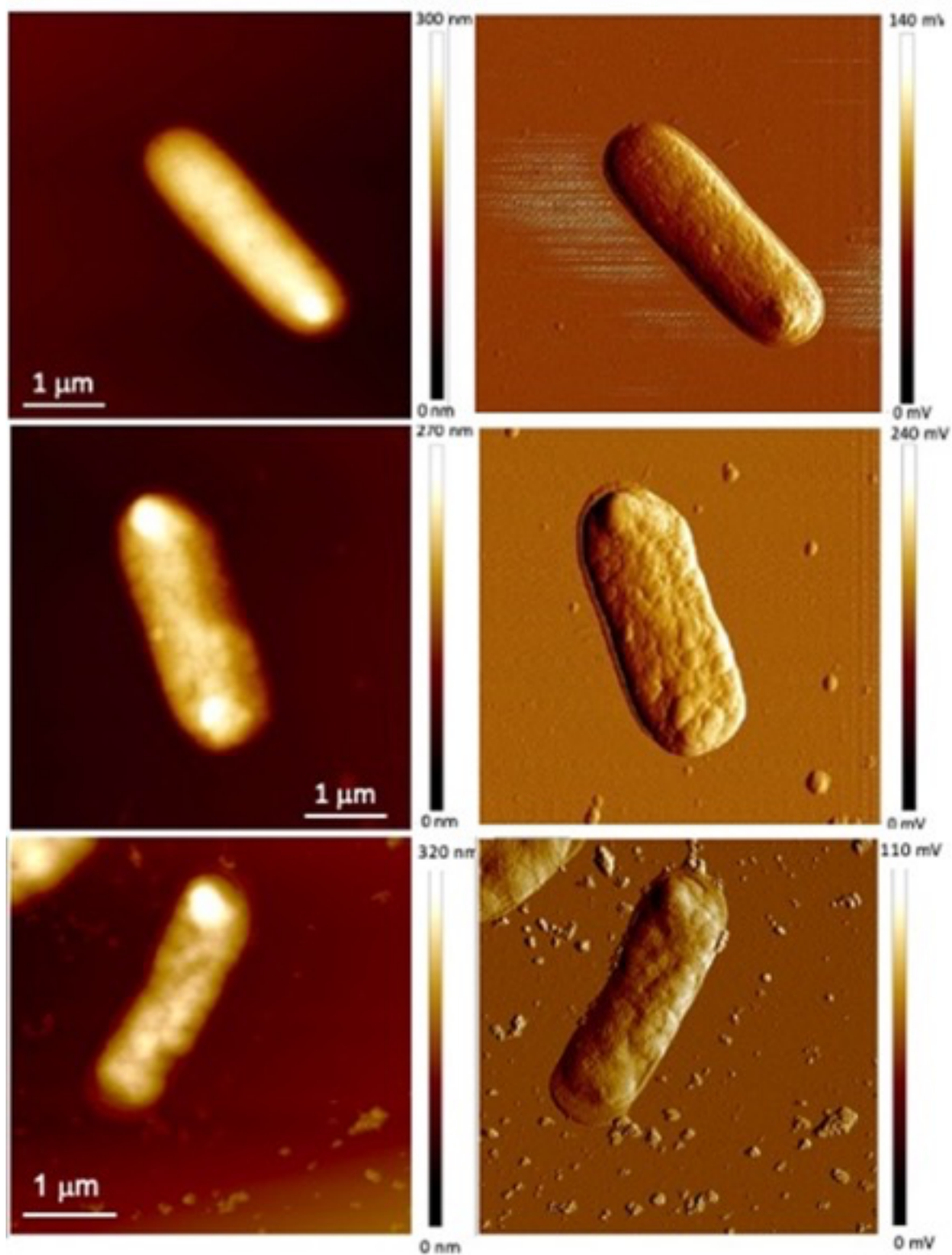


**Fig. 5** - Morphological changes on *E. coli* deposited as described previously. Images shows topological height (left side) and peak force error (right side) of respectively untreated bacteria (1<sup>st</sup> line) and bacteria exposed to AgNO<sub>3</sub> for 1 h (2<sup>nd</sup> line) and 24 h (3<sup>rd</sup> line).

-RESULTS-

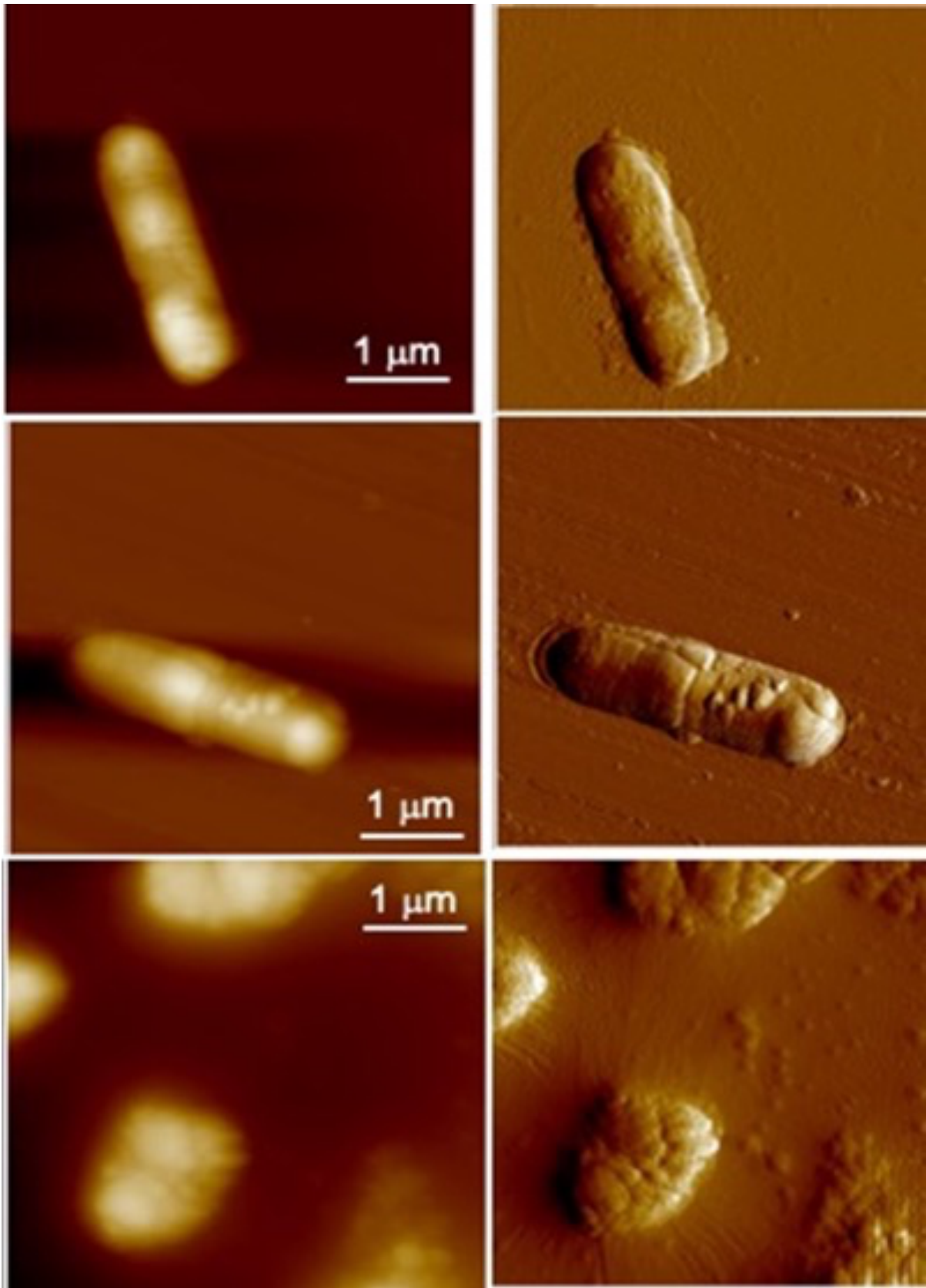


**Fig. 6** - Morphological changes on *B. subtilis* bacteria deposited as described previously. Images shows topological (left side) and peak force error (right side) of respectively untreated bacteria (1<sup>st</sup> line) and bacteria exposed to 1mM AgNO<sub>3</sub> for 1 h (2<sup>nd</sup> line) and 24 h (3<sup>rd</sup> line).

-RESULTS-

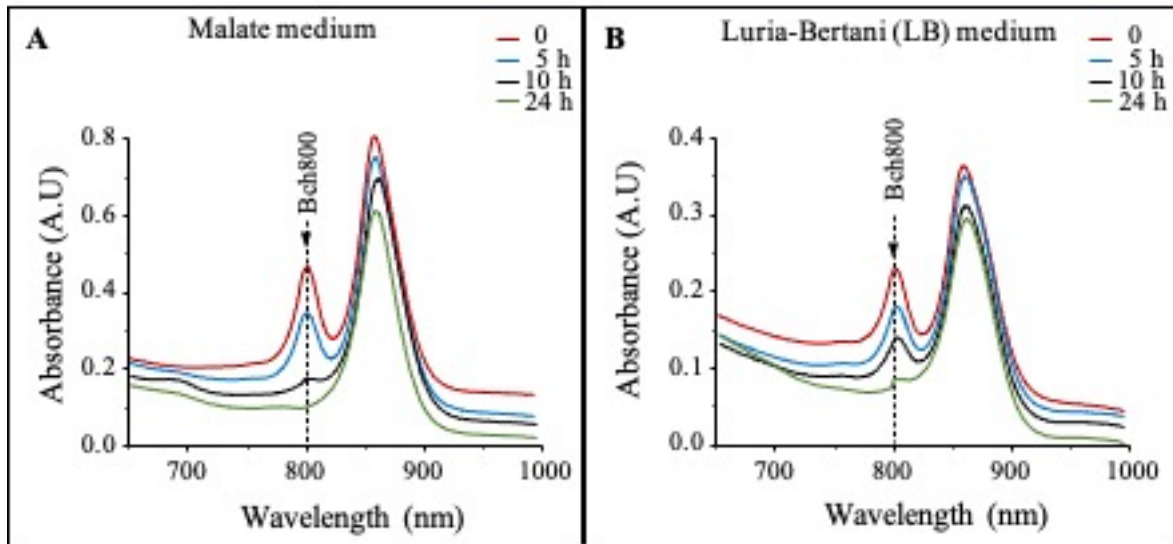


**Fig. 7** - Comparative  $\text{AgNO}_3$  exposure impact on photosystem *in vivo* in *R. gelatinosus* cells grown in Malate (A) and in LB (B) media.

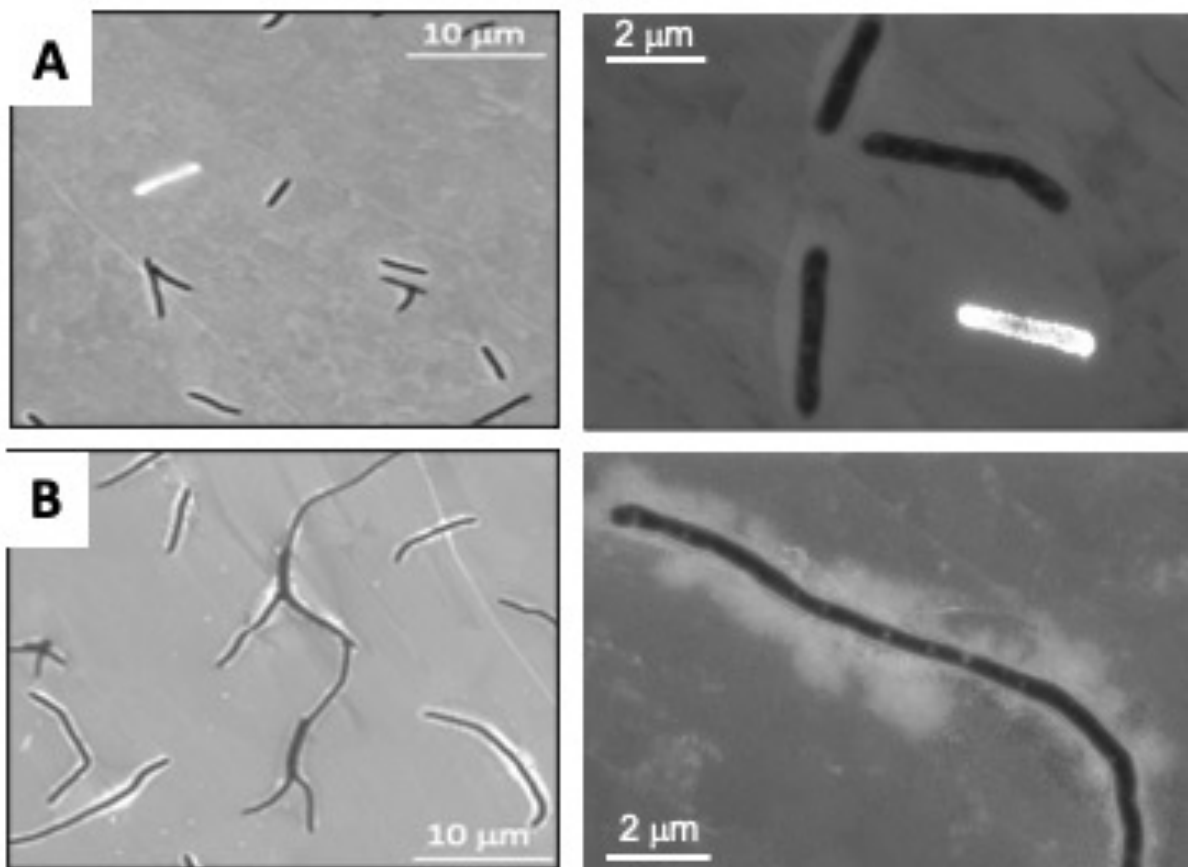


**Fig. 8** - SEM images (and zoom) of *R. gelatinosus* bacteria grown on malate (A) and LB (B) media, exposed during 1 h to  $\text{AgNO}_3$ .

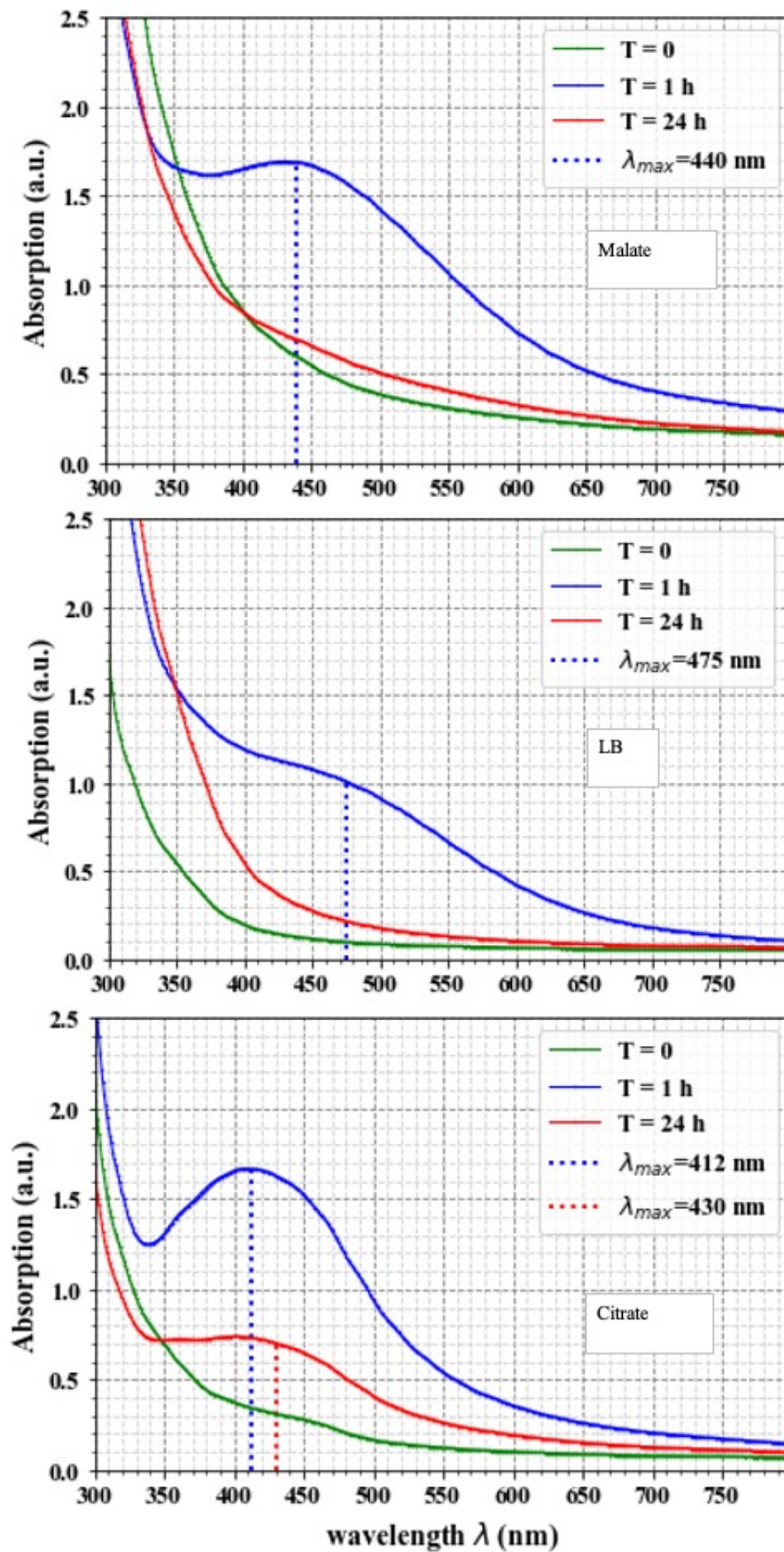


**Fig. 9** - Optical spectroscopy curves for Malate, LB and citrate-phosphate solution toward nanoparticles synthesis. The dashed lines are just an eye-guide around the curve maximum.

-RESULTS-

**Tables**

		Rg CT 1h	Rg CT 24 hrs.	Rg Ag 24 hrs.
Average height $\bar{z}$ (nm)	tra ns.	55	60	90
	lo ng.	55	60	90
Root Mean Square Roughness $R_q$ (nm)	tra ns.	8	9	20
	lo ng.	17	21	33
Average Total Roughness $R_{tm}$ (nm)	tra ns.	40	43	89
	lo ng.	40	70	106
Skewness $S_k$	tra ns.	0.05	0.02	0.34
	lo ng.	-0.51	-0.43	-0.34
Kurtosis $K_u$	tra ns.	1.8	-0.16	+0.18
	lo ng.	-0.8	-1.0	-1.0

**Table 1** - Morphological parameters, obtained using AFM topological imaging, along and across bacteria cell length axis, for *R. gelatinosus*, control (CT) after 1h and 24 h. and exposed to AgNO<sub>3</sub> (Ag) for 24 h.

Supplementary Figures

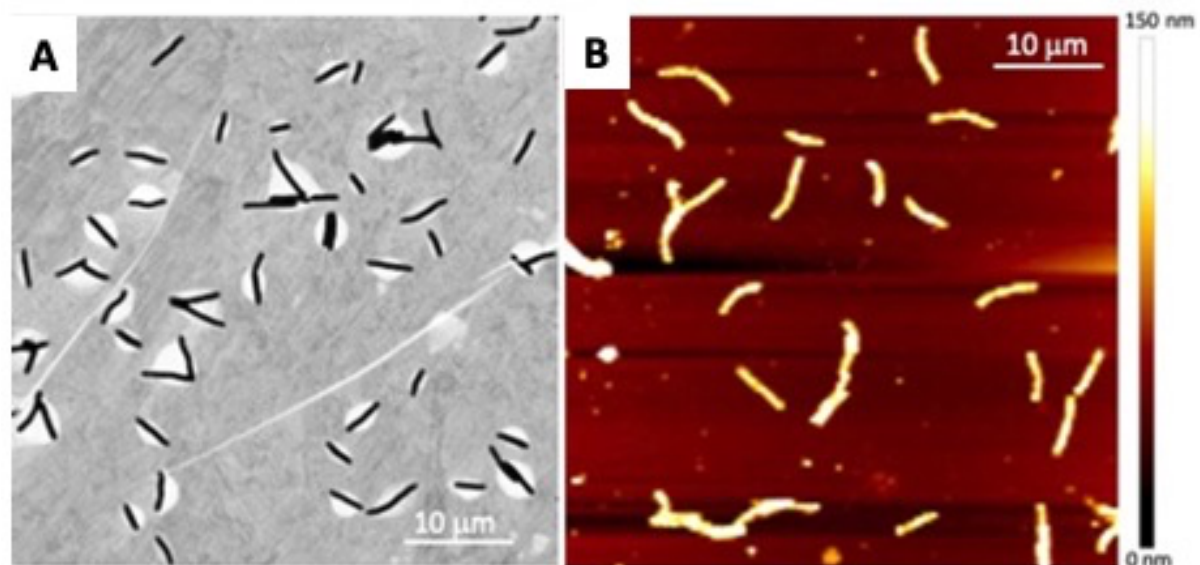


**Fig. S1** - *R. gelatinosus* wt cells grown on malate media (control), deposited by dip coating on graphite HOPG substrate, SEM image (A) and on Mica substrate, AFM image (B).

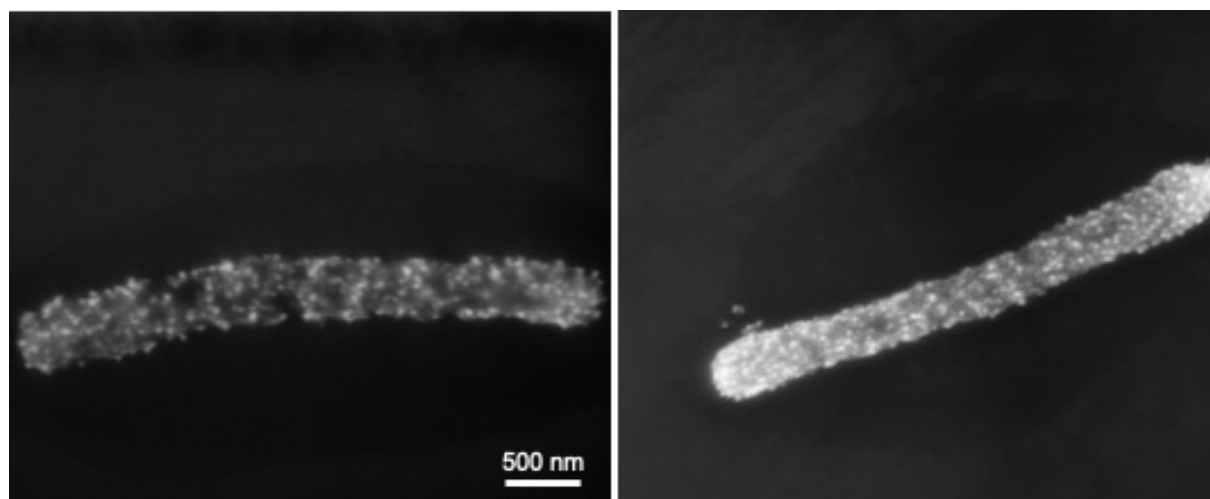


**Fig. S2** - SEM images of *R. gelatinosus* cells grown on malate and exposed to AgNO<sub>3</sub> for 1h.

-RESULTS-

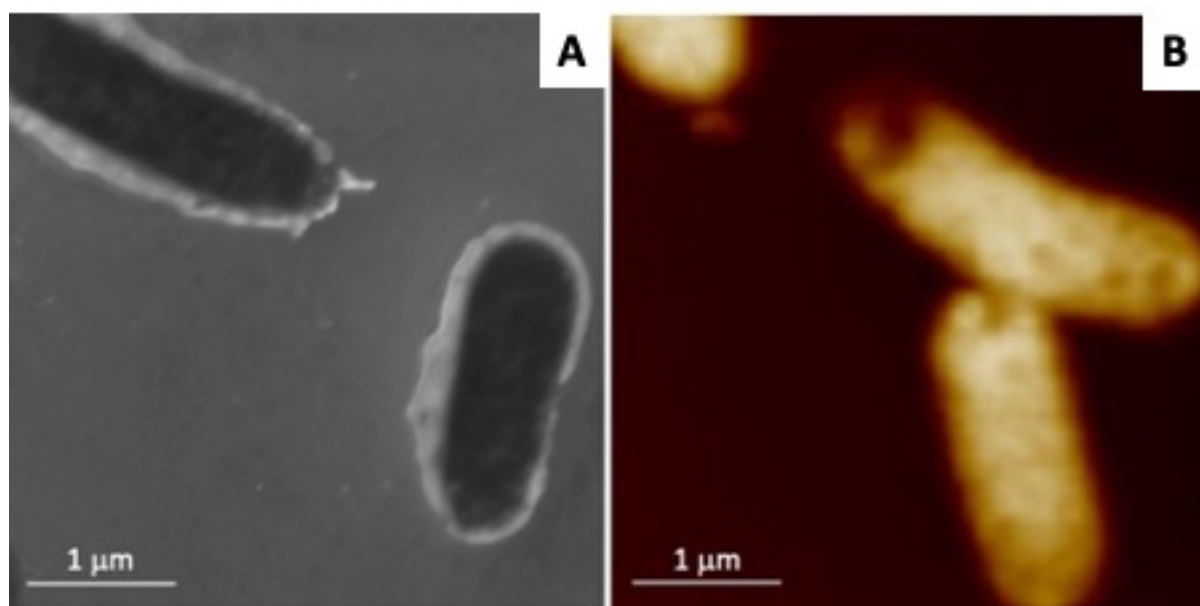


**Fig. S3** - *E. coli* cells grown on LB media, deposited by dip coating, on graphite HOPG substrate, SEM image (A) and on Mica substrate, AFM image (B).

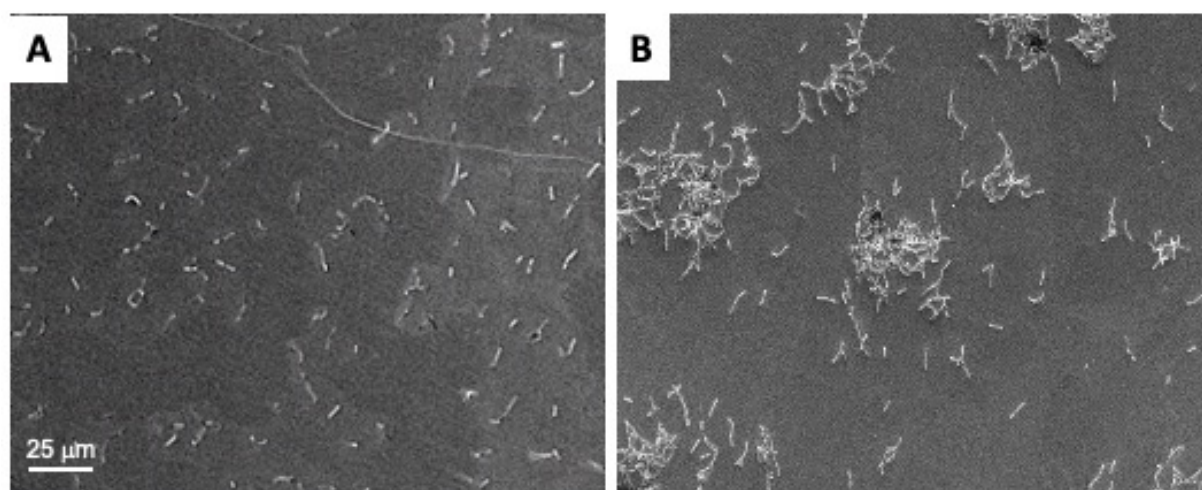


**Fig. S4** - SEM images of *B. subtilis* bacteria grown on LB. Untreated sample (A), and exposed (B) to AgNO<sub>3</sub> for 1h.

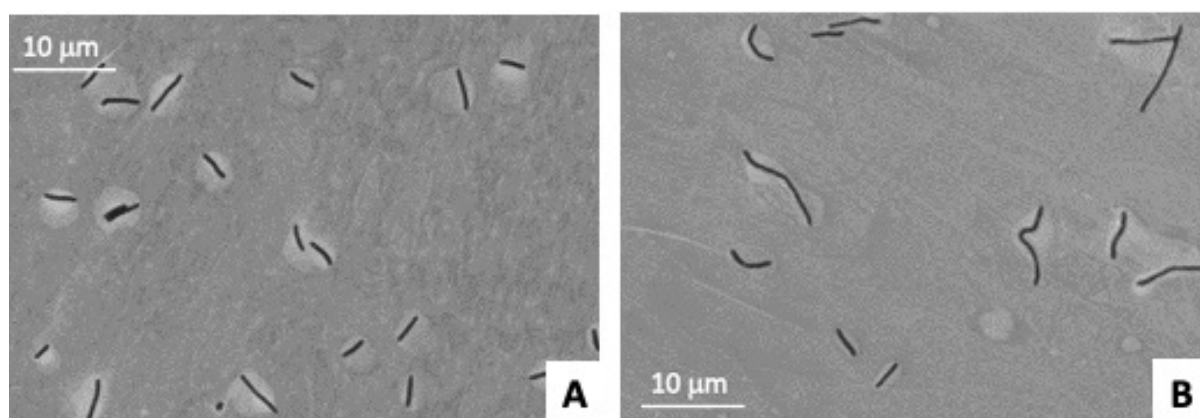


**Fig. S5** - SEM images of *R. gelatinosus* bacteria grown on malate (A) and LB (B) media.

## **Materials and Methods**

**Bacterial strains and growth** - *R. gelatinosus* (wild type S1 strain)<sup>1</sup> was grown at 30°C, in the dark micro-aerobically (low oxygenation: 50 ml flasks containing 50 ml medium) or in light by photosynthesis (filled tubes with residual oxygen in the medium) in malate or LB growth medium.

**Spectrophotometric measurements** - Absorption spectroscopy was performed with an Agilent Cary 500 spectrophotometer for both bacteria measurement and the characterisation of the aggregates described on the culture media influence. For spectra on whole cells, cells were in a 60 % (wt/vol) sucrose solution.

**Atomic Force Microscopy (AFM)** - AFM images were taken under ambient air condition at room temperature, using the tapping mode of a Bruker Nanoscope AFM. Probe and cantilever used from Nanosensors type: (PPP-NCHR, tip radius of curvature < 10 nm, tip height 10-15 mm, highly doped silicon to dissipate static charge with high mechanical Q-factor for high sensitivity, nominal resonance frequency is 330 kHz and a force constant of 45 N/m). Images in this paper are taken at 50 µm for ensemble imaging or at 5 µm scale for individual bacteria imaging. Image resolution are at 512\*512 Pixels. The scan speed is kept at 1 Hz. One image acquisition takes less than 10 min, ensuring a stable observation time window. Data acquired include height (topographical), peak force Error image (mechanical), 3D and cross-section. Data analysis were carried using Gwyddion open-source software.

**Bacterial immobilization for imaging by AFM** - Acquisition of AFM images in air was much more convenient and had higher resolution than that in liquid. Our air/nitrogen dried microbial samples provided a suitable hardness for scanning without significant topographic changes and good resolution. Bacteria were immobilized on Mica substrate with gelatin. MICA substrate was used for its properties as it has no known effect on biological samples, transparent, easy to cut and to manipulate, atomically flat and inexpensive. The substrate must be coated to

## -RESULTS-

immobilize the living cells on it by creating electrostatic interaction between the negative charge of bacteria and the positive charge of gelatin. ***Gelatin preparation (sigma G-6144)***: we used 0.5 g in 100 ml of hot distilled water. We used around 15 ml in a beaker, enough to dip mica substrate in it. We leave substrate to dry, to be used after 24 h. ***Placing bacteria on gelatin coated mica***: 1 ml bacterial culture (0.5 OD at 680 nm) was centrifuged (5000 rpm) washed and rapidly resuspended in 500  $\mu$ l of deionized water. 5  $\mu$ l of this cell suspension was applied on the gelatin-coated mica substrate. Carefully, spread on the surface of the gelatin to avoid damaging it, and let it dry again as described in<sup>29,57</sup>.

**Scanning Electron Microscopy (SEM)** – We imaged bacteria, which had been fixed, dehydrated and dried with a Zeiss Semfeg. It was not necessary to frozen them. We used low tension (2.0 – 3.0 kV) to avoid contamination and electron damaging of structures. Images were taken at different magnifications. The specimen did not release any volatile substance even at high vacuum. We kept same resolution as AFM to enable image comparison and control.

**Preparation of bacterial sample for SEM** – overnight PS grown cells (OD 680nm = 1) were exposed or not to AgNO<sub>3</sub>. After incubation time, samples were washed in deionized water, and then diluted 10 times. Then, we use a clean graphite substrate (freshly cleaved) and dip coat in the cellular culture, and then let to dry<sup>30</sup>.

**Statistical Analysis** - All experiments were performed in triplicate, unless otherwise stated, and data analysis were carried on different bacteria from different samples, showing a great reproducibility.

## References

- (1) Tambosi, R.; Liotenberg, S.; Bourbon, M.-L.; Steunou, A.-S.; Babot, M.; Durand, A.; Kebaili, N.; Ouchane, S. Silver and Copper Acute Effects on Membrane Proteins and Impact on Photosynthetic and Respiratory Complexes in Bacteria. *mBio* **2018**, *9* (6). <https://doi.org/10.1128/mBio.01535-18>.
- (2) Coates, A. R. M.; Halls, G.; Hu, Y. Novel Classes of Antibiotics or More of the Same? *Br. J. Pharmacol.* **2011**, *163* (1), 184–194. <https://doi.org/10.1111/j.1476-5381.2011.01250.x>.
- (3) Aslam, B.; Wang, W.; Arshad, M. I.; Khurshid, M.; Muzammil, S.; Rasool, M. H.; Nisar, M. A.; Alvi, R. F.; Aslam, M. A.; Qamar, M. U.; Salamat, M. K. F.; Baloch, Z. Antibiotic Resistance: A Rundown of a Global Crisis. *Infect Drug Resist* **2018**, *11*, 1645–1658. <https://doi.org/10.2147/IDR.S173867>.
- (4) Sánchez-López, E.; Gomes, D.; Esteruelas, G.; Bonilla, L.; Lopez-Machado, A. L.; Galindo, R.; Cano, A.; Espina, M.; Ettcheto, M.; Camins, A.; Silva, A. M.; Durazzo, A.; Santini, A.; Garcia, M. L.; Souto, E. B. Metal-Based Nanoparticles as Antimicrobial Agents: An Overview. *Nanomaterials (Basel)* **2020**, *10* (2). <https://doi.org/10.3390/nano10020292>.
- (5) Murei, A.; Ayinde, W. B.; Gitari, M. W.; Samie, A. Functionalization and Antimicrobial Evaluation of Ampicillin, Penicillin and Vancomycin with *Pyrenacantha Grandiflora* Baill and Silver Nanoparticles. *Scientific Reports* **2020**, *10* (1), 11596. <https://doi.org/10.1038/s41598-020-68290-x>.
- (6) Zhang; Liu, Z.-G.; Shen, W.; Gurunathan, S. Silver Nanoparticles: Synthesis, Characterization, Properties, Applications, and Therapeutic Approaches. *IJMS* **2016**, *17* (9), 1534. <https://doi.org/10.3390/ijms17091534>.
- (7) Haider, A.; Kang, I.-K. Preparation of Silver Nanoparticles and Their Industrial and Biomedical Applications: A Comprehensive Review <https://www.hindawi.com/journals/amse/2015/165257/> (accessed Sep 1, 2020). <https://doi.org/10.1155/2015/165257>.
- (8) Saravanan, M.; Barik, S. K.; MubarakAli, D.; Prakash, P.; Pugazhendhi, A. Synthesis of Silver Nanoparticles from *Bacillus Brevis* (NCIM 2533) and Their Antibacterial Activity against Pathogenic Bacteria. *Microb. Pathog.* **2018**, *116*, 221–226. <https://doi.org/10.1016/j.micpath.2018.01.038>.
- (9) Li, W.-R.; Xie, X.-B.; Shi, Q.-S.; Zeng, H.-Y.; Ou-Yang, Y.-S.; Chen, Y.-B. Antibacterial Activity and Mechanism of Silver Nanoparticles on *Escherichia Coli*. *Appl. Microbiol. Biotechnol.* **2010**, *85* (4), 1115–1122. <https://doi.org/10.1007/s00253-009-2159-5>.
- (10) Lubick, N. Nanosilver Toxicity: Ions, Nanoparticles—or Both? *Environ. Sci. Technol.* **2008**, *42* (23), 8617–8617. <https://doi.org/10.1021/es8026314>.
- (11) Dias, A. C. P.; Marslin, G.; Selvakesavan; Gregory, F.; Sarmiento, B. Antimicrobial Activity of Cream Incorporated with Silver Nanoparticles Biosynthesized from *Withania Somnifera*. *IJN* **2015**, 5955. <https://doi.org/10.2147/IJN.S81271>.
- (12) Sondi, I.; Salopek-Sondi, B. Silver Nanoparticles as Antimicrobial Agent: A Case Study on *E. Coli* as a Model for Gram-Negative Bacteria. *J Colloid Interface Sci* **2004**, *275* (1), 177–182. <https://doi.org/10.1016/j.jcis.2004.02.012>.

- (13) Barwinska-Sendra, A.; Waldron, K. J. The Role of Intermetal Competition and Mis-Metalation in Metal Toxicity. *Adv. Microb. Physiol.* **2017**, *70*, 315–379. <https://doi.org/10.1016/bs.ampbs.2017.01.003>.
- (14) Chandrangu, P.; Rensing, C.; Helmann, J. D. Metal Homeostasis and Resistance in Bacteria. *Nat. Rev. Microbiol.* **2017**, *15* (6), 338–350. <https://doi.org/10.1038/nrmicro.2017.15>.
- (15) Capdevila, D. A.; Edmonds, K. A.; Giedroc, D. P. Metallochaperones and Metalloregulation in Bacteria. *Essays in Biochemistry* **2017**, *61* (2), 177–200. <https://doi.org/10.1042/EBC20160076>.
- (16) Mealman, T. D.; Blackburn, N. J.; McEvoy, M. M. Metal Export by CusCFBA, the Periplasmic Cu(I)/Ag(I) Transport System of Escherichia Coli. *Curr Top Membr* **2012**, *69*, 163–196. <https://doi.org/10.1016/B978-0-12-394390-3.00007-0>.
- (17) Steunou, A. S.; Durand, A.; Bourbon, M.-L.; Babot, M.; Tambosi, R.; Liotenberg, S.; Ouchane, S. Cadmium and Copper Cross-Tolerance. Cu<sup>+</sup> Alleviates Cd<sup>2+</sup> Toxicity, and Both Cations Target Heme and Chlorophyll Biosynthesis Pathway in *Rubrivivax Gelatinosus*. *Front Microbiol* **2020a**, *11*. <https://doi.org/10.3389/fmicb.2020.00893>.
- (18) Yuan, L.; Gao, T.; He, H.; Jiang, F. L.; Liu, Y. Silver Ion-Induced Mitochondrial Dysfunction via a Nonspecific Pathway. *Toxicol. Res.* **2017**, *6* (5), 621–630. <https://doi.org/10.1039/C7TX00079K>.
- (19) Acharya, D.; Singha, K. M.; Pandey, P.; Mohanta, B.; Rajkumari, J.; Singha, L. P. Shape Dependent Physical Mutilation and Lethal Effects of Silver Nanoparticles on Bacteria. *Sci Rep* **2018**, *8* (1), 201. <https://doi.org/10.1038/s41598-017-18590-6>.
- (20) Silver, S. Bacterial Silver Resistance: Molecular Biology and Uses and Misuses of Silver Compounds. *FEMS Microbiol Rev* **2003**, *27* (2–3), 341–353. [https://doi.org/10.1016/S0168-6445\(03\)00047-0](https://doi.org/10.1016/S0168-6445(03)00047-0).
- (21) Butkus, M. A.; Edling, L.; Labare, M. P. The Efficacy of Silver as a Bactericidal Agent: Advantages, Limitations and Considerations for Future Use. *Journal of Water Supply: Research and Technology-Aqua* **2003**, *52* (6), 407–416. <https://doi.org/10.2166/aqua.2003.0037>.
- (22) Barillo, D. J.; Marx, D. E. Silver in Medicine: A Brief History BC 335 to Present. *Burns* **2014**, *40 Suppl 1*, S3-8. <https://doi.org/10.1016/j.burns.2014.09.009>.
- (23) Navarro, E.; Wagner, B.; Odzak, N.; Sigg, L.; Behra, R. Effects of Differently Coated Silver Nanoparticles on the Photosynthesis of *Chlamydomonas Reinhardtii*. *Environ. Sci. Technol.* **2015**, *49* (13), 8041–8047. <https://doi.org/10.1021/acs.est.5b01089>.
- (24) Salas, P.; Odzak, N.; Echevoyen, Y.; Kägi, R.; Sancho, M. C.; Navarro, E. The Role of Size and Protein Shells in the Toxicity to Algal Photosynthesis Induced by Ionic Silver Delivered from Silver Nanoparticles. *Sci. Total Environ.* **2019**, *692*, 233–239. <https://doi.org/10.1016/j.scitotenv.2019.07.237>.
- (25) Wang, H.; Yan, A.; Liu, Z.; Yang, X.; Xu, Z.; Wang, Y.; Wang, R.; Koohi-Moghadam, M.; Hu, L.; Xia, W.; Tang, H.; Wang, Y.; Li, H.; Sun, H. Deciphering Molecular Mechanism of Silver by Integrated Omic Approaches Enables Enhancing Its Antimicrobial Efficacy in *E. Coli*. *PLOS Biology* **2019**, *17* (6), e3000292. <https://doi.org/10.1371/journal.pbio.3000292>.

- (26) Gabrielyan, L.; Badalyan, H.; Gevorgyan, V.; Trchounian, A. Comparable Antibacterial Effects and Action Mechanisms of Silver and Iron Oxide Nanoparticles on Escherichia Coli and Salmonella Typhimurium. *Sci Rep* **2020**, *10* (1), 13145. <https://doi.org/10.1038/s41598-020-70211-x>.
- (27) Park, S. B.; Steadman, C. S.; Chaudhari, A. A.; Pillai, S. R.; Singh, S. R.; Ryan, P. L.; Willard, S. T.; Feugang, J. M. Proteomic Analysis of Antimicrobial Effects of Pegylated Silver Coated Carbon Nanotubes in Salmonella Enterica Serovar Typhimurium. *Journal of Nanobiotechnology* **2018**, *16* (1), 31. <https://doi.org/10.1186/s12951-018-0355-0>.
- (28) Hussain, S.; Andrews, D.; Hill, B. C. Exposure of Bacillus Subtilis to Silver Inhibits Activity of Cytochrome c Oxidase in Vivo via Interaction with SCO, the CuA Assembly Protein. *Metallomics* **2018**, *10* (5), 735–744. <https://doi.org/10.1039/c7mt00343a>.
- (29) Chaw, K. C.; Manimaran, M.; Tay, F. E. H. Role of Silver Ions in Destabilization of Intermolecular Adhesion Forces Measured by Atomic Force Microscopy in Staphylococcus Epidermidis Biofilms. *AAC* **2005**, *49* (12), 4853–4859. <https://doi.org/10.1128/AAC.49.12.4853-4859.2005>.
- (30) Murtey, M. D.; Ramasamy, P. Sample Preparations for Scanning Electron Microscopy – Life Sciences. In *Modern Electron Microscopy in Physical and Life Sciences*; Janecek, M., Kral, R., Eds.; InTech, 2016. <https://doi.org/10.5772/61720>.
- (31) Naik, A. N.; Patra, S.; Sen, D.; Goswami, A. Evaluating the Mechanism of Nucleation and Growth of Silver Nanoparticles in a Polymer Membrane under Continuous Precursor Supply: Tuning of Multiple to Single Nucleation Pathway. *Phys. Chem. Chem. Phys.* **2019**, *21* (8), 4193–4199. <https://doi.org/10.1039/C8CP06202A>.
- (32) Mulfinger, L.; Solomon, S. D.; Bahadory, M.; Jeyarajasingam, A. V.; Rutkowsky, S. A.; Boritz, C. Synthesis and Study of Silver Nanoparticles. *J. Chem. Educ.* **2007**, *84* (2), 322. <https://doi.org/10.1021/ed084p322>.
- (33) Chakraborty, J.; Mallick, S.; Raj, R.; Das, S. Functionalization of Extracellular Polymers of Pseudomonas Aeruginosa N6P6 for Synthesis of CdS Nanoparticles and Cadmium Bioadsorption. *J Polym Environ* **2018**, *26* (7), 3097–3108. <https://doi.org/10.1007/s10924-018-1195-6>.
- (34) Raposo, M.; Ferreira, Q. A Guide for Atomic Force Microscopy Analysis of Soft-Condensed Matter </paper/A-Guide-for-Atomic-Force-Microscopy-Analysis-of-Raposo-Ferreira/d5359268a9d9ab74a6beaa0f59d23f8ae3f41873> (accessed Sep 21, 2020).
- (35) Mitik-Dineva, N.; Wang, J.; Truong, V. K.; Stoddart, P.; Malherbe, F.; Crawford, R. J.; Ivanova, E. P. Escherichia Coli, Pseudomonas Aeruginosa, and Staphylococcus Aureus Attachment Patterns on Glass Surfaces with Nanoscale Roughness. *Curr Microbiol* **2009**, *58* (3), 268–273. <https://doi.org/10.1007/s00284-008-9320-8>.
- (36) Rafińska, K.; Pomastowski, P.; Buszewski, B. Study of Bacillus Subtilis Response to Different Forms of Silver. *Science of The Total Environment* **2019**, *661*, 120–129. <https://doi.org/10.1016/j.scitotenv.2018.12.139>.
- (37) Yang, X.; Yang, W.; Wang, Q.; Li, H.; Wang, K.; Yang, L.; Liu, W. Atomic Force Microscopy Investigation of the Characteristic Effects of Silver Ions on Escherichia Coli and Staphylococcus Epidermidis. *Talanta* **2010**, *81* (4–5), 1508–1512. <https://doi.org/10.1016/j.talanta.2010.02.061>.

- (38) Dong, X.; Awak, M. A.; Tomlinson, N.; Tang, Y.; Sun, Y.-P.; Yang, L. Antibacterial Effects of Carbon Dots in Combination with Other Antimicrobial Reagents. *PLoS ONE* **2017**, *12* (9), e0185324. <https://doi.org/10.1371/journal.pone.0185324>.
- (39) Mathelié-Guinlet, M.; Grauby-Heywang, C.; Martin, A.; Février, H.; Moroté, F.; Vilquin, A.; Béven, L.; Delville, M.-H.; Cohen-Bouhacina, T. Detrimental Impact of Silica Nanoparticles on the Nanomechanical Properties of Escherichia Coli, Studied by AFM. *Journal of Colloid and Interface Science* **2018**, *529*, 53–64. <https://doi.org/10.1016/j.jcis.2018.05.098>.
- (40) Silhavy, T. J.; Kahne, D.; Walker, S. The Bacterial Cell Envelope. *Cold Spring Harb Perspect Biol* **2010**, *2* (5), a000414. <https://doi.org/10.1101/cshperspect.a000414>.
- (41) Xu, F. F.; Imlay, J. A. Silver(I), Mercury(II), Cadmium(II), and Zinc(II) Target Exposed Enzymic Iron-Sulfur Clusters When They Toxicify Escherichia Coli. *Appl. Environ. Microbiol.* **2012**, *78* (10), 3614–3621. <https://doi.org/10.1128/AEM.07368-11>.
- (42) Johnston, K. A.; Stabryla, L. M.; Smith, A. M.; Gan, X. Y.; Gilbertson, L. M.; Millstone, J. E. Impacts of Broth Chemistry on Silver Ion Release, Surface Chemistry Composition, and Bacterial Cytotoxicity of Silver Nanoparticles. *Environ. Sci.: Nano* **2018**, *5* (2), 304–312. <https://doi.org/10.1039/C7EN00974G>.
- (43) Zhang, S.; Liu, L.; Pareek, V.; Becker, T.; Liang, J.; Liu, S. Effects of Broth Composition and Light Condition on Antimicrobial Susceptibility Testing of Ionic Silver. *Journal of Microbiological Methods* **2014**, *105*, 42–46. <https://doi.org/10.1016/j.mimet.2014.07.009>.
- (44) Eckhardt, S.; Brunetto, P. S.; Gagnon, J.; Priebe, M.; Giese, B.; Fromm, K. M. Nanobio Silver: Its Interactions with Peptides and Bacteria, and Its Uses in Medicine. *Chem. Rev.* **2013**, *113* (7), 4708–4754. <https://doi.org/10.1021/cr300288v>.
- (45) Puchkova, L. V.; Broggin, M.; Polishchuk, E. V.; Ilyechova, E. Y.; Polishchuk, R. S. Silver Ions as a Tool for Understanding Different Aspects of Copper Metabolism. *Nutrients* **2019**, *11* (6), 1364. <https://doi.org/10.3390/nu11061364>.
- (46) Müller, A.; Behnlian, D.; Walz, E.; Gräf, V.; Hogeckamp, L.; Greiner, R. Effect of Culture Medium on the Extracellular Synthesis of Silver Nanoparticles Using Klebsiella Pneumoniae, Escherichia Coli and Pseudomonas Jessinii. *Biocatalysis and Agricultural Biotechnology* **2016**, *6*, 107–115. <https://doi.org/10.1016/j.bcab.2016.02.012>.
- (47) Amornpitoksuk, P.; Intarasuwan, K.; Suwanboon, S.; Baltrusaitis, J. Effect of Phosphate Salts (Na<sub>3</sub>PO<sub>4</sub>, Na<sub>2</sub>HPO<sub>4</sub>, and NaH<sub>2</sub>PO<sub>4</sub>) on Ag<sub>3</sub>PO<sub>4</sub> Morphology for Photocatalytic Dye Degradation under Visible Light and Toxicity of the Degraded Dye Products. *Ind. Eng. Chem. Res.* **2013**, *52* (49), 17369–17375. <https://doi.org/10.1021/ie401821w>.
- (48) Chudobova, D.; Nejd, L.; Gumulec, J.; Krystofova, O.; Rodrigo, M.; Kynicky, J.; Ruttkay-Nedecky, B.; Kopel, P.; Babula, P.; Adam, V.; Kizek, R. Complexes of Silver(I) Ions and Silver Phosphate Nanoparticles with Hyaluronic Acid and/or Chitosan as Promising Antimicrobial Agents for Vascular Grafts. *IJMS* **2013**, *14* (7), 13592–13614. <https://doi.org/10.3390/ijms140713592>.
- (49) Loza, K.; Sengstock, C.; Chernousova, S.; Köller, M.; Epple, M. The Predominant Species of Ionic Silver in Biological Media Is Colloidally Dispersed Nanoparticulate Silver Chloride. **2014**. <https://doi.org/10.1039/C4RA04764H>.

- (50) Xia, Y.; Campbell, D. J. Plasmons: Why Should We Care? *J. Chem. Educ.* **2007**, *84* (1), 91. <https://doi.org/10.1021/ed084p91>.
- (51) Zhang, Z.; Shen, W.; Xue, J.; Liu, Y.; Liu, Y.; Yan, P.; Liu, J.; Tang, J. Recent Advances in Synthetic Methods and Applications of Silver Nanostructures. *Nanoscale Research Letters* **2018**, *13* (1), 54. <https://doi.org/10.1186/s11671-018-2450-4>.
- (52) Agnihotri, S.; Mukherji, S.; Mukherji, S. Size-Controlled Silver Nanoparticles Synthesized over the Range 5–100 Nm Using the Same Protocol and Their Antibacterial Efficacy. *RSC Adv.* **2013**, *4* (8), 3974–3983. <https://doi.org/10.1039/C3RA44507K>.
- (53) Loza, K.; Diendorf, J.; Sengstock, C.; Ruiz-Gonzalez, L.; M. Gonzalez-Calbet, J.; Vallet-Regi, M.; Köller, M.; Epple, M. The Dissolution and Biological Effects of Silver Nanoparticles in Biological Media. *Journal of Materials Chemistry B* **2014**, *2* (12), 1634–1643. <https://doi.org/10.1039/C3TB21569E>.
- (54) De Leersnyder, I.; De Gelder, L.; Van Driessche, I.; Vermeir, P. Influence of Growth Media Components on the Antibacterial Effect of Silver Ions on *Bacillus Subtilis* in a Liquid Growth Medium. *Scientific Reports* **2018**, *8* (1), 9325. <https://doi.org/10.1038/s41598-018-27540-9>.
- (55) Muller, M.; Merrett, N. D. Pyocyanin Production by *Pseudomonas Aeruginosa* Confers Resistance to Ionic Silver. *Antimicrobial Agents and Chemotherapy* **2014**, *58* (9), 5492–5499. <https://doi.org/10.1128/AAC.03069-14>.
- (56) John, M. S.; Nagoth, J. A.; Ramasamy, K. P.; Mancini, A.; Giuli, G.; Natalello, A.; Ballarini, P.; Miceli, C.; Pucciarelli, S. Synthesis of Bioactive Silver Nanoparticles by a *Pseudomonas* Strain Associated with the Antarctic Psychrophilic Protozoon *Euplotes Focardii*. *Mar Drugs* **2020**, *18* (1). <https://doi.org/10.3390/md18010038>.
- (57) Allison, D. P.; Sullivan, C. J.; Mortensen, N. P.; Retterer, S. T.; Doktycz, M. Bacterial Immobilization for Imaging by Atomic Force Microscopy. *JoVE* **2011**, No. 54, 2880. <https://doi.org/10.3791/2880>.

-RESULTS-

### Additional results:

#### 1- Substrate study - toxicity, biocompatibility and suitability for experiment

The aim of this test was to detect any toxicity of surfaces that could be used as substrates, to deposit and fix bacteria cells on them, for AFM and SEM imaging. The candidate substrates were: Mica, HOPG, Si, Al<sub>2</sub>O<sub>3</sub>, MgO, SiO<sub>2</sub> and Copper grid.

In this experiment we prepared solid medium that embedded *R. gelatinosus* bacterial cells. The substrates were cleaned using ethanol, dried and carefully placed on the surface of the medium; all steps under sterilized environment.

The results showed no inhibition zones and that all the substrates used have no toxicity effect on *R. gelatinosus* cells. The growth was normal, expect for the case of copper grid substrate. Thus, we decided to use HOPG (well known in LAC-Nano<sup>3</sup> group) for SEM imaging (conductor, easy to cleave and bake) and Mica for AFM imaging (very flat, easy to cleave and possess a very good wettability).

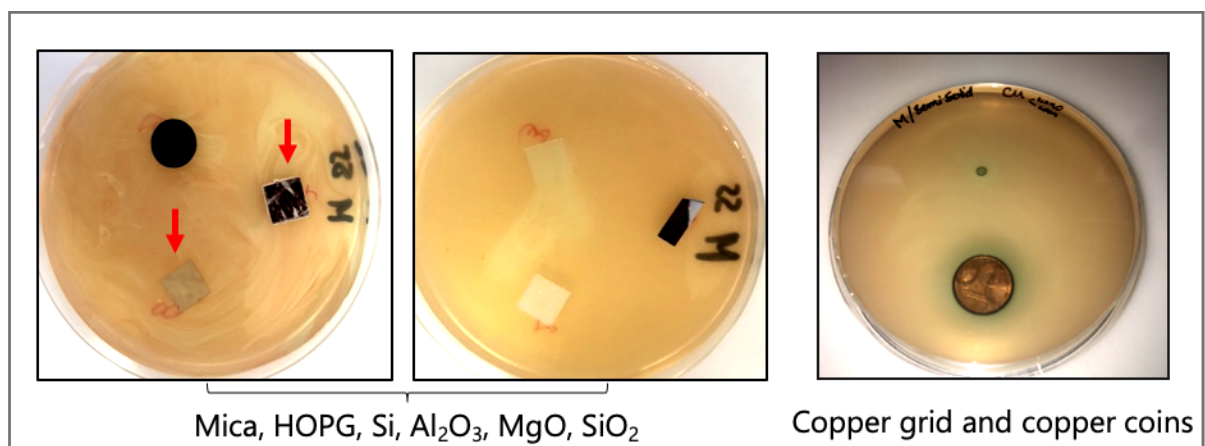


**Figure 65. Substrates: mica and HOPG toxicity test comparing to other types of substrate.**

(arrows pointing mica, left; and HOPG, right). Cultures were let to grow under Photosynthesis condition in 37°C for 48 hrs.

Drying time and deposition techniques had also to be evaluated to setup our protocol. The main goal of this experiment is to find the most suitable substrate to deposit bacteria and silver ions, effectively i.e., in a short period of time and the most appropriate technique of deposition.

Below, table shows relation between drying time and surface tension and figure illustrate the wettability on the substrate by comparing different form of droplets with water as solvent for different type of surface (Guriyanova & Bonaccorso, 2008).



**Figure 66. Different form of droplets with water as solvent and drying time depending on substrate.**

There are several techniques to deposit the contain of a solution (nanoparticles for instance) as a thin film or monolayer onto a substrate. The choice of the techniques depends generally on the nature of the surface that you are trying to cover, the properties (mainly viscosity) of the solution you are trying to deposit and the equipment available. In general, experimental parameters such as choice of solvent, particle concentration, and temperature will all affect the deposition process, and must be controlled to produce a film with the desired thickness and morphology. In our case, drop coating, dip coating and spin coating could be carried.

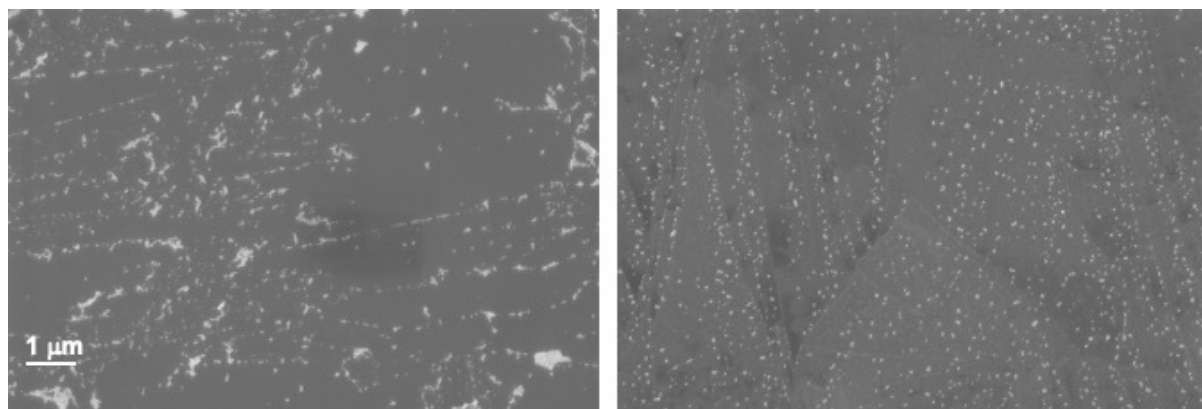
**Spin-coating** is widely used in nanotechnology, mainly because it often provides more uniform film thicknesses across the substrate compared with other coating techniques. In this technique, a substrate is spun at high RPM and a volume of material with known particle concentration is introduced into the center. Centrifugal force leads to uniform spreading of the dispersion across the substrate, followed by

## -RESULTS-

evaporation of solvent to yield a thin particle film. Solvents with some viscosity, other than water are usually favoured. This technique was not kept because we couldn't ensure the sterility of the apparatus, culture media viscosity wasn't high enough, and we couldn't exclude that centrifugal force on drying bacteria will not affect their morphologies.

**Drop-coating** is an easy and tuneable deposition technique for small substrate ( $\sim 1 \text{ cm}^2$ ), spreading a solution contained dispersion over a substrate and allowing it to dry under controlled conditions, (pressure and temperature. In principle, film thickness depends on the volume of dispersion used and the particle concentration, but other less controlled variables can affect the film structure such as how well the solvent wets the substrate, evaporation rate, capillary forces associated with drying, etc. It is more convenient to use solvents that are volatile, wet the substrate, and are not susceptible to thin film instabilities (de-wetting). Water and culture media tend to be poor solvents for drop-coating due to the low vapor pressure and large surface tension. In our case a lot of impurities and mineral streaks were left during drying process.

**Dip-coating** consist on slowly withdrawing a substrate from a solution dispersion. This causes solution contains to be drawn into the meniscus and deposited as the thin liquid layer dries. This technique can produce very uniform, close-packed particle films, but does have a number of inter-related variables to be controlled before producing good films. The substrate pull rate, particle concentration in the solution, and surface tension between substrate and solution are all important. This technique appears to be the most suitable for our experiments, showing a high degree of reproducibility and the less trauma on the bacteria.



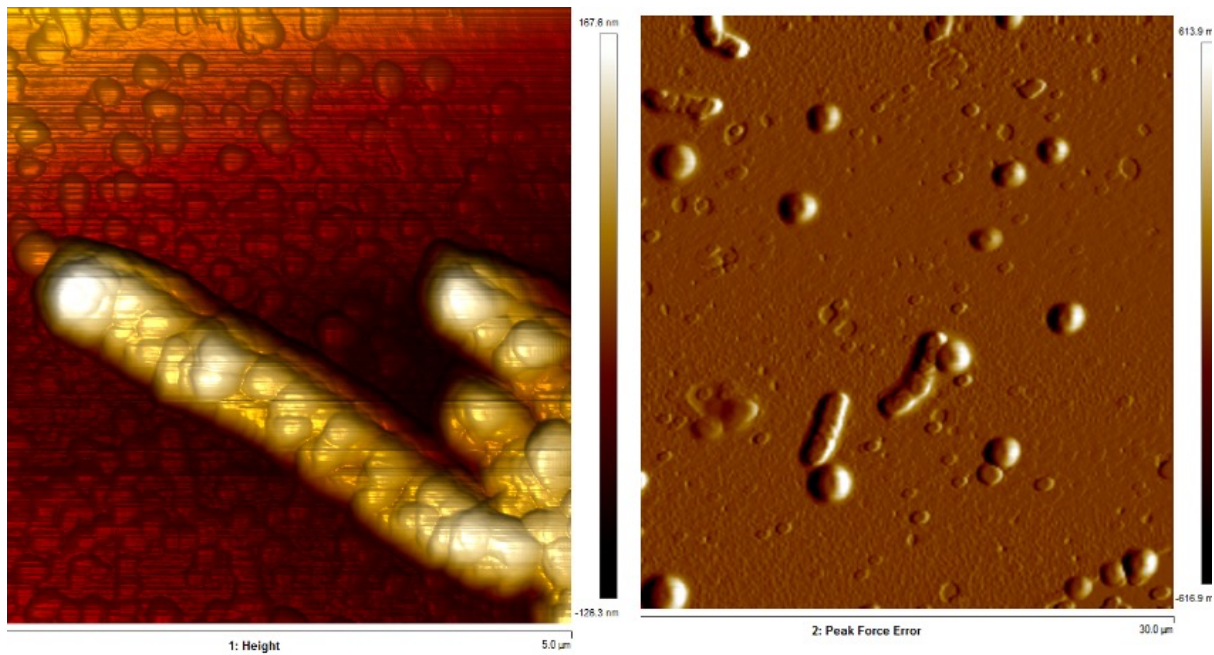
**Figure 67. Ag-NPs on HOPG substrate.**  
Drop-coating (left) and dip-coating (right).

Figure above shows SEM images of Sigma silver nanoparticles (10 nm, concentration 0,05 mg/ml, used as reference) on HOPG surfaces, using drop (left) and dip (right) coating. In the case of dip coating, deposition appears much more homogeneous and undergoing less aggregation (images are at same scale).

## **2- Study of Ag nanoparticles size change by Oswald ripening.**

In our experiment we have found that silver ions precipitates to form aggregates. The size of the obtained aggregates exhibits a complex size distribution density profile, suggesting stochastic nucleation and growth process. Aggregates on the membrane surfaces shows higher and double peaked profile. Despite precipitation processes due to probably both presence of phosphates and chlorates and to a possible defense mechanism (cf Tambosi et al, 2020), some coarsening processes as Oswald ripening seem most likely to be at work.

In this experiment we used commercial silver nanoparticles (Sigma Aldrich and Nanocomposix) incorporated to the culture media and the bacteria to observe the resulting product. We had several sizes of nanoparticles (10 nm, 20 nm; 40 nm and 60 nm), and they are perfectly spherical and stabilized by citrate coating.



**Figure 68. AFM images of *R. gelatinosus* bacterial cells with Ag-NPs incorporated in the culture media.**

Figure (68), above, shows, AFM images of *R. gelatinosus* bacteria with silver nanoparticles incorporated in the culture media. We can observe that the nanoparticles had undergone coarsening process that had considerably increase their apparent sizes. This phenomenon, known as Oswald ripening, is generally observed in solid or liquid solutions. It explains the behaviour and the evolution of an inhomogeneous system. This thermodynamically driven phenomenon was firstly described by Wilhem Ostwald in 1896. The theoretical description of Ostwald ripening derives from Lifshitz, Slyozov And Wagner theory also known as LSW theory (Krapivsky et al., 2010).

It is possible for particles to form islands on the substrate but there would be some local differences in energy. As big islands are stable in size, their energy is remarkably lower compare to unstable small islands. In this case, the system wants to remove the unstable ones and to remain only with stable ones. Eventually, only big islands are remained. This can be easily understood, if you keep in mind that the particle will minimize its surface, leading to a biggest sphere for a given volume as asymptotic behaviour. The density of particle per unit of surface will consequently

being reduced. This growing process can be accelerated by temperature or accented if you give more time for growing.

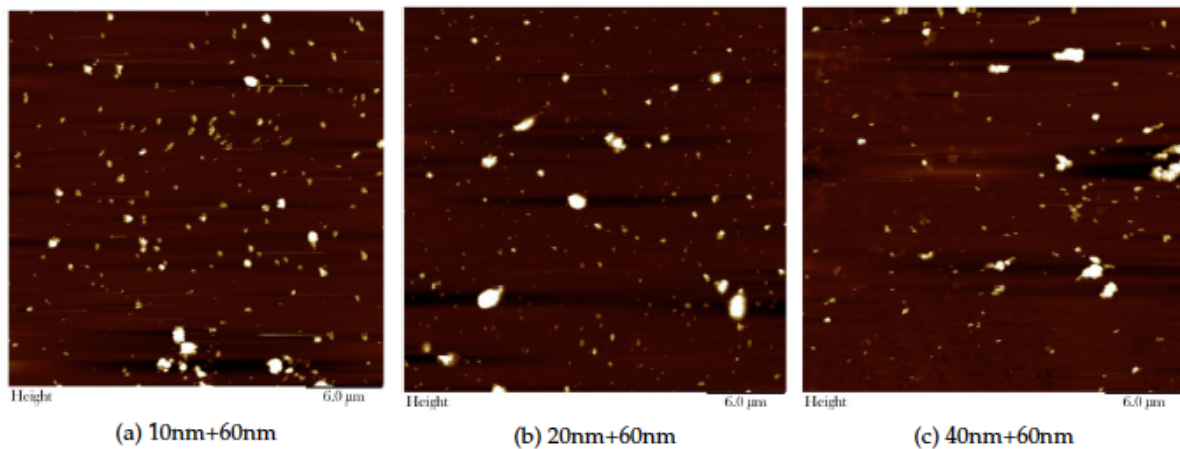


**Figure 69. AFM images of Ag-NPs after 7 days of deposition.**

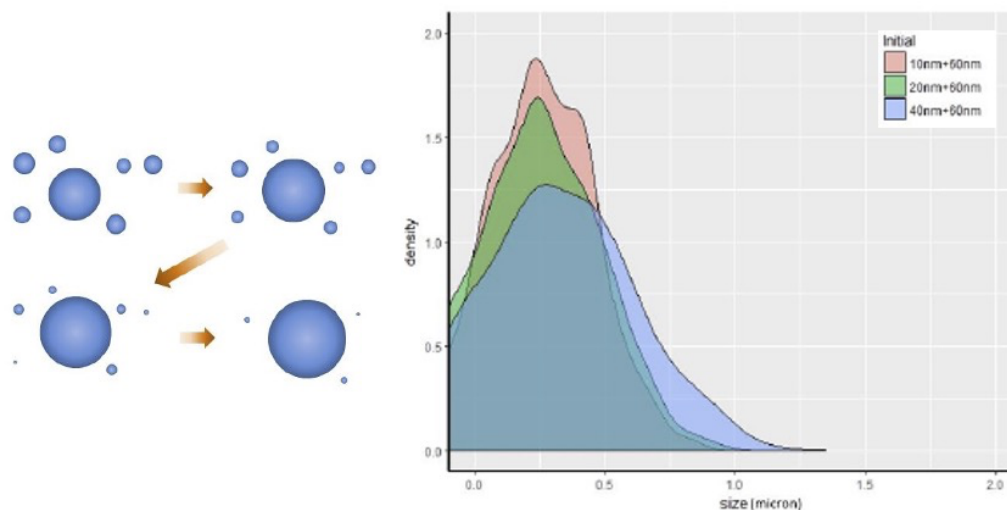


**Figure 70. Mechanism of Ostwald Ripening. Size Distribution depending on the initial size distribution-7 days after.**

To highlight this phenomenon, we had deposited a mix of 60 nm particle with smaller ones (10, 20 or 40 nm) on HOPG and observe the resulting size after they undergo Ostwald ripening process. Figure above shows AFM image and size distribution profile of the discussed mix of nanoparticles after 7 days on the substrate.

We can clearly see a drastic increasing of the size distribution due to coarsening. The fact that the silver aggregates on the bacteria membranes have bigger size, and that after 1 hour of exposure, suggested that the diffusion of silver ions and

nanoparticles is highly enhanced by membranes components. Higher resolution and real time observation of diffusion on the membranes will be needed to go further.

### 3- *Bacillus subtilis* behavior under silver stress by SEM

Cells of *B. subtilis* were seen by SEM as they were aggregate in groups for those that were treated with silver; while the control sample cells were evenly distributed on the surface of the substrate (Fig. 71). It is not clear why cells appeared in such condition. The aggregation might relate to the interactions between cells and  $\text{Ag}^+$  that accumulate on the surface of the cells; in addition to the interaction with the substrate used. This phenomenon was seen with *E. coli* cells exposed to carbon dots stress (Dong et al., 2017). Still, more study needs to be done to reveal this occurrence.

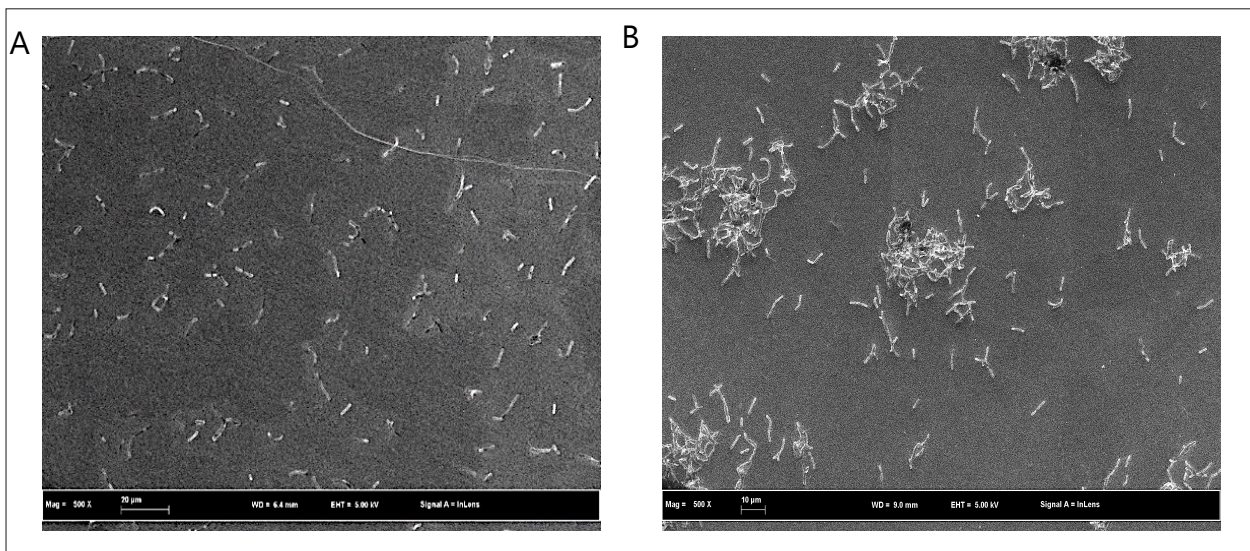


**Figure 71. SEM images of *B. subtilis* cells exposed or not to silver.**

Control (A), incubation with 1mM of  $\text{AgNO}_3$  for 1h. (B).

Cells of *B. subtilis* were seen by SEM as they were aggregate in groups for those that were treated with silver; while the control sample cells were evenly distributed on the surface of the substrate. Differences between gram-positive and gram-negative bacteria, on their appearance under SEM beam and their abilities to group was discussed.

#### **4- Effect of medium on the impact of metal on bacterial cells**

Through this study, we have cross through result that show an effect of culture media used for bacterial growth on the metals addition. This could be due the specific role of different chemical agent present in the media, or the influence of bacteria apparatus. This finding is still under investigation. It was found that silver performs differently in different mediums. It has more toxic impact on cells in malate medium more than when it is in LB medium due, as we proposed, to the presence of phosphate in malate medium. The reaction between  $\text{AgNO}_3$  and  $\text{K}_2\text{HPO}_4$  lead to the precipitation of  $\text{Ag}_3\text{PO}_4$  which was appeared as whitish dotes accumulate on the surface of cells of *R. gelatinosus*. These dotes were detected by the SEM due to the backscattered light of identified Ag atoms on the sample surface. It was suggested that the accumulation of  $\text{Ag}_3\text{PO}_4$  particles are the reason of the enhancement of the toxicity or speeding the toxic effect because of their direct attachment to the membrane and then releasing the  $\text{Ag}^+$ . Thus, we have performed experiments to compare the impact of silver ions, when add them to both malate and LB mediums; on both: the photosynthesis and respiration complexes of grown cell of *R. gelatinosus*.

The spectra in (Fig. 15 in the article II) showed a decrease amount in the photosynthetic complex. Particularly in light harvesting LH2 (B800 Bch) with extended time of incubation with  $\text{Ag}^+$  up to 24 hrs. While it took 10 hrs. for LH2 (B800 Bch) to be decreased in malate medium, it took 24 hrs. in LB medium.

We wanted to check the same impact on respiratory complexes under the same stress. We used cells of *R. gelatinosus* grown aerobically overnight, then shocked with increased concentrations of silver for one hour. We used the BN-PAGE to detect the activity on two of the respiratory chain complexes: *cbb<sub>3</sub>* and SDH. The preliminary result in (Fig. 72) showed that there is a decrease of these proteins activity with the increase concertation of  $\text{Ag}^+$  added into malate medium. While stable and/ or unaffected production in LB medium. Indeed, silver concentration over 50  $\mu\text{M}$  will inactivate the proteins activities.

-RESULTS-

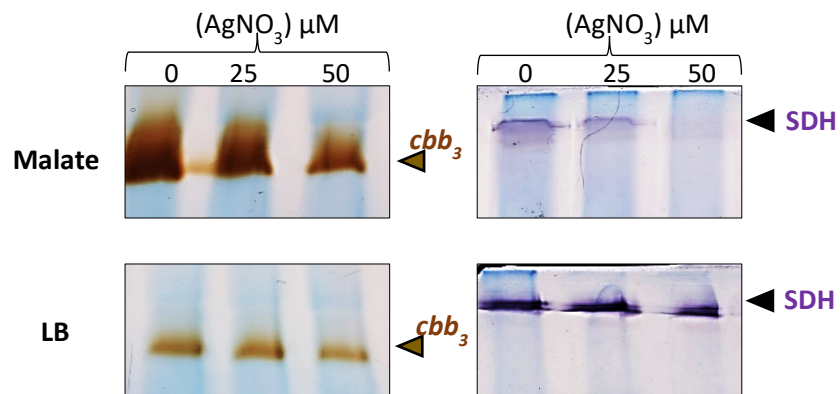


**Figure 72. AgNO<sub>3</sub> effect on respiratory complexes in vivo.**

The WT cells were grown under micro-aerobic respiratory condition and shocked for 1h. with increasing concentration of AgNO<sub>3</sub> grown in Malate and LB mediums. DDM-solubilized membrane proteins were separated on (7.5-15%) gradient BN-PAGE. On the left, *cbb<sub>3</sub>* cytochrome *c* oxidase *in-gel* activity assay. On the right, Succinate dehydrogenase (SDH) *in-gel* activity assay.

## Discussion:

---

Silver has been largely studied concerning its antimicrobial properties since even at low concentration silver ions and/or nanoparticles can be very toxic. Despite numerous studies on its impact on bacteria in general and in *R. gelatinosus* in particular concerning: cells physiology, biochemistry, genetics..., a description of the mechanism of interaction is still incomplete.

In previous chapters, we have demonstrated its effect on membrane proteins on both systems: the photosynthesis and respiration (Tambosi et al., 2018). We presented here, at our knowledge first and direct visualisation of the effect of silver on the structure of membranes using AFM and SEM complementary imaging.

The results helped us to propose a mechanism with two aspect : an early step, where silver ions precipitate around and on the bacteria membranes following apparently different stochastic nucleation and growth mechanism and a later step where silver ions and/or small particles impact and penetrate cell's membrane inducing huge transformation of bacteria membranes morphology and mechanical properties leading to breaking and apoptosis.

Comparison with other bacteria *E. coli* and *B. subtilis* enable to clarify specific behaviour of *R. gelatinosus*. *B. subtilis* ability to resist to silver stress might be explained by understating its cell wall structure as Gram-positive bacteria, since it contains, for instance, a thicker membrane built of layers of peptidoglycan.

Our results show also the effect of culture media. Silver has more toxic impact on cells in malate medium more than in LB medium due, as we proposed, to the presence of phosphate in malate medium. The accumulation of probably  $Ag_3PO_4$  particles are the reason of the enhancement of the toxicity through their direct attachment to the membrane  $Ag^+$  ions releasing for instance.

We should also consider the effect of the bacteria in this precipitation process. Reduction of soluble Ag to colloidal or nanoparticles by various bacterial species have been reported (nano biosynthesis). We could even assume, that this play a role in a

defence strategy, as it enables both, ionic silver concentration reduction around the cells, and particle size increasing regarding efflux systems and intracellular silver binding.

Finally, these results open several other perspectives. We want to study the morphological changes using genetically modified bacteria, with no porins (porinless) which protect cells from inside overload of metals ions. This will have ions to accumulate and adhere on the surface of the cells, thus, should show different results and different characterization of metal toxicity mechanisms. Accordingly, cells will face less challenge for metal homeostasis since they have less overload ionic metals inter inside. Similar finding was seen in *E. coli* cells normal and genetically modified porinless cells, where both were exposed to concentrations of Cu/Ag ions (Rtimi et al., 2017). It is also, expected that this may lead to increase the accumulation and the attachment of silver ions on the cell surface. This attachment performs due to the different charges between the two: bacterial cells and Ag ions. For next, it is suggested to use the *ompW* mutant strain of *R. gelatinosus*. It is known for its role to decrease the overdose of Cu<sup>+</sup> to enter inside cells. Would it be the case with Ag<sup>+</sup>?

For more general perspectives, in order to understand the mechanism of silver toxicity on prokaryotic and eukaryotic, more experiments should address the issue of interaction between membrane complexes involved in cellular bioenergetics and silver in its ions and NPs forms.

In addition, and for immediately following steps, we want to do the same study using silver nanoparticles. It is known that the silver nanoparticles are shape and size dependent. Thus, their toxicity and their impact are unlike silver ions. Furthermore, to open an investigation from chemical point of view regarding the role of medium and its involvement in increase or decrease the metal toxicity.

-RESULTS-

## 4. Silver Nanoparticle Synthesis and Their Effect on Photosynthetic Bacteria

---

### Introduction

---

A lot of improvement had been done regarding the assess of silver on bacteria by the discovery of new and promising material and/or development of new innovative process (Sánchez-López et al., 2020) like for example nanoparticles (NPs) and nanostructured (NSs) materials. The use of silver nanoparticles became a regular field of study since it was proposed as a promising solution against the antibiotic's resistance bacteria (Ferdous & Nemmar, 2020; Keiper, 2003; Lara et al., 2011; Rai et al., 2012). From biological point of view, many studies have been done to understand the metal (ions and NPs) homeostasis and toxicity on various models of bacteria. The mechanism of involved proteins to tolerate silver have yet to be identified and described in detail (Dias et al., 2015; Sondi & Salopek-Sondi, 2004). Still, little has been done on photosynthetic bacteria in general and on *R. gelatinosus* in particular. Most of the studies target applications toward antimicrobial materials or devices. However, many questions remain before the material capabilities translate into device performance, industrial production and commercialization. The main challenge is the optimization of this production, the adaptation to biologically compatible medium and their transposition to industrial use.

Our initial project main goal is still, to develop a highly efficient microbicide material with low toxicity toward human cells by using an original process from bottom-up assembly of NPs materials. Moreover, to have NPs and NSs prepared in the lab with fully control of the characterization of the desired properties.

For this purpose, a multi-disciplinary approach gathering microbiologist and physico-chemists was intended. A multi-scale study will enable us to discriminate between the effect of silver ions (as described previously) and the specific role of silver

## -RESULTS-

nanoparticles (NPs) on environmental bacteria, in the frame of this project, and to extend the study to pathogenic bacteria as a mid-term assignment. In addition, we can also examine their effect on human cell lines as well.

In here, we are presenting preliminary results of the effect of silver nanoparticle, chemically synthesized in the laboratory, on the environmental, photosynthetic and gram-negative bacteria: *Rubrivivax (R.) gelatinosus*. For which there is still a lack of information considering their interaction with Ag-NPs. To our knowledge, this present first evidences of silver NPs physiological impact on *R. gelatinosus* bacterium; in complementary to previous data of silver ions target proteins in the membrane complexes (Tambosi et al., 2018); and their impact on the morphological cell structure (Tambosi et al., 2020 submitted).

Spherical shaped silver nanoparticles (Ag-NPs) was synthesized by a chemical reduction process known as Seed Mediated Growth Method (Agnihotri et al., 2013). In this process, silver nitrate is used as precursor, sodium borohydride as reducing agent and sodium citrate as stabilizing agent. Larger size of Ag-NPs can then be obtained by seed mediated growth method. For Ag-NPs characterization, we used the UV-Visible spectroscopy and TEM imaging. The concentration of Ag-NPs was determined using the Inductively coupled plasma (ICP).

For comparison with silver ions impact, experiments were carried using same method as previously: the synthesized Ag-NPs, at different concentrations were added to the bacteria culture. Bacterial cultures of *R. gelatinosus* were prepared on solid and liquid Malate medium for overnight growth, and under photosynthesis and aerobic conditions.

## Results

### 1- Silver nanoparticles synthesis

Silver nanoparticles with different sizes were synthesized by a seed mediated growth methodology (Wan et al., 2013). This process is based on a two steps reaction, consisting on the synthesis of silver seeds and then, their subsequent growth in solutions containing metal precursors. This synthesis method is based on heterogenous nucleation in solution where the seeds become a nucleation sites for the growth of nanoparticles. We have synthesized silver seeds (AgSeed) using sodium borohydride as reducing agent and trisodium citrate as stabilizing agent. The purified AgSeed obtained have a spherical shape with a LSPR (Localised Surface Plasmon Response) band centered around 392 nm and measures  $12 \pm 2$  nm (Fig. 73).

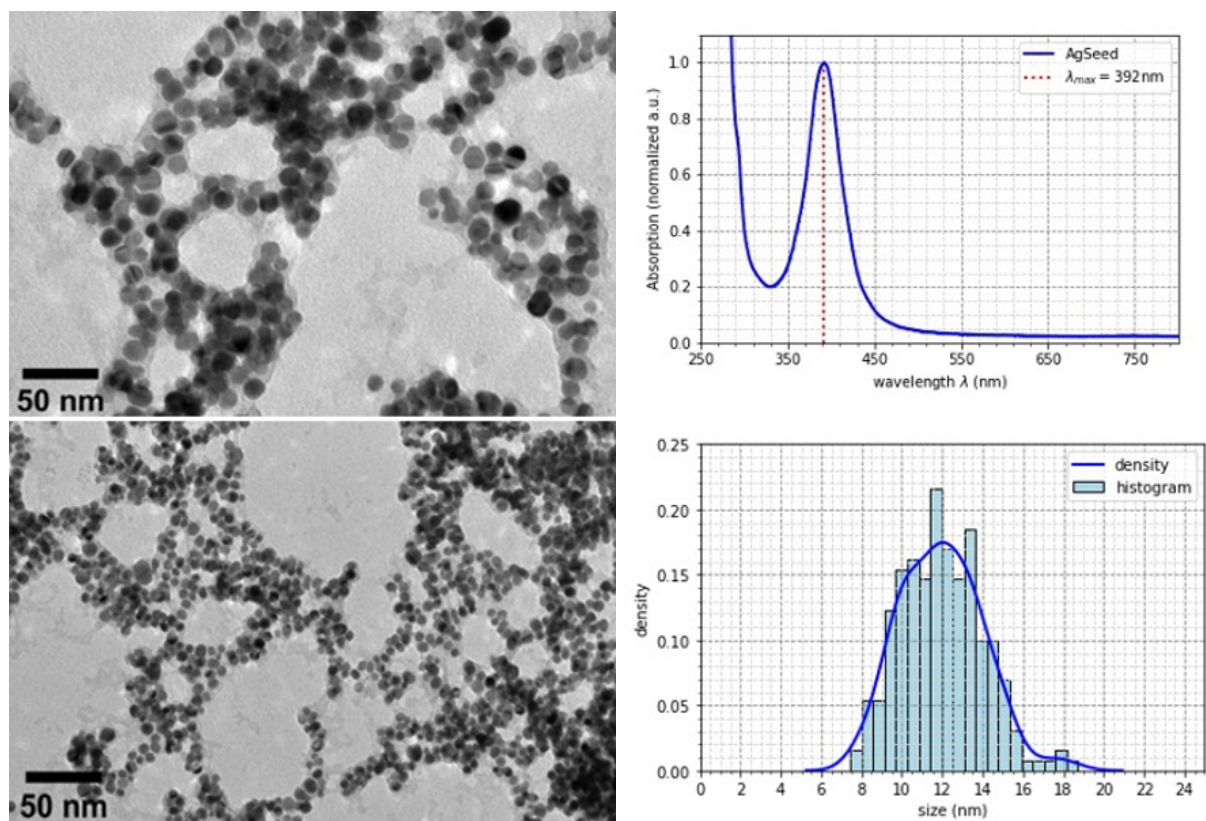


**Figure 73. TEM Images of seed silver nanoparticles AgSeed (left); and their characterization (right) using spectroscopy UV-Visble (up) and size distribution profiles and density given by images analysis (down).**

## -RESULTS-

To obtain bigger size, we can grow this first distribution (AgSeed) in solutions with silver precursor. The growth depends on different empirical parameters, but we were capable of a wide range of size distribution. With one step growth, silver nanoparticles size has increased from initial size  $12 \pm 2$  nm (size of reactional brut reaction, data not shown) to  $22 \pm 15$  nm. The obtained sample, labelled AgSMG1, have a LSPR band centred around 403 nm (characteristic yellowish color solution) (Fig. 74).

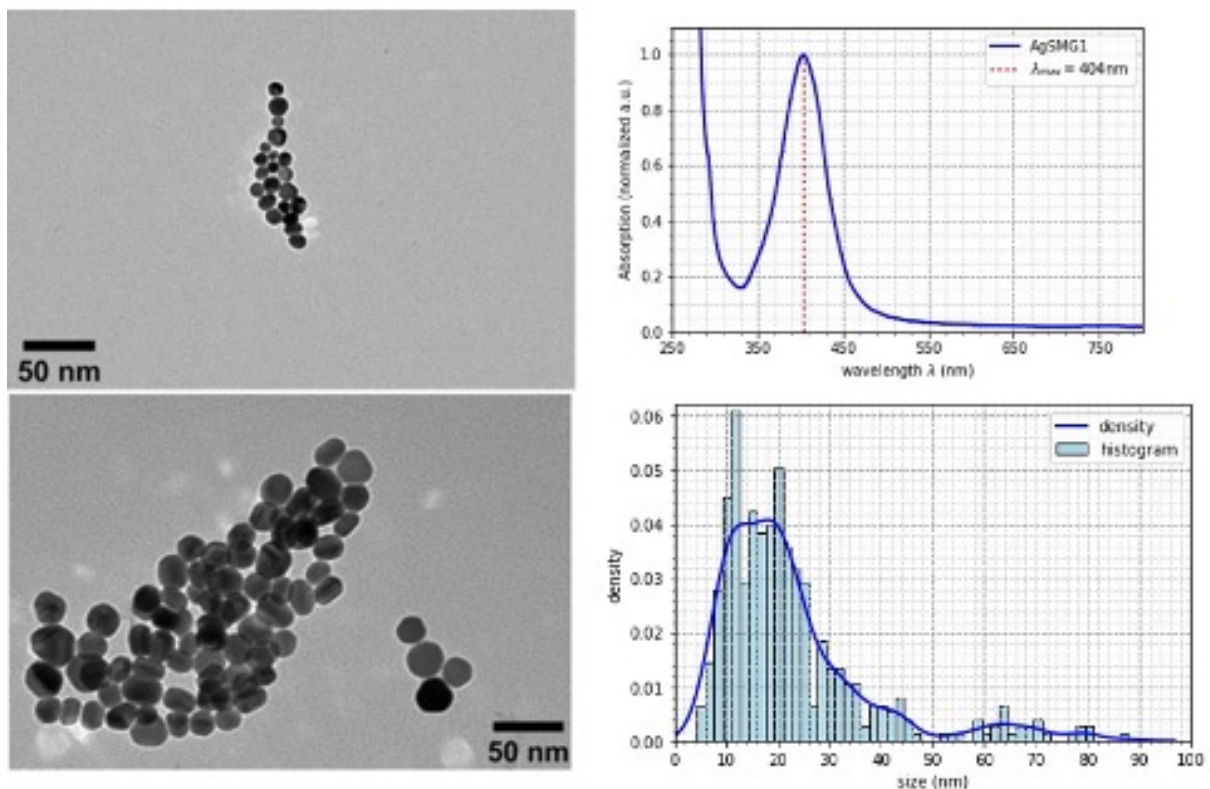


**Figure 74. TEM Images of grown silver nanoparticles AgSMG1 (left); and their characterization (right) using spectroscopy UV-Visible (up) and size distribution profiles and density given by images analysis (down).**

In general, there are many challenges when working with metal nanoparticles to control their stability (no size changes due to aggregation). This size control is crucial if we are concerned by their impact on biological applications. Ag-NPs were coated with sodium citrate (weakly bound capping agents) to avoid aggregation by creating a negatively charged layer around Ag-NPs, coulombic repulsion prevent from agglomeration. Ag-NPs stability checking while processing experiment, can be based

on stable solution color, TEM images and size distribution profiles, and optical spectra measurements.

## 2- Sodium citrate effect on the growth of bacterial cells of *R. gelatinosus*.

Since citrate is used as coating for NPs stability, it was very important to ensure that it had no impact on bacteria or culture medium. Accordingly, we have tested the impact of increased concentration of sodium citrate (SC) [ $\text{HOC}(\text{COONa})(\text{CH}_2\text{COONa})_2 \cdot 2\text{H}_2\text{O}$ ] (*Sodium Citrate / Sigma-Aldrich*). To detect its effect on the growth of cells of *R. gelatinosus* bacteria, we prepared increased concentrations of SC (1 and 2 mM) in  $\text{H}_2\text{O}$  and added them into bacterial cells cultures. They were let to grow under aerobic condition; in comparison to control culture of *wt* cells alone.

The result in (Fig. 75) showed that SC (even up to 2 mM) had no effect on overnight cells growth.

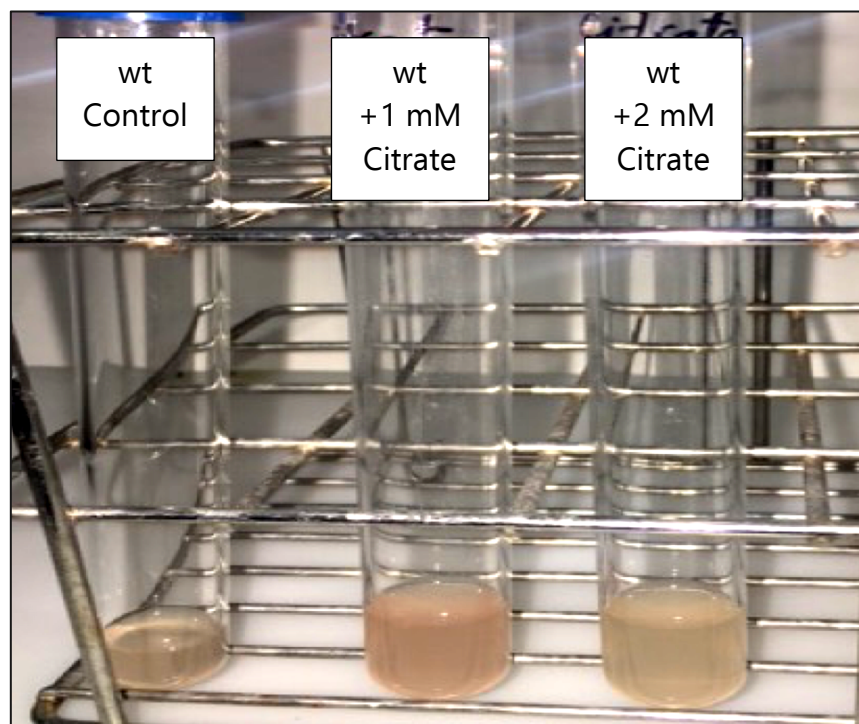


**Figure 75. The *R. gelatinosus* growth under SC effect.**

Wild-type cells of *R. gelatinosus* were grown in the presence of 1 and 2 mM of sodium citrate. Cultures were grown overnight under aerobic condition at 30°C.

### 3- Growth inhibition by silver

Dose-dependent growth kinetics of bacterial cells was used to assess the toxicity of silver nanoparticles (coated with sodium citrate) in comparison to silver ions. Previously, we had shown that sodium citrate alone has no impact on the growth of *R. gelatinosus* cells. Wild types cells of *R. gelatinosus* were treated with increased concentrations of both forms of silver (ions and NPs). Bacterial cultures were prepared on solid malate medium for overnight aerobic growth.

For Ag-NPs, we have tested the effect of two sizes of nanoparticles:  $12 \pm 2$  (AgSeed purified) and  $22 \pm 15$  nm (AgSMG1). Moreover, we had in consideration to monitor the silver mass alone and its impact on bacteria without the effect of other chemical components. Thus, we made sure that silver doses used in (AgNO<sub>3</sub>, AgSeed and AgSMG1) were calculated to indicate the equal silver mass exposure.

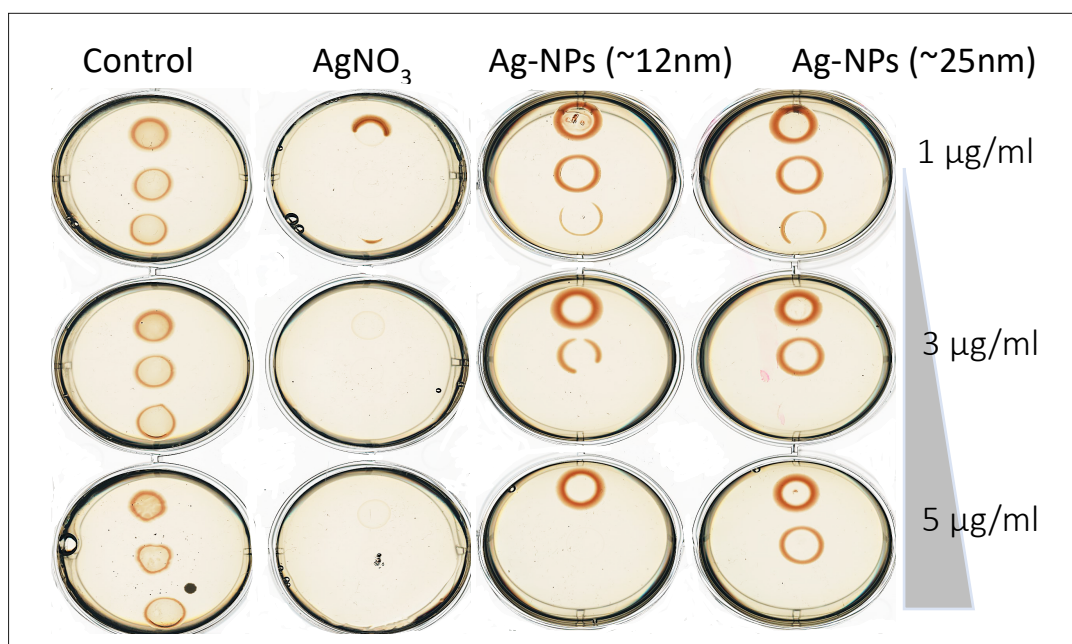


**Figure 76. Growth phenotype of *R. gelatinosus* cells under silver stress.**

Wild-type cells of *R. gelatinosus* were grown in the presence of indicated concentrations (1, 3 and 5 µg/ml) of both AgNO<sub>3</sub> and Ag-NPs on solid Malate media. Cells were spotted in 10 µl drops as undiluted, 10 and 100 times of dilutions; and they were grown aerobically for 24 hrs. at 30°C prior to photography.

## -RESULTS-

The result in (Fig. 76) shows that  $\text{Ag}^+$  are more toxic and 1  $\mu\text{g}/\text{ml}$  of  $\text{AgNO}_3$  is enough for growth inhibition. On one hand, 3  $\mu\text{g}/\text{ml}$  of Ag-NPs  $12 \pm 2$  nm (AgSeed) have an impact on the ability of cells to grow as normal as control; and 5  $\mu\text{g}/\text{ml}$  almost inhibited it. On the other hand, cells were resistant to same silver concentrations (3 and 5  $\mu\text{g}/\text{ml}$ ) of Ag-NPs in range of size  $22 \pm 15$  nm (AgSMG1). It appears that the probability of interaction with bacterial surface and the strength of the impact increase with surface-volume ratio i.e., with decreasing size. Furthermore, we can suppose that smaller NPs diffuse more easily through the cell's membrane (Acharya et al., 2018; Pal et al., 2007; Periasamy et al., 2012). Similar data was reported on *E. coli* by Agnihotri; testing the size-dependent antibacterial efficacy. It was reported that the 5 nm of Ag-NPs have the greatest and fastest bactericidal action comparing to bigger sizes 7 and 10 nm, respectively (Agnihotri et al., 2013).

Dose-dependencie and size-dependencie of Ag-NPs effect on the bacterial cell growth were also studied using Malate liquid medium. Bacterial cultures were prepared to grow under photosynthesis condition for 48 hrs. in the presences of indicated concentrations of silver mass of each:  $\text{AgNO}_3$ , AgSeed and AgSMG1. Despite the silver form and/or the particles size, silver was found highly toxic at doses of 1  $\mu\text{g}/\text{ml}$  and above (Fig. 77). There was no observation of cells growth at all; expect for the control sample of course.

The collective data can explain that the total inhibition bacterial growth observed here is due to most probable interaction between the metal ions and the cell membrane because of the liquid nature of the media. This hugely increase the ability to diffuse through the cell membrane and to interact within the inside cell's components. By comparison in solid media, the diffusion of NPs is more restricted.

-RESULTS-

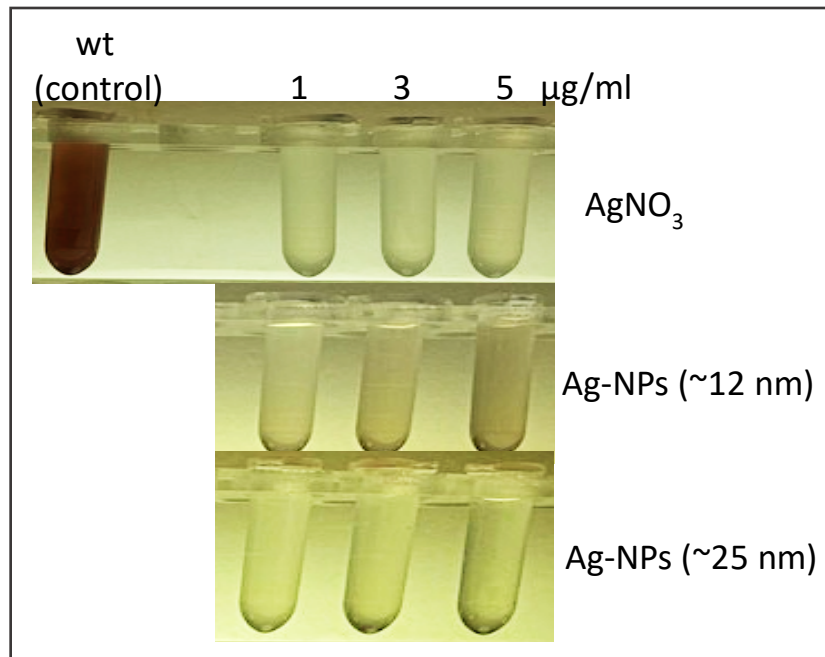


**Figure 77. *R. gelatinosus* growth under silver stress.**

Cells were grown in liquid malate medium under photosynthetic conditions in the presence of increased concentrations of silver.

Some experiments are still on going, since the research program was delayed due to both pandemic situation and LAC laboratory renovation. SEM and AFM imaging and specific NPs protein target identification as done for silver ions, has to be done to fully demonstrate the Ag-NPs specific impact on *R. gelatinosus* in comparison to Ag<sup>+</sup> effect. In addition, and as comparison, we will examine the impact of NPs on other models of bacteria, both in gram negative and gram positive. For Ag-NPs preparation, we want to test other type of coating, to study their impact as well. Silica coating for example, will be used in comparison to sodium citrate coating. We started also the synthesis of non-spherical particles. It was suggested that the triangle shape for silver NPs can be more toxic than the spherical one. This is due to the surface tension and triangular tips effects increasing the efficiency of Ag ions release. The presence of (111) plans (link to higher compacity and density) seems to have also a bigger impact on bacteria (Djafari et al., 2019).

-RESULTS-

# GENERAL DISCUSSION & PERSPECTIVES

---

The past decades have witnessed exciting progress in our understanding of the elements required for the growth and survival of living cells (Crichton, 2020). Valuable data were also collected to understand the harmful effects these nutrients can cause to all types of living cells. Other non-essential elements found in our environment or generated by numerous human activities (chemistry, industry...) provide benefits to humans and still have promising applications. Among these elements, some metal ions are essential to life and other non-essential metals have been used by humans and have largely contributed to the evolution of our civilization.

Over a period of thousands of years, humans learned to extract and shape metals into tools and weapons. Copper (Bronze Age) and iron (Iron Age) were the first to be used by humans; later other metals such as silver and gold were used in ornaments and jewelry making. Metals still continue to shape our lives. Indeed, nowadays other precious and rare metals such as lithium, gallium, zirconium, germanium, etc, are the main building blocks of many electronic and nano-technologies.

Metals were also used for over the years and are still used for their antimicrobial properties: in agriculture, animal feedings and healthcare facilities (Rensing et al., 2018). Because of their toxicity, metal homeostasis and metal impacts on living organisms are interesting and timely topics, in particular with the fast rate of the metal-industrial developments and metal related technologies. Silver for example, has started to gain interest owed to its evolving role in different research fields such as nanotechnologies,

bioengineering, medicine and nutrition. Thus, it is interesting and important to study its impact on the environment and living organisms. In this context, I started my project to study the effect of silver in comparison with other metals on the photosynthetic bacterium *R. gelatinosus*. The study led to interesting results and to a quite comprehensive view of the metal ions effects on bioenergetics complexes within the inner membrane in this bacterium. I have also initiated the study of the interaction of silver nanoparticles with the bacteria using microscopy. Some results, although preliminary, are very promising and suggested that ions and nanoparticles can interact and change the morphology of bacteria. I have also tried to identify genes that could be important for Ag<sup>+</sup> toxicity in the bacterium. However, the obtained results were not conclusive, and some data require further investigations to confirm the obtained results.

This brings me to the perspectives and experiments that we would suggest or do, to get a more complete view of the effect of silver in *R. gelatinosus*.

First, in our analysis of *copA*<sup>-</sup> mutant exposed to AgNO<sub>3</sub>, no phenotype on silver was observed. This could be related to the fact that *cop* operon is not induced by Ag<sup>+</sup> in *R. gelatinosus*. To unambiguously conclude on the role of *copA* in Ag<sup>+</sup> efflux in *R. gelatinosus*, we should first induce *copA* expression by growing cells (WT and *copA*<sup>-</sup> strain) in medium containing sublethal concentration (50 μM) of CuSO<sub>4</sub>, to make sure that the ATPase is expressed in the WT, and then shock those cells with AgNO<sub>3</sub>. If CopA is required to expel Ag<sup>+</sup>, the WT will tolerate AgNO<sub>3</sub> stress, while *copA*<sup>-</sup> strain will be sensitive to AgNO<sub>3</sub>. In contrast, if *copA*<sup>-</sup> strain tolerate AgNO<sub>3</sub> shock, this will indicate that CopA is not involved in silver tolerance. Biochemical studies can also answer this question, but it requires the purification of CopA in liposomes and the set-up of transport experiments protocol with radioisotopic ions in the laboratory as described in (González-Guerrero et al., 2010; Rensing et al., 2000).

On the other hand, since quantitative proteomics analyses are now affordable and can give a global description of changes in the proteome of the bacterium when

subjected to metal stress, I would compare the proteome of Ag<sup>+</sup> stressed and unstressed wild type cells to identify proteins that could be involved in the transport of Ag<sup>+</sup>. Among the up-regulated proteins, I would select efflux transporters and regulators that could be involved in translocation of Ag<sup>+</sup> outside the cell. Genetic inactivation of the genes that code for those proteins will validate our results. Similarly, from the down-regulated proteins, identified transporters may be involved in import and therefore, the inactivation of the encoding genes will be led to Ag<sup>+</sup> resistant cells. Altogether, proteomics combined with genetic analyses can provide answer to the transport, in and out, of silver in *R. gelatinosus*.

Secondly, I have showed that Ag<sup>+</sup> ions damage the bioenergetics membranes and specifically the exposed chlorophyll in the LH2. As stated in the introduction, the toxicity of nanoparticles also related to release of ions, but the nanoparticle itself because of its specific characteristics could be active and toxic. It will be thus, interesting to check the direct effect of AgNPs on these membrane complexes. Unfortunately, we will need concentrated nanoparticle solutions to achieve this experiment either *in vivo* or *in vitro*. Otherwise, to use low concentration of protein membranes and lower the amount of nanoparticles we need adapted devices and spectroscopy to assess the effect on very low concentrated membranes by UV-Vis absorbance. Since now we have identified accurate targets in the membrane of bacteria, this experiment with AgNPs will be very interesting and will show if intact AgNPs can affect those complexes and assess their effect in comparison with Ag<sup>+</sup> ions.

The effect of Ag<sup>+</sup> and Cu<sup>2+</sup> ions on LH2 is most likely related to the exposure of the B800 BCh (Fig. 78). For the electron transfer pathway within the bacterial photosystem (B800 → B850 → B875), light is first absorbed by the B800 BCh in LH2, and transferred to the B850, which then transfers this energy to the core complex of the photosynthetic complex (Saer & Blankenship, 2017). B800 Bch are therefore important to capture and transfer the light excitation to the reaction center.

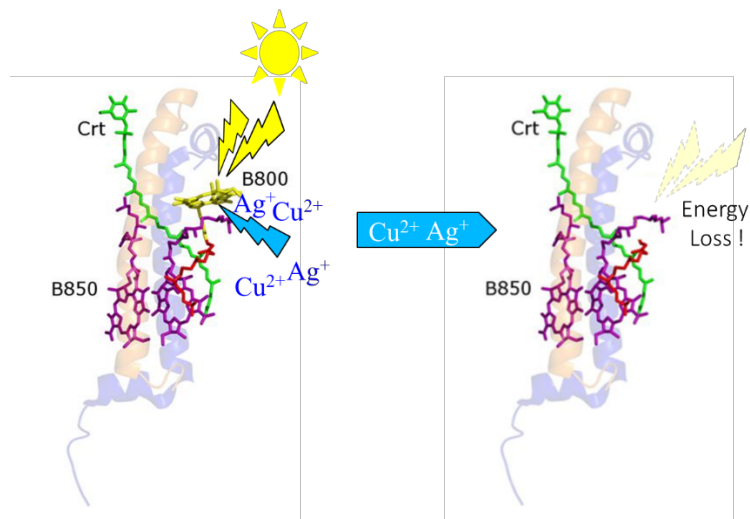


**Figure 78.  $\text{Ag}^+$  and  $\text{Cu}^{2+}$  target B800 BCh and could decrease light capture by LH2.**

Light energy is first trapped by B800 Bch, its damage by metals could therefore result in light trapping deficiency. Modified from (Saer & Blankenship, 2017).

We have found that the loss of the B800 Bch does not lead to the loss of the LH2 complex in the membrane. Nonetheless, given that the B800 Bch is the first trap to capture the light energy within the photosystem, an immediate consequence of its loss could be the loss of light energy trapping or at least the decrease in energy capture efficiency by LH2 complex. Accordingly, photosynthetic growth could be decreased especially under conditions, which require the LH2 complex such as low light condition. This could be assessed by measuring growth rate or doubling time of cells stressed with excess metal under high and low light conditions.

The specific effect of  $\text{Ag}^+$  and  $\text{Cu}^{2+}$  ions on B800 bacteriochlorophyll in the LH2 complex could arise from i- de-metalation (loss of the  $\text{Mg}^{2+}$  atom from the bacteriochlorophyll) or mis-metalation ( $\text{Ag}^+$  instead of  $\text{Mg}^{2+}$ ) of the bacteriochlorophyll and ii- from the loss of the coordination bond that link the bacteriochlorophyll *a* to the protein. In the LH2 structure from both *Rps. acidophila* and *Rs. molischianum*, the  $\alpha$ -His34 and  $\beta$ -His35 form ligands to the central  $\text{Mg}^{2+}$  atoms of the two B850 BCh which are completely buried inside the membrane (Fig. 79 ) (Koepke et al., 1996). The ligand of B800 BCh is a methionine in *Rps. acidophila* or an aspartate of the  $\alpha$  subunit in *Rs. molischianum*. In both structures, a water molecule makes contact with the B800 BCh

(Fig. 79 D), suggesting that this molecule is solvent exposed and that in fact, it could be accessible to ions. An interaction between  $\text{Ag}^+$  and the ligand residue (Met or Asp) would disrupt the link between B800 Bch and the  $\alpha$  polypeptide leading to the release of B800 Bch.

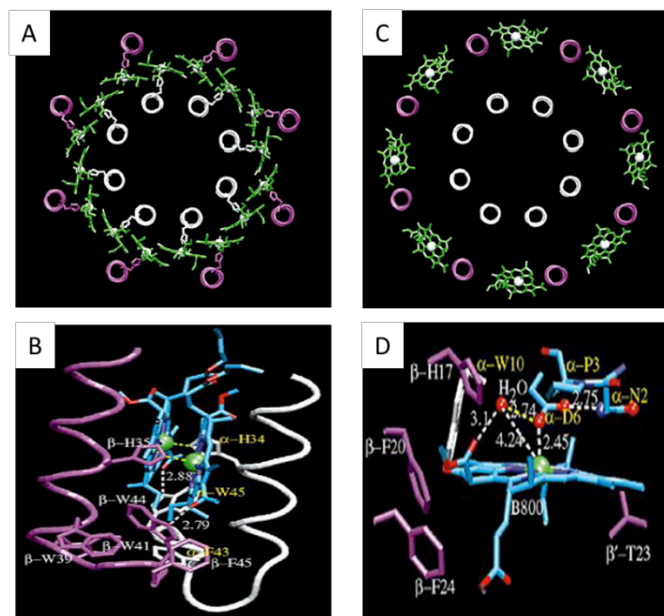


**Figure 79. Position of the Bch molecules and their ligands in the LH2 complex from *Rs. Molischianum*.**

A- The B850 Bch molecules are buried between the  $\alpha$  (in white) and  $\beta$  (magenta) polypeptides inside the membrane. B- The axial ligands of the two B850 molecules are histidines. C- The B800 Bch are exposed between the  $\beta$  polypeptides (outside). D- A close view to the B800 Bch pocket showing the coordination of the  $\text{Mg}^{2+}$  atom by Asp and the presence of water molecule in the structure. (Koepke et al., 1996).

The bacterial LH2, with its simple structure (two small polypeptides with attached pigments), turns out to be an appropriate and relevant model to assay the effect of  $\text{Ag}^+$  and other metal ions on bound chlorophylls. Nevertheless, it will be interesting to assess the effect of  $\text{Ag}^+$  and metals on other photosynthetic complexes, from other organisms, in which the chlorophylls are solvent exposed and therefore accessible to the ions. The structure of most photosynthetic complexes, from bacteria to plants are available, analyses of the pigment positions within the complexes is a prerequisite and will help selecting the complexes, with exposed pigments, to be

tested. If such experiments are feasible with plant photosynthetic complexes, it could shed more light on chlorosis (loss of chlorophyll) caused by the exposure of plants to metals.

Regarding the interaction characterisation, which was imaged by microscopes, we have provided evidences, which to our knowledge are first direct and visual data, regarding the effect of  $\text{Ag}^+$  and its impact on damaging the cells structure of *R. gelatinosus*. The result showed that during the 1<sup>st</sup> hour of exposure with silver, silver ions precipitate around and on the bacteria membranes. The size distribution profiles of the obtained precipitates and/or aggregates suggest different stochastic nucleation and growth mechanism. Diffusion coefficient but also nucleation kinetics seems different on bacteria membrane. A link with the composition of the membrane surface (lipids, ...) need still to be established. For cells exposed to silver for 24 hrs., we observed that silver ions and/or small particles impact and penetrate cell's membrane inducing huge transformation of bacteria membranes morphology and mechanical properties leading to breaking and apoptosis.

Several open questions remain concerning: 1- the localisation of silver fixation points, on the membrane surface first and after membrane penetration 2- the identification of a defence mechanism implying diffusion and nucleation of silver ions on the membranes to reduce for instance silver ions local concentration, 3- the optimal particles size for membranes penetration, probably correlated to pore dimension in the cells and optimal surface-volume ratio. A higher resolution imaging associated to chemical mapping will clarify most of this point (TEM imaging, EDX and/or EELS spectroscopy).

Through this study, we have also confronted the effect of culture media used for bacterial growth on the metal addition. This could be due to the specific role of different chemical agent present in the media, and/or to the influence of bacteria behavior. Preliminary results show that silver performs differently in different media used for cells growth. It has more toxic impact on cells in malate medium than in LB

medium, for example, due, as we proposed, to the presence of phosphate in malate medium. The reaction between  $\text{AgNO}_3$  and  $\text{K}_2\text{HPO}_4$ , for example, leads to the precipitation of  $\text{Ag}_3\text{PO}_4$  which appeared as nanoparticles accumulating on the surface membranes of *R. gelatinosus*. These precipitates were detected by the SEM due to the backscattered light of identified Ag atoms on the sample surface. It was suggested that the accumulation of  $\text{Ag}_3\text{PO}_4$  particles could be the reason of the enhancement of the toxicity or speeding the toxic effect because of their direct attachment to the membrane and their ability to release  $\text{Ag}^+$  ions. We have performed preliminaries experiments to compare the impact of both malate and LB broth media on silver effect on the photosynthesis complexes of grown cell of *R. gelatinosus*. It shows clearly, a silver toxicity affected by the type/nature of the medium used for growing cell cultures. This is true regarding the chemical synthesis of nanoparticles induced. We are also carrying a chemical investigation on silver stress on *R. gelatinosus* grown in different mediums. To have in consideration that medium such as malate contains traces of other metals such as:  $\text{Zn}^+$  and  $\text{Cu}^{2+}$ , and Malic acid as main ingredient for its formula preparation. Furthermore, malate molecules contain carboxylate groups, as the citrate, which can act as stabilizing agent to stabilize smaller particles and prevent their possible aggregation. Thus, the reaction of silver ions ( $\text{AgNO}_3$ ) can go in different directions, accordingly, more data are needed to clarify the phenomena (particles formation) observed and then propose a novel toxic mechanism of silver toxicity on *R. gelatinosus*.

From biological point of view, the formation of particles after silver addition to the bacterial culture could also be related to the interaction with specific produced proteins or enzymes by the bacteria itself. It could be a defence strategy where bacterial cells react with silver beforehand in the environment to prevent its entering inside the cells. Various studies have reported that some bacteria such as *Pseudomonas aeruginosa* have the ability to locate soluble silver and reduce it to colloidal or nanoparticles (biosynthesis nanoparticle method) (Kalimuthu et al., 2008; Klaus et al.,

1999; Kumar & Mamidyala, 2011; Muller & Merrett, 2014; Nanda & Saravanan, 2009; Parikh et al., 2008; Thakkar et al., 2010). However, the reduction mechanism is still unidentified. It was suggested that this could be the case for *R. gelatinosus* as well; and more investigation should also be carried to identify the genes involved in silver reduction mechanism.

Finally, these results open several other perspectives. We want to study the morphological changes using genetically modified bacteria, with no porins (porinless) which protect cells from inside overload of metals ions. The cells exposed, accordingly, will get metal ions accumulated and adhins on their surface. Thus, should show different results and different characterization of metal toxicity mechanisms. For more general perspectives, in order to understand the mechanism of silver toxicity on prokaryotic and eukaryotic, more experiments should address the issue of interaction between membrane complexes involved in cellular bioenergetics and silver in its ions and NPs forms.

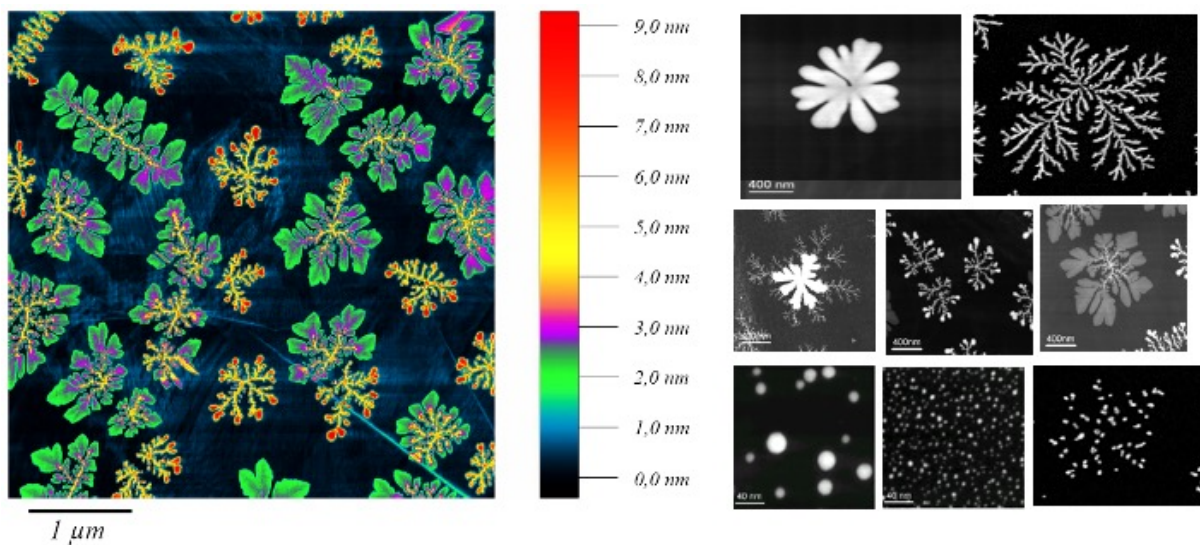


**Figure 80. Different morphologies obtained through self-organization and driven organization of metal or semi-metal preformed nanoparticles deposited on substrate.**

(LAC – Nano<sup>3</sup> group)

The interaction with nanoparticles and nanostructures deposited in substrate can also be a broad field of investigation. Through self-organisation and induced organisation, we are able to build a wide range of morphologies, densities, and nature of nanostructures that can exhibit a multiscale effect on isolated bacteria or bacterial biofilm adhesion and growth.



# APPENDIX

---

## Related Research

---

## Article IV: Cross-Tolerance and Targets of Metals in Bacteria

---

### Summary and main results in Article IV:

---

Heavy metals have a great impact on living cells and the environment around us. Numerous studies have tested and found specific targets of individual metals. However, environments are contaminated with multiple and mixture of metals. Interestingly, cells can respond differently to individual *versus* mixture of metals to meet homeostasis.

In our laboratory, previous studies have studied the effect of copper and cadmium on the photosynthetic bacterium *R. gelatinosus*. The CadA efflux pump, and CopA/CopI detoxification systems are the identified system to tolerate Cd<sup>+</sup> and Cu<sup>+</sup>, respectively. In the frame of this study, it was found that cadmium induced the CadA ATPase and the copper tolerance protein CopI in *R. gelatinosus*. This suggested that copper may help cadmium-exposed cells to tolerate cadmium. In this paper, my contribution was the analyses of  $\Delta cadA$  mutant phenotype under cadmium and zinc excess. Moreover, in this study, it is also shown that cadmium targets the heme and chlorophyll biosynthesis pathway.

In bacteria, the P<sub>1B</sub>-type ATPase CadA (ZntA) protein is known for its role to provide resistance to Cd<sup>2+</sup> and Zn<sup>2+</sup>. The gene encoding CadA was inactivated in *R. gelatinosus* bacterium. As expected, the mutant was sensitive to cadmium and zinc. Exposure of the mutant to excess cadmium resulted in the production of coproporphyrin III in the medium, demonstrating that cadmium affected tetrapyrrole biosynthesis pathway at the level of the coproporphyrin III oxidase HemN as previously shown with copper stress (Azzouzi et al., 2013). It is therefore suggested that cadmium affected the 4Fe-4S cluster of HemN, as demonstrated previously for other enzymes in *E. coli* (Xu & Imlay, 2012). The consequence of tetrapyrrole biosynthesis inhibition is

-APPENDIX –  
-RELATED RESEARCH-

the decrease of heme or chlorophyll containing complexes, namely, the cytochrome *c* oxidase and the light harvesting-reaction center photosynthetic complexes.

Unexpectedly, Western blot analyses showed that the addition of  $\text{Cd}^{2+}$  induced the production of CopI and CopA required for  $\text{Cu}^+$  tolerance. Steunou AS., found that CopI is also involved in cadmium tolerance, although the mechanism is not yet known, CopI could sequester  $\text{Cd}^{2+}$  for example. Most importantly, she showed that copper improved the tolerance towards Cd in *R. gelatinous*  $\Delta\text{cadA}$  mutant, demonstrating that metal mixtures in the environment could also be favorable for some microorganisms. In this context, it is known for example, that excess iron can provide protection against excess metals including copper, cadmium, cobalt or zinc in many organisms including bacteria and eucaryotes. The copper/ cadmium cross-talk or cross-tolerance described in this work was also reported in other bacteria as *P. aeruginosa*, *E. coli* or *B. subtilis*. as discussed in our paper.

**Article IV: Cadmium and Copper Cross-tolerance. Cu<sup>+</sup> alleviates Cd<sup>2+</sup> toxicity, and both cations target heme and chlorophyll biosynthesis pathway in *Rubrivivax gelatinosus***

---

\*Published. *Frontiers in Microbiology* 2020

-APPENDIX –  
-RELATED RESEARCH-



# Cadmium and Copper Cross-Tolerance. Cu<sup>+</sup> Alleviates Cd<sup>2+</sup> Toxicity, and Both Cations Target Heme and Chlorophyll Biosynthesis Pathway in *Rubrivivax gelatinosus*

Anne Soisig Steunou, Anne Durand, Marie-Line Bourbon, Marion Babot, Reem Tambosi, Sylviane Liotenberg and Soufian Ouchane\*

Université Paris-Saclay, CEA, CNRS, Institute for Integrative Biology of the Cell (I2BC), Gif-sur-Yvette, France

## OPEN ACCESS

### Edited by:

Davide Zannoni,  
University of Bologna, Italy

### Reviewed by:

Daniel Raimunda,  
Medical Research Institute Mercedes  
and Martín Ferreyra (INIMEC),  
Argentina

Manuel González-Guerrero,  
Polytechnic University of Madrid,  
Spain

### \*Correspondence:

Soufian Ouchane  
soufian.ouchane@i2bc.paris-saclay.fr

### Specialty section:

This article was submitted to  
Microbial Physiology and Metabolism,  
a section of the journal  
Frontiers in Microbiology

Received: 28 January 2020

Accepted: 16 April 2020

Published: 03 June 2020

### Citation:

Steunou AS, Durand A,  
Bourbon M-L, Babot M, Tambosi R,  
Liotenberg S and Ouchane S (2020)  
Cadmium and Copper  
Cross-Tolerance. Cu<sup>+</sup> Alleviates  
Cd<sup>2+</sup> Toxicity, and Both Cations  
Target Heme and Chlorophyll  
Biosynthesis Pathway in *Rubrivivax  
gelatinosus*. *Front. Microbiol.* 11:893.  
doi: 10.3389/fmicb.2020.00893

Cadmium, although not redox active is highly toxic. Yet, the underlying mechanisms driving toxicity are still to be characterized. In this study, we took advantage of the purple bacterium *Rubrivivax gelatinosus* strain with defective Cd<sup>2+</sup>-efflux system to identify targets of this metal. Exposure of the  $\Delta cadA$  strain to Cd<sup>2+</sup> causes a decrease in the photosystem amount and in the activity of respiratory complexes. As in case of Cu<sup>+</sup> toxicity, the data indicated that Cd<sup>2+</sup> targets the porphyrin biosynthesis pathway at the level of HemN, a S-adenosylmethionine and CxxxCxxC coordinated [4Fe-4S] containing enzyme. Cd<sup>2+</sup> exposure therefore results in a deficiency in heme and chlorophyll dependent proteins and metabolic pathways. Given the importance of porphyrin biosynthesis, HemN represents a key metal target to account for toxicity. In the environment, microorganisms are exposed to mixture of metals. Nevertheless, the biological effects of such mixtures, and the toxicity mechanisms remain poorly addressed. To highlight a potential cross-talk between Cd<sup>2+</sup> and Cu<sup>+</sup> -efflux systems, we show (i) that Cd<sup>2+</sup> induces the expression of the Cd<sup>2+</sup>-efflux pump *CadA* and the Cu<sup>+</sup> detoxification system *CopA* and *CopI*; and (ii) that Cu<sup>+</sup> ions improve tolerance towards Cd<sup>2+</sup>, demonstrating thus that metal mixtures could also represent a selective advantage in the environment.

**Keywords:** *CadA/ZntA*, cadmium/copper, metal homeostasis, metal toxicity, cross-talk, [4Fe-4S], porphyrin biosynthesis

## INTRODUCTION

Metal accumulation, through environmental contamination by anthropogenic release, results in toxicity leading to impaired growth of microorganisms (Nunes et al., 2016). Indeed, excess metal can affect and disrupt different cellular metabolic pathways. Because of their thiophilicity, metals

**Abbreviations:** BN-PAGE, blue native polyacrylamide gel electrophoresis; DAB, 3,3'-diaminobenzidine tetrahydrochloride; DDM, n-dodecyl- $\beta$ -D-maltopyranoside; HRP, horseradish peroxidase; LH-RC, light harvesting-reaction center; PVDF, polyvinylidene difluoride.

can compete or displace each other in the binding sites of metalloproteins. For instance, copper ( $\text{Cu}^+$ ), zinc ( $\text{Zn}^{2+}$ ) or cadmium ( $\text{Cd}^{2+}$ ) represent a standing threat for Fe-S proteins in bacteria. They can either directly damage exposed [4Fe-4S] clusters (Macomber and Imlay, 2009) or inhibit components of the iron-sulfur (Fe-S) biogenesis machinery (Tan et al., 2017; Roy et al., 2018; Li et al., 2019). In *Escherichia coli*,  $\text{Cu}^+$ ,  $\text{Zn}^{2+}$  or  $\text{Cd}^{2+}$  exert their toxic effects by disrupting the solvent exposed [4Fe-4S] clusters of dehydratases (Macomber et al., 2007; Macomber and Imlay, 2009; Xu and Imlay, 2012). These cations can also compete and prevent iron or iron-sulfur cluster binding in IscA, IscU or ferredoxin in the iron-sulfur cluster biogenesis system (Tan et al., 2017; Roy et al., 2018; Li et al., 2019).

In the human pathogen *Neisseria gonorrhoeae*, and the photosynthetic bacterium *Rubrivivax (R.) gelatinosus*, accumulation of  $\text{Cu}^+$  in the cytoplasm affect heme biosynthesis (Azzouzi et al., 2013; Djoko and McEwan, 2013). A hypothesis put forward is that  $\text{Cu}^+$  excess targets HemN, the anaerobic coproporphyrinogen III Oxidase. This enzyme has a conserved cysteine-rich motif, CxxxCxxC, which coordinates a solvent [4Fe-4S] cluster with an iron that anchors a S-adenosylmethionine (SAM) moiety (Layer et al., 2003). It was suggested that  $\text{Cu}^+$  targets this solvent exposed SAM-[4Fe-4S] cluster, thereby affecting the enzyme activity (Azzouzi et al., 2013; Djoko and McEwan, 2013).

Given the importance of Fe-S clusters and heme metabolism in bacteria but also in eukaryotes, the increase of metal concentration in the environment is therefore challenging to all living organisms. Homeostasis maintenance and detoxification of metal excess are therefore crucial to enable bacterial survival in contaminated environments or in macrophages for pathogenic bacteria (Arguello et al., 2007; von Rozycki and Nies, 2009; Capdevila et al., 2017; Chandrangsu et al., 2017).

The intracellular concentration of metals is tightly regulated at the uptake, storage and/or excretion level (Arguello et al., 2007; von Rozycki and Nies, 2009; Capdevila et al., 2017; Chandrangsu et al., 2017). For metals such as copper, cadmium or silver, efflux pumps are effective detoxification systems that allow bacteria to deal with excess metals in their immediate environment (Arguello et al., 2007; von Rozycki and Nies, 2009; Capdevila et al., 2017; Chandrangsu et al., 2017). Indeed, most free-living bacteria possess efflux system to remove metal excess. Members of  $P_{1B}$ -type ATPases family of heavy metal transporters are universally present in bacteria. They are part of the large superfamily of ATP-driven pumps involved in metal transport across bacterial inner membrane (Arguello et al., 2007). These transporters extrude excess or toxic metal ions such as  $\text{Cu}^+$ ,  $\text{Zn}^{2+}$ ,  $\text{Cd}^{2+}$ , or  $\text{Ag}^+$  from the cytoplasm to the periplasm in which metal is handled by other detoxifying proteins (Arguello et al., 2007).  $\text{Cu}^+$ ,  $\text{Zn}^{2+}$ , or  $\text{Cd}^{2+}$  efflux ATPase mutants accumulate these cations in their cytoplasm (Legatzki et al., 2003; Gonzalez-Guerrero et al., 2010; Djoko and McEwan, 2013; Lu et al., 2016) and very often display growth inhibition phenotype.

A strain of *R. gelatinosus* (TN414) efficient at removing  $\text{Cd}^{2+}$  and  $\text{Zn}^{2+}$  from cadmium and zinc contaminated soil has been isolated from paddy fields (Sakpirom et al., 2017). *R. gelatinosus* S1 can also grow in medium containing up to 3 mM of cadmium.

The mechanisms governing  $\text{Cd}^{2+}$  tolerance are however, not yet known. In this study, we first identified the  $\text{Cd}^{2+}$ -efflux system to ask which pathways  $\text{Cd}^{2+}$ , a divalent non-redox active cation, impacts in the absence of an efficient efflux system. Interestingly, it is also shown that  $\text{Cd}^{2+}$  induces  $\text{Cu}^+$  homeostasis system and that  $\text{Cu}^+$  alleviates  $\text{Cd}^{2+}$  toxicity in *R. gelatinosus*, a phenomenon that could represent a selective advantage for bacteria growing in multiple metal-polluted environment.

## MATERIALS AND METHODS

### Bacterial Strains and Growth

*Escherichia coli* was grown at 37°C in LB medium. *R. gelatinosus* (S1) was grown at 30°C, in the dark aerobically (high oxygenation: 250 ml flasks containing 20 ml medium) and microaerobically (low oxygenation: 50 ml flasks filled with 50 ml medium) or in light (photosynthetically in filled tubes with residual oxygen in the medium) in malate growth medium. Antibiotics were used at the following concentrations: kanamycin (Km), ampicillin and trimethoprim (Tp) at 50 µg/ml, tetracycline at 2 µg/ml. Bacterial strains and plasmids are listed in **Supplementary Table SI**. Growth inhibition curves were monitored at OD<sub>680nm</sub> with measurements taken every 15 min for 24 h using a Tecan Infinite M200 luminometer (Tecan, Mannerdorf, Switzerland) for aerobic condition. For photosynthesis conditions, strains were grown as described above and OD was measured after 24 h using the Tecan luminometer. Inhibition growth experiments were done in triplicates starting from a three diluted culture (OD<sub>680</sub> at 0.02).

### Gene Cloning and Plasmid Constructions for Allele Replacement

Standard methods were performed according to Sambrook et al. (1989) unless indicated otherwise. To inactivate *cadA*, a 1.8 kb fragment was amplified using the primers cadAF1 and cadAR1 (**Supplementary Table SII**) and cloned into the PCR cloning vector pGEM-T to give pGcadA. *cadA* gene was inactivated by deletion of 0.8 kb fragment and the insertion of the Tp cassette at the *NarI* sites within the *cadA* coding sequence. The resulting recombinant plasmid was designated pGcadA:Tp. Furthermore, a plasmid (pB106) containing the full *cadA* and *cadR* genes was also isolated from the DNA library. A 6.6 kb fragment containing *cadA* was subcloned from pB106 in pBBR1MCS-2 at the *KpnI*-*SacI* sites. The resulting plasmid was designated pBKCadA. *cadR* was PCR cloned using primers cadRF1 and cadRR1 in pGEMT plasmid. To inactivate *cadR*, the 1.2 kb Km cassette was inserted in the *StuI* site within *cadR* in the pGcadR plasmid. To generate HemN-H6 fusion, hemN was amplified from wild-type genomic DNA using primers hemN-*NdeI* and hemN-*XhoI* and cloned in the corresponding sites within pET-28b.

### Gene Transfer and Strain Selection

Transformation of *R. gelatinosus* cells was performed by electroporation (Ouchane et al., 1996). The plasmid pGcadA:Tp was used to transform the wild-type, *copA*<sup>-</sup>,  $\Delta$ *copI*, or

*copA-H<sub>6</sub>* strains. Transformants were selected on malate plates supplemented with appropriate antibiotics under aerobic conditions. Following transformant selection, template genomic DNA was prepared from the ampicillin sensitive transformants and confirmation of the antibiotic resistance marker's presence at the desired locus was performed by PCR. Finally, selected colonies were spotted on metal containing plates to confirm their metal sensitive phenotype. Plasmid *phemN-H<sub>6</sub>* was used to transform the wild-type strain to generate the HemN-H<sub>6</sub> strain. Clones were selected on kanamycin plates.

### Membrane and Soluble Protein Preparation

The membranes or solubles fractions were prepared by cell disruption with a French press in 0.1 M sodium phosphate buffer (pH 7.4) containing 1 mM phenylmethylsulfonyl fluoride, followed by differential centrifugation. Samples were subjected to a low speed centrifugation step (25,000 g, 30 min, 4°C) and supernatants were subjected to ultracentrifugation (200,000 g, 1h30, 4°C) to purify the soluble proteins and collect the membrane fraction in the pellets.

The membranes were then resuspended in the same buffer. Protein concentration was estimated using the bicinchoninic acid assay (Sigma) with bovine serum albumin as a standard. Periplasmic fractions were purified as previously described by Durand et al. (2015).

### Spectrophotometric Measurements

Absorption spectroscopy was performed with a Cary 500 spectrophotometer. For difference spectra (reduced minus oxidized), total pigments were extracted from cell pellets or membranes with acetone-methanol (7/2 [vol/vol]). For each sample, the spectrum was collected on oxidized sample upon addition of 50 μM K<sub>6</sub>Fe(CN)<sub>3</sub>. The sample was reduced by addition of dithionite (few crystals), and the spectrum was collected to generate the reduced minus oxidized spectrum.

### Blue-Native Gel Electrophoresis

To assay *cbb<sub>3</sub>* and succinate dehydrogenase activities, wild-type and *ΔcadA* strains were grown microaerobically. Membranes were prepared as previously described (Khalifaoui Hassani et al., 2010). Blue-native polyacrylamide gel (BN-PAGE) electrophoresis and in gel-Cox activity assays (DAB staining) were performed as described in (Khalifaoui Hassani et al., 2010) and succinate dehydrogenase activity was assayed using succinate and NBT (Nitroblue tetrazolium) as described for the succinate-NBT reductase assay in reference Wittig et al. (2007).

### Western Blot and Immunodetection

Equal amount of proteins or disrupted cells (OD<sub>680nm</sub> = 1) were separated by SDS-PAGE (15% polyacrylamide) and further transferred to a Hybond ECL PVDF membrane, (GE Healthcare). Coomassie blue of the SDS gels are shown in **Supplementary Material**. Membranes were then probed with the HisProbe-HRP (from Pierce) according to the manufacturer instruction and positive bands

were detected using a chemiluminescent HRP substrate according to the method of Haan and Behrmann (2007). Image capture was performed with a ChemiDoc camera system (Biorad).

## RESULTS

### The P-type ATPase CadA Is the Primary Cadmium Tolerance Element in *R. gelatinosus*

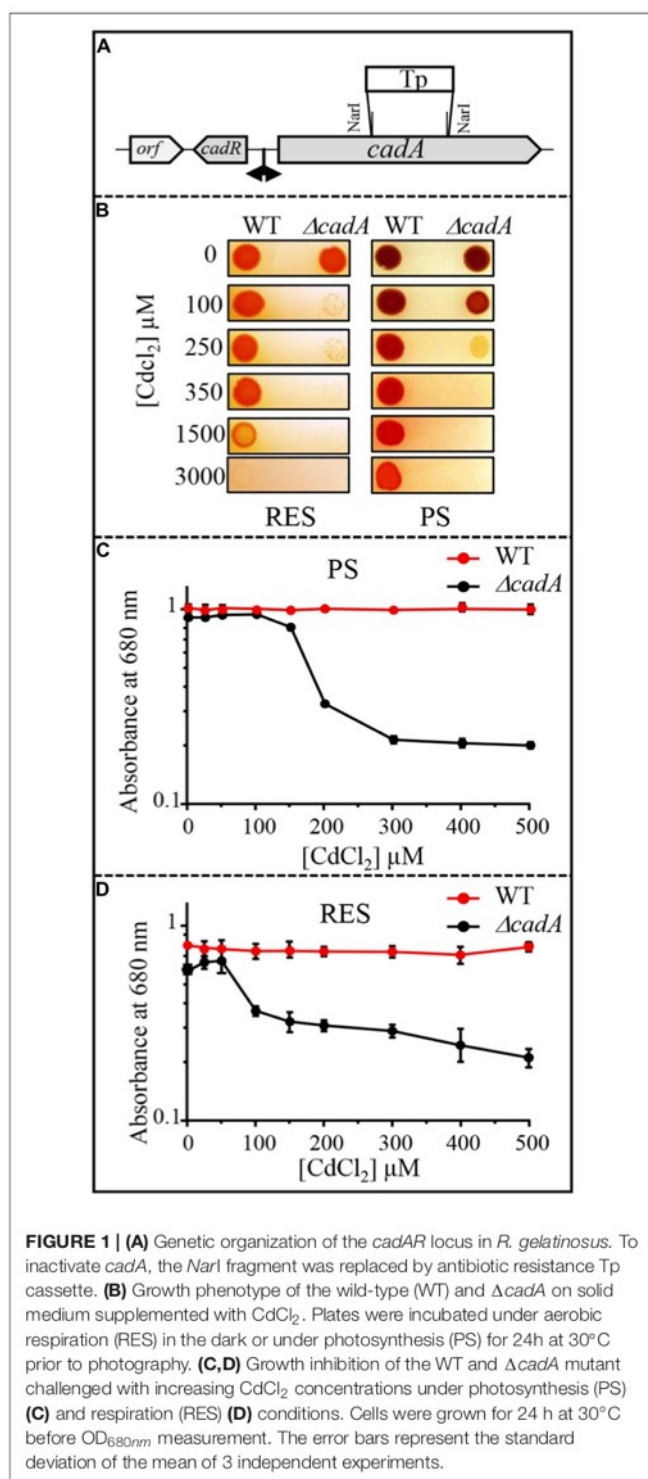
Cadmium tolerance in bacteria usually involves the metal efflux pump P<sub>1B</sub>-type ATPase CadA (ZntA) protein that translocates cadmium from the cytoplasm to the periplasm (Rensing et al., 1998). A gene (hereafter referred to as *cadA*) encoding a putative ATPase involved in Zn<sup>2+</sup> or Cd<sup>2+</sup> efflux was identified in *R. gelatinosus* genome. Sequence analyses showed high similarities with putative heavy metal translocating P<sub>1B</sub>-type ATPases from β-proteobacteria (**Supplementary Figure S1**). In addition to conserved structural features and motifs in the ATPase sequence, an N-terminal 30 amino acids stretch consisting of 14 histidines and 7 acidic residues, flanked by two CxxxC motifs were found in *R. gelatinosus* CadA (**Supplementary Figure S1**). This N-terminal cytoplasmic stretch could play a role in metal binding and transport regulation as reported for other metal transporting ATPases (Mana-Capelli et al., 2003; Baekgaard et al., 2010). A gene (referred to as *cadR*) encoding a MerR regulator protein (CadR) was found upstream *cadA*. To ascertain the role of CadA in Cd<sup>2+</sup> tolerance, the *ΔcadA* deletion strain was generated and its ability to grow on solid medium in presence of CdCl<sub>2</sub> was tested in comparison with wild-type strain under aerobic respiration and photosynthesis conditions (**Figure 1**). When challenged with Cd<sup>2+</sup>, the growth of *ΔcadA* strain is inhibited with 100 or 250 μM CdCl<sub>2</sub> under aerobic or photosynthesis conditions, respectively. In contrast, the wild-type strain was still able to grow in presence of 1.5 or 3 mM CdCl<sub>2</sub> (**Figure 1B**). The tolerance towards Cd<sup>2+</sup> was restored by the expression of the wild-type copy of *cadA* gene *in trans* in *ΔcadA* strain (**Supplementary Figure S2**). Growth inhibition by Cd<sup>2+</sup> of these strains was also assessed in liquid medium in the presence of increasing CdCl<sub>2</sub> concentration. Whereas growth of the wild-type strain remained unaffected under both conditions, growth of *ΔcadA* mutant was reduced starting at 150 μM or 50 μM CdCl<sub>2</sub> under photosynthesis (**Figure 1C**) and respiration (**Figure 1D**) conditions, respectively. *ΔcadA* mutant was also sensitive to excess Zn<sup>2+</sup> as shown by growth inhibition on plates of the wild-type and *ΔcadA* grown in the presence of CdCl<sub>2</sub>, ZnSO<sub>4</sub> or CuSO<sub>4</sub> (**Supplementary Figure S3A**). Similarly, dose response and growth curves in liquid media (**Supplementary Figures S3B-D**) confirmed that *cadA* was also required for full zinc resistance. We should note that *ΔcadA* was more tolerant to Zn<sup>2+</sup> than Cd<sup>2+</sup> probably because under Zn<sup>2+</sup> excess, Zn<sup>2+</sup> uptake (ZnuABC transporter) could be limited by Zur regulator and other Zn<sup>2+</sup>-efflux systems like CzcCBA could mediate Zn<sup>2+</sup> efflux (Arguello et al.,

2007; von Rozycki and Nies, 2009; Capdevila et al., 2017; Chandrangsu et al., 2017). Genes encoding these proteins are present in *R. gelatinosus* genome, but their role was not investigated yet. These data confirmed that *cadA* gene encodes for the  $\text{Cd}^{2+}/\text{Zn}^{2+}$ -efflux ATPase CadA, required for  $\text{Cd}^{2+}$  (and involved in  $\text{Zn}^{2+}$ ) tolerance in *R. gelatinosus*, and that the  $\Delta\text{cadA}$  mutant is more sensitive to cadmium under respiratory conditions.

### Induction of CadA in Response to Excess $\text{Cd}^{2+}$ Involves the MerR-Type Transcriptional Regulator CadR

To cope with excess toxic metal exposure, bacteria usually induce the expression of metal detoxification proteins including the efflux ATPases. To gain better insight into the expression profile of CadA in response to excess  $\text{Cd}^{2+}$ , we analyzed the expression of CadA by Western blot in the wild-type and  $\Delta\text{cadA}$  strains grown under photosynthesis condition in presence of increasing  $\text{CdCl}_2$  concentration. The presence of the histidine stretch within CadA N-terminus sequence allowed the detection of CadA on Western blot using the horseradish peroxidase (HRP)-conjugated HisProbe. As shown in **Figure 2A**, addition of 150  $\mu\text{M}$  or 1 mM  $\text{CdCl}_2$  to the medium during wild-type growth resulted in a significant increase in the amount of an 80 kDa protein, likely corresponding to CadA. This band was not detected in the  $\Delta\text{cadA}$  cells grown without or with the addition of 150  $\mu\text{M}$   $\text{CdCl}_2$ . To confirm that this band was indeed CadA, the  $\Delta\text{cadA}$  complemented strain was also subjected to  $\text{Cd}^{2+}$  stress and Western blot showed the expression and induction of the 80 kDa band encoded by *cadA* gene on the replicative plasmid (**Supplementary Figure S2B**). These findings demonstrated that CadA is induced by cadmium. Unexpectedly, in addition to CadA induction,  $\text{Cd}^{2+}$  also induced an increase in the amount of the periplasmic  $\text{Cu}^+$  tolerance protein CopI (Durand et al., 2015) in both wild-type and  $\Delta\text{cadA}$  cells suggesting a putative role of CopI in  $\text{Cd}^{2+}$  tolerance and very likely a cross talk between  $\text{Cu}^+$  and  $\text{Cd}^{2+}$  (see below). To unequivocally show that the  $\text{Cd}^{2+}$ -induced band correspond to CopI, we generated a mutant ( $\Delta\text{cadA}\text{-}\Delta\text{copI}$ ) in which *cadA* and *copI* were deleted, and probed the presence of CopI in the periplasmic fractions. As shown in **Figure 2B**, while CopI was induced in  $\Delta\text{cadA}$  under  $\text{Cd}^{2+}$  excess, the band was absent in the  $\Delta\text{cadA}\text{-}\Delta\text{copI}$  mutant showing that the cadmium-induced band correspond to CopI.

It has been reported that the transcription regulator CadR/ZntR recognizes a palindromic sequence in the promoter region of *cadA/zntA* genes (Singh et al., 1999). In the intergenic sequence (54 bp) between *cadA* and *cadR* (**Figure 1**), an inverted repeat sequence ( $-^{27}\text{-ACCCGCTACAGGGT-}^{-13}$ ) might allow the binding of regulatory proteins was identified. To further highlight the role of CadR, the gene was inactivated and the resulting *cadR*<sup>-</sup> strain was shown to be sensitive to cadmium (**Supplementary Figure S4**) suggesting its involvement in *cadA* expression. To unambiguously show the role of *cadR* in *CadA* expression, we checked the expression level of CadA in the wild-type and the *cadR*<sup>-</sup> strains challenged with excess  $\text{Cd}^{2+}$ . For this



purpose, cells were grown overnight under photosynthesis in the presence of increasing  $\text{CdCl}_2$  concentration and *CadA* expression profile was assessed by Western blot. In contrast to the wild-type, overnight growth of *cadR*<sup>-</sup> cells was inhibited beyond 600  $\mu\text{M}$   $\text{CdCl}_2$ . Western blot analysis confirmed that *CadA* is induced

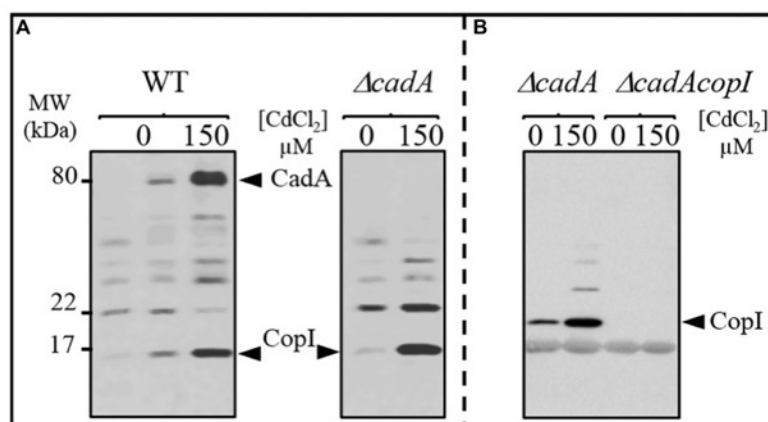


**FIGURE 2 |** Expression profile of CadA and CopI in *R. gelatinosus* wild-type (WT) and  $\Delta cadA$  cells challenged with  $Cd^{2+}$ . Cells were grown overnight (18 h) under photosynthesis and total protein extract from the same amount of cells ( $OD_{680nm} = 0.1$ ) were separated on a 15% Tris-glycine SDS-PAGE (A). Periplasmic fractions were purified from  $\Delta cadA$  and  $\Delta cadA_{\Delta copI}$  cells challenged or not with  $Cd^{2+}$  and separated on a 15% Tris-glycine SDS-PAGE (B). Proteins were visualized after Western blotting using the HRP-HisProbe (Pierce).

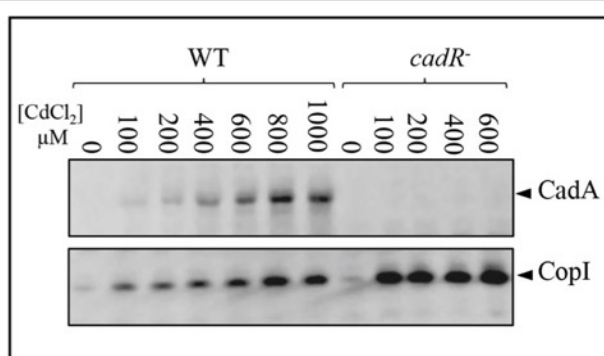


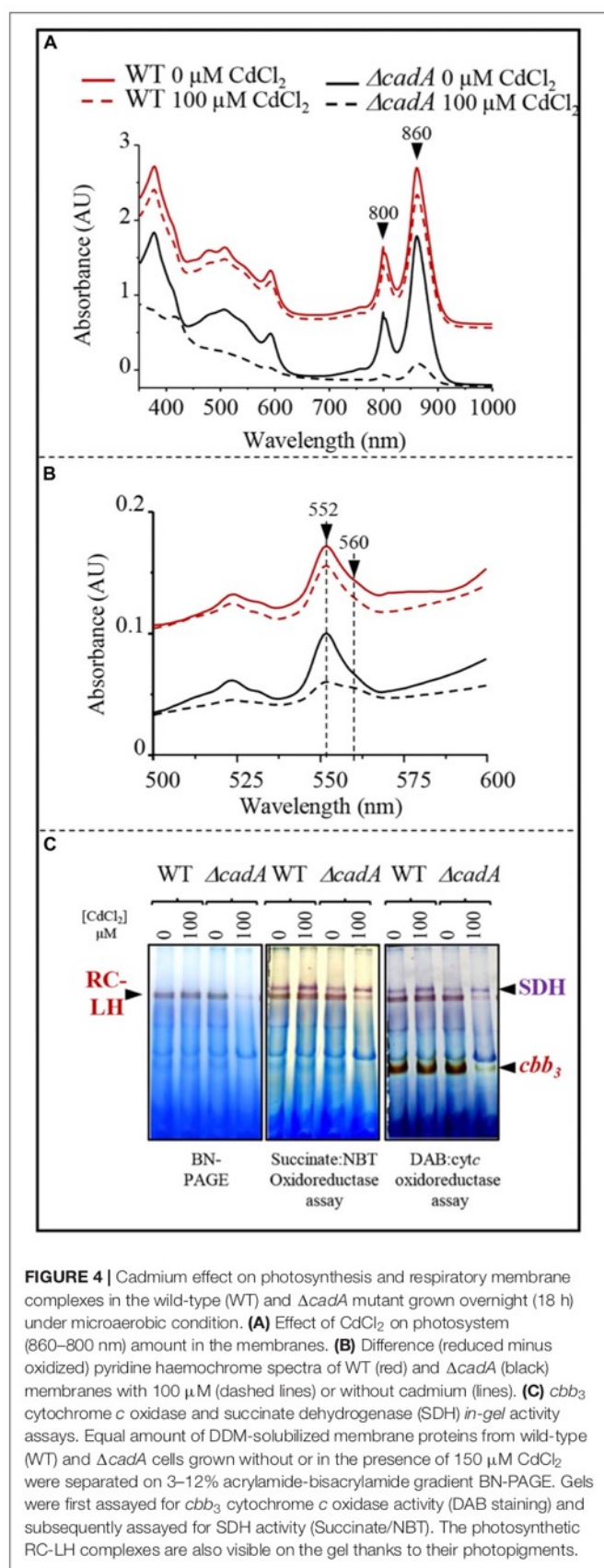
**FIGURE 3 |** Expression level of CadA and CopI in *R. gelatinosus* wild-type (WT) and  $cadR^-$  mutant cells challenged with increasing concentration of  $CdCl_2$ . Cells were grown overnight (18 h) under photosynthetic condition. Total protein extract from the same amount of cells ( $OD_{680nm} = 0.1$ ) were separated on a 15% Tris-glycine SDS-PAGE. Proteins were visualized after Western blotting using the HRP-HisProbe.

with increasing concentration of  $CdCl_2$  (Figure 3) in the wild-type and this induction is CadR-dependent since CadA was not detected in  $cadR^-$  cells. In conclusion, these data showed that the CadA efflux ATPase is required for cadmium detoxification and its expression is induced by  $CdCl_2$  under the control of CadR. Note that the  $cadR^-$  mutant tolerates a higher cadmium concentration than the  $\Delta cadA$  mutant, but less than the wild-type (Supplementary Figure S4). This difference could be due to a low expression of CadA (undetectable on Western blot) in  $cadR^-$ , but sufficient enough to warrant tolerance toward low cadmium concentrations. The Western blot also confirmed the induction of CopI expression in response to  $Cd^{2+}$  stress and showed that induction of CopI by  $Cd^{2+}$  occurred, even in the absence of CadR.

### Cadmium Effect on Photosynthesis and Respiratory Membrane Complexes

The toxic effect of  $Cu^+$  on photosynthesis and respiration in *R. gelatinosus* was previously assessed in the  $Cu^+$ - $P_{1B}$ -type ATPase efflux mutant  $copA^-$  (Azzouzi et al., 2013; Liotenberg et al., 2015). Because photosynthetic organisms can also be exposed to  $Cd^{2+}$  in their environment, we took advantage of the  $\Delta cadA$  strain that should likely accumulate  $Cd^{2+}$  in the cytoplasm, to ask whether  $Cd^{2+}$  affects protein complexes and cytochromes involved in photosynthesis and microaerobic respiration. Membranes from the wild-type and  $\Delta cadA$  cells grown microaerobically in medium supplemented or not with  $100 \mu M Cd^{2+}$  were enriched and the amount of photosynthetic complexes (RC-LH 860 nm and 800 nm) was assessed with UV-visible absorbance spectra. In contrast to the wild-type, the amount of the photosynthetic complexes was shown to significantly decrease in the membrane of  $\Delta cadA$  cells exposed to  $Cd^{2+}$  (Figure 4A). We also performed redox spectral analyses (reduced minus oxidized spectra) to checked the effect of  $Cd^{2+}$  on cytochromes *c* (peak at 552 nm) and *b* (peak at 560 nm) in these membranes by comparing the total cytochrome content in the wild-type and  $\Delta cadA$  membranes (Figure 4B). Comparable spectra were recorded for  $Cd^{2+}$  treated and untreated wild-type membrane. Unlike the wild-type, in the  $\Delta cadA$  cells,  $Cd^{2+}$  addition resulted in a drastic decrease of cytochrome *c* and *b* content within the membranes.

BN-PAGE analysis confirmed the decreased amount of reaction centre and light harvesting antenna (RC-LH) in the  $Cd^{2+}$  stressed  $\Delta cadA$  mutant membranes (Figure 4C). Furthermore, cytochrome *c* oxidase *in-gel* assay revealed comparable amount of active cytochrome *c* oxidase *cbb3* in the wild-type membrane from cells grown with or without  $Cd^{2+}$ ; whereas in  $\Delta cadA$  membrane, the *cbb3* active band decreased significantly in the  $Cd^{2+}$  stressed mutant. Concomitantly, succinate-NBT reductase *in-gel* assay revealed an active band,

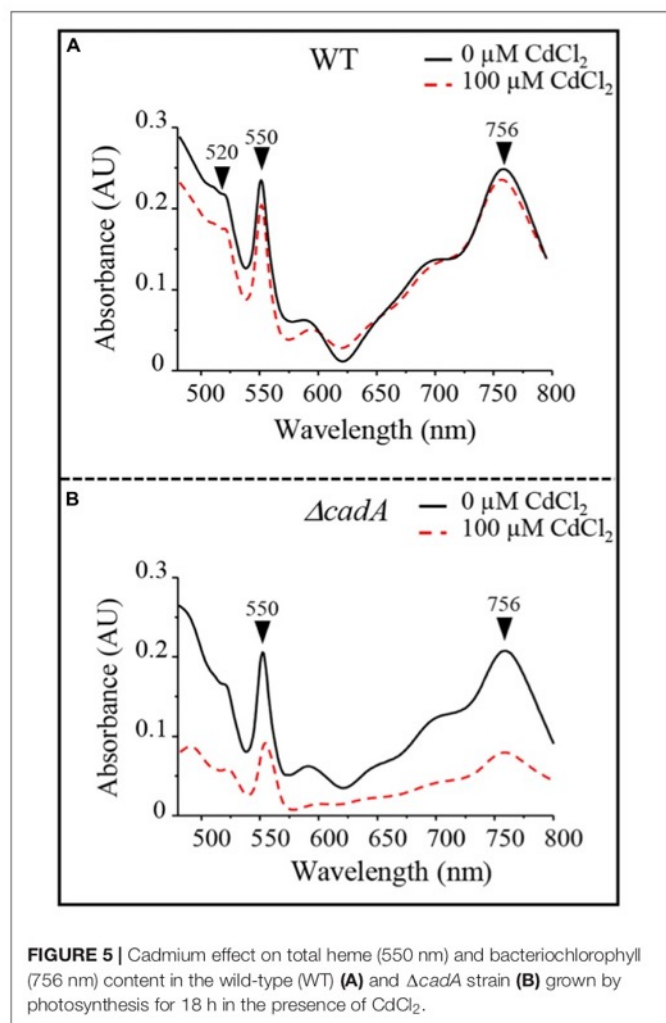


likely corresponding to SDH, in the wild-type and  $\Delta cadA$  membranes. This band increased slightly in the presence of  $Cd^{2+}$  in both strains. However, the activity was also slightly reduced in  $\Delta cadA$  membranes compared to the wild-type membranes (Figure 4C). The decrease in active cytochrome *c* oxidase  $cbb_3$  was more pronounced than the SDH. The SDH complex requires only one heme per complex while the  $cbb_3$  oxidase requires five hemes for its assembly and activity.

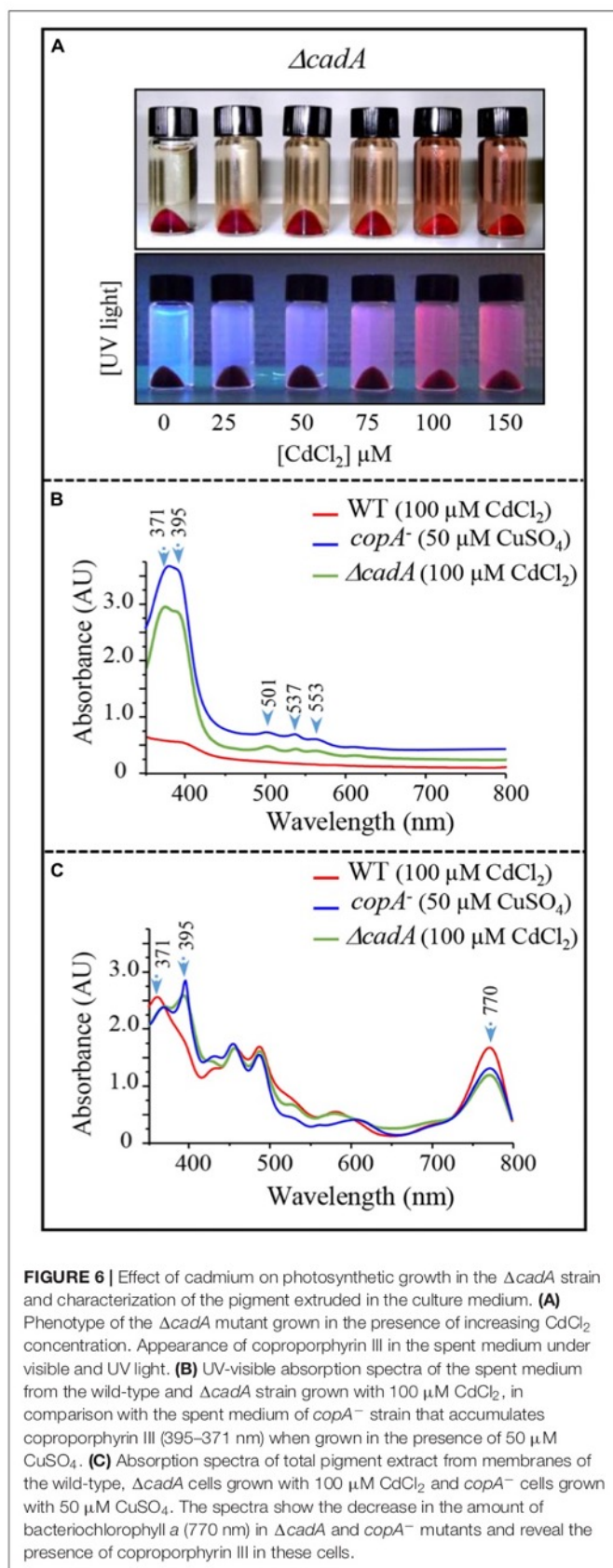
Photosynthetic and respiratory complexes require chlorophylls and heme cofactors respectively for their assembly and activity. The decreased level of these complexes in presence of excess  $Cd^{2+}$  could be attributed to a decreased amount of cofactors under  $Cd^{2+}$  stress condition in the  $\Delta cadA$  mutant. The total heme and chlorophylls were extracted from cells exposed or not to  $Cd^{2+}$  and dithionite-reduced and ferricyanide-oxidized pyridine haemochromes spectra were recorded. The reduced minus oxidized spectra showed a comparable amount of heme (peaks  $\alpha$  and  $\beta$  at 550 nm and 520 nm respectively) and bacteriochlorophylls (756 nm) for photosynthetic grown wild-type strain in presence/absence of  $Cd^{2+}$  in these samples (Figure 5A). The  $\Delta cadA$  mutant cells stressed by 100  $\mu M$  of  $Cd^{2+}$  presented a strong decrease of the heme and bacteriochlorophylls content compared to the unstressed mutant strain (Figure 5B). Heme and chlorophyll share the same biosynthesis pathway down to protoporphyrin IX. An effect of cadmium on the porphyrin biosynthesis pathway upstream protoporphyrin IX would then affect concomitantly heme and chlorophyll biosynthesis.

### Cadmium Excess Is Associated With an Accumulation of Coproporphyrin III

The wild-type strain and the  $\Delta cadA$  mutant were subjected to increasing sub-lethal concentrations of  $CdCl_2$  (0–150  $\mu M$   $CdCl_2$ ) under photosynthetic growth conditions. No effect of excess  $CdCl_2$  was observed on the wild-type cells (not shown). Conversely, for the  $\Delta cadA$  cells, growth was affected by increasing  $CdCl_2$  concentration and a UV-fluorescent pigment was released in the spent medium as a  $CdCl_2$  concentration-dependent manner (Figure 6A). This phenotype also seen under microaerobic conditions, is presumably due to the excretion of porphyrin intermediate and is reminiscent of the  $copA^-$  strain one when exposed to  $Cu^+$  (Azzouzi et al., 2013). The spent medium of the  $\Delta cadA$  strain was therefore compared to that of wild-type and  $copA^-$  strains using UV-Vis absorbance spectra (Figure 6B). In view of these spectra, the  $\Delta cadA$  strain extrudes the same pigment as the  $copA^-$  strain exposed to  $Cu^+$ . Two absorbance peaks in the Soret region at 371 and 395 nm with minor peaks at 501, 537, and 553 nm were observed. These peaks are characteristic of coproporphyrin III (oxidized coproporphinogen III), a protoporphyrin IX precursor. The presence of coproporphyrin III in the medium may correlate with a decreased amount of chlorophylls and heme in the  $\Delta cadA$  cells exposed to  $Cd^{2+}$ . To ascertain this assumption, UV-vis spectra were recorded on total pigments extracted from wild-type and  $\Delta cadA$  strains grown with 100  $\mu M$   $CdCl_2$  or from  $copA^-$  strain grown with 50  $\mu M$   $CuSO_4$



under the same conditions. In both  $\Delta cadA$  and  $copA^-$  strains, the addition of  $\text{CdCl}_2$  or  $\text{CuSO}_4$  respectively to the growth medium correlated with a decrease in the bacteriochlorophyll *a* content (peak at 770 nm) and an increase of the 395 nm peak (Figure 6C). In contrast, in the wild-type strain grown in the presence of 100  $\mu\text{M}$   $\text{CdCl}_2$ , the higher amount of bacteriochlorophyll *a* correlated with the absence of the 395 nm peak in the extract (Figure 6C). These data confirm the accumulation of coproporphyrin III and reflects the decrease of bacteriochlorophyll *a* and heme under photosynthetic and microaerobic conditions in  $\Delta cadA$  cells exposed to  $\text{Cd}^{2+}$  as previously reported for the  $copA^-$  mutant exposed to excess  $\text{CuSO}_4$ . As for  $\text{Cu}^+$  toxicity, accumulation of coproporphyrin III in the  $\Delta cadA$  strain when stressed with  $\text{Cd}^{2+}$  suggested that excess  $\text{Cd}^{2+}$  affected the enzyme for which coproporphyrinogen III is a substrate. We therefore assumed that  $\text{Cd}^{2+}$  targets the coproporphyrinogen III oxidase HemN in the porphyrin biosynthesis pathway. This is the first *in vivo* demonstration that, as oxygen and  $\text{Cu}^+$ ,  $\text{Cd}^{2+}$  affects the porphyrin biosynthesis pathway presumably at the level of the SAM and [4Fe-4S] containing HemN enzyme.



## HemN Is a Target of Cd<sup>2+</sup> and Cu<sup>+</sup> Toxicity in *R. gelatinosus*

Accumulation of coproporphyrin III in the  $\Delta cadA$  strain when exposed to excess cadmium, or in the CopA defective strains when challenged with excess copper both in *R. gelatinosus* and *N. gonorrhoea*, strongly suggests that HemN activity is affected by excess metal (Azzouzi et al., 2013; Djoko and McEwan, 2013). Inactivating the [4Fe-4S] of HemN by Cd<sup>2+</sup> or Cu<sup>+</sup> would be consistent with the published evidences showing that Cd<sup>2+</sup> or Cu<sup>+</sup> damage exposed [4Fe-4S] in dehydratases (Macomber and Imlay, 2009; Xu and Imlay, 2012). Attempt to express and purify HemN of *R. gelatinosus* and *N. gonorrhoea* (Djoko and McEwan, 2013) in *E. coli* to assess the effect of metal on the enzyme activity were unfortunately unsuccessful. Therefore, to provide direct evidence that Cd<sup>2+</sup> or Cu<sup>+</sup> damage HemN, we hypothesized that the amount of the enzyme would decrease if the [4Fe-4S] cluster is damaged by excess Cu<sup>+</sup> or Cd<sup>2+</sup>. To test this assumption, we generated a strain in which the wild-type *hemN* gene was substituted by a histidine tagged copy on the chromosome. In this strain, the *hemN-H<sub>6</sub>* gene is under its own FNR-regulated promoter and should therefore be inducible under micro-aerobic and photosynthesis conditions. This strain was subjected to elevated concentrations of CdCl<sub>2</sub> or CuSO<sub>4</sub> and the amount of HemN-H<sub>6</sub> in the soluble fraction was assessed on Western blot.

A band of 54 kDa likely corresponding to HemN-H<sub>6</sub> was detected on Western blot in the soluble fraction of HemN-H<sub>6</sub> strain but not in the wild-type soluble fraction (Figure 7). This band was however significantly decreased in the soluble fractions purified from HemN-H<sub>6</sub> strain grown in the medium supplemented either with 1000  $\mu$ M CdCl<sub>2</sub> or with 500  $\mu$ M CuSO<sub>4</sub> (Figure 7). In contrast to the decrease of HemN-H<sub>6</sub>, CopI protein expression was increased in presence of Cd<sup>2+</sup> and highly increased by Cu<sup>+</sup> as expected in these samples (Figure 7), confirming the Cd<sup>2+</sup> and Cu<sup>+</sup> stress status encountered by these cells. These results, clearly demonstrated that *in vivo*, HemN stability is affected by excess Cd<sup>2+</sup> and Cu<sup>+</sup>, thus elucidating the effect of metal excess on heme biosynthesis and the cause of coproporphyrin III accumulation.

## Cadmium and Copper Cross-Tolerance: CopI Is Involved in Cadmium Tolerance

On Western Blot, we observed an increase of the periplasmic copper tolerance protein CopI with the addition of CdCl<sub>2</sub> in both wild-type and  $\Delta cadA$  cells (Figure 2). This CopI induction, in presence of 150  $\mu$ M CdCl<sub>2</sub>, is higher in the  $\Delta cadA$  mutant than in the wild-type, very likely resulting from Cd<sup>2+</sup> accumulation in the cytoplasm of the  $\Delta cadA$  strain. CopI induction by Cd<sup>2+</sup> suggested a cross-talk between the Cd<sup>2+</sup> and Cu<sup>+</sup> response systems and a role of CopI and/or the copper detoxification system in Cd<sup>2+</sup> response. A band at about 22 kDa apparent molecular weight was also noticeably induced in the  $\Delta cadA$  mutant. This band corresponds to the cytosolic superoxide dismutase SodB (Steunou et al., 2020a). Similarly, in the *cadR*<sup>-</sup> mutant, CopI is also more induced compared to the wild-type

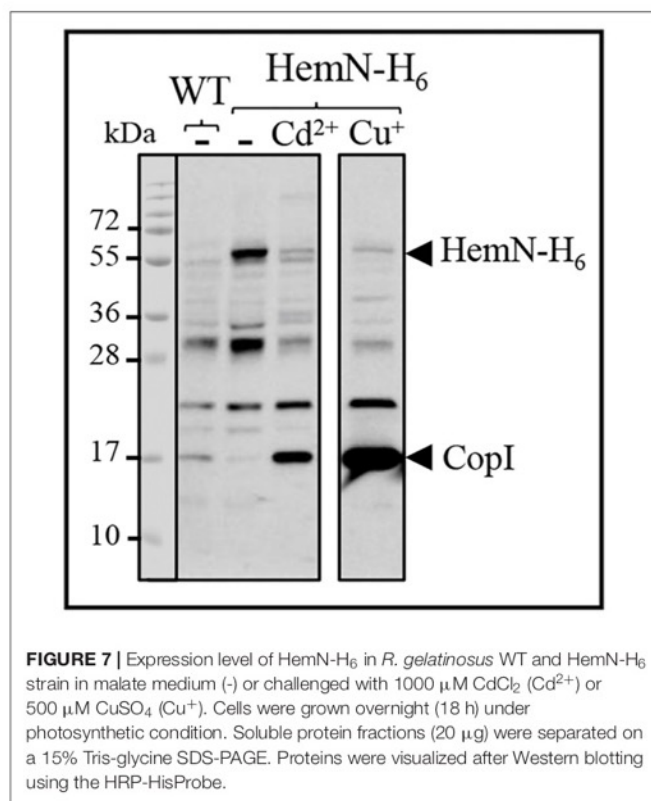


**FIGURE 7** | Expression level of HemN-H<sub>6</sub> in *R. gelatinosus* WT and HemN-H<sub>6</sub> strain in malate medium (-) or challenged with 1000  $\mu$ M CdCl<sub>2</sub> (Cd<sup>2+</sup>) or 500  $\mu$ M CuSO<sub>4</sub> (Cu<sup>+</sup>). Cells were grown overnight (18 h) under photosynthetic condition. Soluble protein fractions (20  $\mu$ g) were separated on a 15% Tris-glycine SDS-PAGE. Proteins were visualized after Western blotting using the HRP-HisProbe.

strain. Once again, this difference in expression could arise from the accumulation of Cd<sup>2+</sup> in the cytoplasm of *cadR*<sup>-</sup> cells devoid of the Cd<sup>2+</sup>-efflux ATPase. The data suggested that either CopR can interact with Cd<sup>2+</sup> to induce CopI or that other regulators can induce CopI expression in the *cadR*<sup>-</sup> strain.

Given the induction of CopI, the periplasmic copper tolerance protein, by excess Cd<sup>2+</sup> (Figures 2, 3), we wondered whether CopI was required for Cd<sup>2+</sup> resistance. The  $\Delta copI$  mutant was sensitive only to high Cd<sup>2+</sup> concentration. However, the presence of CadA in the  $\Delta copI$  mutant made the conclusion elusive. To confirm its requirement for Cd<sup>2+</sup> tolerance, we question whether inactivation of *copI* in the  $\Delta cadA$  background could give rise to a higher Cd<sup>2+</sup> sensitivity in such a strain. The double mutant  $\Delta cadA_{\Delta copI}$  was constructed and its tolerance towards Cd<sup>2+</sup> was compared to that of  $\Delta cadA$  strain on plates (Figure 8A) and liquid (Figure 8B and Supplementary Figure S5) under photosynthesis conditions. The double mutant  $\Delta cadA_{\Delta copI}$  was indeed more sensitive to Cd<sup>2+</sup> than the  $\Delta cadA$  mutant when exposed to 150  $\mu$ M and 200  $\mu$ M CdCl<sub>2</sub> on plates, and to 75  $\mu$ M CdCl<sub>2</sub> in liquid, thus confirming that CopI is somehow involved in Cd<sup>2+</sup> tolerance. The underlying mechanism is not yet known, however, CopI was shown to be periplasmic and displays conserved His and Met residues that could interact with cations (Durand et al., 2015). It is then tempting to speculate that CopI may handle Cd<sup>2+</sup> within the periplasm.

Cd<sup>2+</sup> detoxification. The involvement of CopA in Cd<sup>2+</sup> or Zn<sup>2+</sup> efflux has never been demonstrated and seems very unlikely. Nevertheless, the cross-talk between Cu<sup>+</sup> and Zn<sup>2+</sup>/Cd<sup>2+</sup> efflux systems, at least at the expression level, was previously reported in other bacteria. In *P. aeruginosa*, both PA3920 gene encoding CopA and PA3690 encoding ZntA/CadA homologue are induced by Cu<sup>+</sup> stress (Teitzel et al., 2006). We should stress out that in this study, *P. aeruginosa* wild type cells were exposed to a very high concentration of CuSO<sub>4</sub> (10 mM). In a more recent study, Arguello's group used RNA-Seq to characterize the response of *P. aeruginosa* to 0.5 mM CuSO<sub>4</sub> to avoid pleiotropic effects that could be related to elevated concentration of CuSO<sub>4</sub> (Quintana et al., 2017). PA3690 (ZntA/CadA) was not induced in the wild type, nevertheless, in the  $\Delta cueR$  and  $\Delta copR$  mutant, a 3.6 and 2 fold change in the expression of PA3690 was observed in these mutants (Quintana et al., 2017). Likewise, in the filamentous cyanobacterium *Oscillatoria brevis*, expression of the ATPase Bxa1 is also induced by both Cd<sup>2+</sup> and Cu<sup>+</sup> cations (Liu et al., 2004). Cross-tolerance towards Cu<sup>+</sup> and Zn<sup>2+</sup> or Cd<sup>2+</sup> involving these ATPases, was not investigated in these bacteria.

Although the mechanism and physiological significance behind Cu<sup>+</sup>/Cd<sup>2+</sup> growth improvement reported in this work remain unclear and require further investigation, the cross-talk and cross-tolerance reported in all these studies emphasize on the importance of interactions and toxicity that could arise from metal mixtures and show that research should further consider mixtures effects.

Metal ability to undergo redox reactions is important for its function as protein cofactor but also for its intrinsic toxicity. Cd<sup>2+</sup> is not redox active and cannot directly trigger ROS formation, yet, it is very toxic. It was suggested that Cd<sup>2+</sup> could indirectly promote ROS production by displacing and releasing redox active ions such as iron or copper from proteins

(Xu and Imlay, 2012; Barwinska-Sendra and Waldron, 2017). Induction of SodB expression in the  $\Delta cadA$  strain suggests an increase in ROS production or a dysregulation of iron homeostasis since SodB is known to be regulated by Fur regulator in bacteria. Together with the degradation of solvent exposed [4Fe-4S] cluster from key metabolic enzymes, iron homeostasis dysregulation and ROS should be considered to account for the Cd<sup>2+</sup> toxicity in the  $\Delta cadA$  strain (Steunou et al., 2020b).

## DATA AVAILABILITY STATEMENT

The raw data supporting the conclusions of this article will be made available by the authors, without undue reservation, to any qualified researcher.

## AUTHOR CONTRIBUTIONS

AS, AD, MB, SL, and SO designed the research. AS, AD, M-LB, RT, and SO performed the research. AS, AD, MB, SL, M-LB, and SO analyzed the data. AS and SO wrote the manuscript.

## ACKNOWLEDGMENTS

We gratefully acknowledge the support of the CNRS and the Microbiology department of I2BC.

## SUPPLEMENTARY MATERIAL

The Supplementary Material for this article can be found online at: <https://www.frontiersin.org/articles/10.3389/fmicb.2020.00893/full#supplementary-material>

## REFERENCES

- Arguello, J. M., Eren, E., and Gonzalez-Guerrero, M. (2007). The structure and function of heavy metal transport PIB-ATPases. *Biomol. Biophys. Acta* 1577, 233–248. doi: 10.1016/j.bba.2006.09.055-6
- Azzouzi, A., Steunou, A. S., Durand, A., Khalifaoui-Hassani, B., Bourbon, M. L., Astier, C., et al. (2013). Coproporphyrin III excretion identifies the anaerobic coproporphyrinogen III oxidase HemN as a copper target in the Cu<sup>+</sup>-ATPase mutant *copA*<sup>-</sup> of *Rubrivivax gelatinosus*. *Mol. Microbiol.* 88, 339–351. doi: 10.1111/mmi.12188
- Baekgaard, L., Mikkelsen, M. D., Sorensen, D. M., Hegelund, J. N., Persson, D. P., Mills, R. F., et al. (2010). A combined zinc/cadmium sensor and zinc/cadmium export regulator in a heavy metal pump. *J. Biol. Chem.* 285, 31243–31252. doi: 10.1074/jbc.M110.111260
- Barwinska-Sendra, A., and Waldron, K. J. (2017). The Role of Intermetal Competition and Mis-Metalation in Metal Toxicity. *Adv. Microb. Physiol.* 70, 315–379. doi: 10.1016/bs.ampbs.2017.01.003
- Breckau, D., Mahlitz, E., Sauerwald, A., Layer, G., and Jahn, D. (2003). Oxygen-dependent coproporphyrinogen III oxidase (HemF) from *Escherichia coli* is stimulated by manganese. *J. Biol. Chem.* 278, 46625–46631. doi: 10.1074/jbc.M308553200
- Caille, O., Rossier, C., and Perron, K. (2007). A copper-activated two-component system interacts with zinc and imipenem resistance in *Pseudomonas aeruginosa*. *J. Bacteriol.* 189, 4561–4568. doi: 10.1128/jb.00095-07
- Capdevila, D. A., Edmonds, K. A., and Giedroc, D. P. (2017). Metallochaperones and metalloregulation in bacteria. *Essays Biochem.* 61, 177–200. doi: 10.1042/ebc20160076
- Chandrangsu, P., Rensing, C., and Helmann, J. D. (2017). Metal homeostasis and resistance in bacteria. *Nat. Rev. Microbiol.* 15, 338–350. doi: 10.1038/nrmicro.2017.15
- Djoko, K. Y., and McEwan, A. G. (2013). Antimicrobial action of copper is amplified via inhibition of heme biosynthesis. *ACS Chem. Biol.* 8, 2217–2223. doi: 10.1021/cb4002443
- Durand, A., Azzouzi, A., Bourbon, M. L., Steunou, A. S., Liotenberg, S., Maeshima, A., et al. (2015). c-type cytochrome assembly is a key target of copper toxicity within the bacterial periplasm. *mBio* 6, e01007–e01015.
- Gonzalez-Guerrero, M., Raimunda, D., Cheng, X., and Arguello, J. M. (2010). Distinct functional roles of homologous Cu<sup>+</sup> efflux ATPases in *Pseudomonas aeruginosa*. *Mol. Microbiol.* 78, 1246–1258. doi: 10.1111/j.1365-2958.2010.07402.x
- Haan, C., and Behrmann, I. (2007). A cost effective non-commercial ECL-solution for Western blot detections yielding strong signals and low background. *J. Immunol. Methods* 318, 11–19. doi: 10.1016/j.jim.2006.07.027
- Khalifaoui Hassani, B., Steunou, A. S., Liotenberg, S., Reiss-Husson, F., Astier, C., and Ouchane, S. (2010). Adaptation to oxygen: Role of terminal oxidases in photosynthesis initiation in the purple photosynthetic bacterium. *Rubrivivax gelatinosus*. *J. Biol. Chem.* 285, 19891–19899. doi: 10.1074/jbc.M109.086066

-APPENDIX -  
-RELATED RESEARCH-

- Kihlken, M. A., Singleton, C., and Le Brun, N. E. (2008). Distinct characteristics of Ag<sup>+</sup> and Cd<sup>2+</sup> binding to CopZ from *Bacillus subtilis*. *J. Biol. Inorg. Chem.* 13, 1011–1023. doi: 10.1007/s00775-008-0388-1
- Layer, G., Heinz, D. W., Jahn, D., and Schubert, W. D. (2004). Structure and function of radical SAM enzymes. *Curr. Opin. Chem. Biol.* 8, 468–476. doi: 10.1016/j.cbpa.2004.08.001
- Layer, G., Moser, J., Heinz, D. W., Jahn, D., and Schubert, W. D. (2003). Crystal structure of coproporphyrinogen III oxidase reveals cofactor geometry of Radical SAM enzymes. *EMBO J.* 22, 6214–6224. doi: 10.1093/emboj/cdg598
- Legatzki, A., Grass, G., Anton, A., Rensing, C., and Nies, D. H. (2003). Interplay of the Czc system and two P-type ATPases in conferring metal resistance to *Ralstonia metallidurans*. *J. Bacteriol.* 185, 4354–4361. doi: 10.1128/jb.185.15.4354-4361.2003
- Li, J., Ren, X., Fan, B., Huang, Z., Wang, W., Zhou, H., et al. (2019). Zinc Toxicity and Iron-Sulfur Cluster Biogenesis in *Escherichia coli*. *Appl. Environ. Microbiol.* 85, e1967–e1918.
- Liottenberg, A., Steunou, A. S., Durand, A., Bourbon, M. L., Bollivar, D. W., Hansson, M., et al. (2015). Oxygen-dependent copper toxicity: targets in the chlorophyll biosynthesis pathway identified in the copper efflux ATPase CopA deficient mutant. *Environ. Microbiol.* 17, 1963–1976. doi: 10.1111/1462-2920.12733
- Liu, T., Nakashima, S., Hirose, K., Shibasaki, M., Katsuhara, M., Ezaki, B., et al. (2004). A novel cyanobacterial SmtB/ArsR family repressor regulates the expression of a CPx-ATPase and a metallothionein in response to both Cu(I)/Ag(I) and Zn(II)/Cd(II). *J. Biol. Chem.* 279, 17810–17818. doi: 10.1074/jbc.m310560200
- Lu, M., Li, Z., Liang, J., Wei, Y., Rensing, C., and Wei, G. (2016). Zinc Resistance Mechanisms of P1B-type ATPases in *Sinorhizobium meliloti* CCNWSX0020. *Sci. Rep.* 6:29355.
- Macomber, L., and Imlay, J. A. (2009). The iron-sulfur clusters of dehydratases are primary intracellular targets of copper toxicity. *Proc. Natl. Acad. Sci. U.S.A.* 106, 8344–8349. doi: 10.1073/pnas.0812808106
- Macomber, L., Rensing, C., and Imlay, J. A. (2007). Intracellular copper does not catalyze the formation of oxidative DNA damage in *Escherichia coli*. *J. Bacteriol.* 189, 1616–1626. doi: 10.1128/jb.01357-06
- Mana-Capelli, S., Mandal, A. K., and Arguello, J. M. (2003). *Archaeoglobus fulgidus* CopB is a thermophilic Cu<sup>2+</sup>-ATPase: functional role of its histidine-rich-N-terminal metal binding domain. *J. Biol. Chem.* 278, 40534–40541. doi: 10.1074/jbc.m306907200
- Moore, C. M., Gaballa, A., Hui, M., Ye, R. W., and Helmann, J. D. (2005). Genetic and physiological responses of *Bacillus subtilis* to metal ion stress. *Mol. Microbiol.* 57, 27–40. doi: 10.1111/j.1365-2958.2005.04642.x
- Nunes, I., Jacquioud, S., Brejnrod, A., Holm, P. E., Johansen, A., Brandt, K. K., et al. (2016). Coping with copper: legacy effect of copper on potential activity of soil bacteria following a century of exposure. *FEMS Microbiol. Ecol.* 92:fiw175. doi: 10.1093/femsec/fiw175
- Ouchane, S., Picaud, M., Reiss-Husson, F., Vernotte, C., and Astier, C. (1996). Development of gene transfer methods for *Rubrivivax gelatinosus* S1: construction, characterization and complementation of a puf operon deletion strain. *Mol. Genet.* 252, 379–385. doi: 10.1007/bf02173002
- Quintana, J., Novoa-Aponte, L., and Arguello, J. M. (2017). Copper homeostasis networks in the bacterium *Pseudomonas aeruginosa*. *J. Biol. Chem.* 292, 15691–15704. doi: 10.1074/jbc.m117.804492
- Rensing, C., Sun, Y., Mitra, B., and Rosen, B. P. (1998). Pb(II)-translocating P-type ATPases. *J. Biol. Chem.* 273, 32614–32617. doi: 10.1074/jbc.273.49.32614
- Roy, P., Bauman, M. A., Almutairi, H. H., Jayawardhana, W. G., Johnson, N. M., and Torelli, A. T. (2018). Comparison of the response of bacterial IscU and SufU to Zn(2+) and select transition-metal ions. *ACS Chem. Biol.* 13, 591–599. doi: 10.1021/acscchembio.7b00442
- Sakpirom, J., Kantachote, D., Nunkaew, T., and Khan, E. (2017). Characterizations of purple non-sulfur bacteria isolated from paddy fields, and identification of strains with potential for plant growth-promotion, greenhouse gas mitigation and heavy metal bioremediation. *Res. Microbiol.* 168, 266–275. doi: 10.1016/j.resmic.2016.12.001 doi: 10.1016/j.resmic.2016.12.001
- Sambrook, J., Fritsch, E. F., and Maniatis, T. (1989). *Molecular Cloning, A Laboratory Manual*, 2nd Edn. New York, NY: Cold Spring Harbor.
- Singh, V. K., Xiong, A., Usgaard, T. R., Chakrabarti, S., Deora, R., Misra, T. K., et al. (1999). ZntR is an autoregulatory protein and negatively regulates the chromosomal zinc resistance operon znt of *Staphylococcus aureus*. *Mol. Microbiol.* 33, 200–207. doi: 10.1046/j.1365-2958.1999.01466.x
- Solovieva, I. M., and Entian, K. D. (2004). Metalloregulation in *Bacillus subtilis*: the copZ chromosomal gene is involved in cadmium resistance. *FEMS Microbiol. Lett.* 236, 115–122. doi: 10.1111/j.1574-6968.2004.tb09636.x
- Steunou, A. S., Babot, M., Bourbon, M. L., Tambosi, R., Durand, A., Liottenberg, S., et al. (1999). Additive effects of metal excess and superoxide, a highly toxic mixture in bacteria. *Microb. Biotechnol.* (In press)
- Steunou, A. S., Babot, M., Bourbon, M. L., Tambosi, R., Durand, A., Liottenberg, S., et al. (2020a). Additive effects of metal excess and superoxide, a highly toxic mixture in bacteria. *Microb. Biotechnol.* (in press).
- Steunou, A. S., Bourbon, M. L., Babot, M., Durand, A., Liottenberg, S., Yamaichi, Y., et al. (2020b). Increasing the copper sensitivity of microorganisms by restricting iron supply, a strategy for bio-management practices. *Microb. Biotechnol.* (in press).
- Tan, G., Yang, J., Li, T., Zhao, J., Sun, S., Li, X., et al. (2017). Anaerobic copper toxicity and iron-sulfur cluster biogenesis in *Escherichia coli*. *Appl. Environ. Microbiol.* 83:e00867-17.
- Teitzel, G. M., Geddie, A., De Long, S. K., Kirisits, M. J., Whiteley, M., and Parsek, M. R. (2006). Survival and growth in the presence of elevated copper: transcriptional profiling of copper-stressed *Pseudomonas aeruginosa*. *J. Bacteriol.* 188, 7242–7256. doi: 10.1128/jb.00837-06
- von Rozyccki, T., and Nies, D. H. (2009). Cupriavidus metallidurans: evolution of a metal-resistant bacterium. *Antonie Van Leeuwenhoek* 96, 115–139. doi: 10.1007/s10482-008-9284-5
- Wittig, I., Karas, M., and Schagger, H. (2007). High resolution clear native electrophoresis for in-gel functional assays and fluorescence studies of membrane protein complexes. *Mol. Cell Proteomics* 6, 1215–1225. doi: 10.1074/mcp.m700076-mcp200
- Xu, F. F., and Imlay, J. A. (2012). Silver(I), mercury(II), cadmium(II), and zinc(II) target exposed enzymic iron-sulfur clusters when they toxify *Escherichia coli*. *Appl. Environ. Microbiol.* 78, 3614–3621. doi: 10.1128/aem.07368-11
- Ye, J., Rensing, C., Su, J., and Zhu, Y. G. (2017). From chemical mixtures to antibiotic resistance. *J. Environ. Sci.* 62, 138–144. doi: 10.1016/j.jes.2017.09.003

**Conflict of Interest:** The authors declare that the research was conducted in the absence of any commercial or financial relationships that could be construed as a potential conflict of interest.

Copyright © 2020 Steunou, Durand, Bourbon, Babot, Tambosi, Liottenberg and Ouchane. This is an open-access article distributed under the terms of the Creative Commons Attribution License (CC BY). The use, distribution or reproduction in other forums is permitted, provided the original author(s) and the copyright owner(s) are credited and that the original publication in this journal is cited, in accordance with accepted academic practice. No use, distribution or reproduction is permitted which does not comply with these terms.

-APPENDIX –  
-RELATED RESEARCH-

## Article V: Interplay Between Metals Efflux and ROS Detoxifying Systems

---

### Summary and main results in Article V:

---

In general, bacterial cells rely on various defense strategies in order to survive environmental stresses. For metal stress, as metal could target metallo-proteins and generate reactive oxygen species, bacteria can induce metal efflux systems and/or the ROS detoxification enzymes to deal with excess metal and/or increased ROS production.

Reactive oxygen species include oxygen singlet, superoxide, hydroxyl radicals, hydrogen peroxide etc. Many respiratory and photosynthetic complexes produce superoxide in presence of oxygen. Superoxide dismutase (SOD) catalyze the dismutation of superoxide anion ( $O_2^-$ ) and generates hydrogen peroxide ( $H_2O_2$ ) that can be inactivated by catalases or peroxidases to oxygen and water. The role of these enzymes in protecting bacteria from oxidative stress is well known (Storz & Imlay, 1999). Their contribution to tolerate excess metal was also suggested based on transcriptomic data for example showing the induction of ROS detoxification enzymes encoding genes (*sod*, *kat*, *prx*, *ahp...*), upon copper or cadmium stress (Imlay, 2013). Nevertheless, the consequences of the simultaneous loss of metal and ROS detoxification systems was not reported.

While assessing the expression of CadA in *cadR*<sup>-</sup> (*cadR* is the  $Cd^{2+}$ -sensor-regulator of CadA) mutant, on Western blot, using the His probe (because of the presence of histidine residues in CadA sequence (Steunou et al., 2020a), I have revealed the induction of a protein under excess cadmium. This protein was identified as the cytosolic Fe-superoxide dismutase SodB. Analyses of the SodB sequence showed the presence of five histidines in its N-ter domain that is recognized by the His probe on the Western blot.

-APPENDIX –  
-RELATED RESEARCH-

Anne Soisig Steunou has made the mutant of *sodB* and showed that it is sensitive to superoxide generator (menadione), but resistant to metal ( $\text{Cd}^{2+}$  or  $\text{Cu}^{2+}$ ). On the contrary, SodB protein became essential to tolerate metal in the medium when the detoxification systems (ATPases) were deficient. Indeed, the double mutant  $\Delta cadAsodB$  was extremely sensitive to  $\text{Cd}^{2+}$  compared to the single mutant  $\Delta cadA$ . Similarly, the double mutant  $copAsodB$  was extremely sensitive to  $\text{Cu}^{2+}$  compared to the single mutant  $copA$ . These results showed that expression of SodB is important to face metal toxicity. To explain the toxicity encountered in the double mutants, we suggested that since both  $\text{Cd}^{2+}$  or  $\text{Cu}^{2+}$  and superoxide damage 4Fe-4S, accumulation of both in the double mutant would accentuate the loss of 4Fe-4S proteins and release of iron that may generate more ROS through the Fenton reaction. Such conditions would be unendurable by the cell and would lead to growth inhibition or cell death.

**Article V: Additive effects of metal excess and superoxide, a highly toxic mixture in bacteria**

---

\*Published. *Microbial Biotechnology* 2020

-APPENDIX –  
-RELATED RESEARCH-



## Additive effects of metal excess and superoxide, a highly toxic mixture in bacteria

Anne Soisig Steunou,\* Marion Babot, Marie-Line Bourbon, Reem Tambosi, Anne Durand, Sylviane Liotenberg, Anja Krieger-Liszkay, Yoshiharu Yamaichi and Soufian Ouchane\*\*   
Institute for Integrative Biology of the Cell (I2BC), CEA, CNRS, Université Paris-Saclay, 91198, Gif-sur-Yvette, France.

### Summary

Heavy metal contamination is a serious environmental problem. Understanding the toxicity mechanisms may allow to lower concentration of metals in the metal-based antimicrobial treatments of crops, and reduce metal content in soil and groundwater. Here, we investigate the interplay between metal efflux systems and the superoxide dismutase (SOD) in the purple bacterium *Rubrivivax gelatinosus* and other bacteria through analysis of the impact of metal accumulation. Exposure of the Cd<sup>2+</sup>-efflux mutant  $\Delta cadA$  to Cd<sup>2+</sup> caused an increase in the amount and activity of the cytosolic Fe-Sod SodB, thereby suggesting a role of SodB in the protection against Cd<sup>2+</sup>. In support of this conclusion, inactivation of *sodB* gene in the  $\Delta cadA$  cells alleviated detoxification of superoxide and enhanced Cd<sup>2+</sup> toxicity. Similar findings were described in the Cu<sup>+</sup>-efflux mutant with Cu<sup>+</sup>. Induction of the Mn-Sod or Fe-Sod in response to metals in other bacteria, including *Escherichia coli*, *Pseudomonas aeruginosa*, *Pseudomonas putida*, *Vibrio cholera* and *Bacillus subtilis*, was also shown. Both excess Cd<sup>2+</sup> or Cu<sup>+</sup> and superoxide can damage [4Fe-4S] clusters. The additive effect of metal and superoxide on the [4Fe-4S] could therefore explain the hypersensitive phenotype in mutants lacking SOD and the efflux ATPase. These findings underscore that ROS defence system

becomes decisive for bacterial survival under metal excess.

### Introduction

Heavy metal pollution, mainly caused by anthropogenic activities, may have adverse effects on the ecosystems and living organisms unless sustainable management practices are implemented. Cu<sup>2+</sup> and Cd<sup>2+</sup> pollution originating from activities including excessive use of fertilizers, antimicrobials and agrochemicals is an important environmental concern (Ballabio *et al.*, 2018).

[https://ec.europa.eu/environment/integration/research/newsalert/pdf/agricultural\\_management\\_practices\\_influence\\_copper\\_concentrations\\_european\\_topsoils\\_518\\_na2\\_en.pdf](https://ec.europa.eu/environment/integration/research/newsalert/pdf/agricultural_management_practices_influence_copper_concentrations_european_topsoils_518_na2_en.pdf)

Metal pollution contributes also to the selection and spread of antibiotic resistance factors. In fact, cross-resistance in bacteria can occur through transfer of genes encoding efflux pumps that can expel antibiotics in addition to metals (Baker-Austin *et al.*, 2006; Rensing *et al.*, 2018; Asante and Osei Sekyere, 2019). Metal pollution affects groundwater and soils properties by altering the microbial diversity and evenness (Nunes *et al.*, 2016). Limiting the concentration of heavy metals in agrochemicals or in metal-based antimicrobial treatments can lead to a sustainable use of metals in agriculture and farming (Turner, 2017) and may limit the metal-related co-selection for metal and antibiotic resistance in bacteria.

In contaminated soils, exposed organisms have to deal with excess metal. In bacteria, most metal ions presumably reach the bacterial cytoplasm through porins and specific or non-specific transporters in the inner membrane. The lack of rigorous control or specific uptake system for some metals is often compensated for by the presence of effective efflux systems. This allows cells to tolerate the excess of metal(s) in their immediate environment by expelling the surplus of metal ions (Arguello *et al.*, 2007; von Rozycki and Nies, 2009; Capdevila *et al.*, 2017; Chandrangsu *et al.*, 2017). The P<sub>1B</sub>-type ATPases family of heavy metal transporters is the most frequently present in bacteria. They are efficient efflux pumps that extrude excess of toxic metal ions such as copper (Cu<sup>+</sup>), zinc (Zn<sup>2+</sup>), cadmium (Cd<sup>2+</sup>) or silver (Ag<sup>+</sup>) from the cytoplasm to the

Received 27 January, 2020; revised 15 April, 2020; accepted 16 April, 2020.

For correspondence. \*E-mail [anne.soisig.steunou@i2bc.paris-saclay.fr](mailto:anne.soisig.steunou@i2bc.paris-saclay.fr); Tel. +(33)-169823137; Fax +(33)-169823230. \*\*E-mail [soufian.ouchane@i2bc.paris-saclay.fr](mailto:soufian.ouchane@i2bc.paris-saclay.fr); Tel. +(33)-169823137; Fax +(33)-169823230.

*Microbial Biotechnology* (2020) 0(0), 1–15  
doi:10.1111/1751-7915.13589

### Funding information

We gratefully acknowledge the support of the CNRS and the Microbiology Department of I2BC.

2 A. S. Steunou et al.

periplasm in which metal is handled by other detoxifying proteins (Arguello *et al.*, 2007). The effectiveness of these metal efflux systems prevents the molecular and physiological damages that metal can cause. Therefore, mutants defective in metal homeostasis machineries, specifically in the efflux systems, shed light on the toxicity mechanisms and the molecular events following metal accumulation within the cell. Lines of evidence showed that while excess of metal can cause damage to [4Fe-4S] clusters and mismetallation of metalloproteins under strict anaerobic condition (Macomber and Imlay, 2009), contribution of reactive oxygen species (ROS) should be taken into account under aerobic condition.

Superoxide is produced in presence of oxygen by some aerobic respiratory complexes and other non-respiratory flavoproteins, like the lipoamide or xanthine dehydrogenases. It can directly damage exposed catalytic [4Fe-4S] clusters in dehydratases or mononuclear Fe<sup>2+</sup> enzymes, or indirectly damage other cell components by contributing to the production of hydroxyl radicals (Imlay, 2013; Imlay, 2019). To deal with superoxide in the cytoplasm, bacteria possess either one or two superoxide dismutases (Fe-Sod and Mn-Sod) whose expression is differently regulated by redox-cycling compounds and by iron (Imlay, 2013; Imlay, 2019). In enteric bacteria such as *Escherichia (E.) coli*, *sodA* gene is regulated by the SoxRS system. The transcriptional factor SoxR functions as a sensor of oxidative stress in response to changes in the redox state of its [2Fe-2S] cluster (Imlay, 2013; Kobayashi, 2017; Imlay, 2019). SoxR activates the transcriptional factor SoxS that in turn induces the transcription of many genes including *sodA*. Nonetheless, the majority of SoxR regulons in bacteria, including *Vibrio* and *Pseudomonas*, lack the *soxS* gene (Dietrich *et al.*, 2008). Expression of Sod in these bacteria does not involve SoxR and relies mainly on iron homeostasis and regulators. In *E. coli* and other bacteria, when iron is available, the Fe<sup>2+</sup>-Fur repressor inhibits Mn-Sod and small RNA RyhB production and activates the Fe-Sod synthesis. In contrast, under iron limitation, Fur is inactivated, which induces the synthesis of the Mn-Sod and the transcription of the small RyhB RNA. RyhB interaction with Fe-Sod mRNA triggers degradation of the mRNA and thus promotes decrease of Fe-Sod in the cells (Masse and Gottesman, 2002; Imlay, 2013; Imlay, 2019).

Metal stress promotes increase in the level of oxidative stress-associated defence enzymes such as superoxide dismutases (SOD), catalases and peroxidases, which suggest elevated ROS in metal-stressed cells (Krumnschnabel *et al.*, 2005; Macomber *et al.*, 2007; Helbig *et al.*, 2008; Ray *et al.*, 2013; Xu *et al.*, 2019). The involvement of these enzymes in metal stress

response was further supported by the metal-sensitive phenotype of *E. coli* mutant of which two genes encoding SOD were concomitantly inactivated (Geslin *et al.*, 2001).

Macomber and co-workers reported that while copper did not induce significant oxidative DNA damage in copper-overloaded *E. coli* cells, they exhibited increased catalase (KatG and KatE) and superoxide dismutase activities. This suggested an induction of SoxRS regulons and the presence of elevated amounts of hydrogen peroxide and superoxide in these cells (Macomber *et al.*, 2007). Metals such as Fe<sup>2+</sup> and Cu<sup>+</sup> are redox-active ions which, in presence of oxygen, can induce the formation of reactive oxygen species *via* Fenton and Haber-Weiss-type reactions (Gunther *et al.*, 1995). These metals are also toxic under anaerobic condition, as Cu<sup>+</sup> was shown to directly poison bacteria by damaging the exposed [4Fe-4S] clusters of dehydratases in *E. coli* (Macomber and Imlay, 2009) and those of porphyrin biosynthesis enzymes in the photosynthetic bacterium *Rubrivivax (R.) gelatinosus* and the human pathogen *Neisseria gonorrhoea* (Azzouzi *et al.*, 2013; Djoko and McEwan, 2013). Toxicity of non-redox-active metals such as Cd<sup>2+</sup> or Zn<sup>2+</sup> was also associated with destruction of exposed [4Fe-4S] clusters, and release of iron, which in turn might produce hydroxyl radicals *via* the Fenton reaction (18).

In the present study, we investigated the role of superoxide dismutase and superoxide stress in heavy metal toxicity. We found that Cd<sup>2+</sup> or Cu<sup>+</sup> stress induced the expression and activity of the cytosolic Fe-Sod or Mn-Sod in many bacteria including *R. gelatinosus*, *E. coli*, *Vibrio (V.) cholerae*, *Pseudomonas (P.) aeruginosa*, *P. putida* and *Bacillus (B.) subtilis*, when the metal efflux systems are missing.

Although SOD induction by excess metal was previously reported in many transcriptomic data sets, the importance and consequences of SOD inactivation under excess metal in metal efflux deficient mutants were never reported. Here, the Cd<sup>2+</sup> and Cu<sup>+</sup> hypersensitive phenotypes of mutants lacking SOD along with the Cd<sup>2+</sup> and Cu<sup>+</sup>-ATPases, respectively, were shown to emphasize the importance of SOD and ROS detoxification in metal toxicity. Altogether, the data demonstrated the involvement of SOD in the protection of heavy metal-exposed cells and shed light on the synergy of excess metal and superoxide in heavy metal toxicity.

## Results

### *Induction of a 22 kDa protein in cadR<sup>-</sup> and ΔcadA deficient strains*

To deal with toxic Cd<sup>2+</sup> exposure, bacteria usually induce the expression of gene encoding the metal efflux

ATPase, CadA (also known as ZntA in some species, as it expels  $Zn^{2+}$  as well). The major transcriptional regulator CadR interacts with  $Cd^{2+}$ , thereby allowing induction of the expression of the CadA ATPase. While these genes are widely distributed in bacterial species, purple photosynthetic bacteria can encounter  $Cd^{2+}$  in their environment and are therefore suitable models to assess the effect of  $Cd^{2+}$  on their growth. Requirement for CadR in CadA expression and metal tolerance was assessed in the purple photosynthetic bacterium *R. gelatinosus* wild-type and *cadR*<sup>-</sup> mutant cells. To this end, total cell extracts from overnight culture of wild-type and *cadR*<sup>-</sup> mutant grown under photosynthetic condition with different concentrations of  $CdCl_2$  were analysed by Western blot. Note that CadA and the periplasmic copper protein CopI can be readily detected by conventional HisProbe due to the presence of histidine-rich motifs within these proteins. In the wild-type,  $Cd^{2+}$  induced a steady increase in the amount of CadA and CopI proteins (Fig. 1A). In the *cadR*<sup>-</sup> mutant, CadA was not induced below 600  $\mu M$  of  $CdCl_2$ . Unexpectedly, however, apparent induction of CadA was observed with excess  $CdCl_2$  (800 and 1000  $\mu M$ ). Furthermore, a 22 kDa protein band revealed by the HisProbe was clearly induced up to 600 but not with 800 and 1000  $\mu M$  of  $CdCl_2$  (Fig. 1A). Interestingly, the corresponding band was only slightly expressed in the wild-type cells, even for those challenged with excess  $Cd^{2+}$ . Concomitantly to CadA induction, the 22 kDa protein amount decreased upon elevated  $Cd^{2+}$  stress (800 and 1000  $\mu M$ ) in the *cadR*<sup>-</sup> mutant (Fig. 1A). Taken together, these data confirmed that  $Cd^{2+}$  induced the expression of the  $Cd^{2+}$ -efflux ATPase CadA and the production of a 22 kDa protein in CadR-deficient cells. Moreover, these data

suggested a direct link between the expressions of these two proteins. To test this possibility, CadA-deficient mutant  $\Delta cadA$  of *R. gelatinosus* was subjected to  $Cd^{2+}$  stress. In contrast to *cadR*<sup>-</sup>, growth of the  $\Delta cadA$  mutant was inhibited beyond 200  $\mu M$   $CdCl_2$  (see below); therefore, the analysis included only low  $CdCl_2$  concentrations. As expected,  $Cd^{2+}$  excess (100 or 200  $\mu M$ ) caused an increase in the amount of CadA and CopI proteins, but the amount of the 22 kDa protein remained unchanged in the wild-type strain (Fig. 1B). In contrast, both CopI and the 22 kDa protein were induced in the  $Cd^{2+}$ -stressed  $\Delta cadA$  mutant cells (Fig. 1B). Therefore, in the absence of the CadA ATPase,  $Cd^{2+}$  induced the expression of the 22 kDa protein which could be involved in  $Cd^{2+}$  response and tolerance. Similar results showing the induction of the 22 kDa protein in *cadR*<sup>-</sup> and  $\Delta cadA$  strains were obtained under respiratory (aerobic) condition (Fig. S1). Alongside this study, biochemical experiments in our group suggested that the 22 kDa protein may correspond to the Fe-Sod superoxide dismutase, SodB (unpublished data).

#### Induction of SodB in response to excess $Cd^{2+}$ in the $\Delta cadA$ mutant

Various SOD genes encode the enzymes responsible for superoxide dismutation and contribute to the protection of bacteria against ROS (Beyer *et al.*, 1991; Imlay, 2003). These SODs vary by their metal cofactors but also by their subcellular localization. Analysis of the genome of *R. gelatinosus* highlighted the presence of two SOD encoding genes: *sodC* and *sodB*, which, respectively, encode the 15 kDa periplasmic Cu-Zn SodC and a cytosolic 21.5 kDa Fe-Sod. SodB displays

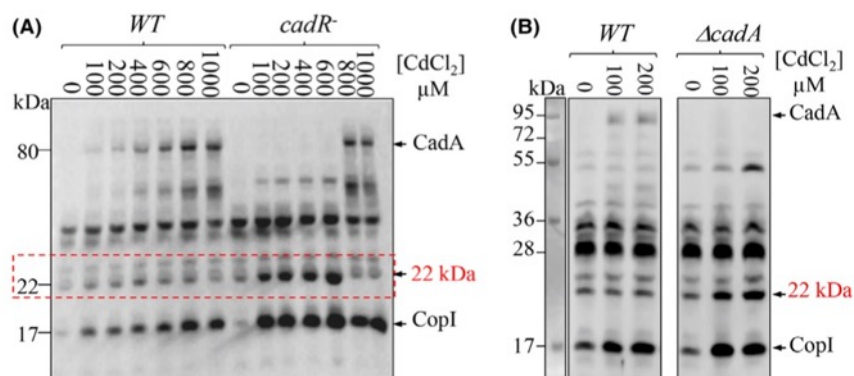


**Fig. 1.** Induction of His-rich 22 kDa protein in  $Cd^{2+}$  efflux pump mutants in *R. gelatinosus*. Induction of CadA, CopI and the 22 kDa proteins in *R. gelatinosus* wild-type (WT) strain, *cadR*<sup>-</sup> (A) and  $\Delta cadA$  mutants (B). Total protein extracts from the same amount of cells (0.1 OD<sub>680nm</sub>) grown overnight in photosynthetic condition with indicated concentration of  $CdCl_2$  were separated on 15% SDS-PAGE and analysed by Western blot using the HRP-HisProbe. Growth of *cadR*<sup>-</sup> with 800 and 1000  $\mu M$  of  $CdCl_2$  started after 3 days (very likely suppressors). CadA, CopI and the 22 kDa protein are indicated.

6 A. S. Steunou et al.

grown with excess  $\text{CuSO}_4$  showed increased level of CopI, while amount and activity of SodB remained unchanged (Fig. 4A and B). In contrast, induction of CopI in the  $\text{copA}^-$  cells was associated with an increased amount and activity of the superoxide dismutase SodB, with similar degree to  $\Delta\text{cadA}$  cells exposed to  $\text{CdCl}_2$  (Fig. 4A and B). Then, it is conceivable that SodB would also be required for tolerance to excess  $\text{Cu}^+$ . To address this, growth inhibition of the double mutant  $\Delta\text{sodB}\text{copA}^-$  strain in presence of increasing concentration of  $\text{CuSO}_4$  was monitored under photosynthetic and respiratory conditions and compared with  $\Delta\text{sodB}$  or  $\text{copA}^-$  single mutants (Fig. 4C and D). Disruption of the  $\text{sodB}$  gene in the wild-type background did not affect copper tolerance since  $\Delta\text{sodB}$  mutant growth was comparable to that of the wild-type. However, disruption of  $\text{sodB}$  gene in the  $\text{copA}^-$  mutant background led to a strong decrease in  $\text{Cu}^+$  tolerance (Fig. 4C and D). Disc diffusion assay was also performed in presence of  $\text{CuSO}_4$  and menadione, and the results indicated the hypersusceptibility of the  $\Delta\text{sodB}\text{copA}^-$  strain to  $\text{Cu}^{2+}$  and superoxide on solid medium (Fig. S5). These results confirmed that SOD was also required for bacterial survival under copper stress when the  $\text{Cu}^+$ -efflux system was defective.

Altogether, association between the induction of SodB by metal excess and the hypersensitivity to the cognate metal in the SOD-efflux pump double mutant appeared to

be common in *R. gelatinosus*. To understand whether this is a general phenomenon in bacteria, we tested induction of SOD by excess metal in different bacterial species.

*Fe-Sod activity and amount were also increased in V. cholerae under  $\text{Cd}^{2+}$  stress*

*Vibrio cholerae* is an aquatic bacterium but can infect human intestine to cause diarrhoeal diseases. *V. cholerae* encodes genes for two cytoplasmic SODs, the Mn-Sod (*vc2696* or *sodA*) and the Fe-Sod (*vc2045* or *sodB*) on the genome. However, *in-gel* SOD activity assay indicated that only SodB was active in our condition (Fig. 5A). *V. cholerae* also possesses  $\text{Cd}^{2+}/\text{Zn}^{2+}$ - and  $\text{Cu}^+$ -efflux ATPases, encoded by *zntA* (*vc1033*, hereafter referred to as *cadA* for clarity) and *copA* (*vc2215*) respectively. To assess the effect of increasing concentration of  $\text{Cd}^{2+}$  on SodB activity in *V. cholerae*, wild-type and the  $\text{cadA}^-$  mutants were grown in the presence of excess  $\text{CdCl}_2$  and the soluble fractions were analysed on non-denaturing PAGE for SOD activity. In the wild-type fractions, SodB activity was comparable between  $\text{CdCl}_2$  exposed and non-exposed cells (Fig. 5B). In contrast, the  $\text{cadA}^-$  mutant exposed to  $5 \mu\text{M}$   $\text{CdCl}_2$  showed significant increase in SodB activity in comparison with non-exposed cells and the wild-type. Western blot analysis confirmed the increase in SodB amount only in the

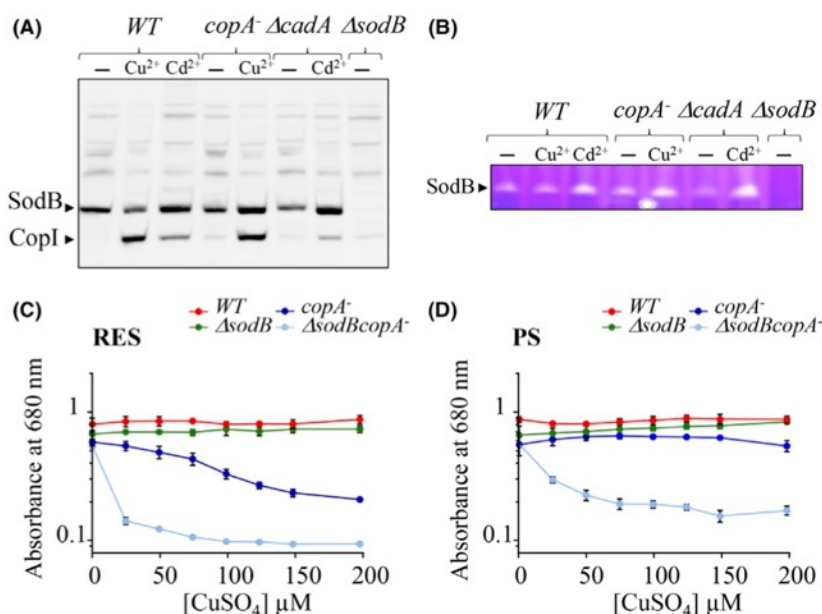


**Fig. 4.** Involvement of SodB in copper stress in *R. gelatinosus*. Western blot analysis of wild-type (WT),  $\Delta\text{cadA}$ ,  $\text{copA}^-$  and  $\Delta\text{sodB}$  mutants grown in malate medium supplemented or not (-) with  $100 \mu\text{M}$   $\text{CdCl}_2$  ( $\text{Cd}^{2+}$ ) or  $\text{CuSO}_4$  ( $\text{Cu}^{2+}$ ) (A). Cells were grown by photosynthesis, and total protein extracts from the same amount of cells ( $0.1 \text{ OD}_{680\text{nm}}$ ) were analysed by Western blot using the HRP-HisProbe. SOD activity assay on non-denaturing PAGE. Soluble fractions from the  $\Delta\text{cadA}$ ,  $\text{copA}^-$  and  $\Delta\text{sodB}$  mutants were separated on 15% PAGE (B). Dose-response curves of the WT,  $\Delta\text{sodB}$ ,  $\text{copA}^-$  and  $\Delta\text{sodB}\text{copA}^-$  strains. Cells were grown in presence of increasing concentration of  $\text{CuSO}_4$  by respiration (C) or under photosynthesis condition (D) for 24 h. Results represent mean  $\pm$  stdev from 3 independent experiments.

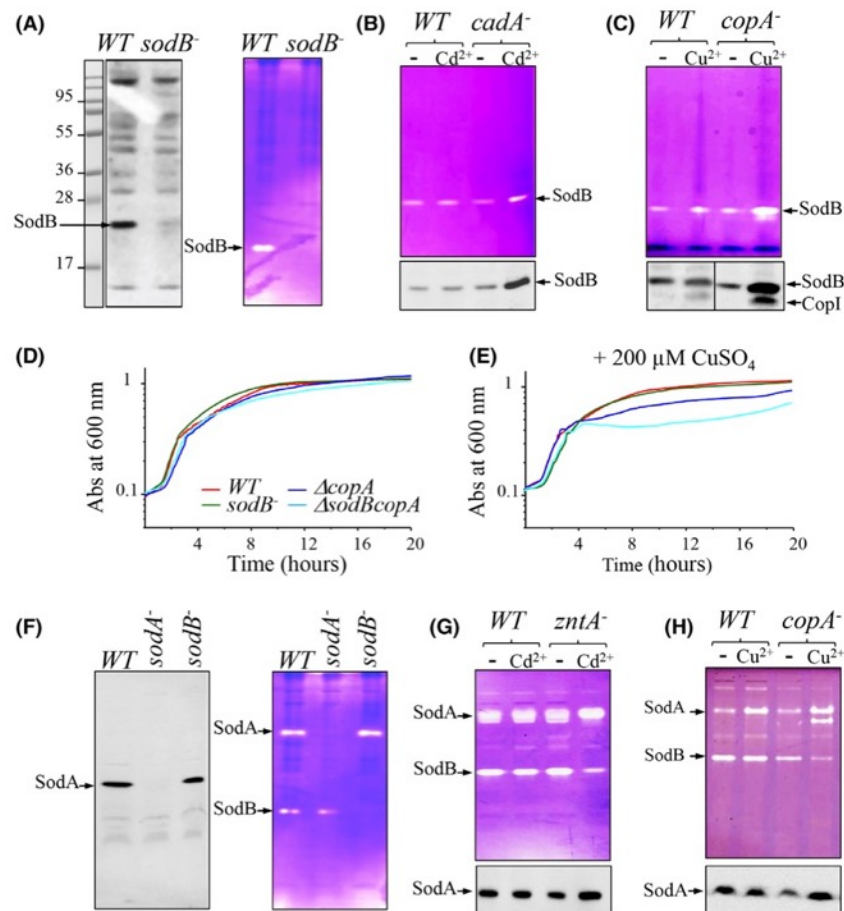


**Fig. 5.** SOD activity was induced in the ATPase mutants of *V. cholerae* and *E. coli*. Western blot and SOD *in-gel* activity assay of soluble fractions from wild-type (*WT*) and *SodB*<sup>-</sup> strains of *V. cholerae* (A). *SodB* activity and expression in *V. cholerae* were induced in the ATPase-deficient mutants *cadA*<sup>-</sup> and *copA*<sup>-</sup> in response to 5 μM CdCl<sub>2</sub> (Cd<sup>2+</sup>) (B) or 200 μM CuSO<sub>4</sub> (Cu<sup>2+</sup>) (C) as shown by the *in-gel* activity assay and on the Western blots. Effect of excess CuSO<sub>4</sub> on growth of the *V. cholerae* Δ*sodBcopA* deletion strain. *WT*, the single mutants Δ*copA*, *sodB*<sup>-</sup> and the Δ*sodBcopA* mutant were grown overnight in LB (D) or LB supplemented with 200 μM of CuSO<sub>4</sub> (E), growth was monitored at 600 nm with a Tecan Infinite. Western blot and SOD *in-gel* activity assay of soluble fractions from *WT*, *SodA*<sup>-</sup> and *SodB*<sup>-</sup> strains of *E. coli* (F). *SodB* activity was reduced, while *SodA* increased in the ATPase mutants *zntA*<sup>-</sup> and *copA*<sup>-</sup> in response to 20 μM CdCl<sub>2</sub> (Cd<sup>2+</sup>) (G) or 100 μM CuSO<sub>4</sub> (Cu<sup>2+</sup>) (H) as shown by the *in-gel* activity assays and on the Western blots.

*cadA*<sup>-</sup> deficient mutant when exposed to CdCl<sub>2</sub> (Fig. 5B).

Similarly to the effect of cadmium in *cadA*<sup>-</sup>, both the activity and amount of *SodB* were also induced in the *copA*<sup>-</sup> *V. cholerae* cells when challenged with 200 μM CuSO<sub>4</sub> (Fig. 5C). Note that induction of *CopI* (*vc0260*) was appreciated in *copA*<sup>-</sup> mutant and not in *cadA*<sup>-</sup> *V. cholerae* cells (Fig. 5B and C). We then assessed the requirement of *SodB* for excess Cu<sup>+</sup> tolerance in the absence of *CopA*. We introduced Δ*copA* mutation in *sodB*<sup>-</sup> strain and showed that the Δ*sodBcopA* double mutant has comparable growth rate in LB medium with the wild-type and the single mutants (Fig. 5D). When cells were challenged by 200 μM CuSO<sub>4</sub>, *sodB* mutation did not affect copper tolerance, while Δ*copA* mutant showed slight growth defect (Fig. 5E). Importantly, the Δ*sodBcopA* double mutant

showed more sensitivity to copper than the Δ*copA* mutant (Fig. 5E). Altogether, even though the phenotype was not as strong as in *R. gelatinosus*, we concluded that *SodB* was also important for metal tolerance in *V. cholerae* given its high induction under excess metal and the sensitive phenotype of the double mutant.

*Mn-Sod* and *Fe-Sod* activity and amount, respectively, increased and decreased in response to excess Cd<sup>2+</sup> or Cu<sup>+</sup> in *E. coli*

In contrast to *R. gelatinosus* and *V. cholerae*, both the *Fe-Sod* (*SodB*) and the *Mn-Sod* (*SodA*) are active in *E. coli* (Carlioz and Touati, 1986) (Fig. 5F). Note that unlike *R. gelatinosus* and *V. cholerae*, *E. coli* *SodB* contains only four histidines in its amino terminus and is not detectable

sufficient active [Fe-S] clusters to sustain growth (Fig. 7). In addition, the presence of elevated level of superoxide with released iron from damaged clusters or imported by the uptake systems would participate in Fenton chemistry and catalyse hydroxyl radical formation in these cells, thereby contributing to cell growth inhibition. A similar scenario was reported to explain the toxicity of copper in macrophages, in which bacterial killing is caused by copper overloading and hydrogen peroxide production (White *et al.*, 2009). Our findings, with both redox-active  $\text{Cu}^+$  and non-active  $\text{Cd}^{2+}$ , support this scenario and suggest that metal overloading and superoxide synergistically poison cells because they both destabilize exposed [4Fe-4S] clusters and likely target the same [4Fe-4S] enzymes.

One remarkable finding in this study is the induction of SOD expression and activity in the efflux ATPase mutants from different bacterial species when exposed to excess metal. This raised the question of the molecular mechanisms that underpinned SOD induction by excess  $\text{Cd}^{2+}$  or  $\text{Cu}^+$ . It is well established in *E. coli* and other bacteria that Mn-Sod and Fe-Sod expressions are partly regulated by the iron status within the cell. This regulation involves the Fur repressor and the sRNA RyhB that downregulate non-essential iron-containing proteins when iron is limiting (Masse and Gottesman, 2002; Imlay, 2019). Under such condition, the Fe-Sod expression is repressed, whereas the Mn-Sod is upregulated to convert superoxide into  $\text{H}_2\text{O}_2$  and protect cells from oxidative stress. Excess  $\text{Cu}^{2+}$  or  $\text{Cd}^{2+}$  in bacteria and eukaryotes was shown to interfere with iron homeostasis. Many studies suggest that excess  $\text{Cd}^{2+}$ ,  $\text{Ni}^{2+}$ ,  $\text{Co}^{2+}$ ,  $\text{Zn}^{2+}$  or  $\text{Cu}^+$  may generate an Fe-starvation signal and lead to the induction of iron uptake systems (Stadler and Schweyen, 2002; Yoshihara *et al.*, 2006; Houot *et al.*, 2007; Chillappagari *et al.*, 2010; Xu *et al.*, 2019). This could be a direct effect of [4Fe-4S] cluster degradation. Indeed, Keyer and Imlay elegantly showed that 'released iron' originating from [4Fe-4S] degradation was rapidly sequestered, and iron uptake was then required to supply iron to the Fe-S machinery in response to peroxynitrite stress (Keyer and Imlay, 1997). In *E. coli*, we observed a decrease of the Fe-Sod and increase of the Mn-Sod, which suggest that under excess  $\text{Cu}^+$  or  $\text{Cd}^{2+}$  stress, cells encounter a state of iron limitation. Furthermore, in *E. coli*, SoxR/SoxS directly induced the expression of the Mn-Sod in response to superoxide or redox-recycling compounds (Imlay, 2019). Therefore, if superoxide is produced under metal stress, then it could also explain the induction of Mn-Sod under  $\text{Cu}^+$  or  $\text{Cd}^{2+}$  stress by SoxRS. Oxidation of the 2Fe-2S cluster of SoxR by superoxide or redox-active compounds activates SoxR (Imlay, 2013; Kobayashi, 2017; Imlay, 2019).  $\text{Cu}^+$  is a potent

oxidant,  $\text{Cd}^{2+}$  is not. We observed the same SodA induction in cells challenged with excess  $\text{Cu}^+$  or  $\text{Cd}^{2+}$ , suggesting that if  $\text{Cu}^+$  and  $\text{Cd}^{2+}$  induction of SodA involves SoxRS, SoxR would be indirectly activated by these cations.

Unlike *E. coli*, *soxRS* genes are missing in *R. gelatinosus* genome. *V. cholerae* encodes SoxR homologue but not SoxS; however, the only available superoxide dismutase to protect the cell from the deleterious effects of superoxide is the iron-dependent SodB. Therefore, in these bacteria, there is no other choice but to express SodB in spite of the putative iron limitation status. To corroborate this hypothesis, we have shown that like iron starvation,  $\text{Cu}^+$  and  $\text{Cd}^{2+}$  excess induced iron uptake system as attested by the accumulation of the iron-binding protein FbpA in the periplasm of *R. gelatinosus* (Steunou *et al.*, 2020b). The induction of Sod in the ATPase mutants is therefore indirect and is probably the consequence of iron homeostasis dysregulation by excess  $\text{Cd}^{2+}$  or  $\text{Cu}^+$ .

Metals such as  $\text{Cd}^{2+}$  or  $\text{Cu}^+$  can displace or replace  $\text{Fe}^{2+}$  in the ferric uptake regulator Fur and may therefore affect Fur-DNA binding (Adrait *et al.*, 1999; Mills & Marletta, 2005; Vitale *et al.*, 2009). Nevertheless, if  $\text{Cd}^{2+}$  or  $\text{Cu}^+$  metallates Fur *in vivo* and allows binding to the Fur box, we may then expect a repression of the iron uptake systems and induction of the Fe-Sod. Our results showed, however, an induction of Fe-Sod and the FbpABC iron uptake system (Steunou *et al.*, 2020b), which rather suggest that Fur is unloaded in the presence of  $\text{Cd}^{2+}$  or  $\text{Cu}^+$ .

In *Vibrio tasmaniensis*, a pathogenic strain of oysters, the Mn-Sod is active. In this *vibrio*, it was shown that the  $\text{Cu}^+$ -efflux system (including CopA) and the ROS detoxification system (including SodA) were highly induced intracellularly (more than 50 fold) and that they are required for *vibrio* intracellular survival in phagocytes and cytotoxicity to haemocytes (Vanhove *et al.*, 2016). As for *V. cholerae*, for *Vibrio shiloi* (a coral pathogen), the Fe-Sod was required for survival of the bacterium in the coral ectodermal cells (Vanhove *et al.*, 2016).

In *P. aeruginosa*, transcriptional profiles of exposed cells to  $\text{Cu}^{2+}$  ions (Teitzel *et al.*, 2006),  $\text{Cd}^{2+}$  or  $\text{Zn}^{2+}$  nanoparticles also showed an increase in the relative amount of the Mn-Sod superoxide dismutase SodA transcript (Manara *et al.*, 2012; Yang *et al.*, 2012). The increase of SodA in these strains could be also related to iron homeostasis, as several genes induced under iron-limiting condition were upregulated in copper-stressed cells. In *P. putida*, quantitative proteomic studies showed upregulation of SOD in  $\text{Ni}^{2+}$ ,  $\text{Co}^{2+}$  or  $\text{Cd}^{2+}$ -treated cells, suggesting an increased production of superoxide radicals due to the presence of metal (Cheng *et al.*, 2009; Manara *et al.*, 2012; Ray *et al.*, 2013). These studies also pointed out for a role of iron

starvation in the induction of SOD since they also report the increased level of iron import proteins under metal stress. In Gram + bacteria, the superoxide dismutase SodM was also significantly induced by CuSO<sub>4</sub> in *Staphylococcus aureus* (Tarrant *et al.*, 2019). In *B. subtilis*, transcriptional profiles of exposed cells to Cu<sup>2+</sup> ions also demonstrated that copper stress induced genes required for iron uptake and a slight increase in the SodA transcript (Chillappagari *et al.*, 2010). In the cyanobacterium *Synechocystis sp.* PCC 6803, high copper treatment also induced the expression of the iron superoxide dismutase *sodB* (Giner-Lamia *et al.*, 2014). Very recently, mercury (Hg<sup>2+</sup>) was shown to induce ROS scavenging genes transcripts including the Mn-Sod in the thermophilic aerobe *Thermus thermophilus*. *T. thermophilus*  $\Delta$ *sod* mutant exhibited an increased sensitivity to Hg<sup>2+</sup> (Norambuena *et al.*, 2019).

Collectively, these results showed that SOD was induced under metal excess stress in bacteria. The mechanisms of induction might be both direct and indirect and very likely involved iron homeostasis dysregulation and SoxRS system when present as in *E. coli*. The data also showed that the SOD scavenging activity was vital when the metal efflux systems were defective. Increase in the SOD amount and activity would protect metal-exposed cells by decreasing superoxide concentration and hence would save some exposed [4Fe-4S] clusters from degradation (Imlay, 2019).

Extensive use of antibiotics in health care and agriculture has led to an increase in antibiotic resistance (Asante and Osei Sekyere, 2019). Copper and zinc exhibit antimicrobial properties and are used as alternatives to antibiotics in farming and agriculture. Nevertheless, the use of high concentrations of these cations led to environment contamination and to co-selection of antibiotic resistance genes (Baker-Austin *et al.*, 2006; Purves *et al.*, 2018; Rensing *et al.*, 2018; Bischofberger *et al.*, 2020). To avoid such impacts, we need to significantly reduce the concentration of metal in metal-based antimicrobial treatments. Our findings showed that superoxide detoxification system became determinant for bacterial survival under metal stress. Moreover, induction of SOD by excess metal appears to be a general phenomenon in bacteria; therefore, targeting the ROS defence system together with the metal efflux systems may allow lowering the concentration of metals in the metal-based antimicrobial treatments in agriculture and farming.

## Experimental procedures

### Bacterial strains and construction of mutants

Bacterial strains and plasmids used in this study are listed in Table S1. Standard methods were performed according to Sambrook *et al.* (1989) unless indicated

otherwise. To inactivate *sodB*, a 1.7 kb fragment was amplified using the primers RG345\_*sodBF* and RG346\_*sodBR* (Table S2) and cloned into the PCR cloning vector pGEM-T to give *pGsodB*. *sodB* gene was inactivated by deletion of a 50 bp fragment and the insertion of the 1.2 kb Km cassette at the MscI and StuI sites within the *sodB* coding sequence. The resulting recombinant plasmid was designated *pGsodB::Km*. A 2.4 kb fragment obtained by PCR using RG369\_*xseAF* and RG370\_*sodBR* containing the entire *xseAsodB* gene was cloned into pGEM-T to give *pGxseAsodB*. *xseAsodB* was sub-cloned in pBBR1MCS-3 at the SmaI-SacI sites. The resulting plasmid was designated *pBxseAsodB*. From this plasmid, *xseA* was deleted by digestion with SacI and SmaI giving the *pBsodB* plasmid. Those plasmids were used for the complementation of  $\Delta$ *sodB*. Transformation of *R. gelatinosus* cells was performed by electroporation (Ouchane *et al.*, 1996). The plasmid *pGsodB::Km* was used to transform the wild-type, the *copA*<sup>-</sup> and  $\Delta$ *cadA* strains. Transformants were selected on malate plates supplemented with the appropriate antibiotics under respiratory condition. Following transformant selection, template genomic DNA was prepared from the ampicillin-sensitive transformants and confirmation of the antibiotic resistance marker's presence at the desired locus was performed by PCR.

To construct  $\Delta$ *copA* in *V. cholerae*, ~ 600 bp fragments upstream and downstream to the *copA* were amplified using primers oYo848 and oYo849, and oYo850 and oYo851 respectively (Table S2). Resulting fragments were cloned into SmaI site of pCVD442 vector (Donnenberg and Kaper, 1991) using Gibson Assembly (Gibson *et al.*, 2009), resulting in pEYY345.  $\Delta$ *copA* mutation was then introduced in C6706 (wild-type) and C6706 *sodB::Tn* strains, kindly provided by J. Mekalanos (Cameron *et al.*, 2008), by allelic exchange (Donnenberg and Kaper, 1991).

Single-gene deletion mutant library of *E. coli* (KEIO collection (Baba *et al.*, 2006)) was obtained from the National BioResource Project, National Institute of Genetics, Japan. *P. aeruginosa* mutants were obtained from the Comprehensive *P. aeruginosa* Transposon Mutant Library at the University of Washington Genome Center (Jacobs *et al.*, 2003). *P. putida* strains were kindly provided by Sanjay Swarup (Adaikkalam and Swarup, 2002), and *B. subtilis* strains were gift from Peter Graumann (Chillappagari *et al.*, 2010).

### Cell preparation, growth and growth inhibition

*Rubrivivax gelatinosus* was grown at 30°C, in the dark aerobically (high oxygenation: 250 ml flasks containing 20 ml medium, referred to as respiratory condition) or under light microaerobically (in filled tubes with residual

12 A. S. Steunou et al.

oxygen in the medium, termed as photosynthetic condition) in malate growth medium. *E. coli*, *V. cholerae*, *B. subtilis* and *P. aeruginosa* were grown overnight at 37°C in LB medium. *P. putida* was grown at 30°C in LB medium. Antibiotics were added at following concentrations when appropriate: kanamycin, ampicillin, tetracycline, spectinomycin and trimethoprim (50 µg ml<sup>-1</sup>), streptomycin (100 µg ml<sup>-1</sup>).

Growth curves in respiratory condition were monitored at OD<sub>680nm</sub> with measurements taken every 15 min for 24 h using a Tecan Infinite M200 luminometer (Tecan, Mannerdorf, Switzerland). For growth inhibition under photosynthetic condition, strains were grown in filled tubes and OD<sub>680nm</sub> was measured after 24 h using the Tecan luminometer.

For disc diffusion assay, 200 µl (1 OD<sub>680nm</sub>) of overnight grown cells was mixed with 7 ml semi-solid agar and uniformly spread onto solidified agar plates. Sterile discs (6 mm) were soaked with 10 µl of 10 mM menadione and placed in the middle of the plate. Plates were incubated overnight at 30°C under either photosynthetic or respiratory condition. The disc diffusion method was performed in triplicate, and the mean of the measured inhibition zones was calculated.

#### *SOD in-gel activity assay on non-denaturing gel electrophoresis*

About 20 µg of soluble proteins was separated on a 10% non-denaturing polyacrylamide gel and stained for SOD activity as described in Weydert and Cullen (2010), with minor modifications. Incubation with TEMED (0.85%) and Riboflavin-5-Phosphate (56 µM) was performed for 15 min at light and room temperature (RT), followed by the addition of nitroblue tetrazolium (2 mg ml<sup>-1</sup>) and a 15 min incubation in the dark at RT. Gel was washed twice in ddH<sub>2</sub>O and left in ddH<sub>2</sub>O at RT on a light box until SOD-positive staining appeared.

#### *Western blot and HisProbe-HRP detection*

Equal amount of soluble proteins (20 µg) or disrupted cells (1 OD<sub>680nm</sub>) when indicated was separated on SDS-PAGE and transferred onto a Hybond ECL Polyvinylidene difluoride membrane (GE Healthcare). Membrane was then probed with the HisProbe-HRP (horseradish peroxidase, from Pierce) according to the manufacturer's instruction. The HisProbe-HRP allows detection of proteins (including Sod) exhibiting at least five His residues in their N-ter domain. Those with only four His residues (*E. coli* SodB) are not detected with this probe. Positive bands were detected using a chemiluminescent HRP substrate according to the method of

Haan and Behrmann (Haan and Behrmann, 2007). Image capture was performed with a ChemiDoc camera system (Bio-Rad).

#### **Acknowledgements**

We gratefully acknowledge the support of the CNRS and the Microbiology Department of I2BC. We are very grateful to Prof. Peter Graumann and Antje Schäfer at Marburg, Germany, and to Prof. Sanjay Swarup and Miko Poh Chin Hong at NUS Singapore for providing strains. We also acknowledge the National BioResource Project, National Institute of Genetics, Japan, for providing *E. coli* strains.

#### **Conflict of interest**

The authors declare that they have no conflicts of interest with the contents of this manuscript.

#### **Author contributions**

ASS and SO conceived of the study. ASS, MB, MLB, RT, AD, YY and SO acquired and analysed data. ASS, MB, AD, AKL and SO interpreted the data. ASS and SO wrote the manuscript.

#### **References**

- Adaikkalam, V., and Swarup, S. (2002) Molecular characterization of an operon, *cueAR*, encoding a putative P1-type ATPase and a MerR-type regulatory protein involved in copper homeostasis in *Pseudomonas putida*. *Microbiology* **148**: 2857–2867.
- Adrait, A., Jacquamet, L., Le Pape, L., Gonzalez de Peredo, A., Aberdam, D., Hazemann, J.L., et al. (1999) Spectroscopic and saturation magnetization properties of the manganese- and cobalt-substituted Fur (ferric uptake regulation) protein from *Escherichia coli*. *Biochemistry* **38**: 6248–6260.
- Arguello, J.M., Eren, E., and Gonzalez-Guerrero, M. (2007) The structure and function of heavy metal transport P1B-ATPases. *Biometals* **20**: 233–248.
- Asante, J., and Osei Sekyere, J. (2019) Understanding antimicrobial discovery and resistance from a metagenomic and metatranscriptomic perspective: advances and applications. *Environ Microbiol Rep* **11**: 62–86.
- Azzouzi, A., Steunou, A.S., Durand, A., Khalifaoui-Hassani, B., Bourbon, M.L., Astier, C., et al. (2013) Coproporphyrin III excretion identifies the anaerobic coproporphyrinogen III oxidase HemN as a copper target in the Cu<sup>+</sup>-ATPase mutant *copA*<sup>-</sup> of *Rubrivivax gelatinosus*. *Mol Microbiol* **88**: 339–351.
- Baba, T., Ara, T., Hasegawa, M., Takai, Y., Okumura, Y., Baba, M., et al. (2006) Mori H (2006) construction of *Escherichia coli* K-12 in-frame, single-gene knockout mutants: the Keio collection. *Mol Syst Biol* **2**: 0008.

- Baker-Austin, C., Wright, M.S., Stepanauskas, R., and McArthur, J.V. (2006) Co-selection of antibiotic and metal resistance. *Trends Microbiol* **14**: 176–182.
- Ballabio, C., Panagos, P., Lugato, E., Huang, J.H., Orgiazzi, A., Jones, A., *et al.* (2018) Copper distribution in European topsoils: an assessment based on LUCAS soil survey. *Sci Total Environ* **636**: 282–298.
- Barwinska-Sendra, A., and Waldron, K.J. (2017) The role of intermetal competition and mis-metalation in metal toxicity. *Adv Microb Physiol* **70**: 315–379.
- Beyer, W., Imlay, J., and Fridovich, I. (1991) Superoxide dismutases. *Prog Nucleic Acid Res Mol Biol* **40**: 221–253.
- Bischofberger, A.M., Baumgartner, M., Pfrunder-Cardozo, K.R., Allen, R.C., and Hall, A.R. (2020) Associations between sensitivity to antibiotics, disinfectants and heavy metals in natural, clinical and laboratory isolates of *Escherichia coli*. *Environ Microbiol*. <https://doi.org/10.1111/1462-2920.14986>
- Cameron, D.E., Urbach, J.M., and Mekalanos, J.J. (2008) A defined transposon mutant library and its use in identifying motility genes in *Vibrio cholerae*. *Proc Natl Acad Sci USA* **105**: 8736–8741.
- Capdevila, D.A., Edmonds, K.A., and Giedroc, D.P. (2017) Metallochaperones and metalloregulation in bacteria. *Essays Biochem* **61**: 177–200.
- Carlioz, A., and Touati, D. (1986) Isolation of superoxide dismutase mutants in *Escherichia coli*: is superoxide dismutase necessary for aerobic life? *The EMBO journal* **5**: 623–630.
- Chandrangsu, P., Rensing, C., and Helmann, J.D. (2017) Metal homeostasis and resistance in bacteria. *Nat Rev Microbiol* **15**: 338–350.
- Cheng, Z., Wei, Y.Y., Sung, W.W., Glick, B.R., and McConkey, B.J. (2009) Proteomic analysis of the response of the plant growth-promoting bacterium *Pseudomonas putida* UW4 to nickel stress. *Proteome Sci* **7**: 18.
- Chillappagari, S., Seubert, A., Trip, H., Kuipers, O.P., Marahiel, M.A., and Miethke, M. (2010) Copper stress affects iron homeostasis by destabilizing iron-sulfur cluster formation in *Bacillus subtilis*. *J Bacteriol* **192**: 2512–2524.
- Dietrich, L.E., Teal, T.K., Price-Whelan, A., and Newman, D.K. (2008) Redox-active antibiotics control gene expression and community behavior in divergent bacteria. *Science* **321**: 1203–1206.
- Djoko, K.Y., and McEwan, A.G. (2013) Antimicrobial action of copper is amplified via inhibition of heme biosynthesis. *ACS Chem Biol* **8**: 2217–2223.
- Donnenberg, M.S., and Kaper, J.B. (1991) Construction of an eae deletion mutant of enteropathogenic *Escherichia coli* by using a positive-selection suicide vector. *Infect Immun* **59**: 4310–4317.
- Elzanowska, H., Wolcott, R.G., Hannum, D.M., and Hurst, J.K. (1995) Bactericidal properties of hydrogen peroxide and copper or iron-containing complex ions in relation to leukocyte function. *Free Radic Biol Med* **18**: 437–449.
- Geslin, C., Llanos, J., Prieur, D., and Jeanthon, C. (2001) The manganese and iron superoxide dismutases protect *Escherichia coli* from heavy metal toxicity. *Res Microbiol* **152**: 901–905.
- Gibson, D.G., Young, L., Chuang, R.Y., Venter, J.C., Hutchison, C.A. 3rd, and Smith, H.O. (2009) Enzymatic assembly of DNA molecules up to several hundred kilobases. *Nat Methods* **6**: 343–345.
- Giner-Lamia, J., Lopez-Maury, L., and Florencio, F.J. (2014) Global transcriptional profiles of the copper responses in the cyanobacterium *Synechocystis* sp. PCC 6803. *PLoS ONE* **9**: e108912.
- Gunther, M.R., Hanna, P.M., Mason, R.P., and Cohen, M.S. (1995) Hydroxyl radical formation from cuprous ion and hydrogen peroxide: a spin-trapping study. *Arch Biochem Biophys* **316**: 515–522.
- Haan, C., and Behrmann, I. (2007) A cost effective non-commercial ECL-solution for Western blot detections yielding strong signals and low background. *J Immunol Methods* **318**: 11–19.
- Heim, S., Ferrer, M., Heuer, H., Regenhart, D., Nimtz, M., and Timmis, K.N. (2003) Proteome reference map of *Pseudomonas putida* strain KT2440 for genome expression profiling: distinct responses of KT2440 and *Pseudomonas aeruginosa* strain PAO1 to iron deprivation and a new form of superoxide dismutase. *Environ Microbiol* **5**: 1257–1269.
- Helbig, K., Grosse, C., and Nies, D.H. (2008) Cadmium toxicity in glutathione mutants of *Escherichia coli*. *J Bacteriol* **190**: 5439–5454.
- Henriques, A.O., Melsen, L.R., and Moran, C.P. Jr (1998) Involvement of superoxide dismutase in spore coat assembly in *Bacillus subtilis*. *J Bacteriol* **180**: 2285–2291.
- Houot, L., Floutier, M., Marteyn, B., Michaut, M., Picciocchi, A., Legrain, P., *et al.* (2007) Cadmium triggers an integrated reprogramming of the metabolism of *Synechocystis* PCC6803, under the control of the Slr1738 regulator. *BMC Genom* **8**: 350.
- Imlay, J.A. (2003) Pathways of oxidative damage. *Annu Rev Microbiol* **57**: 395–418.
- Imlay, J.A. (2013) The molecular mechanisms and physiological consequences of oxidative stress: lessons from a model bacterium. *Nat Rev Microbiol* **11**: 443–454.
- Imlay, J.A. (2019) Where in the world do bacteria experience oxidative stress? *Environ Microbiol* **21**: 521–530.
- Inaoka, T., Matsumura, Y., and Tsuchido, T. (1998) Molecular cloning and nucleotide sequence of the superoxide dismutase gene and characterization of its product from *Bacillus subtilis*. *J Bacteriol* **180**: 3697–3703.
- Jacobs, M.A., Alwood, A., Thaipisuttikul, I., Spencer, D., Haugen, E., Ernst, S., *et al.* (2003) Comprehensive transposon mutant library of *Pseudomonas aeruginosa*. *Proc Natl Acad Sci USA* **100**: 14339–14344.
- Keyer, K., and Imlay, J.A. (1996) Superoxide accelerates DNA damage by elevating free-iron levels. *Proc Natl Acad Sci USA* **93**: 13635–13640.
- Keyer, K., and Imlay, J.A. (1997) Inactivation of dehydratase [4Fe-4S] clusters and disruption of iron homeostasis upon cell exposure to peroxyntrite. *J Biol Chem* **272**: 27652–27659.
- Kobayashi, K. (2017) Sensing mechanisms in the Redox-Regulated, [2Fe-2S] cluster-containing, bacterial transcriptional factor SoxR. *Acc Chem Res* **50**: 1672–1678.
- Krumschnabel, G., Manzl, C., Berger, C., and Hofer, B. (2005) Oxidative stress, mitochondrial permeability transition, and cell death in Cu-exposed trout hepatocytes. *Toxicol Appl Pharmacol* **209**: 62–73.

Yang, Y., Mathieu, J.M., Chattopadhyay, S., Miller, J.T., Wu, T., Shibata, T., *et al.* (2012) Defense mechanisms of *Pseudomonas aeruginosa* PAO1 against quantum dots and their released heavy metals. *ACS Nano* **6**: 6091–6098.

Yoshihara, T., Hodoshima, H., Miyano, Y., Shoji, K., Shimada, H., and Goto, F. (2006) Cadmium inducible Fe deficiency responses observed from macro and molecular views in tobacco plants. *Plant Cell Rep* **25**: 365–373.

### Supporting information

Additional supporting information may be found online in the Supporting Information section at the end of the article.

**Table S1.** Bacterial strains and plasmids used in this work.

**Table S2.** DNA primers used in this work.

**Fig. S1.** A 22 kDa protein was induced in the Cd<sup>2+</sup>-ATPase deficient mutants under respiration. Induction of SodB in *R. gelatinosus* wild-type (WT), *cadR* and  $\Delta cadA$  strains with the increase of CdCl<sub>2</sub> concentration. Cells were grown under respiration. Total protein extracts from the same amount of cells (OD<sub>680nm</sub> = 1) were separated on 15% SDS-PAGE and analyzed by western blot using the HisProbe.

**Fig. S2.** XseA is not required for menadione tolerance. A. Menadione disc-diffusion assay (as described in Experimental procedures) results showing the complementation by pB*xseAsodB* and pB*sodB*. pBTc: empty plasmid. B. *sodB* constructs used in this work. pG*sodB*::Km was used to generate the  $\Delta sodB$  mutant. pB derivatives (pB*xseAsodB* and pB*sodB*) were used for complementations of  $\Delta sodB$  strain.

**Fig. S3.** Genetic organization of *xseA sodB* orfs. A. *xseAsodB* gene fusion. *xseA* coding sequence is in blue and *sodB* in red. No stop codon was found between the two orfs. Putative promoters and transcripts and primers used in

RT-PCR are indicated. B. Protein sequence of the fusion. The five His detected by the HisProbe in SodB are shown in black and boldstyle. C. Analysis of *sodB* expression by RT-PCR. Total RNA from wild-type (WT) and  $\Delta sodB$  strains grown under respiration was extracted according to Steunou *et al.* (2004). 2  $\mu$ g of total RNA was reverse transcribed with the superscript II (Invitrogen) using the specific *sodB* primer RG348. 2  $\mu$ l of the RT reaction was used for the PCR. We used either the primers RG433-RG434 specific to *xseA* or the RG347-RG348 primers specific to *sodB*. Both PCRs were positive showing the presence of the *xseAsodB* transcript (arrow). Genomic DNA and 16SrRNA were used for controls. This experiment suggested the presence of *xseAsodB* transcript but does not exclude the presence of an internal promoter upstream of *sodB*. Putative promoters are shown in gray.

**Fig. S4.** Effect of Cd<sup>2+</sup> and menadione stress in  $\Delta sodB$ , and  $\Delta cadAsodB$  strains. A. Menadione disc-diffusion assay. Plates were incubated at 30°C overnight either under photosynthetic (PS) or respiratory (RES) conditions. B. Western blot analysis of wild-type (WT),  $\Delta sodB$ ,  $\Delta cadA$ , and  $\Delta cadAsodB$  strains grown by photosynthesis with (50  $\mu$ M) or without (–) cadmium, showing the induction of SodB. C. Effect of Cd<sup>2+</sup> and menadione stress in  $\Delta sodB$ , and  $\Delta cadAsodB$  strains. Menadionedisc-diffusion assay in plates supplemented or not with 25 mM CdCl<sub>2</sub>. Plates were incubated at 30°C over night under aerobic respiration conditions. The simultaneous presence of Cd<sup>2+</sup> and menadione is deleterious for the  $\Delta cadAsodB$  hyper-sensitive strain.

**Fig. S5.** Effect of CuSO<sub>4</sub> and menadione stress in the wild-type (WT),  $\Delta sodB$ , *copA*<sup>–</sup>, and  $\Delta sodBcopA$ <sup>–</sup> strains. Menadione disc-diffusion assay in plates supplemented or not with 25 mM CuSO<sub>4</sub> (as described in Experimental procedures). Plates were incubated at 30°C overnight under aerobic respiration conditions. The simultaneous presence of Cu<sup>2+</sup> and menadione is deleterious for the  $\Delta sodBcopA$ <sup>–</sup> hyper-sensitive strain.

-APPENDIX –  
-RELATED RESEARCH-

# **MATERIALS & METHODS**

---

### **Principles and application of DAB staining**

DAB (3,3'-Diaminobenzidine) is a derivative of benzene. It is most often used in immunohistochemically (IHC) staining as a chromogen. It is also used in *in situ* hybridization (ISH) and sometimes in dot blots and in western blotting. In DAB staining, DAB is oxidized by hydrogen peroxide in a reaction typically catalyzed by horseradish peroxidase (HRP). The oxidized DAB forms a brown precipitate, at the location of the HRP, which can be visualized using light microscopy. The DAB precipitate is insoluble in water, alcohol, and other organic solvents most commonly used in the lab (such as xylene and isopropanol). This allows for great flexibility in the subsequent treatment of the tissue section, such as in the choice of counterstain and mounting medium. DAB staining is also heat-resistant, so it can be used in double labeling IHC/ISH experiments and is extremely stable in fact stained slides are often stable for many years. When used together with a nickel or cobalt solution as a DAB enhancer, DAB staining becomes a more intense, black color. OD of overnight growth culture is  $3.10^9$  / ml.

### **Bacterial strains and growth.**

*E. coli* and *B. subtilis* were grown aerobically (500 ml flasks containing 50 ml medium) at 37°C in LB medium. *R. gelatinosus* was grown at 30°C, in the Dark micro-aerobically (low oxygenation: 50 ml flasks containing 50 ml medium) or in light by photosynthesis (filled tubes with residual oxygen in the medium) in malate growth medium. Antibiotics kanamycin (km) and trimethoprim (Tp) were used at a final concentration of 50 µg/ml. Growth inhibition curves were monitored at OD 680 nm with measurements taken every 15 min for 24 h using a Tecan Infinite M200 luminometer (Tecan, Mannerdorf, Switzerland) for aerobic condition. For photosynthesis conditions, strains were grown as described above and OD was measured after 24 h using the Tecan luminometer.

### **Membrane proteins preparation.**

Cells were disrupted by sonication in 0.1 M sodium phosphate buffer (pH 7.4) containing 1 mM phenylmethylsulfonyl fluoride. Unbroken cells were removed by a low-speed centrifugation step (25000 g, 30min, 4°C) and supernatants were subjected to ultracentrifugation (200.000g, 1h30, 4°C) to collect the membrane fraction. Membrane fractions were then resuspended in the same buffer. Membrane protein concentration was estimated using the bicinchoninic acid assay (Sigma) with bovine serum albumin as standard. For membrane proteins metal treatment, required concentration of metal solution was mixed with 50 mg/ml membrane proteins at room temperature. Spectra were recorded every 30 min.

### **Spectrophotometric measurements.**

Absorption spectroscopy was performed with a Cary 500 spectrophotometer. For spectra on whole cells, cells were resuspended in a 60% (wt/v) sucrose solution. Membrane fractions were in 0.1 M sodium phosphate buffer (pH 7.4).

### **Blue-native gel electrophoresis and *in-gel* assays.**

To assay *cbb<sub>3</sub>* and succinate dehydrogenase activities, *R. gelatinosus* wild-type cells were grown micro-aerobically. For *E. coli* and *B. subtilis*, cells were grown aerobically. Membranes were prepared as previously described. Blue-native polyacrylamide gel electrophoresis (BN-PAGE) and in gel Cox activity assays (DAB:CytC staining), and succinate dehydrogenase activity was assayed using succinate and NBT (Nitroblue tetrazolium) as described in reference.

### **Western blot and His Probe-HRP detection.**

Equal number of cells (OD<sub>680nm</sub>=1) were disrupted in SDS loading buffer, proteins were then separated on a 15% SDS-PAGE and further transferred to a Hybond ECL PVDF membrane (GE Healthcare). Membranes were then probed with the His Probe-HRP (Pierce) according to the manufacturer's instruction and positive bands

were detected using a chemiluminescent HRP substrate according to the method of Haan and Behrmann. Image capture was performed with a ChemiDoc camera system (Biorad).

**Gene transfer and strain selection:**

Transformation of *R. gelatinosus* cells was produced by electroporation as previously described (Ouchane et al., 1996). The transformants were selected on plates of malate medium containing the appropriate antibiotic under aerobic conditions. Ampicillin-sensitive transformants are from two homologous recombination events and have not integrated the recombinant plasmid. After the selection of the transformant, the genomic DNA was prepared from these ampicillin-sensitive strains and confirmation of the presence of the resistance to the antibiotic was checked by PCR.

**Table: Primers used in the experiments**

<i>cusA</i>	F5'- CTCGACGCTGCTGATCGG	Rev5'- GAACATCACCGGCGTCAAC
<i>cdfA</i>	NdeI 5'- ACAGTCGGGCGCATATGAGTTCG	BamHI 5'-TCTAGTGAGACGGATCCTATCCG
<i>cdfA</i>	F5'- ATCACCACGATCACCACCAC	Rev5'- CCTGCAGCCGTTAACTCTAG
<i>ompW</i>	F5'-AAGATGGAAGGCTTCATGGAC	Rev5'- CAGAAGATGGTGCAGCTTC

**Table: Antibiotics used for genes inactivation**

	Conc. In Malate liquid (µg/ml)	Conc. In LB liquid µg/ml)
<b>Kanamycine (Km)</b>	50	50
<b>Trimethoprim (Tp)</b>	50	50
<b>Streptomycine (Sp)</b>	25	25
<b>Spectinomycine (Sm)</b>	25	25
<b>Ampicilline (Amp)</b>	50	100

### **Bacterial Immobilizing for imaging by AFM**

Acquisition of AFM images in air was much more convenient and had higher resolution than that in liquid. Our air/nitrogen dried microbial samples provided a suitable hardness for scanning without significant topographic changes and good resolution. Bacteria were immobilized on Mica Substrate with gelatin. **MICA substrates** are used for its properties as it has no known effect on biological subject, transparent, easy to cut and to manipulate, atomically flat and inexpensive. The substrate must be coated to immobilize the living cells on it by creating electrostatic interaction between the negative charge of bacteria and the positive charge of gelatin. **Gelatin preparation** (*sigma G-6144*): we used 0.5 g in 100 ml of hot distilled water. We used around 15 ml in a beaker, enough to dip mica substrate in it. We leave substrate to dry, to be used after 24 hours. **Placing bacteria on gelatin coated mica:** we centrifuge 1 mL of a bacterial culture (0.5 - 1.0 OD at 680 nm) at 500 rpm; use the minimum rpm to get the pellet of cells for 5 minutes. Then, we wash the pellet using an equal volume of deionized water, then, by centrifugation collect the cells again. In 500  $\mu$ L of deionized water resuspend the pellet rapidly. Finally, we apply 5  $\mu$ l of suspension cell on the gelatin-coated mica substrate. Carefully, spread on the surface using a pipette tip and make sure not touching the surface of the gelatin to avoid damaging it, and let it dry again (Allison et al., 2011).

### **Atomic Force Microscopy (AFM)**

AFM images were taken under ambient air condition at room temperature, using the tapping mode of a Bruker Nanoscope AFM. Probe and cantilever used from Nanosensors type: (PPP-NCHR, tip radius of curvature < 10 nm, tip height 10-15 nm, highly doped silicon to dissipate static charge with high mechanical Q-factor for high sensitivity, nominal resonance frequency is 330 kHz and a force constant of 45 N/m). Images in this paper are taken at 50  $\mu$ m for ensemble imaging or at 5  $\mu$ m scale for individual bacteria imaging. Image resolution are at 512\*512 Pixels. The scan speed is

kept at 1 Hz. One image acquisition takes less than 10 min, ensuring a stable observation time window. Data acquired include height (topographical), peak force Error image (mechanical), 3D and cross-section. Data analysis were carried using Gwyddion open source software.

### **Preparation of bacterial sample for SEM**

We prepare 2 ml of new culture of bacteria to grow overnight in PS condition. At (OD 680 nm = 1) treat with 200  $\mu$ l with AgNO<sub>3</sub> and in another tube keep 200  $\mu$ l as control. When the incubation time is finished, samples must be washed in DI H<sub>2</sub>O. Then diluted 10 times with DI water; then vortex. Then, we use a clean graphite substrate (freshly cleaved before) and dip coat in the cellular culture, and then let to dry (Murtey & Ramasamy, 2016).

### **Scanning Electron Microscopy (SEM)**

We imaged bacteria, which had been fixed, dehydrated and dried with a Zeiss Semfeg. It wasn't necessarily to frozen them. We used low tension (2.0 – 3.0 kV) to avoid contamination and electron damaging of structures. Images were taken at different magnifications. The specimen didn't release any volatile substance even at high vacuum. We kept same resolution as AFM to enable image comparison and control.

### **TEM Images**

Images were acquired using a microscope JEOL1400 operating at 80 kV. Colloidal solutions were ultrasonicated and diluted in water or citrate 1 mM aqueous solution. A drop of 5  $\mu$ L of nanoparticles solutions was added to Formvar/Carbon-Cu 200 mesh TEM grids and let dry at ambient temperature

### **Silver Seed Synthesis – AgSeed purified**

Silver nanoparticles were synthesized by seed mediated growth methodology based on previous report (Wan et al., 2013). Briefly, seeds were prepared by mixing 20 mL of 1% (w/v) citrate solution in 75 mL of water during 15 minutes at 70 °C. Then, AgNO<sub>3</sub> was added to the mixture (Final concentration of 1 mM), followed by the quick addition of freshly prepared NaBH<sub>4</sub> solution (Final concentration of 0,525 mM). The reaction mixture was left under stirring at open atmosphere with a condenser, during 1 h at 70°C. After the cooling of the reaction mixture, the NPs were centrifugated twice at 13000 rpm for 70 min and resuspended in citrate 1 mM. Another quick centrifugation step was realized to collect smallest nanoparticles from the supernatant.

### **Seed Mediated Growth of AgSeed - 1 Step – AgSMG1**

We have prepared two growth samples from the AgSeed. A solution containing 0,87 mM of citrate was brought to ebullition. Then, 10 mL of AgSeed unpurified is added to the mixture followed by 1,5 mL of 1% AgNO<sub>3</sub> aqueous solution. The solution mixture is vigorously stirred under reflux during 1h.

The reaction solution turned yellow and became browner. AgSMG1 was centrifugated twice at 10000 rpm for 15 min, washed in citrate 1mM and resuspended in citrate 1mM or water for further analysis.

### **Ag-NPs Characterization Apparatus**

**UV-Visible spectroscopy (Spectrophotometric measurements)** was performed with a Cary 500 spectrophotometer. For spectra on whole cells, cells were resuspended in a 60% (wt/vol) sucrose solution. For the Ag-NPs spectra, we used Thermo Scientific Multiskan GO from Thermo Scientific in wavelength between 200 to 900 nm.

### **ICP Results - AgNPs by Seed mediated growth synthesis**

Samples of synthesized silver nanoparticles were prepared and sent to CEA for concentration characterization was performed by Icap Q from Thermo Scientific. Ag-

-MATERIALS & METHODS-

NPs were prepared in H<sub>2</sub>O and in sodium citrate; in different sizes as shown in the table below.

Sample List	Sample identification	Size (nm)	Concentration (mg/L) = (µg/ml)	Silver (mmol/L)
A	AgSeed5 in H <sub>2</sub> O	11,9 ± 2,05	90,6	0,84
B	AgSeed5 in Citrate 1 mM	11,9 ± 2,05	92,4	0,86
C	AgS5MG1 in H <sub>2</sub> O	22,55 ± 14,7	132,33	1,22
D	AgS5MG1 in Citrate 1 mM	22,55 ± 14,7	144,95	1,34
E	AgS5MG2a in H <sub>2</sub> O	23,2 ± 5,66	349,87	3,24
F	AgS5MG2a in Citrate 1 mM	23,2 ± 5,66	350,6	3,25



# REFERENCES

---

- Abbaszadegan, A., Ghahramani, Y., Gholami, A., Hemmateenejad, B., Dorostkar, S., Nabavizadeh, M., & Sharghi, H. (2015, February 15). *The Effect of Charge at the Surface of Silver Nanoparticles on Antimicrobial Activity against Gram-Positive and Gram-Negative Bacteria: A Preliminary Study* [Research Article]. *Journal of Nanomaterials*; Hindawi. <https://doi.org/10.1155/2015/720654>
- AbdelRahim, K., Mahmoud, S. Y., Ali, A. M., Almaary, K. S., Mustafa, A. E.-Z. M. A., & Hussein, S. M. (2017). Extracellular biosynthesis of silver nanoparticles using *Rhizopus stolonifer*. *Saudi Journal of Biological Sciences*, *24*(1), 208–216. <https://doi.org/10.1016/j.sjbs.2016.02.025>
- AFM Microscopes. Bruker.* (n.d.). Bruker.com. Retrieved October 15, 2020, from <https://www.bruker.com/products/surface-and-dimensional-analysis/atomic-force-microscopes/campaigns/afm-microscopes.html>
- Agalidis, I., Othman, S., Boussac, A., Reiss-Husson, F., & Desbois, A. (1999). Purification, redox and spectroscopic properties of the tetraheme cytochrome c isolated from *Rubrivivax gelatinosus*. *European Journal of Biochemistry*, *261*(1), 325–336. <https://doi.org/10.1046/j.1432-1327.1999.00277.x>
- Agalidis, & Reiss-Husson, F. (1991). Resolution of *Rhodocyclus gelatinosus* photoreceptor unit components by temperature-induced phase separation in the presence of decyltetraoxyethylene. *Biochemical and Biophysical Research Communications*, *177*(3), 1107–1112. [https://doi.org/10.1016/0006-291x\(91\)90653-o](https://doi.org/10.1016/0006-291x(91)90653-o)
- Agnihotri, S., Mukherji, S., & Mukherji, S. (2013). Size-controlled silver nanoparticles synthesized over the range 5–100 nm using the same protocol and their antibacterial efficacy. *RSC Advances*, *4*(8), 3974–3983. <https://doi.org/10.1039/C3RA44507K>
- Ahmad, F., Ashraf, N., Ashraf, T., Zhou, R.-B., & Yin, D.-C. (2019). Biological synthesis of metallic nanoparticles (MNPs) by plants and microbes: Their cellular uptake, biocompatibility, and biomedical applications. *Applied Microbiology and Biotechnology*, *103*(7), 2913–2935. <https://doi.org/10.1007/s00253-019-09675-5>
- Allen, J. P., Feher, G., Yeates, T. O., Komiya, H., & Rees, D. C. (1988). Structure of the Reaction Center from *Rhodobacter sphaeroides* R-26 and 2.4.1. In J. Breton & A. Verméglio (Eds.), *The Photosynthetic Bacterial Reaction Center: Structure and Dynamics* (pp. 5–11). Springer US. [https://doi.org/10.1007/978-1-4899-0815-5\\_2](https://doi.org/10.1007/978-1-4899-0815-5_2)
- Allison, D. P., Sullivan, C. J., Mortensen, N. P., Retterer, S. T., & Doktycz, M. (2011). Bacterial Immobilization for Imaging by Atomic Force Microscopy. *Journal of Visualized Experiments*, *54*, 2880. <https://doi.org/10.3791/2880>
- Alonso, J., Barandiarán, J. M., Fernández Barquín, L., & García-Arribas, A. (2018). Chapter 1—Magnetic Nanoparticles, Synthesis, Properties, and Applications. In A. A. El-Gendy, J. M. Barandiarán, & R. L. Hadimani (Eds.), *Magnetic Nanostructured Materials* (pp. 1–40). Elsevier. <https://doi.org/10.1016/B978-0-12-813904-2.00001-2>
- Ansari, A., Pervez, S., Javed, U., Abro, M. I., Nawaz, M. A., Qader, S. A. U., & Aman, A. (2018). Characterization and interplay of bacteriocin and exopolysaccharide-mediated silver

- nanoparticles as an antibacterial agent. *International Journal of Biological Macromolecules*, *115*, 643–650. <https://doi.org/10.1016/j.ijbiomac.2018.04.104>
- Argüello, J. M., Eren, E., & González-Guerrero, M. (2007). The structure and function of heavy metal transport P1B-ATPases. *Biometals: An International Journal on the Role of Metal Ions in Biology, Biochemistry, and Medicine*, *20*(3–4), 233–248. <https://doi.org/10.1007/s10534-006-9055-6>
- Asiani, K. R., Williams, H., Bird, L., Jenner, M., Searle, M. S., Hobman, J. L., Scott, D. J., & Soutanas, P. (2016). SilE is an intrinsically disordered periplasmic “molecular sponge” involved in bacterial silver resistance. *Molecular Microbiology*, *101*(5), 731–742. <https://doi.org/10.1111/mmi.13399>
- Aslam, B., Wang, W., Arshad, M. I., Khurshid, M., Muzammil, S., Rasool, M. H., Nisar, M. A., Alvi, R. F., Aslam, M. A., Qamar, M. U., Salamat, M. K. F., & Baloch, Z. (2018). Antibiotic resistance: A rundown of a global crisis. *Infection and Drug Resistance*, *11*, 1645–1658. <https://doi.org/10.2147/IDR.S173867>
- Azai, C., Tsukatani, Y., Itoh, S., & Oh-oka, H. (2010). C-type cytochromes in the photosynthetic electron transfer pathways in green sulfur bacteria and heliobacteria. *Photosynthesis Research*, *104*(2), 189–199. <https://doi.org/10.1007/s11120-009-9521-4>
- Azzouzi, A., Steunou, A.-S., Durand, A., Khalfaoui-Hassani, B., Bourbon, M.-L., Astier, C., Bollivar, D. W., & Ouchane, S. (2013). Coproporphyrin III excretion identifies the anaerobic coproporphyrinogen III oxidase HemN as a copper target in the Cu<sup>+</sup>-ATPase mutant copA<sup>-</sup> of *Rubrivivax gelatinosus*. *Molecular Microbiology*, *88*(2), 339–351. <https://doi.org/10.1111/mmi.12188>
- Bao, Z., & Lan, C. Q. (2019). Advances in biosynthesis of noble metal nanoparticles mediated by photosynthetic organisms-A review. *Colloids and Surfaces. B, Biointerfaces*, *184*, 110519. <https://doi.org/10.1016/j.colsurfb.2019.110519>
- Baradaran, R., Berrisford, J. M., Minhas, G. S., & Sazanov, L. A. (2013). Crystal structure of the entire respiratory complex I. *Nature*, *494*(7438), 443–448. <https://doi.org/10.1038/nature11871>
- Barwinska-Sendra, A., & Waldron, K. J. (2017). The Role of Intermetal Competition and Mis-Metalation in Metal Toxicity. *Advances in Microbial Physiology*, *70*, 315–379. <https://doi.org/10.1016/bs.ampbs.2017.01.003>
- Bauer, C., Buggy, J., & Mosley, C. (1993). Control of photosystem genes in *Rhodobacter capsulatus*. *Trends in Genetics: TIG*, *9*(2), 56–60. [https://doi.org/10.1016/0168-9525\(93\)90188-N](https://doi.org/10.1016/0168-9525(93)90188-N)
- Bhattacharya, R., & Mukherjee, P. (2008). Biological properties of “naked” metal nanoparticles. *Advanced Drug Delivery Reviews*, *60*(11), 1289–1306. <https://doi.org/10.1016/j.addr.2008.03.013>
- Binnig, G., Quate, C. F., & Gerber, Ch. (1986). Atomic Force Microscope. *Physical Review Letters*, *56*(9), 930–933. <https://doi.org/10.1103/PhysRevLett.56.930>

- Blaby-Haas, C. E., & Merchant, S. S. (2017). Regulating cellular trace metal economy in algae. *Current Opinion in Plant Biology*, *39*, 88–96. <https://doi.org/10.1016/j.pbi.2017.06.005>
- Bondarczuk, K., & Piotrowska-Seget, Z. (2013). Molecular basis of active copper resistance mechanisms in Gram-negative bacteria. *Cell Biology and Toxicology*, *29*(6), 397–405. <https://doi.org/10.1007/s10565-013-9262-1>
- Brown, N. L., Stoyanov, J. V., Kidd, S. P., & Hobman, J. L. (2003). The MerR family of transcriptional regulators. *FEMS Microbiology Reviews*, *27*(2–3), 145–163. [https://doi.org/10.1016/S0168-6445\(03\)00051-2](https://doi.org/10.1016/S0168-6445(03)00051-2)
- Bryant, D. A., Hunter, C. N., & Warren, M. J. (2020). Biosynthesis of the modified tetrapyrroles—The pigments of life. *Journal of Biological Chemistry*, *295*(20), 6888–6925. <https://doi.org/10.1074/jbc.REV120.006194>
- Buschmann, S., Warkentin, E., Xie, H., Langer, J. D., Ermler, U., & Michel, H. (2010). The Structure of cbb3 Cytochrome Oxidase Provides Insights into Proton Pumping. *Science*, *329*(5989), 327–330. <https://doi.org/10.1126/science.1187303>
- Butkus, M. A., Edling, L., & Labare, M. P. (2003). The efficacy of silver as a bactericidal agent: Advantages, limitations and considerations for future use. *Journal of Water Supply: Research and Technology-Aqua*, *52*(6), 407–416. <https://doi.org/10.2166/aqua.2003.0037>
- Cassier-Chauvat, C., & Chauvat, F. (2014). Responses to Oxidative and Heavy Metal Stresses in Cyanobacteria: Recent Advances. *International Journal of Molecular Sciences*, *16*(1), 871–886. <https://doi.org/10.3390/ijms16010871>
- Chacón, K. N., Mealman, T. D., McEvoy, M. M., & Blackburn, N. J. (2014). Tracking metal ions through a Cu/Ag efflux pump assigns the functional roles of the periplasmic proteins. *Proceedings of the National Academy of Sciences*, *111*(43), 15373–15378. <https://doi.org/10.1073/pnas.1411475111>
- Chandrangsu, P., Rensing, C., & Helmann, J. D. (2017). Metal homeostasis and resistance in bacteria. *Nature Reviews. Microbiology*, *15*(6), 338–350. <https://doi.org/10.1038/nrmicro.2017.15>
- Chen, X., Pu, H., Fang, Y., Wang, X., Zhao, S., Lin, Y., Zhang, M., Dai, H.-E., Gong, W., & Liu, L. (2015). Crystal structure of the catalytic subunit of magnesium chelatase. *Nature Plants*, *1*(9), 1–5. <https://doi.org/10.1038/nplants.2015.125>
- Chew, A. G. M., & Bryant, D. A. (2007). Chlorophyll Biosynthesis in Bacteria: The Origins of Structural and Functional Diversity. *Annual Review of Microbiology*, *61*(1), 113–129. <https://doi.org/10.1146/annurev.micro.61.080706.093242>
- Chillappagari, S., Seubert, A., Trip, H., Kuipers, O. P., Marahiel, M. A., & Miethke, M. (2010). Copper Stress Affects Iron Homeostasis by Destabilizing Iron-Sulfur Cluster Formation in *Bacillus subtilis*. *Journal of Bacteriology*, *192*(10), 2512–2524. <https://doi.org/10.1128/JB.00058-10>

- Choudhary, M., & Kaplan, S. (2000). DNA sequence analysis of the photosynthesis region of *Rhodobacter sphaeroides* 2.4.1T. *Nucleic Acids Research*, *28*(4), 862–867. <https://doi.org/10.1093/nar/28.4.862>
- Coates, A. R. M., Halls, G., & Hu, Y. (2011). Novel classes of antibiotics or more of the same? *British Journal of Pharmacology*, *163*(1), 184–194. <https://doi.org/10.1111/j.1476-5381.2011.01250.x>
- Cogdell, Isaacs, N. W., Howard, T. D., McLuskey, K., Fraser, N. J., & Prince, S. M. (1999). How photosynthetic bacteria harvest solar energy. *Journal of Bacteriology*, *181*(13), 3869–3879. <https://doi.org/10.1128/JB.181.13.3869-3879.1999>
- Cogdell, R. J., & Gardiner, A. T. (1993). [18] Functions of carotenoids in photosynthesis. In *Methods in Enzymology* (Vol. 214, pp. 185–193). Academic Press. [https://doi.org/10.1016/0076-6879\(93\)14065-Q](https://doi.org/10.1016/0076-6879(93)14065-Q)
- Crichton, R. R. (2020). *An overview of the role of metals in biology*. <https://doi.org/10.1016/B978-0-444-64225-7.00001-8>
- Curtis, P. D. (2016). Essential Genes Predicted in the Genome of *Rubrivivax gelatinosus*. *Journal of Bacteriology*, *198*(16), 2244–2250. <https://doi.org/10.1128/JB.00344-16>
- Dailey, H. A., Dailey, T. A., Gerdes, S., Jahn, D., Jahn, M., O'Brian, M. R., & Warren, M. J. (2017). Prokaryotic Heme Biosynthesis: Multiple Pathways to a Common Essential Product. *Microbiology and Molecular Biology Reviews*, *81*(1). <https://doi.org/10.1128/MMBR.00048-16>
- Dakal, T. C., Kumar, A., Majumdar, R. S., & Yadav, V. (2016). Mechanistic Basis of Antimicrobial Actions of Silver Nanoparticles. *Frontiers in Microbiology*, *7*. <https://doi.org/10.3389/fmicb.2016.01831>
- DalCorso, G., Manara, A., & Furini, A. (2013). An overview of heavy metal challenge in plants: From roots to shoots. *Metallomics*, *5*(9), 1117–1132. <https://doi.org/10.1039/C3MT00038A>
- Dalecki, A. G., Crawford, C. L., & Wolschendorf, F. (2017). Chapter Six - Copper and Antibiotics: Discovery, Modes of Action, and Opportunities for Medicinal Applications. In Robert K. Poole (Ed.), *Advances in Microbial Physiology* (Vol. 70, pp. 193–260). Academic Press. <https://doi.org/10.1016/bs.ampbs.2017.01.007>
- Dangel, A. W., & Tabita, F. R. (2015). CbbR, the Master Regulator for Microbial Carbon Dioxide Fixation. *Journal of Bacteriology*, *197*(22), 3488–3498. <https://doi.org/10.1128/JB.00442-15>
- Darrouzet, E., & Daldal, F. (2003). Protein-protein interactions between cytochrome b and the Fe-S protein subunits during QH<sub>2</sub> oxidation and large-scale domain movement in the bc1 complex. *Biochemistry*, *42*(6), 1499–1507. <https://doi.org/10.1021/bi026656h>
- Darrouzet, E., Valkova-Valchanova, M. B., Moser, C., Dutton, P., & Daldal, F. (2000). Uncovering the [2Fe2S] domain movement in cytochrome bc1 and its implications for energy conversion. *Proceedings of the National Academy of Sciences of the United States of America*, *97*, 4567–4572. <https://doi.org/10.1073/pnas.97.9.4567>

- De Leersnyder, I., De Gelder, L., Van Driessche, I., & Vermeir, P. (2018). Influence of growth media components on the antibacterial effect of silver ions on *Bacillus subtilis* in a liquid growth medium. *Scientific Reports*, *8*(1), 9325. <https://doi.org/10.1038/s41598-018-27540-9>
- Deisenhofer, J., & Michel, H. (1989). Nobel lecture. The photosynthetic reaction centre from the purple bacterium *Rhodospseudomonas viridis*. *The EMBO Journal*, *8*(8), 2149–2170. <https://doi.org/10.1002/j.1460-2075.1989.tb08338.x>
- Delmar, J. A., Su, C.-C., & Yu, E. W. (2015). Heavy metal transport by the CusCFBA efflux system. *Protein Science*, *24*(11), 1720–1736. <https://doi.org/10.1002/pro.2764>
- Dennison, C., David, S., & Lee, J. (2018). Bacterial copper storage proteins. *The Journal of Biological Chemistry*, *293*(13), 4616–4627. <https://doi.org/10.1074/jbc.TM117.000180>
- Dias, A. C. P., Marslin, G., Selvakesavan, Gregory, F., & Sarmiento, B. (2015). Antimicrobial activity of cream incorporated with silver nanoparticles biosynthesized from *Withania somnifera*. *International Journal of Nanomedicine*, 5955. <https://doi.org/10.2147/IJN.S81271>
- Djafari, J. (2019). *Synthesis, Characterization and Applications of Gold and Silver Nanoparticles: From Antibacterial to Optoelectronic Nanomaterials*. <https://run.unl.pt/handle/10362/72827>
- Djafari, J., Fernández-Lodeiro, C., Fernández-Lodeiro, A., Silva, V., Poeta, P., Igrejas, G., Lodeiro, C., Capelo, J. L., & Fernández-Lodeiro, J. (2019). Exploring the Control in Antibacterial Activity of Silver Triangular Nanoplates by Surface Coating Modulation. *Frontiers in Chemistry*, *6*. <https://doi.org/10.3389/fchem.2018.00677>
- Djoko, K. Y., & McEwan, A. G. (2013). Antimicrobial Action of Copper Is Amplified via Inhibition of Heme Biosynthesis. *ACS Chemical Biology*, *8*(10), 2217–2223. <https://doi.org/10.1021/cb4002443>
- Domenech, B., Bastos-Arrieta, J., Alonso, A., Macanas, J., Munoz, M., & N., D. (2012). Bifunctional Polymer-Metal Nanocomposite Ion Exchange Materials. In A. Kilislioglu (Ed.), *Ion Exchange Technologies*. InTech. <https://doi.org/10.5772/51579>
- Dong, X., Awak, M. A., Tomlinson, N., Tang, Y., Sun, Y.-P., & Yang, L. (2017). Antibacterial effects of carbon dots in combination with other antimicrobial reagents. *PloS One*, *12*(9), e0185324. <https://doi.org/10.1371/journal.pone.0185324>
- Donohue, T. J., & Kaplan, S. (1991). [22] Genetic techniques in rhodospirillaceae. In *Methods in Enzymology* (Vol. 204, pp. 459–485). Academic Press. [https://doi.org/10.1016/0076-6879\(91\)04024-I](https://doi.org/10.1016/0076-6879(91)04024-I)
- Dufrêne, Y. F. (2014). Atomic Force Microscopy in Microbiology: New Structural and Functional Insights into the Microbial Cell Surface. *MBio*, *5*(4). <https://doi.org/10.1128/mBio.01363-14>
- Dufrêne, Y. F., Ando, T., Garcia, R., Alsteens, D., Martinez-Martin, D., Engel, A., Gerber, C., & Müller, D. J. (2017). Imaging modes of atomic force microscopy for application in

- molecular and cell biology. *Nature Nanotechnology*, 12(4), 295–307. <https://doi.org/10.1038/nnano.2017.45>
- Dupont, C. L., Grass, G., & Rensing, C. (2011). Copper toxicity and the origin of bacterial resistance—New insights and applications. *Metallomics: Integrated Biometal Science*, 3(11), 1109–1118. <https://doi.org/10.1039/c1mt00107h>
- Durand, A., Azzouzi, A., Bourbon, M.-L., Steunou, A.-S., Liotenberg, S., Maeshima, A., Astier, C., Argentini, M., Saito, S., & Ouchane, S. (2015). C-Type Cytochrome Assembly Is a Key Target of Copper Toxicity within the Bacterial Periplasm. *MBio*, 6(5), e01007-15. <https://doi.org/10.1128/mBio.01007-15>
- Durand, A., Bourbon, M.-L., Steunou, A.-S., Khalfaoui-Hassani, B., Legrand, C., Guitton, A., Astier, C., & Ouchane, S. (2018). Biogenesis of the bacterial cbb3 cytochrome c oxidase: Active subcomplexes support a sequential assembly model. *The Journal of Biological Chemistry*, 293(3), 808–818. <https://doi.org/10.1074/jbc.M117.805184>
- Elsen, S., Jaubert, M., Pignol, D., & Giraud, E. (2005). PpsR: A multifaceted regulator of photosynthesis gene expression in purple bacteria. *Molecular Microbiology*, 57(1), 17–26. <https://doi.org/10.1111/j.1365-2958.2005.04655.x>
- Elsen, S., Swem, L. R., Swem, D. L., & Bauer, C. E. (2004). RegB/RegA, a Highly Conserved Redox-Responding Global Two-Component Regulatory System. *Microbiology and Molecular Biology Reviews*, 68(2), 263–279. <https://doi.org/10.1128/MMBR.68.2.263-279.2004>
- Faber, F., Egli, T., & Harder, W. (1993). Transient repression of the synthesis of OmpF and aspartate transcarbamoylase in *Escherichia coli* K12 as a response to pollutant stress. *FEMS Microbiology Letters*, 111(2–3), 189–196. <https://doi.org/10.1111/j.1574-6968.1993.tb06384.x>
- Faghri Zonooz, N., & Salouti, M. (2011). Extracellular biosynthesis of silver nanoparticles using cell filtrate of *Streptomyces* sp. ERI-3. *Scientia Iranica*, 18(6), 1631–1635. <https://doi.org/10.1016/j.scient.2011.11.029>
- Flores, S. M., & Toca-Herrera, J. L. (2009). The new future of scanning probe microscopy: Combining atomic force microscopy with other surface-sensitive techniques, optical microscopy and fluorescence techniques. *Nanoscale*, 1(1), 40–49. <https://doi.org/10.1039/B9NR00156E>
- Foster, A. W., Osman, D., & Robinson, N. J. (2014). Metal Preferences and Metallation. *Journal of Biological Chemistry*, 289(41), 28095–28103. <https://doi.org/10.1074/jbc.R114.588145>
- Francki, K. T., Chang, B. J., Mee, B. J., Collignon, P. J., Susai, V., & Keese, P. K. (2000). Identification of genes associated with copper tolerance in an adhesion-defective mutant of *Aeromonas veronii* biovar *sobria*. *FEMS Immunology and Medical Microbiology*, 29(2), 115–121. <https://doi.org/10.1111/j.1574-695X.2000.tb01513.x>
- Frank, H. A., & Cogdell, R. J. (1996). Carotenoids in Photosynthesis. *Photochemistry and Photobiology*, 63(3), 257–264. <https://doi.org/10.1111/j.1751-1097.1996.tb03022.x>

- Fuchs, B. M., Spring, S., Teeling, H., Quast, C., Wulf, J., Schattenhofer, M., Yan, S., Ferriera, S., Johnson, J., Glockner, F. O., & Amann, R. (2007). Characterization of a marine gammaproteobacterium capable of aerobic anoxygenic photosynthesis. *Proceedings of the National Academy of Sciences*, *104*(8), 2891–2896. <https://doi.org/10.1073/pnas.0608046104>
- Galdiero, S., Falanga, A., Vitiello, M., Cantisani, M., Marra, V., & Galdiero, M. (2011). Silver nanoparticles as potential antiviral agents. *Molecules (Basel, Switzerland)*, *16*(10), 8894–8918. <https://doi.org/10.3390/molecules16108894>
- Gall, A., Cogdell, R. J., & Robert, B. (2003). Influence of carotenoid molecules on the structure of the bacteriochlorophyll binding site in peripheral light-harvesting proteins from *Rhodobacter sphaeroides*. *Biochemistry*, *42*(23), 7252–7258. <https://doi.org/10.1021/bi0268293>
- Gallardo-Navarro, Ó. A., & Santillán, M. (2019). Three-Way Interactions in an Artificial Community of Bacterial Strains Directly Isolated From the Environment and Their Effect on the System Population Dynamics. *Frontiers in Microbiology*, *10*. <https://doi.org/10.3389/fmicb.2019.02555>
- Gnida, M., Ferner, R., Gremer, L., Meyer, O., & Meyer-Klaucke, W. (2003). A novel binuclear [CuSMo] cluster at the active site of carbon monoxide dehydrogenase: Characterization by X-ray absorption spectroscopy. *Biochemistry*, *42*(1), 222–230. <https://doi.org/10.1021/bi026514n>
- Golding, C. G., Lamboo, L. L., Beniac, D. R., & Booth, T. F. (2016). The scanning electron microscope in microbiology and diagnosis of infectious disease. *Scientific Reports*, *6*, 26516. <https://doi.org/10.1038/srep26516>
- Gomelsky, L., Moskvin, O. V., Stenzel, R. A., Jones, D. F., Donohue, T. J., & Gomelsky, M. (2008). Hierarchical Regulation of Photosynthesis Gene Expression by the Oxygen-Responsive PrrBA and AppA-PpsR Systems of *Rhodobacter sphaeroides*. *Journal of Bacteriology*, *190*(24), 8106–8114. <https://doi.org/10.1128/JB.01094-08>
- González-Guerrero, M., Raimunda, D., Cheng, X., & Argüello, J. M. (2010). Distinct functional roles of homologous Cu<sup>+</sup> efflux ATPases in *Pseudomonas aeruginosa*. *Molecular Microbiology*, *78*(5), 1246–1258. <https://doi.org/10.1111/j.1365-2958.2010.07402.x>
- Gray, K. A., & Daldal, F. (1995). Mutational Studies of the Cytochrome bc<sub>1</sub> Complexes. In R. E. Blankenship, M. T. Madigan, & C. E. Bauer (Eds.), *Anoxygenic Photosynthetic Bacteria* (pp. 747–774). Springer Netherlands. [https://doi.org/10.1007/0-306-47954-0\\_35](https://doi.org/10.1007/0-306-47954-0_35)
- Gudipaty, S. A., Larsen, A. S., Rensing, C., & McEvoy, M. M. (2012). Regulation of Cu(I)/Ag(I) efflux genes in *Escherichia coli* by the sensor kinase CusS. *FEMS Microbiology Letters*, *330*(1), 30–37. <https://doi.org/10.1111/j.1574-6968.2012.02529.x>
- Guerrero, R. (2000). Brock Biology of Microorganisms (9th edn). Michael E. Madigan, John M. Martinko, Jack Parker. *International Microbiology*, *3*(2), 129. <https://doi.org/10.2436/im.v3i2.9260>

- Guriyanova, S., & Bonaccorso, E. (2008). Influence of wettability and surface charge on the interaction between an aqueous electrolyte solution and a solid surface. *Physical Chemistry Chemical Physics*, *10*(32), 4871–4878. <https://doi.org/10.1039/B806236F>
- Haefeli, C., Franklin, C., & Hardy, K. (1984). Plasmid-determined silver resistance in *Pseudomonas stutzeri* isolated from a silver mine. *Journal of Bacteriology*, *158*(1), 389–392.
- Haider, A., & Kang, I.-K. (2015, March 1). *Preparation of Silver Nanoparticles and Their Industrial and Biomedical Applications: A Comprehensive Review* [Review Article]. *Advances in Materials Science and Engineering*; Hindawi. <https://doi.org/10.1155/2015/165257>
- Hamouda, R. A., Hussein, M. H., Abo-elmagd, R. A., & Bawazir, S. S. (2019). Synthesis and biological characterization of silver nanoparticles derived from the cyanobacterium *Oscillatoria limnetica*. *Scientific Reports*, *9*(1), 13071. <https://doi.org/10.1038/s41598-019-49444-y>
- Hansson, M. D., Karlberg, T., Söderberg, C. A. G., Rajan, S., Warren, M. J., Al-Karadaghi, S., Rigby, S. E. J., & Hansson, M. (2011). Bacterial ferrochelatase turns human: Tyr13 determines the apparent metal specificity of *Bacillus subtilis* ferrochelatase. *JBIC Journal of Biological Inorganic Chemistry*, *16*(2), 235–242. <https://doi.org/10.1007/s00775-010-0720-4>
- Hassani, Astier, C., Nitschke, W., & Ouchane, S. (2010a). CtpA, a Copper-translocating P-type ATPase Involved in the Biogenesis of Multiple Copper-requiring Enzymes. *The Journal of Biological Chemistry*, *285*(25), 19330–19337. <https://doi.org/10.1074/jbc.M110.116020>
- Hassani, Steunou, A.-S., Liotenberg, S., Reiss-Husson, F., Astier, C., & Ouchane, S. (2010). Adaptation to Oxygen ROLE OF TERMINAL OXIDASES IN PHOTOSYNTHESIS INITIATION IN THE PURPLE PHOTOSYNTHETIC BACTERIUM, RUBRIVIVAX GELATINOSUS. *Journal of Biological Chemistry*, *285*(26), 19891–19899. <https://doi.org/10.1074/jbc.M109.086066>
- He, Z. L., Yang, X. E., & Stoffella, P. J. (2005). Trace elements in agroecosystems and impacts on the environment. *Journal of Trace Elements in Medicine and Biology: Organ of the Society for Minerals and Trace Elements (GMS)*, *19*(2–3), 125–140. <https://doi.org/10.1016/j.jtemb.2005.02.010>
- Heiligtag, F. J., & Niederberger, M. (2013). The fascinating world of nanoparticle research. *Materials Today*, *16*(7), 262–271. <https://doi.org/10.1016/j.mattod.2013.07.004>
- Helbig, K., Bleuel, C., Krauss, G. J., & Nies, D. H. (2008). Glutathione and Transition-Metal Homeostasis in *Escherichia coli*. *Journal of Bacteriology*, *190*(15), 5431–5438. <https://doi.org/10.1128/JB.00271-08>
- Hiniker, A., Collet, J.-F., & Bardwell, J. C. A. (2005). Copper Stress Causes an in Vivo Requirement for the *Escherichia coli* Disulfide Isomerase DsbC. *Journal of Biological Chemistry*, *280*(40), 33785–33791. <https://doi.org/10.1074/jbc.M505742200>

- Ho, C. H., Thiel, M., Celik, S., Odermatt, E. K., Berndt, I., Thomann, R., & Tiller, J. C. (2012). Conventional and microwave-assisted synthesis of hyperbranched and highly branched polylysine towards amphiphilic core-shell nanocontainers for metal nanoparticles. *Polymer*, *53*(21), 4623–4630. <https://doi.org/10.1016/j.polymer.2012.08.032>
- Huang, Q., Wu, H., Cai, P., Fein, J. B., & Chen, W. (2015). Atomic force microscopy measurements of bacterial adhesion and biofilm formation onto clay-sized particles. *Scientific Reports*, *5*(1), 16857. <https://doi.org/10.1038/srep16857>
- Huang, Xu, Y., Packianathan, C., Gao, F., Chen, C., Zhang, J., Shen, Q., Rosen, B. P., & Zhao, F.-J. (2018). Arsenic methylation by a novel ArsM As(III) S-adenosylmethionine methyltransferase that requires only two conserved cysteine residues. *Molecular Microbiology*, *107*(2), 265–276. <https://doi.org/10.1111/mmi.13882>
- Huertas, M. J., López-Maury, L., Giner-Lamia, J., Sánchez-Riego, A. M., & Florencio, F. J. (2014). Metals in Cyanobacteria: Analysis of the Copper, Nickel, Cobalt and Arsenic Homeostasis Mechanisms. *Life*, *4*(4), 865–886. <https://doi.org/10.3390/life4040865>
- Hülsen, T., Barry, E. M., Lu, Y., Puyol, D., Keller, J., & Batstone, D. J. (2016). Domestic wastewater treatment with purple phototrophic bacteria using a novel continuous photo anaerobic membrane bioreactor. *Water Research*, *100*, 486–495. <https://doi.org/10.1016/j.watres.2016.04.061>
- Hunter, C. N., Daldal, F., Thurnauer, M. C., & Beatty, J. T. (Eds.). (2009). *The Purple Phototrophic Bacteria*. Springer Netherlands. <https://doi.org/10.1007/978-1-4020-8815-5>
- Igarashi, N., Harada, J., Nagashima, S., Matsuura, K., Shimada, K., & Nagashima, K. V. (2001). Horizontal transfer of the photosynthesis gene cluster and operon rearrangement in purple bacteria. *Journal of Molecular Evolution*, *52*(4), 333–341. <https://doi.org/10.1007/s002390010163>
- Imhoff, J. F. (2006). The Phototrophic Beta-Proteobacteria. In M. Dworkin, S. Falkow, E. Rosenberg, K.-H. Schleifer, & E. Stackebrandt (Eds.), *The Prokaryotes: Volume 5: Proteobacteria: Alpha and Beta Subclasses* (pp. 593–601). Springer. [https://doi.org/10.1007/0-387-30745-1\\_25](https://doi.org/10.1007/0-387-30745-1_25)
- Imhoff, Rahn, T., Künzel, S., & Neulinger, S. C. (2018). Photosynthesis Is Widely Distributed among Proteobacteria as Demonstrated by the Phylogeny of PufLM Reaction Center Proteins. *Frontiers in Microbiology*, *8*. <https://doi.org/10.3389/fmicb.2017.02679>
- Imlay, J. A. (2013). The molecular mechanisms and physiological consequences of oxidative stress: Lessons from a model bacterium. *Nature Reviews Microbiology*, *11*(7), 443–454. <https://doi.org/10.1038/nrmicro3032>
- Javid, A., Oloketuyi, S. F., Khan, M. M., & Khan, F. (2018). Diversity of Bacterial Synthesis of Silver Nanoparticles. *BioNanoScience*, *8*(1), 43–59. <https://doi.org/10.1007/s12668-017-0496-x>
- Johnston, K. A., Stabryla, L. M., Smith, A. M., Gan, X. Y., Gilbertson, L. M., & Millstone, J. E. (2018). Impacts of broth chemistry on silver ion release, surface chemistry composition, and

- bacterial cytotoxicity of silver nanoparticles. *Environmental Science: Nano*, 5(2), 304–312. <https://doi.org/10.1039/C7EN00974G>
- Jones, M. (n.d.). *BACTERIAL PHOTOSYNTHESIS*. 23.
- José-Yacaman, M., Gutierrez-Wing, C., Miki, M., Yang, D.-Q., Piyakis, K. N., & Sacher, E. (2005). Surface diffusion and coalescence of mobile metal nanoparticles. *The Journal of Physical Chemistry. B*, 109(19), 9703–9711. <https://doi.org/10.1021/jp0509459>
- Kaláb, M., Yang, A.-F., & Chabot, D. (2008). Conventional Scanning Electron Microscopy of Bacteria. *Infocus Magazine*, 42–61. <https://doi.org/10.22443/rms.inf.1.33>
- Kalimuthu, K., Suresh Babu, R., Venkataraman, D., Bilal, Mohd., & Gurunathan, S. (2008). Biosynthesis of silver nanocrystals by *Bacillus licheniformis*. *Colloids and Surfaces B: Biointerfaces*, 65(1), 150–153. <https://doi.org/10.1016/j.colsurfb.2008.02.018>
- Karcz, D., Boroń, B., Matwiczuk, A., Furso, J., Staroń, J., Ratuszna, A., & Fiedor, L. (2014). Lessons from Chlorophylls: Modifications of Porphyrinoids Towards Optimized Solar Energy Conversion. *Molecules*, 19(10), 15938–15954. <https://doi.org/10.3390/molecules191015938>
- Kébaili, N., Benrezzak, S., Cahuzac, P., Masson, A., & Bréchnignac, C. (2009). Diffusion of silver nanoparticles on carbonaceous materials. Cluster mobility as a probe for surface characterization. *The European Physical Journal D*, 52(1), 115–118. <https://doi.org/10.1140/epjd/e2009-00067-y>
- Kemper, A. F., Cheng, H.-P., Kébaili, N., Benrezzak, S., Schmidt, M., Masson, A., & Bréchnignac, C. (2009). Curvature effect on the interaction between folded graphitic surface and silver clusters. *Physical Review B*, 79(19), 193403. <https://doi.org/10.1103/PhysRevB.79.193403>
- Khan, I., Saeed, K., & Khan, I. (2019). Nanoparticles: Properties, applications and toxicities. *Arabian Journal of Chemistry*, 12(7), 908–931. <https://doi.org/10.1016/j.arabjc.2017.05.011>
- Khardori, N., Stevaux, C., & Ripley, K. (2020). Antibiotics: From the Beginning to the Future: Part 1. *Indian Journal of Pediatrics*, 87(1), 39–42. <https://doi.org/10.1007/s12098-019-03087-z>
- Khlebtsov, N. G., & Dykman, L. A. (2010). Optical properties and biomedical applications of plasmonic nanoparticles. *Journal of Quantitative Spectroscopy and Radiative Transfer*, 111(1), 1–35. <https://doi.org/10.1016/j.jqsrt.2009.07.012>
- Kim, J. S., Kuk, E., Yu, K. N., Kim, J.-H., Park, S. J., Lee, H. J., Kim, S. H., Park, Y. K., Park, Y. H., Hwang, C.-Y., Kim, Y.-K., Lee, Y.-S., Jeong, D. H., & Cho, M.-H. (2007). Antimicrobial effects of silver nanoparticles. *Nanomedicine: Nanotechnology, Biology, and Medicine*, 3(1), 95–101. <https://doi.org/10.1016/j.nano.2006.12.001>
- Kim, Nevitt, T., & Thiele, D. J. (2008). Mechanisms for copper acquisition, distribution and regulation. *Nature Chemical Biology*, 4(3), 176–185. <https://doi.org/10.1038/nchembio.72>

- Klaus, T., Joerger, R., & Olsson, E. (1999). *Silver-based crystalline nanoparticles, microbially fabricated*. 4.
- Klueh, U., Wagner, V., Kelly, S., Johnson, A., & Bryers, J. D. (2000). Efficacy of silver-coated fabric to prevent bacterial colonization and subsequent device-based biofilm formation. *Journal of Biomedical Materials Research*, *53*(6), 621–631. [https://doi.org/10.1002/1097-4636\(2000\)53:6<621::aid-jbm2>3.0.co;2-q](https://doi.org/10.1002/1097-4636(2000)53:6<621::aid-jbm2>3.0.co;2-q)
- Koch, M., Breithaupt, C., Kiefersauer, R., Freigang, J., Huber, R., & Messerschmidt, A. (2004). Crystal structure of protoporphyrinogen IX oxidase: A key enzyme in haem and chlorophyll biosynthesis. *The EMBO Journal*, *23*(8), 1720–1728. <https://doi.org/10.1038/sj.emboj.7600189>
- Koepke, J., Hu, X., Muenke, C., Schulten, K., & Michel, H. (1996). The crystal structure of the light-harvesting complex II (B800-850) from *Rhodospirillum rubrum*. *Structure (London, England: 1993)*, *4*(5), 581–597. [https://doi.org/10.1016/s0969-2126\(96\)00063-9](https://doi.org/10.1016/s0969-2126(96)00063-9)
- Krapivsky, P. L., Redner, S., & Ben-Naim, E. (2010). *A Kinetic View of Statistical Physics*. Cambridge University Press. <https://doi.org/10.1017/CBO9780511780516>
- Kumar, C. G., & Mamidyala, S. K. (2011). Extracellular synthesis of silver nanoparticles using culture supernatant of *Pseudomonas aeruginosa*. *Colloids and Surfaces. B, Biointerfaces*, *84*(2), 462–466. <https://doi.org/10.1016/j.colsurfb.2011.01.042>
- Küpper, H., Küpper, F., & Spiller, M. (1998a). In situ detection of heavy metal substituted chlorophylls in water plants. *Photosynthesis Research*, *58*(2), 123–133. <https://doi.org/10.1023/A:1006132608181>
- Küpper, H., Küpper, F., & Spiller, M. (1998b). In situ detection of heavy metal substituted chlorophylls in water plants. *Photosynthesis Research*, *58*(2), 123–133. <https://doi.org/10.1023/A:1006132608181>
- Lane, T. W., Saito, M. A., George, G. N., Pickering, I. J., Prince, R. C., & Morel, F. M. M. (2005). A cadmium enzyme from a marine diatom. *Nature*, *435*(7038), 42–42. <https://doi.org/10.1038/435042a>
- Lang, H. P., & Hunter, C. N. (1994). The relationship between carotenoid biosynthesis and the assembly of the light-harvesting LH2 complex in *Rhodobacter sphaeroides*. *Biochemical Journal*, *298*(Pt 1), 197–205.
- Langridge, G. C., Phan, M.-D., Turner, D. J., Perkins, T. T., Parts, L., Haase, J., Charles, I., Maskell, D. J., Peters, S. E., Dougan, G., Wain, J., Parkhill, J., & Turner, A. K. (2009). Simultaneous assay of every *Salmonella Typhi* gene using one million transposon mutants. *Genome Research*, *19*(12), 2308–2316. <https://doi.org/10.1101/gr.097097.109>
- Layer, G., Moser, J., Heinz, D. W., Jahn, D., & Schubert, W.-D. (2003). Crystal structure of coproporphyrinogen III oxidase reveals cofactor geometry of Radical SAM enzymes. *The EMBO Journal*, *22*(23), 6214–6224. <https://doi.org/10.1093/emboj/cdg598>

- Lee, E. J. H., Ribeiro, C., Longo, E., & Leite, E. R. (2005). Oriented attachment: An effective mechanism in the formation of anisotropic nanocrystals. *The Journal of Physical Chemistry. B*, *109*(44), 20842–20846. <https://doi.org/10.1021/jp0532115>
- Liang, M.-H., Zhu, J., & Jiang, J.-G. (2018). Carotenoids biosynthesis and cleavage related genes from bacteria to plants. *Critical Reviews in Food Science and Nutrition*, *58*(14), 2314–2333. <https://doi.org/10.1080/10408398.2017.1322552>
- Liottenberg, S., Steunou, A.-S., Durand, A., Bourbon, M.-L., Bollivar, D., Hansson, M., Astier, C., & Ouchane, S. (2015). Oxygen-dependent copper toxicity: Targets in the chlorophyll biosynthesis pathway identified in the copper efflux ATPase CopA deficient mutant. *Environmental Microbiology*, *17*(6), 1963–1976. <https://doi.org/10.1111/1462-2920.12733>
- Liottenberg, S., Steunou, A.-S., Picaud, M., Reiss-Husson, F., Astier, C., & Ouchane, S. (2008). Organization and expression of photosynthesis genes and operons in anoxygenic photosynthetic proteobacteria. *Environmental Microbiology*, *10*(9), 2267–2276. <https://doi.org/10.1111/j.1462-2920.2008.01649.x>
- Liu, T., Nakashima, S., Hirose, K., Shibasaka, M., Katsuhara, M., Ezaki, B., Giedroc, D. P., & Kasamo, K. (2004). A Novel Cyanobacterial SmtB/ArsR Family Repressor Regulates the Expression of a CPx-ATPase and a Metallothionein in Response to Both Cu(I)/Ag(I) and Zn(II)/Cd(II). *Journal of Biological Chemistry*, *279*(17), 17810–17818. <https://doi.org/10.1074/jbc.M310560200>
- Liu, & Wang, Y. (2010). Application of AFM in microbiology: A review. *Scanning*, *32*(2), 61–73. <https://doi.org/10.1002/sca.20173>
- Lopez-Redondo, M. L., Coudray, N., Zhang, Z., Alexopoulos, J., & Stokes, D. L. (2018). Structural basis for the alternating access mechanism of the cation diffusion facilitator YiiP. *Proceedings of the National Academy of Sciences*, *115*(12), 3042–3047. <https://doi.org/10.1073/pnas.1715051115>
- Lu, M., & Fu, D. (2007). Structure of the Zinc Transporter YiiP. *Science*, *317*(5845), 1746–1748. <https://doi.org/10.1126/science.1143748>
- Lubick, N. (2008). Nanosilver toxicity: Ions, nanoparticles—or both? *Environmental Science & Technology*, *42*(23), 8617–8617. <https://doi.org/10.1021/es8026314>
- Macomber, L., & Imlay, J. A. (2009). The iron-sulfur clusters of dehydratases are primary intracellular targets of copper toxicity. *Proceedings of the National Academy of Sciences of the United States of America*, *106*(20), 8344–8349. <https://doi.org/10.1073/pnas.0812808106>
- Madigan, M. T., & Jung, D. O. (2009). An Overview of Purple Bacteria: Systematics, Physiology, and Habitats. In C. Neil Hunter, F. Daldal, M. C. Thurnauer, & J. T. Beatty (Eds.), *The Purple Phototrophic Bacteria* (pp. 1–15). Springer Netherlands. [https://doi.org/10.1007/978-1-4020-8815-5\\_1](https://doi.org/10.1007/978-1-4020-8815-5_1)
- Mann, S. (2001). *Biomineralization: Principles and Concepts in Bioinorganic Materials Chemistry*. Oxford University Press.

- Marambio-Jones, C., & Hoek, E. M. V. (2010). A review of the antibacterial effects of silver nanomaterials and potential implications for human health and the environment. *Journal of Nanoparticle Research*, *12*(5), 1531–1551. <https://doi.org/10.1007/s11051-010-9900-y>
- Masindi, V., & Muedi, K. L. (2018). Environmental Contamination by Heavy Metals. *Heavy Metals*. <https://doi.org/10.5772/intechopen.76082>
- Masuda, S., Dong, C., Swem, D., Setterdahl, A. T., Knaff, D. B., & Bauer, C. E. (2002). Repression of photosynthesis gene expression by formation of a disulfide bond in CrtJ. *Proceedings of the National Academy of Sciences*, *99*(10), 7078–7083. <https://doi.org/10.1073/pnas.102013099>
- McDermott, G., Prince, S. M., Freer, A. A., Hawthornthwaite-Lawless, A. M., Papiz, M. Z., Cogdell, R. J., & Isaacs, N. W. (1995). Crystal structure of an integral membrane light-harvesting complex from photosynthetic bacteria. *Nature*, *374*(6522), 517–521. <https://doi.org/10.1038/374517a0>
- Mealman, T. D., Blackburn, N. J., & McEvoy, M. M. (2012). Metal export by CusCFBA, the periplasmic Cu(I)/Ag(I) transport system of Escherichia coli. *Current Topics in Membranes*, *69*, 163–196. <https://doi.org/10.1016/B978-0-12-394390-3.00007-0>
- Medici, S., Peana, M., Nurchi, V. M., & Zoroddu, M. A. (2019). Medical Uses of Silver: History, Myths, and Scientific Evidence. *Journal of Medicinal Chemistry*, *62*(13), 5923–5943. <https://doi.org/10.1021/acs.jmedchem.8b01439>
- Mettert, E. L., & Kiley, P. J. (2018). Reassessing the Structure and Function Relationship of the O<sub>2</sub> Sensing Transcription Factor FNR. *Antioxidants & Redox Signaling*, *29*(18), 1830–1840. <https://doi.org/10.1089/ars.2017.7365>
- Mikhailov, O. V., & Mikhailova, E. O. (2019). Elemental Silver Nanoparticles: Biosynthesis and Bio Applications. *Materials (Basel, Switzerland)*, *12*(19). <https://doi.org/10.3390/ma12193177>
- Miller, L. C., Zhao, L., Canniffe, D. P., Martin, D., & Liu, L.-N. (2020). Unfolding pathway and intermolecular interactions of the cytochrome subunit in the bacterial photosynthetic reaction center. *Biochimica et Biophysica Acta (BBA) - Bioenergetics*, *1861*(8), 148204. <https://doi.org/10.1016/j.bbabi.2020.148204>
- Mills, E. L., Kelly, B., Logan, A., Costa, A. S. H., Varma, M., Bryant, C. E., Tourlomousis, P., Däbritz, J. H. M., Gottlieb, E., Latorre, I., Corr, S. C., McManus, G., Ryan, D., Jacobs, H. T., Szibor, M., Xavier, R. J., Braun, T., Frezza, C., Murphy, M. P., & O'Neill, L. A. (2016). Succinate Dehydrogenase Supports Metabolic Repurposing of Mitochondria to Drive Inflammatory Macrophages. *Cell*, *167*(2), 457–470.e13. <https://doi.org/10.1016/j.cell.2016.08.064>
- Möhler, J. S., Sim, W., Blaskovich, M. A. T., Cooper, M. A., & Ziora, Z. M. (2018). Silver bullets: A new lustre on an old antimicrobial agent. *Biotechnology Advances*, *36*(5), 1391–1411. <https://doi.org/10.1016/j.biotechadv.2018.05.004>

–REFERENCES–

- Montealegre, M. C., Roy, S., Böni, F., Hossain, M. I., Navab-Daneshmand, T., Caduff, L., Faruque, A. S. G., Islam, M. A., & Julian, T. R. (2018). Risk Factors for Detection, Survival, and Growth of Antibiotic-Resistant and Pathogenic *Escherichia coli* in Household Soils in Rural Bangladesh. *Applied and Environmental Microbiology*, *84*(24), e01978-18, /aem/84/24/e01978-18.atom. <https://doi.org/10.1128/AEM.01978-18>
- Moore, L. J., & Kiley, P. J. (2001). Characterization of the Dimerization Domain in the FNR Transcription Factor. *Journal of Biological Chemistry*, *276*(49), 45744–45750. <https://doi.org/10.1074/jbc.M106569200>
- Moore, A., & Goettmann, F. (2006). The plasmon band in noble metal nanoparticles: An introduction to theory and applications. *New Journal of Chemistry*, *30*(8), 1121–1132. <https://doi.org/10.1039/B604038C>
- Morones, J. R., Elechiguerra, J. L., Camacho, A., Holt, K., Kouri, J. B., Ramírez, J. T., & Yacaman, M. J. (2005). The bactericidal effect of silver nanoparticles. *Nanotechnology*, *16*(10), 2346–2353. <https://doi.org/10.1088/0957-4484/16/10/059>
- Moser, J., Lange, C., Krausze, J., Rebelein, J., Schubert, W.-D., Ribbe, M. W., Heinz, D. W., & Jahn, D. (2013). Structure of ADP-aluminium fluoride-stabilized protochlorophyllide oxidoreductase complex. *Proceedings of the National Academy of Sciences of the United States of America*, *110*(6), 2094–2098. <https://doi.org/10.1073/pnas.1218303110>
- Mulfinger, L., Solomon, S. D., Bahadory, M., Jeyarajasingam, A. V., Rutkowsky, S. A., & Boritz, C. (2007). Synthesis and Study of Silver Nanoparticles. *Journal of Chemical Education*, *84*(2), 322. <https://doi.org/10.1021/ed084p322>
- Müller, D. J., Helenius, J., Alsteens, D., & Dufrêne, Y. F. (2009). Force probing surfaces of living cells to molecular resolution. *Nature Chemical Biology*, *5*(6), 383–390. <https://doi.org/10.1038/nchembio.181>
- Muller, M., & Merrett, N. D. (2014). Pyocyanin Production by *Pseudomonas aeruginosa* Confers Resistance to Ionic Silver. *Antimicrobial Agents and Chemotherapy*, *58*(9), 5492–5499. <https://doi.org/10.1128/AAC.03069-14>
- Muraki, N., Nomata, J., Ebata, K., Mizoguchi, T., Shiba, T., Tamiaki, H., Kurisu, G., & Fujita, Y. (2010). X-ray crystal structure of the light-independent protochlorophyllide reductase. *Nature*, *465*(7294), 110–114. <https://doi.org/10.1038/nature08950>
- Murtey, M. D., & Ramasamy, P. (2016). Sample Preparations for Scanning Electron Microscopy – Life Sciences. In M. Janecek & R. Kral (Eds.), *Modern Electron Microscopy in Physical and Life Sciences*. InTech. <https://doi.org/10.5772/61720>
- Nagashima, S., Kamimura, A., Shimizu, T., Nakamura-Isaki, S., Aono, E., Sakamoto, K., Ichikawa, N., Nakazawa, H., Sekine, M., Yamazaki, S., Fujita, N., Shimada, K., Hanada, S., & Nagashima, K. V. P. (2012). Complete Genome Sequence of Phototrophic Betaproteobacterium *Rubrivivax gelatinosus* IL144. *Journal of Bacteriology*, *194*(13), 3541–3542. <https://doi.org/10.1128/JB.00511-12>

- Nanda, A., & Saravanan, M. (2009). Biosynthesis of silver nanoparticles from *Staphylococcus aureus* and its antimicrobial activity against MRSA and MRSE. *Nanomedicine: Nanotechnology, Biology, and Medicine*, 5(4), 452–456. <https://doi.org/10.1016/j.nano.2009.01.012>
- Nateghi, M. R., & Hajimirzababa, H. (2014). Effect of silver nanoparticles morphologies on antimicrobial properties of cotton fabrics. *The Journal of The Textile Institute*, 105(8), 806–813. <https://doi.org/10.1080/00405000.2013.855377>
- Navarro Gallón, S. M., Alpaslan, E., Wang, M., Larese-Casanova, P., Londoño, M. E., Atehortúa, L., Pavón, J. J., & Webster, T. J. (2019). Characterization and study of the antibacterial mechanisms of silver nanoparticles prepared with microalgal exopolysaccharides. *Materials Science & Engineering. C, Materials for Biological Applications*, 99, 685–695. <https://doi.org/10.1016/j.msec.2019.01.134>
- Nel, A. E., Mädler, L., Velegol, D., Xia, T., Hoek, E. M. V., Somasundaran, P., Klaessig, F., Castranova, V., & Thompson, M. (2009). Understanding biophysicochemical interactions at the nano–bio interface. *Nature Materials*, 8(7), 543–557. <https://doi.org/10.1038/nmat2442>
- Nel, Xia, T., Mädler, L., & Li, N. (2006, March 2). *Toxic potential of materials at the nanolevel*. Science (New York, N.Y.); Science. <https://doi.org/10.1126/science.1114397>
- Nguyen-Tri, P., Ghassemi, P., Carriere, P., Nanda, S., Assadi, A. A., & Nguyen, D. D. (2020). Recent Applications of Advanced Atomic Force Microscopy in Polymer Science: A Review. *Polymers*, 12(5). <https://doi.org/10.3390/polym12051142>
- Nies, D. H. (2003). Efflux-mediated heavy metal resistance in prokaryotes. *FEMS Microbiology Reviews*, 27(2–3), 313–339. [https://doi.org/10.1016/S0168-6445\(03\)00048-2](https://doi.org/10.1016/S0168-6445(03)00048-2)
- Nyquist, R. M., Heitbrink, D., Bolwien, C., Gennis, R. B., & Heberle, J. (2003). Direct observation of protonation reactions during the catalytic cycle of cytochrome c oxidase. *Proceedings of the National Academy of Sciences*, 100(15), 8715–8720. <https://doi.org/10.1073/pnas.1530408100>
- Oldenburg, S. (Sigma-Aldrich). *Silver Nanomaterials: Properties & Applications*. Sigma-Aldrich. <https://www.sigmaaldrich.com/technical-documents/articles/technology-spotlights/silver-nanomaterials.html>
- Olson, J. A. (1993). Vitamin A and carotenoids as antioxidants in a physiological context. *Journal of Nutritional Science and Vitaminology*, 39 Suppl, S57–65. [https://doi.org/10.3177/jnsv.39.supplement\\_s57](https://doi.org/10.3177/jnsv.39.supplement_s57)
- Oreopoulos, J., & Yip, C. M. (2008). Combined scanning probe and total internal reflection fluorescence microscopy. *Methods*, 46(1), 2–10. <https://doi.org/10.1016/j.ymeth.2008.05.011>
- Osman, D., Martini, M. A., Foster, A. W., Chen, J., Scott, A. J. P., Morton, R. J., Steed, J. W., Lurie-Luke, E., Huggins, T. G., Lawrence, A. D., Deery, E., Warren, M. J., Chivers, P. T., & Robinson, N. J. (2019). Bacterial sensors define intracellular free energies for correct

–REFERENCES–

- enzyme metalation. *Nature Chemical Biology*, 15(3), 241–249. <https://doi.org/10.1038/s41589-018-0211-4>
- Ouchane, Picaud, M., & Astier, C. (1995). A new mutation in the *pufL* gene responsible for the terbutryn resistance phenotype in *Rubrivivax gelatinosus*. *FEBS Letters*, 374(1), 130–134. [https://doi.org/10.1016/0014-5793\(95\)01055-J](https://doi.org/10.1016/0014-5793(95)01055-J)
- Ouchane, Picaud, M., Therizols, P., Reiss-Husson, F., & Astier, C. (2007). Global Regulation of Photosynthesis and Respiration by FnrL THE FIRST TWO TARGETS IN THE TETRAPYRROLE PATHWAY. *Journal of Biological Chemistry*, 282(10), 7690–7699. <https://doi.org/10.1074/jbc.M605985200>
- Ouchane, Picaud, M., Vernotte, C., & Astier, C. (1997). Photooxidative stress stimulates illegitimate recombination and mutability in carotenoid-less mutants of *Rubrivivax gelatinosus*. *The EMBO Journal*, 16, 4777–4787. <https://doi.org/10.1093/emboj/16.15.4777>
- Ouchane, S., Picaud, M., Reiss-Husson, F., Vernotte, C., & Astier, C. (1996). Development of gene transfer methods for *Rubrivivax gelatinosus* S1: Construction, characterization and complementation of *apuf* operon deletion strain. *Molecular and General Genetics MGG*, 252(4), 379–385. <https://doi.org/10.1007/BF02173002>
- Ouchane, Steunou, A.-S., Picaud, M., & Astier, C. (2004). Aerobic and Anaerobic Mg-Protoporphyrin Monomethyl Ester Cyclases in Purple Bacteria A STRATEGY ADOPTED TO BYPASS THE REPRESSIVE OXYGEN CONTROL SYSTEM. *Journal of Biological Chemistry*, 279(8), 6385–6394. <https://doi.org/10.1074/jbc.M309851200>
- Outten, F. W., Huffman, D. L., Hale, J. A., & O'Halloran, T. V. (2001). The Independent *cue* and *cus* Systems Confer Copper Tolerance during Aerobic and Anaerobic Growth in *Escherichia coli*. *Journal of Biological Chemistry*, 276(33), 30670–30677. <https://doi.org/10.1074/jbc.M104122200>
- Pal, S., Tak, Y. K., & Song, J. M. (2007). Does the Antibacterial Activity of Silver Nanoparticles Depend on the Shape of the Nanoparticle? A Study of the Gram-Negative Bacterium *Escherichia coli*. *Applied and Environmental Microbiology*, 73(6), 1712–1720. <https://doi.org/10.1128/AEM.02218-06>
- Palmgren, M. G., & Nissen, P. (2011). P-Type ATPases. *Annual Review of Biophysics*, 40(1), 243–266. <https://doi.org/10.1146/annurev.biophys.093008.131331>
- Panáček, A., Kolár, M., Vecerová, R., Pucek, R., Soukupová, J., Krystof, V., Hamal, P., Zboril, R., & Kvítek, L. (2009). Antifungal activity of silver nanoparticles against *Candida* spp. *Biomaterials*, 30(31), 6333–6340. <https://doi.org/10.1016/j.biomaterials.2009.07.065>
- Pandey, R., Armitage, J. P., & Wadhams, G. H. (2017). Use of transcriptomic data for extending a model of the AppA/PpsR system in *Rhodobacter sphaeroides*. *BMC Systems Biology*, 11(1), 146. <https://doi.org/10.1186/s12918-017-0489-y>
- Pandey, R., Flockerzi, D., Hauser, M. J. B., & Straube, R. (2011). Modeling the Light- and Redox-Dependent Interaction of PpsR/AppA in *Rhodobacter sphaeroides*. *Biophysical Journal*, 100(10), 2347–2355. <https://doi.org/10.1016/j.bpj.2011.04.017>

- Papiz, M. Z., Prince, S. M., Howard, T., Cogdell, R. J., & Isaacs, N. W. (2003). The structure and thermal motion of the B800-850 LH2 complex from *Rps.acidophila* at 2.0Å resolution and 100K: New structural features and functionally relevant motions. *Journal of Molecular Biology*, *326*(5), 1523–1538. [https://doi.org/10.1016/s0022-2836\(03\)00024-x](https://doi.org/10.1016/s0022-2836(03)00024-x)
- Parikh, R. Y., Singh, S., Prasad, B. L. V., Patole, M. S., Sastry, M., & Shouche, Y. S. (2008). Extracellular Synthesis of Crystalline Silver Nanoparticles and Molecular Evidence of Silver Resistance from *Morganella* sp.: Towards Understanding Biochemical Synthesis Mechanism. *ChemBioChem*, *9*(9), 1415–1422. <https://doi.org/10.1002/cbic.200700592>
- Pavičić, I., Milić, M., Pongrac, I. M., Brkić Ahmed, L., Matijević Glavan, T., Ilić, K., Zapletal, E., Ćurlin, M., Mitrečić, D., & Vinković Vrček, I. (2020). Neurotoxicity of silver nanoparticles stabilized with different coating agents: In vitro response of neuronal precursor cells. *Food and Chemical Toxicology*, *136*, 110935. <https://doi.org/10.1016/j.fct.2019.110935>
- Philips, S. J., Canalizo-Hernandez, M., Yildirim, I., Schatz, G. C., Mondragón, A., & O'Halloran, T. V. (2015). Allosteric transcriptional regulation via changes in the overall topology of the core promoter. *Science*, *349*(6250), 877–881. <https://doi.org/10.1126/science.aaa9809>
- Phototropic bacteria – purple non sulfur bacteria. (2012, October 10). *All About the Little Microbes*. <https://littlemicrobes.wordpress.com/bmm-usage/phototropic-bacteria-purple-non-sulfur-bacteria/>
- Pi, H., & Helmann, J. D. (2017). Ferrous iron efflux systems in bacteria. *Metallomics*, *9*(7), 840–851. <https://doi.org/10.1039/C7MT00112F>
- Pilon, M., Cohu, C. M., Ravet, K., Abdel-Ghany, S. E., & Gaymard, F. (2009). Essential transition metal homeostasis in plants. *Current Opinion in Plant Biology*, *12*(3), 347–357. <https://doi.org/10.1016/j.pbi.2009.04.011>
- Pinochet-Barros, A., & Helmann, J. D. (2018). Redox Sensing by Fe<sup>2+</sup> in Bacterial Fur Family Metalloregulators. *Antioxidants & Redox Signaling*, *29*(18), 1858–1871. <https://doi.org/10.1089/ars.2017.7359>
- Pinta, V., Picaud, M., Reiss-Husson, F., & Astier, C. (2002). Rubrivivax gelatinosus acsF (previously orf358) codes for a conserved, putative binuclear-iron-cluster-containing protein involved in aerobic oxidative cyclization of Mg-protoporphyrin IX monomethylester. *Journal of Bacteriology*, *184*(3), 746–753. <https://doi.org/10.1128/jb.184.3.746-753.2002>
- Pontel, L. B., Pezza, A., & Soncini, F. C. (2010). Copper Stress Targets the Rcs System To Induce Multiaggregative Behavior in a Copper-Sensitive Salmonella Strain. *Journal of Bacteriology*, *192*(23), 6287–6290. <https://doi.org/10.1128/JB.00781-10>
- Poole, R. K., & Cook, G. M. (2000). Redundancy of aerobic respiratory chains in bacteria? Routes, reasons and regulation. *Advances in Microbial Physiology*, *43*, 165–224. [https://doi.org/10.1016/s0065-2911\(00\)43005-5](https://doi.org/10.1016/s0065-2911(00)43005-5)

- Porter, S. L., Wadhams, G. H., & Armitage, J. P. (2011). Signal processing in complex chemotaxis pathways. *Nature Reviews Microbiology*, *9*(3), 153–165. <https://doi.org/10.1038/nrmicro2505>
- Rademacher, C., & Masepohl, B. (2012). Copper-responsive gene regulation in bacteria. *Microbiology*, *158*(10), 2451–2464. <https://doi.org/10.1099/mic.0.058487-0>
- Rademacher, C., Moser, R., Lackmann, J.-W., Klinkert, B., Narberhaus, F., & Masepohl, B. (2012). Transcriptional and Posttranscriptional Events Control Copper-Responsive Expression of a *Rhodobacter capsulatus* Multicopper Oxidase. *Journal of Bacteriology*, *194*(8), 1849–1859. <https://doi.org/10.1128/JB.06274-11>
- Rai, M. K., Deshmukh, S. D., Ingle, A. P., & Gade, A. K. (2012). Silver nanoparticles: The powerful nanoweapon against multidrug-resistant bacteria: Activity of silver nanoparticles against MDR bacteria. *Journal of Applied Microbiology*, *112*(5), 841–852. <https://doi.org/10.1111/j.1365-2672.2012.05253.x>
- Ranck, J.-L., Halgand, F., Lapr evote, O., & Reiss-Husson, F. (2005). Characterization of the core complex of *Rubrivivax gelatinosus* in a mutant devoid of the LH2 antenna. *Biochimica Et Biophysica Acta*, *1709*(3), 220–230. <https://doi.org/10.1016/j.bbabi.2005.08.002>
- Raposo, M., & Ferreira, Q. (2007). *A Guide for Atomic Force Microscopy Analysis of Soft-Condensed Matter*. Undefined. /paper/A-Guide-for-Atomic-Force-Microscopy-Analysis-of-Raposo-Ferreira/d5359268a9d9ab74a6beaa0f59d23f8ae3f41873
- Raza, M. A., Kanwal, Z., Rauf, A., Sabri, A. N., Riaz, S., & Naseem, S. (2016). Size- and Shape-Dependent Antibacterial Studies of Silver Nanoparticles Synthesized by Wet Chemical Routes. *Nanomaterials*, *6*(4). <https://doi.org/10.3390/nano6040074>
- Rensing, C., & Grass, G. (2003). *Escherichia coli* mechanisms of copper homeostasis in a changing environment. *FEMS Microbiology Reviews*, *27*(2–3), 197–213. [https://doi.org/10.1016/S0168-6445\(03\)00049-4](https://doi.org/10.1016/S0168-6445(03)00049-4)
- Rensing, C., & McDevitt, S. F. (2013). The copper metallome in prokaryotic cells. *Metal Ions in Life Sciences*, *12*, 417–450. [https://doi.org/10.1007/978-94-007-5561-1\\_12](https://doi.org/10.1007/978-94-007-5561-1_12)
- Rensing, C., Moodley, A., Cavaco, L. M., & McDevitt, S. F. (2018). Resistance to Metals Used in Agricultural Production. *Microbiology Spectrum*, *6*(2). <https://doi.org/10.1128/microbiolspec.ARBA-0025-2017>
- Rensing, Fan, B., Sharma, R., Mitra, B., & Rosen, B. P. (2000). CopA: An *Escherichia coli* Cu(I)-translocating P-type ATPase. *Proceedings of the National Academy of Sciences of the United States of America*, *97*(2), 652–656. <https://doi.org/10.1073/pnas.97.2.652>
- Richardson, D. J. (2000). Bacterial respiration: A flexible process for a changing environment. *Microbiology (Reading, England)*, *146* ( Pt 3), 551–571. <https://doi.org/10.1099/00221287-146-3-551>
- Rigoulet, M., Mourier, A., & Devin, A. (2007). Organization and Regulation of Mitochondrial Oxidative Phosphorylation. In *Molecular System Bioenergetics* (pp. 29–58). John Wiley & Sons, Ltd. <https://doi.org/10.1002/9783527621095.ch2>

- Robinson, N. J., & Winge, D. R. (2010). Copper Metallochaperones. *Annual Review of Biochemistry*, 79(1), 537–562. <https://doi.org/10.1146/annurev-biochem-030409-143539>
- Rtimi, S., Nadtochenko, V., Khmel, I., & Kiwi, J. (2017). Evidence for differentiated ionic and surface contact effects driving bacterial inactivation by way of genetically modified bacteria. *Chemical Communications*, 53(65), 9093–9096. <https://doi.org/10.1039/C7CC05013E>
- Sadeghi, B., Garmaroudi, F. S., Hashemi, M., Nezhad, H. R., Nasrollahi, A., Ardalan, S., & Ardalan, S. (2012). Comparison of the anti-bacterial activity on the nanosilver shapes: Nanoparticles, nanorods and nanoplates. *Advanced Powder Technology*, 23(1), 22–26. <https://doi.org/10.1016/j.appt.2010.11.011>
- Saer, R. G., & Blankenship, R. E. (2017). Light harvesting in phototrophic bacteria: Structure and function. *Biochemical Journal*, 474(13), 2107–2131. <https://doi.org/10.1042/BCJ20160753>
- Sánchez-López, E., Gomes, D., Esteruelas, G., Bonilla, L., Lopez-Machado, A. L., Galindo, R., Cano, A., Espina, M., Ettcheto, M., Camins, A., Silva, A. M., Durazzo, A., Santini, A., Garcia, M. L., & Souto, E. B. (2020). Metal-Based Nanoparticles as Antimicrobial Agents: An Overview. *Nanomaterials (Basel, Switzerland)*, 10(2). <https://doi.org/10.3390/nano10020292>
- Sautron, E., Mayerhofer, H., Giustini, C., Pro, D., Crouzy, S., Ravaud, S., Pebay-Peyroula, E., Rolland, N., Catty, P., & Seigneurin-Berny, D. (2015). HMA6 and HMA8 are two chloroplast Cu<sup>+</sup>-ATPases with different enzymatic properties. *Bioscience Reports*, 35(3). <https://doi.org/10.1042/BSR20150065>
- Scheuring, S., Reiss-Husson, F., Engel, A., Rigaud, J.-L., & Ranck, J.-L. (2001). High-resolution AFM topographs of *Rubrivivax gelatinosus* light-harvesting complex LH2. *The EMBO Journal*, 20(12), 3029–3035. <https://doi.org/10.1093/emboj/20.12.3029>
- Schindel, H. S., & Bauer, C. E. (2016). The RegA regulon exhibits variability in response to altered growth conditions and differs markedly between *Rhodobacter* species. *Microbial Genomics*, 2(10). <https://doi.org/10.1099/mgen.0.000081>
- Schmidt, M., Kébaili, N., Lando, A., Benrezzak, S., Baraton, L., Cahuzac, Ph., Masson, A., & Bréchnignac, C. (2008). Bent graphite surfaces as guides for cluster diffusion and anisotropic growth. *Physical Review B*, 77(20), 205420. <https://doi.org/10.1103/PhysRevB.77.205420>
- Sedlak, R. H., Hnilova, M., Grosh, C., Fong, H., Baneyx, F., Schwartz, D., Sarikaya, M., Tamerler, C., & Traxler, B. (2012). Engineered *Escherichia coli* Silver-Binding Periplasmic Protein That Promotes Silver Tolerance. *Applied and Environmental Microbiology*, 78(7), 2289–2296. <https://doi.org/10.1128/AEM.06823-11>
- Selamoglu, N., Önder, Ö., Öztürk, Y., Khalfaoui-Hassani, B., Blaby-Haas, C. E., Garcia, B. A., Koch, H.-G., & Daldal, F. (2020). Comparative differential cuproproteomes of *Rhodobacter*

- capsulatus reveal novel copper homeostasis related proteins. *Metallomics*, 12(4), 572–591. <https://doi.org/10.1039/C9MT00314B>
- Sganga, M. W., & Bauer, C. E. (1992). Regulatory factors controlling photosynthetic reaction center and light-harvesting gene expression in *Rhodobacter capsulatus*. *Cell*, 68(5), 945–954. [https://doi.org/10.1016/0092-8674\(92\)90037-D](https://doi.org/10.1016/0092-8674(92)90037-D)
- Sharma, R., Rensing, C., Rosen, B. P., & Mitra, B. (2000). The ATP Hydrolytic Activity of Purified ZntA, a Pb(II)/Cd(II)/Zn(II)-translocating ATPase from *Escherichia coli*. *Journal of Biological Chemistry*, 275(6), 3873–3878. <https://doi.org/10.1074/jbc.275.6.3873>
- Shcolnick, S., & Keren, N. (2006). Metal Homeostasis in Cyanobacteria and Chloroplasts. Balancing Benefits and Risks to the Photosynthetic Apparatus. *Plant Physiology*, 141(3), 805–810. <https://doi.org/10.1104/pp.106.079251>
- Shen, L., Li, Z., Wang, J., Liu, A., Li, Z., Yu, R., Wu, X., Liu, Y., Li, J., & Zeng, W. (2018). Characterization of extracellular polysaccharide/protein contents during the adsorption of Cd(II) by *Synechocystis* sp. PCC6803. *Environmental Science and Pollution Research*, 25(21), 20713–20722. <https://doi.org/10.1007/s11356-018-2163-3>
- Sheu, S.-Y., Li, Z.-H., Young, C.-C., & Chen, W.-M. (2020). *Rubrivivax albus* sp. Nov., isolated from a freshwater pond. *International Journal of Systematic and Evolutionary Microbiology*, 70(2), 805–813. <https://doi.org/10.1099/ijsem.0.003829>
- Silver, S. (2003). Bacterial silver resistance: Molecular biology and uses and misuses of silver compounds. *FEMS Microbiology Reviews*, 27(2–3), 341–353. [https://doi.org/10.1016/S0168-6445\(03\)00047-0](https://doi.org/10.1016/S0168-6445(03)00047-0)
- Simkiss, K., & Wilbur, K. M. (2012). *Biomineralization*. Elsevier.
- Singh, P., Kim, Y. J., Singh, H., Mathiyalagan, R., Wang, C., & Yang, D. C. (2015, May 18). *Biosynthesis of Anisotropic Silver Nanoparticles by Bhargavaea indica and Their Synergistic Effect with Antibiotics against Pathogenic Microorganisms* [Research Article]. *Journal of Nanomaterials*; Hindawi. <https://doi.org/10.1155/2015/234741>
- Smith, K. F., Bibb, L. A., Schmitt, M. P., & Oram, D. M. (2009). Regulation and Activity of a Zinc Uptake Regulator, Zur, in *Corynebacterium diphtheriae*. *Journal of Bacteriology*, 191(5), 1595–1603. <https://doi.org/10.1128/JB.01392-08>
- Soliman, D. (2016). *Augmented microscopy: Development and application of high-resolution optoacoustic and multimodal imaging techniques for label-free biological observation*. <https://doi.org/10.13140/RG.2.2.24410.03525>
- Solioz, M. (2018). *Copper and Bacteria: Evolution, Homeostasis and Toxicity*. Springer International Publishing. <https://doi.org/10.1007/978-3-319-94439-5>
- Solioz, M. (2019). Chapter 11—Copper Disposition in Bacteria. In N. Kerkar & E. A. Roberts (Eds.), *Clinical and Translational Perspectives on WILSON DISEASE* (pp. 101–113). Academic Press. <https://doi.org/10.1016/B978-0-12-810532-0.00011-2>
- Solov'yov, I. A., Solov'yov, A. V., Kébaili, N., Masson, A., & Bréchnignac, C. (2014). Thermally induced morphological transition of silver fractals. *Physica Status Solidi (b)*, 251(3), 609–622. <https://doi.org/10.1002/pssb.201349254>

- Sondi, I., & Salopek-Sondi, B. (2004). Silver nanoparticles as antimicrobial agent: A case study on *E. coli* as a model for Gram-negative bacteria. *Journal of Colloid and Interface Science*, *275*(1), 177–182. <https://doi.org/10.1016/j.jcis.2004.02.012>
- Steunou, A. S., Babot, M., Bourbon, M.-L., Tambosi, R., Durand, A., Liotenberg, S., Krieger-Liszkay, A., Yamaichi, Y., & Ouchane, S. (2020b). Additive effects of metal excess and superoxide, a highly toxic mixture in bacteria. *Microbial Biotechnology*, *13*(5), 1515–1529. <https://doi.org/10.1111/1751-7915.13589>
- Steunou, A. S., Bourbon, M., Babot, M., Durand, A., Liotenberg, S., Yamaichi, Y., & Ouchane, S. (2020c). Increasing the copper sensitivity of microorganisms by restricting iron supply, a strategy for bio-management practices. *Microbial Biotechnology*, *13*(5), 1530–1545. <https://doi.org/10.1111/1751-7915.13590>
- Steunou, A. S., Durand, A., Bourbon, M.-L., Babot, M., Tambosi, R., Liotenberg, S., & Ouchane, S. (2020a). Cadmium and Copper Cross-Tolerance. Cu<sup>+</sup> Alleviates Cd<sup>2+</sup> Toxicity, and Both Cations Target Heme and Chlorophyll Biosynthesis Pathway in *Rubrivivax gelatinosus*. *Frontiers in Microbiology*, *11*. <https://doi.org/10.3389/fmicb.2020.00893>
- Steunou, Astier, & Ouchane. (2004). Regulation of Photosynthesis Genes in *Rubrivivax gelatinosus*: Transcription Factor PpsR Is Involved in both Negative and Positive Control. *Journal of Bacteriology*, *186*(10), 3133–3142. <https://doi.org/10.1128/JB.186.10.3133-3142.2004>
- Storz, G., & Imlay, J. A. (1999). Oxidative stress. *Current Opinion in Microbiology*, *2*(2), 188–194. [https://doi.org/10.1016/s1369-5274\(99\)80033-2](https://doi.org/10.1016/s1369-5274(99)80033-2)
- Stoyanov, J. V., Magnani, D., & Solioz, M. (2003). Measurement of cytoplasmic copper, silver, and gold with a lux biosensor shows copper and silver, but not gold, efflux by the CopA ATPase of *Escherichia coli*. *FEBS Letters*, *546*(2–3), 391–394. [https://doi.org/10.1016/s0014-5793\(03\)00640-9](https://doi.org/10.1016/s0014-5793(03)00640-9)
- Stroebel, D., Choquet, Y., Popot, J.-L., & Picot, D. (2003). An atypical haem in the cytochrome b6f complex. *Nature*, *426*(6965), 413–418. <https://doi.org/10.1038/nature02155>
- Sundström, V., Pullerits, T., & van Grondelle, R. (1999). Photosynthetic Light-Harvesting: Reconciling Dynamics and Structure of Purple Bacterial LH2 Reveals Function of Photosynthetic Unit. *The Journal of Physical Chemistry B*, *103*(13), 2327–2346. <https://doi.org/10.1021/jp983722+>
- Svensson-Ek, M., Abramson, J., Larsson, G., Törnroth, S., Brzezinski, P., & Iwata, S. (2002). The X-ray crystal structures of wild-type and EQ(I-286) mutant cytochrome c oxidases from *Rhodobacter sphaeroides*. *Journal of Molecular Biology*, *321*(2), 329–339. [https://doi.org/10.1016/s0022-2836\(02\)00619-8](https://doi.org/10.1016/s0022-2836(02)00619-8)
- Swainsbury, D. J. K., Faries, K. M., Niedzwiedzki, D. M., Martin, E. C., Flinders, A. J., Canniffe, D. P., Shen, G., Bryant, D. A., Kirmaier, C., Holten, D., & Hunter, C. N. (2019). Engineering of B800 bacteriochlorophyll binding site specificity in the *Rhodobacter sphaeroides* LH2 antenna. *Biochimica et Biophysica Acta (BBA) - Bioenergetics*, *1860*(3), 209–223. <https://doi.org/10.1016/j.bbabi.2018.11.008>

- Swem, L. R., Gong, X., Yu, C.-A., & Bauer, C. E. (2006). Identification of a Ubiquinone-binding Site That Affects Autophosphorylation of the Sensor Kinase RegB. *The Journal of Biological Chemistry*, *281*(10), 6768–6775. <https://doi.org/10.1074/jbc.M509687200>
- Tacconelli, E., & Magrini. (2017). *GLOBAL PRIORITY LIST OF ANTIBIOTIC-RESISTANT BACTERIA TO GUIDE RESEARCH, DISCOVERY, AND DEVELOPMENT OF NEW ANTIBIOTICS*. 7.
- Takaichi, S. (2013). Tetraterpenes: Carotenoids. In K. G. Ramawat & J.-M. Mérillon (Eds.), *Natural Products: Phytochemistry, Botany and Metabolism of Alkaloids, Phenolics and Terpenes* (pp. 3251–3283). Springer. [https://doi.org/10.1007/978-3-642-22144-6\\_141](https://doi.org/10.1007/978-3-642-22144-6_141)
- Tamayo, L. A., Zapata, P. A., Vejar, N. D., Azócar, M. I., Gulppi, M. A., Zhou, X., Thompson, G. E., Rabagliati, F. M., & Páez, M. A. (2014). Release of silver and copper nanoparticles from polyethylene nanocomposites and their penetration into *Listeria monocytogenes*. *Materials Science and Engineering: C*, *40*, 24–31. <https://doi.org/10.1016/j.msec.2014.03.037>
- Tambosi, R., Liotenberg, S., Bourbon, M.-L., Steunou, A.-S., Babot, M., Durand, A., Kebaili, N., & Ouchane, S. (2018). Silver and Copper Acute Effects on Membrane Proteins and Impact on Photosynthetic and Respiratory Complexes in Bacteria. *MBio*, *9*(6). <https://doi.org/10.1128/mBio.01535-18>
- Tang, Y., Li, F., Tan, B., Liu, G., Kong, X., Hardwidge, P. R., & Yin, Y. (2014). Enterotoxigenic *Escherichia coli* infection induces intestinal epithelial cell autophagy. *Veterinary Microbiology*, *171*(1), 160–164. <https://doi.org/10.1016/j.vetmic.2014.03.025>
- Tchounwou, P. B., Yedjou, C. G., Patlolla, A. K., & Sutton, D. J. (2012). Heavy Metals Toxicity and the Environment. *EXS*, *101*, 133–164. [https://doi.org/10.1007/978-3-7643-8340-4\\_6](https://doi.org/10.1007/978-3-7643-8340-4_6)
- Thakkar, K. N., Mhatre, S. S., & Parikh, R. Y. (2010). Biological synthesis of metallic nanoparticles. *Nanomedicine: Nanotechnology, Biology and Medicine*, *6*(2), 257–262. <https://doi.org/10.1016/j.nano.2009.07.002>
- Thöny-Meyer, L. (1997). Biogenesis of respiratory cytochromes in bacteria. *Microbiology and Molecular Biology Reviews: MMBR*, *61*, 337–376. <https://doi.org/10.1128/61.3.337-376.1997>
- Troup, B., Hungerer, C., & Jahn, D. (1995). Cloning and characterization of the *Escherichia coli* hemN gene encoding the oxygen-independent coproporphyrinogen III oxidase. *Journal of Bacteriology*, *177*(11), 3326–3331.
- Trumpower, B. L. (1990). Cytochrome bc<sub>1</sub> complexes of microorganisms. *Microbiological Reviews*, *54*(2), 101–129.
- Uffen, R. L. (1976). Anaerobic growth of a *Rhodopseudomonas* species in the dark with carbon monoxide as sole carbon and energy substrate. *Proceedings of the National Academy of Sciences*, *73*(9), 3298–3302. <https://doi.org/10.1073/pnas.73.9.3298>
- Venter, H., Mowla, R., Ohene-Agyei, T., & Ma, S. (2015). RND-type drug efflux pumps from Gram-negative bacteria: Molecular mechanism and inhibition. *Frontiers in Microbiology*, *6*, 377. <https://doi.org/10.3389/fmicb.2015.00377>

- Ventola, C. L. (2015). The Antibiotic Resistance Crisis. *Pharmacy and Therapeutics*, *40*(4), 277–283.
- Verissimo, A. F., & Daldal, F. (2014). Cytochrome c biogenesis System I: An intricate process catalyzed by a maturase supercomplex? *Biochimica Et Biophysica Acta*, *1837*(7), 989–998. <https://doi.org/10.1016/j.bbabi.2014.03.003>
- Wang, S., Li, X., Williams, J. C., Allen, J. P., & Mathis, P. (1994). Interaction between cytochrome c<sub>2</sub> and reaction centers from purple bacteria. *Biochemistry*, *33*(27), 8306–8312. <https://doi.org/10.1021/bi00193a018>
- Wang, Singh, P., Kim, Y. J., Mathiyalagan, R., Myagmarjav, D., Wang, D., Jin, C.-G., & Yang, D. C. (2016). Characterization and antimicrobial application of biosynthesized gold and silver nanoparticles by using *Microbacterium resistens*. *Artificial Cells, Nanomedicine, and Biotechnology*, *44*(7), 1714–1721. <https://doi.org/10.3109/21691401.2015.1089253>
- Wang, Yanfang, Hodgkinson, V., Zhu, S., Weisman, G. A., & Petris, M. J. (2011). Advances in the Understanding of Mammalian Copper Transporters<sup>12</sup>. *Advances in Nutrition*, *2*(2), 129–137. <https://doi.org/10.3945/an.110.000273>
- Wang, Yuliang, & Xia, Y. (2004). Bottom-Up and Top-Down Approaches to the Synthesis of Monodispersed Spherical Colloids of Low Melting-Point Metals. *Nano Letters*, *4*(10), 2047–2050. <https://doi.org/10.1021/nl048689j>
- Willems, A., Gillis, M., & De Ley, J. (1991). Transfer of *Rhodocyclus gelatinosus* to *Rubrivivax gelatinosus* gen. Nov., comb. Nov., and Phylogenetic Relationships with *Leptothrix*, *Sphaerotilus natans*, *Pseudomonas saccharophila*, and *Alcaligenes latus*. *International Journal of Systematic Bacteriology*, *41*(1), 65–73. <https://doi.org/10.1099/00207713-41-1-65>
- Williams, C. L., Neu, H. M., Gilbreath, J. J., Michel, S. L. J., Zurawski, D. V., & Merrell, D. S. (2016). Copper Resistance of the Emerging Pathogen *Acinetobacter baumannii*. *Applied and Environmental Microbiology*, *82*(20), 6174–6188. <https://doi.org/10.1128/AEM.01813-16>
- Wiseman, B., Nitharwal, R. G., Fedotovskaya, O., Schäfer, J., Guo, H., Kuang, Q., Benlekbir, S., Sjöstrand, D., Ädelroth, P., Rubinstein, J. L., Brzezinski, P., & Högbom, M. (2018). Structure of a functional obligate complex III<sub>2</sub> IV<sub>2</sub> respiratory supercomplex from *Mycobacterium smegmatis*. *Nature Structural & Molecular Biology*, *25*(12), 1128–1136. <https://doi.org/10.1038/s41594-018-0160-3>
- Wu, J., Zheng, Y., Wen, X., Lin, Q., Chen, X., & Wu, Z. (2014). Silver nanoparticle/bacterial cellulose gel membranes for antibacterial wound dressing: Investigation in vitro and in vivo. *Biomedical Materials*, *9*(3), 035005. <https://doi.org/10.1088/1748-6041/9/3/035005>
- Wu, K., Su, D., Liu, J., Saha, R., & Wang, J.-P. (2019). Magnetic nanoparticles in nanomedicine: A review of recent advances. *Nanotechnology*, *30*(50), 502003. <https://doi.org/10.1088/1361-6528/ab4241>

- Wu, Kébaïli, N., Cheng, H.-P., Cahuzac, P., Masson, A., & Bréchnignac, C. (2012). Enhancement of Ag cluster mobility on Ag surfaces by chloridation. *The Journal of Chemical Physics*, *137*(18), 184705. <https://doi.org/10.1063/1.4759266>
- Xia, Y., Gilroy, K. D., Peng, H.-C., & Xia, X. (2017). Seed-Mediated Growth of Colloidal Metal Nanocrystals. *Angewandte Chemie (International Ed. in English)*, *56*(1), 60–95. <https://doi.org/10.1002/anie.201604731>
- Xu, F. F., & Imlay, J. A. (2012). Silver(I), Mercury(II), Cadmium(II), and Zinc(II) Target Exposed Enzymic Iron-Sulfur Clusters when They Toxicify Escherichia coli. *Applied and Environmental Microbiology*, *78*(10), 3614–3621. <https://doi.org/10.1128/AEM.07368-11>
- Yacamán, M. J., Ascencio, J. A., Liu, H. B., & Gardea-Torresdey, J. (2001). Structure shape and stability of nanometric sized particles. *Journal of Vacuum Science & Technology B: Microelectronics and Nanometer Structures Processing, Measurement, and Phenomena*, *19*(4), 1091–1103. <https://doi.org/10.1116/1.1387089>
- Yang, X., Cai, W., & Shao, X. (2007). Structural Variation of Silver Clusters from Ag<sub>13</sub> to Ag<sub>160</sub>. *The Journal of Physical Chemistry A*, *111*(23), 5048–5056. <https://doi.org/10.1021/jp0711895>
- Yankovskaya, V., Horsefield, R., Törnroth, S., Luna-Chavez, C., Miyoshi, H., Léger, C., Byrne, B., Cecchini, G., & Iwata, S. (2003). Architecture of succinate dehydrogenase and reactive oxygen species generation. *Science (New York, N.Y.)*, *299*(5607), 700–704. <https://doi.org/10.1126/science.1079605>
- Yoneyama, H., & Nakae, T. (1996). Protein C (OprC) of the outer membrane of *Pseudomonas aeruginosa* is a copper-regulated channel protein. *Microbiology (Reading, England)*, *142* ( Pt 8), 2137–2144. <https://doi.org/10.1099/13500872-142-8-2137>
- Youvan, D., Bylina, E., Alberti, M., Begusch, H., & Hearst, J. (1984). Nucleotide and deduced polypeptide sequences of the photosynthetic reaction-center, B870 antenna, and flanking polypeptides from *R. capsulata*. *Cell*, *37*, 949–957. [https://doi.org/10.1016/0092-8674\(84\)90429-X](https://doi.org/10.1016/0092-8674(84)90429-X)
- Zeilstra-Ryalls, J., Gomelsky, M., Eraso, J. M., Yeliseev, A., O’Gara, J., & Kaplan, S. (1998). Control of photosystem formation in *Rhodobacter sphaeroides*. *Journal of Bacteriology*, *180*(11), 2801–2809. <https://doi.org/10.1128/JB.180.11.2801-2809.1998>
- Zeilstra-Ryalls, J. H., & Kaplan, S. (1995). Aerobic and anaerobic regulation in *Rhodobacter sphaeroides* 2.4.1: The role of the *fnrL* gene. *Journal of Bacteriology*, *177*(22), 6422–6431.
- Zeilstra-Ryalls, J. H., & Kaplan, S. (2004). Oxygen intervention in the regulation of gene expression: The photosynthetic bacterial paradigm. *Cellular and Molecular Life Sciences: CMLS*, *61*(4), 417–436. <https://doi.org/10.1007/s00018-003-3242-1>
- Zhang, Chaker, M., Ma, D., & Riabinina, D. (2010). *Influence of Sodium Citrate Concentration on Morphology Transformation of Gold Nanoparticles during Laser Irradiation*.

–REFERENCES–

- Zhang, Liu, Z.-G., Shen, W., & Gurunathan, S. (2016). Silver Nanoparticles: Synthesis, Characterization, Properties, Applications, and Therapeutic Approaches. *International Journal of Molecular Sciences*, *17*(9), 1534. <https://doi.org/10.3390/ijms17091534>
- Zhang, Yan, S., Tyagi, R. D., & Surampalli, R. Y. (2011). Synthesis of nanoparticles by microorganisms and their application in enhancing microbiological reaction rates. *Chemosphere*, *82*(4), 489–494. <https://doi.org/10.1016/j.chemosphere.2010.10.023>
- Zhang, Z., Shen, W., Xue, J., Liu, Y., Liu, Y., Yan, P., Liu, J., & Tang, J. (2018). Recent advances in synthetic methods and applications of silver nanostructures. *Nanoscale Research Letters*, *13*(1), 54. <https://doi.org/10.1186/s11671-018-2450-4>
- Zhou, Y., Kong, Y., Kundu, S., Cirillo, J. D., & Liang, H. (2012). Antibacterial activities of gold and silver nanoparticles against *Escherichia coli* and *Bacillus Calmette-Guérin*. *Journal of Nanobiotechnology*, *10*(1), 19. <https://doi.org/10.1186/1477-3155-10-19>
- Zickermann, V., Wirth, C., Nasiri, H., Siegmund, K., Schwalbe, H., Hunte, C., & Brandt, U. (2015). Mechanistic insight from the crystal structure of mitochondrial complex I. *Science*, *347*(6217), 44–49. <https://doi.org/10.1126/science.1259859>
- Ziller, A., & Fraissinet-Tachet, L. (2018). Metallothionein diversity and distribution in the tree of life: A multifunctional protein. *Metallomics: Integrated Biometal Science*, *10*(11), 1549–1559. <https://doi.org/10.1039/c8mt00165k>
- Zsigmondy. (1926). *Properties of Colloids*.



**Titre : STRESS et TOXICITÉ des MÉTAUX dans LES BACTÉRIES PHOTOSYNTHÉTIQUES :**

Étude multi-échelles de l'effet et de la cible des ions métalliques et des nanoparticules

**Mots clés :** Stress métallique, Cuivre et Argent, Métabolisme, nanoparticules, Toxicité, AFM et SEM

**Résumé :** L'usage extensif des métaux et des ions métalliques dans l'industrie et l'agriculture représente une menace sérieuse pour l'environnement et pour tous les êtres vivants en raison de la toxicité aiguë de ces ions. Cependant, cela peut aussi être un outil prometteur. En effet, les ions comme les nanoparticules d'argent sont très utilisés dans diverses applications médicales, industrielles et sanitaires. L'effet antimicrobien de ces nanoparticules est en partie lié aux ions  $\text{Ag}^+$  libérés et à leur capacité à interagir avec les membranes bactériennes.

L'objectif de ce projet est d'étudier l'interaction entre un objet biologique (les bactéries) et des objets physiques (métaux), pour comprendre l'impact des métaux sous différentes formes (ions, nanoparticules et nanostructures) sur les cellules bactériennes en utilisant différentes approches : de physiologie, biochimie, génétique et de biologie cellulaire. Nous avons utilisé comme modèles biologiques, principalement la bactérie photosynthétique pourpre *Rubrivivax (R.) gelatinosus*, mais aussi *Escherichia coli*; et pour les objets physiques, nous avons utilisé l'argent comme métal principal mais aussi d'autres métaux (cuivre, cadmium et nickel) à titre de comparaison.

Les principaux objectifs de ce travail sont : 1- d'étudier l'impact et les mécanismes de toxicité de ces ions métalliques / NPs sur les métabolismes bactériens respiratoire et photosynthétique. 2- Identifier des gènes bactériens impliqués dans la réponse à un excès d'ions  $\text{Ag}^+$ . 3- Etudier l'internalisation et l'interaction des ions métalliques et des NPs au sein des membranes biologiques. Ainsi, nous avons pu identifier, à la fois *in vitro et in vivo*, des cibles spécifiques d'ions  $\text{Ag}^+$  et  $\text{Cu}^{2+}$  dans la membrane des bactéries. Cela inclut des complexes impliqués dans la photosynthèse, mais également des complexes de la chaîne respiratoire. Il a été démontré que les ions  $\text{Ag}^+$  et  $\text{Cu}^{2+}$  ciblent spécifiquement une bactériochlorophylle exposée au solvant dans les antennes de collecte de lumière du photosystème de la bactérie. Ceci présente également, à notre connaissance, la première preuve directe de dommages induits par des ions  $\text{Ag}^+$  sur les protéines membranaires impliquées dans ces métabolismes. Par ailleurs, nous avons également réalisé une étude comparative par microscopie (AFM/ SEM) de l'effet de l' $\text{Ag}^+$  en solution ou des Ag-NPs synthétisés dans notre laboratoire, sur la morphologie des cellules bactériennes.

**Title: STRESS and TOXICITY of METALS in PHOTOSYNTHETIC BACTERIA:**

Multi-scale study of the effects and targets of metal ions and nanoparticles

**Keywords:** Metallic stress, Copper and Silver, Metabolism, nanoparticles, Toxicity, AFM and SEM

**Abstract:** The extensive use of metal ions in industry and agriculture represents a serious threat to the environment and to all living being because of the acute toxicity of these ions. However, it can also be a promising tool, silver ions and nanoparticles are some of the most widely used metals in various industrial and health applications. The antimicrobial effect of these nanoparticles is in part related to the released  $\text{Ag}^+$  ions and their ability to interact with bacterial membranes.

The goal of this project is to study the interaction between biological subject (the bacteria) and physical objects (metals), and more specifically to understand the impact of metals in different forms (ions, nanoparticles and nanostructures) on the growth of the bacterial cells using different approaches : physiology, biochemistry, genetics and cell biology.

We used as biological models, principally the purple photosynthetic bacterium *Rubrivivax (R.) gelatinosus*, but also *Escherichia coli*, and for physical objects, we used silver as main metal but also other metals (copper, cadmium and nickel) for comparison.

The main objectives are: 1- to study the impact and the mechanisms of toxicity of these metallic ions/NPs on the bacterial respiratory and photosynthesis metabolisms. 2- To identify the bacterial genes involved in response to excess silver. 3- To study the internalization and interaction of metals ions and NPs within biological membranes.

The results showed that we were able to identify, both *in vitro* and *in vivo*, specific targets of  $\text{Ag}^+$  and  $\text{Cu}^{2+}$  ions within the membrane of bacteria. This include complexes involved in photosynthesis, but also complexes involved in respiration.  $\text{Ag}^+$  and  $\text{Cu}^{2+}$  were shown to specifically target a solvent exposed bacteriochlorophyll in the light harvesting antennae of the photosystem. This also presents, in our knowledge, the first direct evidence of silver ions damages to membrane proteins involved in these metabolisms. We also carried out a microscopy (AFM/ SEM) comparative study of the effect of  $\text{Ag}^+$  ions or Ag-NPs synthesized in our laboratory, on the bacterial cell morphology.